UC Santa Barbara

UC Santa Barbara Electronic Theses and Dissertations

Title

Physical Properties and Experimental Platform of Symmetry Protected Topological Phases

Permalink

https://escholarship.org/uc/item/37q1k2rj

Author

Bi, Zhen

Publication Date

2017

Peer reviewed|Thesis/dissertation

eScholarship.org Powered by the California Digital Library
University of California

University of California
Santa Barbara

Physical Properties and Experimental Platform of Symmetry Protected Topological Phases

A dissertation submitted in partial satisfaction
of the requirements for the degree

Doctor of Philosophy
in
Physics

by

Zhen Bi

Committee in charge:

Professor Cenke Xu, Chair
Professor Chetan Nayak
Professor Andrea F. Young

June 2017

The Dissertation of Zhen Bi is approved.

Professor Chetan Nayak

Professor Andrea F. Young

Professor Cenke Xu, Committee Chair

June 2017

Physical Properties and Experimental Platform of

Symmetry Protected Topological Phases

Copyright © 2017

by

Zhen Bi

Acknowledgements

This is probably the hardest part of this thesis for me. I feel deeply in debt to many people during the five years of my graduate school.

First and foremost, I would like to thank my advisor, Cenke Xu. Cenke is always a legendary figure in my mind. He is extremely creative, insightful and productive. It is impossible to enumerate his contributions to my Ph.D. life. Cenke's endless and selfless advices and helps are the main driving force for this dissertation. In addition, Cenke has provided me a very diversified education by teaching me many different topics outside physics, such as Chinese history, world history, Chinese pop music, American election. Thank you, Cenke, for being such a incredible advisor, collaborator and friend.

I am deeply grateful for Yi-Zhuang You. Yi-Zhuang has in many ways acted as my second advisor. Discussions with him always expand my knowledge, and he always has the clearest explanation for my questions. Yi-Zhuang's dedication to physics is contagious. We have collaborated on ten projects during his three years at KITP. I cannot thank Yi-Zhuang enough for being such a productive collaborate and thoughtful friend.

During my time at UCSB, I have benefitted enormously from talking with Leon. I am very grateful that Leon allowed me to attend his group meetings. I learned many aspects about quantum spin liquids and disorder systems from Leon. Leon always has a unique and clear angle to physics, and discussions with Leon always refresh my mind. Leon has selflessly helped me on postdoc applications. I could not thank you enough, Leon, for all your support.

I would like to acknowledge Zhenghan Wang and Meng Cheng from Station Q. Zhenghan and Meng countlessly educated me on the mathematical aspects of topological phases of matter. Without their patient teaching, I cannot keep up with the rapid development of this field. Zhenghan and Meng also supported me a lot on postdoc applications. I am

forever in debt to their help.

I want to thank Andrea Young and Chetan Nayak for serving on my Ph.D. committee. I also thank Matthew Fisher and David Weld for my advance exam committee.

I really enjoyed discussions with postdocs and graduate fellows from KITP and Station Q during the five years. I thank Yizhi You, Chao-Ming Jian, Xueda Wen, Laimei Nie, Thomas Scaffidi, Max Metlitski, Turan Grover, Tim Hsieh, Louk Rademaker, Jianpeng Liu, Gbor Halsz, Dong Liu and Eun-Gook Moon for countless insightful discussions.

I also want to address my thanks to my fellow graduate students. I always learned a lot from talking with our group members, Alex Rasmussen, Kevin Slagle, Kelly Ann Pawlak, and Farzan Vafa. I thank the many body journal club for introducing me to many of my fellow condensed matter physicists. It is a great platform for me to learn from other students and practice my presentation skills. I would like to thank everyone that has contributed to this journal club: Keith Fratus, Ru Chen, Lucile Savary, Yoni BenTov, Eugeniu Plamadeala, Jen Cano, James Garrison, Teddy Parker, Brayden Ware, Kaushal Patel, Dominic Else, Jason Iaconis, Katie Haytt, Alan Tran, Christina Knapp, Chaitanya Murthy, Dan Ish, Chunxiao Liu, ...

I am very lucky to be teaching assistants for Andrew Jayich, Dirk Bouwmeester, Tony Zee, Joe Incandela, Jean Carlson, Douglas Eardley, Sathya Guruswamy, Robert Geller, and Robert Pizzi during my five years of graduate school. These teaching experiences are extremely valuable to me.

I thank all my friends. In particular, I thank Wei Du, Lixin Sun, Junwu Huang, Xin Liang, Yunkun Xie, Quan Zhou, Xu Yi, Zhongbo Yan, Yingfei Gu, Biao Lian, Wenbo Fu, Yumeng Liu, and Liujun Zou for their endless mental support. And I thank Junkai Jiang, Rui Wu and Peter Dotti for being my great roommates.

Finally, I want to thank the never-ending love and support from my family. I would never make it this far without you.

Curriculum Vitæ

Zhen Bi

Education

2017	Ph.D. in Physics (Expected), University of California, Santa Barbara.
2015	M.A. in Physics, University of California, Santa Barbara.
2012	B.S. in Physics, Peking University.

Awards and Honors

2017	Outstanding Teaching Assistant, Physics Department, UCSB
2016	Dissertation Fellowship, Graduate Division, UCSB
2012	Herbert P. Broida Fellowship, Physics Department, UCSB

Professional Experiences

2017 Winter	Teaching Assistant for Phys. 110B Electrodynamics
2015 Winter	Teaching Assistant for Phys. 101 Complex Analysis, and Phys. 105B Quantum Mechanics
2015 Fall	Teaching Assistant for Phys. 119A Thermal Physics and Statistical Mechanics, and Phys. 123A Condensed Matter Physics
2014 Fall	Teaching Assistant for Phys. 205 Classical Mechanics

Publications

[1] C.-M. Jian, Z. Bi, and C. Xu, *A model for continuous thermal Metal to Insulator Transition,* arXiv:1703.07793.

[2] Z. Bi, C.-M. Jian, Y.-Z. You, K. Pawlak, and C. Xu, *Instability of the non-Fermi liquid state of the Sachdev-Ye-Kitaev Model,* arXiv:1701.07081.

[3] K. Slagle, Z. Bi, Y.-Z. You, and C. Xu, *Out-of-Time-Order Correlation in Marginal Many-Body Localized Systems,* arXiv:1611.04058.

[4] Z. Bi, A. Rasmussen, Y. BenTov, and C. Xu, *Stable Interacting* $(2+1)d$ *Conformal Field Theories at the Boundary of a Class of* $(3+1)d$ *Symmetry Protected Topological Phases* arXiv:1605.05336.

[5] Z. Bi, RX. Zhang, Y.-Z. You, A. Young, L. Balents, CX. Liu, and C. Xu. *Bilayer Graphene as a Platform for Bosonic Symmetry Protected Topological States,* arXiv:1512.-01547, Phys. Rev. Lett. **118**, 126801 (2017)

[6] Z. Bi, Y.-Z. You, and C. Xu, *Exotic Quantum Critical Point on the Surface of 3d Topological Insulator,* arXiv:1512.01547, Phys. Rev. B **94**, 024433 (2016).

[7] Y.-Z. You, Z. Bi, D. Mao, and C. Xu, *Quantum Phase Transitions Between Bosonic Symmetry Protected Topological States Without Sign Problem: Nonlinear Sigma Model with a Topological Term,* arXiv:1510.04278, Phys. Rev. B **93**, 125101 (2016).

[8] K. Slagle, Z. Bi, Y.-Z. You, and C. Xu, *Many-Body Localization of Symmetry Protected Topological States,* arXiv:1505.05147.

[9] Z. Bi, K. Slagle, and C. Xu, *Self-dual Quantum Electrodynamics on the Boundary of 4d Bosonic Symmetry Protected Topological States,* arXiv:1504.04373.

[10] Z. Bi, and C. Xu, *Construction and Field Theory of Bosonic Symmetry Protected Topological States beyond Group Cohomology,* arXiv: 1501.02271, Phys. Rev. B **91**, 184404 (2015).

[11] M. Cheng, Z. Bi, Y.-Z. You, and Z.-C Gu, *Towards a Complete Classification of Symmetry-Protected Phases for Interacting Fermions in Two Dimensions,* arXiv:1501.01313.

[12] Z. Bi, Y.-Z. You, and C. Xu, *Anyon and Loop Braiding Statistics in Field Theories with a Topological Θ-term,* arXiv: 1407.2994, Phys. Rev. B **90**, 081110 (2014).

[13] Y.-Z. You, Z. Bi, A. Rasmussen, M. Cheng, and C. Xu. *Bridging Fermionic and Bosonic Short Range Entangled States,* arXiv: 1404.6256, New J. Phys. **17**, 075010 (2015).

[14] Y.-Z. You, Z. Bi, A. Rasmussen, K. Slagle, and C. Xu. *Wave Function and Strange Correlator of Short Range Entangled States,* arXiv: 1312.0626, Phys. Rev. Lett. **112**, 247202 (2014).

[15] Z. Bi, A. Rasmussen, K. Slagle, and C. Xu, *Classification and Description of Bosonic Symmetry Protected Topological Phases with Semiclassical Nonlinear Sigma Models,* arXiv: 1309.0515, Phys. Rev. B **91**, 134404 (2015).

[16] Z. Bi, A. Rasmussen, and C. Xu, *Line Defects in Three Dimensional Symmetry Protected Topological Phases,* arXiv: 1304.7272, Phys. Rev. B **89**, 184424 (2014).

Abstract

Physical Properties and Experimental Platform of

Symmetry Protected Topological Phases

by

Zhen Bi

As condensed matter theorists, we always try to seek new quantum phases of matter that are not possible in classical physics. In this dissertation, I discussed a new type of quantum disordered phases known as symmetry protected topological (SPT) phases, which is a generalization of the topological insulator to interacting fermion or boson/spin systems with various symmetries. In the first part of this thesis, a nonlinear σ-model (NLσM) field theory is introduced as a powerful tool to describe the properties of the bosonic SPT phases. Secondly, we want to answer the question of how to detect the SPT states from their bulk properties. Introducing gauge fields was shown to be an effective theoretical tool to study bulk properties of SPT phases. Furthermore, we investigated anyon and loop statistics of gauged SPT states in the framework of NLσM. We also designed a new numerical probe, so-called strange correlator, which can distinguish SPT states from trivial states based on the bulk wavefunction on a closed manifold. Thirdly, several aspects of surface states of SPT phases are discussed. 1. A surface phase transition of $3d$ topological insulator is studied through a new controlled expansion method with the help of the recently discovered fermion-vortex duality. 2. A new strongly interacting conformal field theory on the surface of $3d$ bosonic SPT state is also found by a controlled renormalization group calculation. 3. we made a connection between the surface of SPT phase and the Lieb-Schultz-Mattis (LSM) theorem, which enables us to identity the $SU(N)$ and $SO(N)$ spin systems that permit a featureless ground state in $2d$ and $3d$.

Finally, we proposed the first experimental realization of bosonic SPT state in dimension higher than 1. We established a general relation between interacting multi-layer fermionic SPTs and bosonic SPT with the same symmetry, which motivates a proposal of realizing $2+1d$ bosonic SPT phase in bilayer graphene system.

Contents

Chapter 1

Introduction

From our experience of solving problems in classical mechanics, we know that the complexity of a problem grows very fast with the number of objects in consideration. Condensed matter physics deals with macroscopic systems composed of an enormous number of microscopic degrees of freedom, so-called many-body systems. A first principle solution of a generic interacting condensed matter system is virtually unreachable with the computational power today. On the other hand, strongly correlated many-body systems can give rise to many striking emergent phenomena, which provide a playground for theoretical condensed matter study.

Interacting electrons in crystalline materials are historically the central player in "hard" condensed matter physics. We are interested in the properties at low temperature where quantum effects play an essential role. Surprisingly, as we zoom into the low energy physics of electron systems, we often find emergent degrees of freedom that are related to but different from the original electrons. One famous example arises in graphene. Although the system is composed of ordinary massive electrons, its low energy theory has features resembling the so-called gapless Dirac fermion. Another well known example is the Hubbard model with large onsite repulsive interaction at half filling, in which at

energy lower than the onsite interaction the effective theory is the Heisenberg model of electron spins and the charge degrees of freedom of the electrons are completely frozen. Interacting spin models on various lattices, so-called quantum magnetism, is also an active topic in condensed matter. With the rapid development of cold atom experiments, it is possible to engineer lattice systems with interacting bosonic degrees of freedom. As can be seen from these examples, modern theoretical condensed matter physics is focused on determining the low energy properties of all kinds of lattices models of interacting electrons, spins or bosons.

1.1 Some common notions

To further specify the subject of our study, we need the notions of phases of matter and phase transitions. Let us consider a macroscopic system in its thermal equilibrium state. Usually we will have several "experimental knobs" which correspond to theoretical tuning parameters, such as pressure, temperature and electromagnetic field, to play with. If all macroscopic properties of the system(*e.g.* magnetization, magnetic susceptibility, specific heat) change smoothly as we slowly change from one set of parameters, then we say that the system with these two sets of parameters are in the same phase. If instead some of the system's macroscopic quantities go through a discontinuous change with smoothly changing of parameters, we will say that the system undergoes a phase transition. Gas, liquid and solid are three well known examples of phases of matter. It is less commonly known that gas and liquid actually belong to the same phase since gas can be turned into liquid without going through a phase transition by a particular parameter path in the temperature and pressure plane. The gas-liquid-solid classification of phases is a very crude one. As we now realize that for ice molecules there can exist up to 16 different phases differing by their microscopic packing geometries. Another example is

solid iron, which can, depending on the temperature, exhibit two different phases: the ferromagnetic phase and the paramagnetic phase.

A more advanced guiding principle for classifying phases of matter is symmetry and *spontaneous symmetry breaking*, also known as the Landau-Ginzburg paradigm. Let us take the Heisenberg model of spins as an example.

$$\mathcal{H}_{Heisenberg} = J \sum_{<i,j>} \hat{\boldsymbol{S}}_i \cdot \hat{\boldsymbol{S}}_j \tag{1.1}$$

This microscopic spin hamiltonian has spin rotational symmetry, which means that if we rotate every spin by the same angle, the hamiltonian remains invariant. (This is not the only symmetry of the system. There is also spatial symmetry associated with the lattice structure, but we will focus on the spin rotation now.) With $J < 0$, in the ground states, the spins tend to be parallel to each other to achieve minimal energy. The ground states of the hamiltonian (there are uncountably many ground states in this case) are product states of all spins pointing in the same direction, in other words, the spins are ordering along that direction. Notice that the ground states are not invariant under the full spin rotational symmetry anymore. Instead, each ground state will transform into another ground state under some spin rotation operation (except in the case of rotation about the ordering axis). At zero temperature, the system randomly picks one of the ground states and spontaneously breaks the spin rotational symmetry. The system will have macroscopic magnetization and hence is in the ferromagnetic phase. The symmetry breaking phase is also referred as the *ordered phase*. In the ordered phase, the spin operator, which is also identified as the *order parameter* (The order parameter by definition must have nontrivial transformation under the broken symmetry.), has *long range correlation*, namely the correlation function $\langle GS| \hat{\boldsymbol{S}}_i \cdot \hat{\boldsymbol{S}}_j |GS\rangle \sim$ const. as $|\boldsymbol{i} - \boldsymbol{j}| \to \infty$.

Raising the temperature will introduce *thermal fluctuation* to the system. In thermodynamics, the equilibrium state has to minimize the free energy.

$$\mathcal{F} = \mathcal{E} - T\mathcal{S} \tag{1.2}$$

Finite temperature allows the system to explore more spin configurations to gain entropy, and consequently the thermal average value of the spin operator will decrease relative to the zero temperature result. Above a critical temperature, $T_c \sim J$, the order parameter decays to zero, $\langle \hat{\boldsymbol{S}} \rangle_\beta = 0$, and the system restores the spin rotational symmetry. The spin system then enters the so-called paramagnetic phase, which preserves all the symmetry of the microscopic model. Therefore, it is also referred as the symmetric or *disordered phase*. In the disordered phase, although the average value of the spin operator is zero, the spin operators have *short range correlations* which means that the nearby spins still tend to aline to each other locally. Typically, the correlation function decays as a exponential function $\langle \hat{\boldsymbol{S}}_i \cdot \hat{\boldsymbol{S}}_j \rangle_\beta \sim \exp[-|\boldsymbol{i} - \boldsymbol{j}|/\xi]$. ξ is a length scale beyond which the spins lose their correlation, and hence it is called the correlation length. As we approach the transition by lowering the temperature, ξ will increase and eventually diverge at the critical point. Below the transition temperature, the spins have long range correlation. The divergence of correlation length is a defining signature for a continuous *second order phase transition*. In contrast, the system will not have any diverging length scale when crossing a first order transition. A generic symmetry breaking phase transition, or order-disorder transition, is usually continuous second order. Right at the continuous phase transition point, the correlation function decays with distance in a *power-law* form, $\langle \hat{\boldsymbol{S}}_i \cdot \hat{\boldsymbol{S}}_j \rangle_\beta \sim 1/|\boldsymbol{i} - \boldsymbol{j}|^\alpha$, and the *exponent* is a *universal property* for the *critical point*.

We are more interested in quantum phases of matter, so we will restrict ourselves to systems with zero temperature from now on. In other words, we are only going

to look at properties of the ground states and the nearby states. In the case of the ferromagnetic Heisenberg model, it is very easy to identify the ground states. However, it is not always easy (in fact it is usually impossible) to determine the ground states of a quantum many-body hamiltonian. Take the Heisenberg model with $J > 0$ as an example (the so-called anti-ferromagnetic Heisenberg model). A guess for a typical ground state would look like $|\psi\rangle \sim |\uparrow\downarrow\uparrow ...\rangle$ in the S^z basis. However, this state is actually not an eigenstate of the hamiltonian. In particular, some terms in the hamiltonian, $\hat{S}_i^x \hat{S}_j^x$ and $\hat{S}_i^y \hat{S}_j^y$, acting on the state $|\psi\rangle$ can flip the spins in the state and lead to a different state in the Hilbert space. This phenomenon is called *quantum fluctuation*. It happens because different terms in the hamiltonian do not mutually commute, and the system must make a compromise between different terms to lower the energy. Now we see that whether the anti-ferromagnetic Heisenberg model has a symmetry breaking ground state does not have an obvious answer because of the quantum fluctuation. The results also highly depend on the dimension and geometric properties of the underlying lattice structure. On a bipartite lattice in two and higher spatial dimensions, for instance the square lattice, the ground state has so-called *Neel order*. The ground state is predominately $|\psi\rangle \sim |\uparrow\downarrow\uparrow ...\rangle$, but with corrections to make sure the whole state is an eigenstate. (Of course, this is only one of the uncountable many ground states that are all related by spin rotations.) The spin operators have long range correlation $\langle GS| \hat{\boldsymbol{S}}_i \cdot \hat{\boldsymbol{S}}_j |GS\rangle \sim (-1)^{|\boldsymbol{i}-\boldsymbol{j}|}$. The Neel state breaks the $SU(2)$ spin symmetry down to $U(1)$ rotation along the ordering direction. The situation for triangular lattice is trickier. The triangluar lattice has the property of so-called *geometric frustration*. That is to say, there is no way to perfectly assign an anti-ferromagnetic pattern to this lattice without upsetting some subset of the spins. Convincing numerical results have shown that the ground state still exhibits ordering but in a coplanar 120 degree fashion, which completely breaks all the spin rotational symmetries. However, the fate of the anti-ferromagnetic Heisenberg model

on the Kagome lattice, another type of frustrated lattice, is still unsettled. Recent numerical tests suggest that it may remain quantum disordered and host some exotic gapless states[1].

A rather well understood iconic quantum spin model is the transverse field Ising model or the quantum Ising model.

$$\mathcal{H}_{Ising} = -J \sum_{<i,j>} S_i^z S_j^z - h \sum_i S_i^x \tag{1.3}$$

It's a spin model with a discrete $G = Z_2$ symmetry, where the action of the Z_2 symmetry is to flip the S^z operators while keeps S^x invariant. Therefore, expectation value of the S^z operator corresponds to the order parameter in this case. Let us assume $J \geq 0$ and $h \geq 0$. The model is solvable in $h/J \to 0$ and $h/J \to \infty$ limits, which are representative points in the ordered and disordered phase, respectively. We comment on some properties of this model:

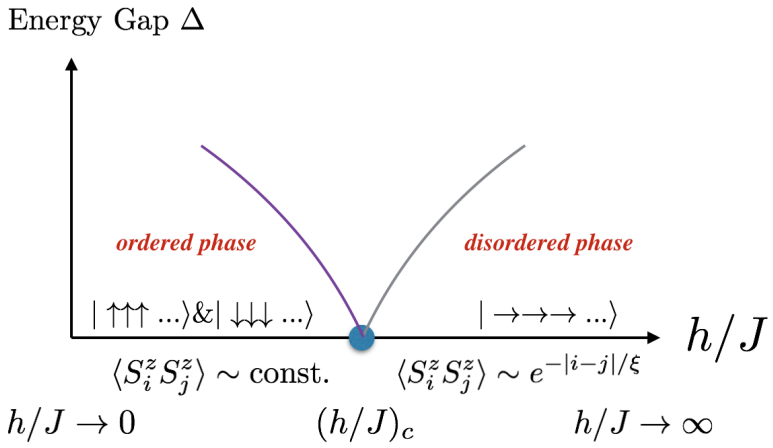

Figure 1.1: phase diagram of quantum Ising model

1. With $h/J \to 0$, the first term, *i.e.*, the Ising coupling dominates. We have two-fold degenerate ground states, in the S^z basis: $|\psi_{up}\rangle \sim |\uparrow\uparrow\uparrow ...\rangle$ and $|\psi_{down}\rangle \sim |\downarrow\downarrow\downarrow ...\rangle$.

They spontaneously break the Z_2 symmetry and the system is in an ordered phase. Adding S^x terms introduces quantum fluctuations to flip the spins and weaken the S^z order. However, the ground state wavefunctions of the symmetry breaking phase with finite h are still predominately $|\psi_{up}\rangle$ and $|\psi_{down}\rangle$ with only small corrections. Additionally, the energy spectrum in the ordered phase has a finite gap of order J above the ground state.

2. In the other limit, $h/J \to \infty$, S^x terms dominate and the ground state is unique, $|\psi\rangle \sim |\to\to\to ...\rangle$, where $|\to\rangle$ is the eigenstate of S^x with eigenvalue $1/2$. This is a state that respects the Z_2 symmetry, and it represents the quantum disordered phase of this model. The disordered phase also has a finite energy gap of order h.

3. If the two sets of parameters belong to the same gapped phase, then their ground state wavefunctions can be adiabatically connected to each other. In this example, the ground state wavefunctions of the ordered and disordered phase are both adiabatically connected to a *direct product state*.

4. The energy gap closes at the order-disorder transition point. This is a second order quantum phase transition. Correlation functions of local operators have power-law forms with universal exponents that characterize the critical point.

In general, the symmetry of a microscopic hamiltonian is characterized by a symmetry group G. $G = SU(2)$ for the Heisenberg model. Any element $g \in G$ will leave the hamiltonian invariant, $g\mathcal{H}g^{-1} = \mathcal{H}$. In a symmetry breaking phase, the ground state is not invariant under the whole group G. However, it may still be invariant under a subgroup of G. Let us call this residue symmetry group H. In the ferromagnetic and antiferromagnetic examples, $H = U(1)$, which is the rotation along the ordering direction. The space for the ground states, or the *ground state manifold*, is $\mathcal{M} = G/H$, which is

$\mathcal{M}_{ferro} = SU(2)/U(1) \sim S^2$ in the ferromagnetic phase. If $\dim(\mathcal{M}) \geq 1$, a small change of the ground state along any direction in $\mathcal{M}$ costs no energy. Therefore, the spectrum of the system is gapless, and the gapless modes are called *Goldstone modes*. The number of Goldstone modes is exactly $\dim(\mathcal{M})$. If the $\dim(\mathcal{M}) = 0$, then the spectrum will be gapped, and the ground state degeneracy will be the number of disconnected points in $\mathcal{M}$. For example, the Ising model is a spin model with a discrete Z_2 symmetry. In the ordered phase, its ground state is two-fold degenerate, which can be understood by $\mathcal{M}_{Ising} = G/H = Z_2/Z_1 = Z_2$. To summarize, spontaneous symmetry breaking leads to either a gapless spectrum or a gapped spectrum with ground state degeneracy depending on whether the broken symmetry is continuous or discrete.

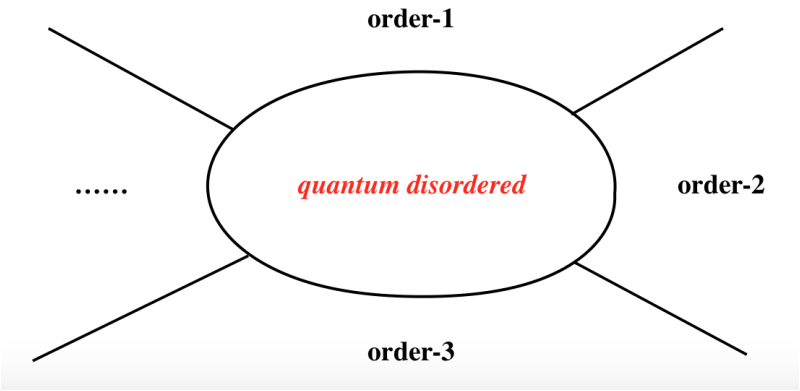

Figure 1.2: schematic classification of quantum phases according to spontaneous symmetry breaking paradigm

The schematic classification of quantum phases according to Landau's spontaneous symmetry breaking principle can be pictured as in Fig. 1.2. The quantum disordered phase respects all the symmetries of the microscopic model. The system may be driven into different ordered states by different tuning parameters, and different ordered states can be labeled by their symmetry breaking patterns. The symmetry breaking phases may have gapless or gapped but degenerate spectra depending on the broken symmetry. The

transitions between disordered and ordered phases are typically second order transitions. The transitions between different ordered states are typically first order.

1.2 Symmetry protected topological (SPT) phases

Traditionally, given a microscopic system with a certain symmetry group there is one canonical disordered phase whose ground state wavefunction is adiabatically connect to a direct product state, which is essentially classical. This type of quantum disordered phase is featureless. It has a non-degenerate ground state a finite energy gap in the bulk. If the system has spatial boundaries, the boundary energy spectrum can also generically be gapped and non-degenerate without breaking any symmetry of the system.

However, recent studies reveal that disordered phases driven by quantum fluctuation can have far richer structure than just direct product states. In quantum many-body systems, several types of exotic/nontrivial quantum disordered phases are possible: (1) algebraic liquid phases with gapless spectra and power-law correlations, (2) intrinsic topological order with a gapped spectrum and topological degeneracy, and (3) symmetry protected topological (SPT) phases. Each of these topics deserves its own thesis. We are going to focus on the last one, symmetry protected topological phase, although aspects of other two will naturally appear throughout the discussion.

The symmetry protected topological phase is a new type of quantum disordered phase. It is intrinsically different from a trivial direct product state, when and only when the system preserves a certain symmetry G. In terms of its phenomena, a SPT phase on a $d-$dimensional lattice should satisfy at least the following three criteria:

(i). On a $d-$dimensional lattice without boundary, this phase is fully gapped, and nondegenerate;

(ii). On a $d-$dimensional lattice with a $(d-1)-$dimensional boundary, if the Hamilto-

nian of the entire system (including both the bulk and boundary Hamiltonian) preserves a certain symmetry G, this phase is either gapless, or gapped but degenerate.

(*iii*). The boundary state of this $d-$dimensional system cannot be realized as a $(d-1)$-dimensional lattice system with the same symmetry G. Stated theoretically, the boundary is anomalous with symmetry G.

The $2d$ quantum spin Hall (QSH) insulator[2, 3, 4] and $3d$ topological insulator (TI) [5, 6, 7] are perfect examples of fermionic SPT phases protected by charge conservation and time reversal symmetry, $G = U(1) \rtimes \mathcal{T}$. In the free limit, the $1d$ boundary of a $2d$ QSH insulator has a pair of gapless counter propagating edge modes, and the $2d$ surface of a $3d$ TI hosts a single gapless Dirac fermion. These gapless modes are protected by symmetry because there are no symmetry preserving fermion bilinear terms we can add to gap out the boundary. Electron interactions on the boundary of a QSH insulator are either irrelevant and do not change the gapless nature, or they are relevant and may lead to spontaneous breaking of $\mathcal{T}$ symmetry, which leaves a two-fold degeneracy on the boundary[8, 9, 10]. There are more possible surface states of a TI if we include electron interactions. With interaction it can be (*i*) symmetric gapless, (*ii*) spontaneous symmetry breaking (either $U(1)$ or $\mathcal{T}$), or (*iii*) symmetric gapped but with intrinsic topological order[11, 12, 13, 14]. We will encounter some aspects of interacting surface states of a TI later in the main text.

SPT phases also exist in boson and spin systems. Unlike fermion systems, bosonic SPT phases are always strongly interacting phases of boson systems because free boson system at low temperature always falls into Bose-Einstein condensates. Since bosonic SPTs are strongly interacting phases of bosons, we have fewer theoretical tools with which to study their properties. Also, it is relatively difficult to realize them experimentally than free fermion topological phases. One of the goals of this thesis is to develop formalism for understanding bosonic SPT states as well as to provide some experimental suggestions

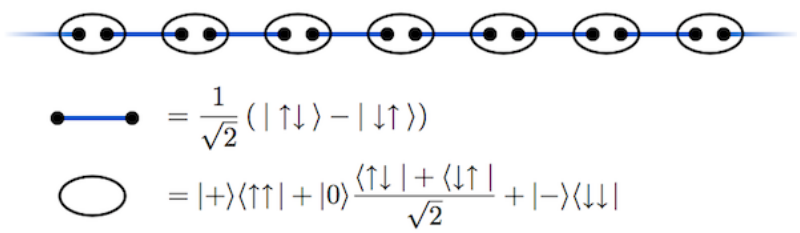

Figure 1.3: The solid points represent spin-$\frac{1}{2}$'s, which are put into singlet states. The lines connecting the spin-$\frac{1}{2}$'s are the valence bonds indicating the pattern of singlets. The ovals are projection operators which"tie" together two spin$\frac{1}{2}$'s into a single spin 1, projecting out the spin-0 or singlet subspace and keeping only the spin-1 or triplet subspace. Picture from wikipedia page on AKLT model.

to realize these bosonic topological states.

Let us discuss one of the earliest examples of SPT in $1d$ integer spin systems. Because we are considering integer spins, the spin symmetry is actually $SO(3)$ instead of $SU(2)$. The example goes by the name of the Haldane phase[15, 16] of $1d$ antiferromagnetic spin-1 chain. There exists an exact soluble point in the Haldane phase, which is the so-called Affleck-Lieb-Kennedy-Tasaki (AKLT) model[17]. The model hamiltonian is motived by the construction of a certain valance bond state that preserves all of the spin and lattice translational symmetry. The idea is that we can break the spin-1 representation on each site into two spin-$\frac{1}{2}$ representations and then form singlet state out of two spin-$\frac{1}{2}$'s from adjacent sites. Eventually, we want to project the state on each site onto the spin-1 sector. The construction of the state can be seen pictorially in Fig. 1.3. The projector hamiltonian that selects the AKLT state as the ground state is the following.

$$\mathcal{H}_{AKLT} = \sum_{i=1}^{\mathcal{N}} \boldsymbol{S}_i \cdot \boldsymbol{S}_{i+1} + \frac{1}{3}(\boldsymbol{S}_i \cdot \boldsymbol{S}_{i+1})^2 \tag{1.4}$$

Any change of the state will involve breaking the singlet bounds, which costs finite energy. Therefore, we have a gapped non-degenerate ground state if the spins form a ring. However, if we break the ring, at each boundary of the system there is a leftover spin-$\frac{1}{2}$

degree of freedom, which is a fractional/projective representation of $SO(3)$ symmetry. The boundary spin-$\frac{1}{2}$ carries robust two-fold degeneracy, and there is no way to split them with $SO(3)$ invariant perturbations. This inability to split the boundary degeneracy while preserving the symmetry is the signature for SPT phases in $1d$.

It turns out that $1d$ spin-1 antiferromagnetic Heisenberg model is in the same Haldane phase as the AKLT state[18]. The AKLT state is a representative state with zero correlation length for the Haldane phase. The antiferromagnetic Heisenberg model is not exactly soluble. Various approximation methods have been tried to solve this model. We are going to review the nonlinear σ-model field theory for the Heisenberg model in the next section.

1.3 The nonlinear σ-model description of $1d$ Heisenberg model

Let's derive the effective field theory for the $1d$ spin-S antiferromagnetic Heisenberg model, using standard techniques which can be found in various textbooks[19, 20]. We start from the coherent state path integral formalism for spins. The spin-S coherent states are defined as follows.

$$|\hat{\Omega}\rangle = e^{i\hat{S}^z\phi}e^{i\hat{S}^y\theta}e^{i\hat{S}^z\chi}|S,S\rangle \tag{1.5}$$

$$\hat{\Omega} = (\sin\theta\cos\phi, \sin\theta\sin\phi, \cos\theta) \tag{1.6}$$

χ is a gauge degree of freedom that we will fix to be zero from now on. Notice that these coherent state basis are not orthogonal to each other

$$\langle \hat{\Omega} \, | \hat{\Omega}' \rangle = \left(\frac{1 + \hat{\Omega} \cdot \hat{\Omega}'}{2} \right)^S e^{-iS\psi} \tag{1.7}$$

$$\psi = 2 \arctan \left[\tan \left(\frac{\phi - \phi'}{2} \right) \frac{\cos[(\theta + \theta')/2]}{\cos(\theta - \theta')/2} \right] \tag{1.8}$$

The expectation value of the Heisenberg model in a coherent state is

$$H[\hat{\Omega}] = \langle \hat{\Omega} | \, \mathcal{H} \, | \hat{\Omega} \rangle = JS^2 \sum_{<i,j>} \hat{\Omega}_i \cdot \hat{\Omega}_j \tag{1.9}$$

We see that the hamiltonian is essentially classical. The coherent state is a bridge between classical and quantum spins. The exact classical case is achieved in the limit $S \to \infty$, where the overlap of different coherent states vanishes.

The partition function of the spin model can be written as

$$\mathcal{Z} = \mathrm{Tr}[e^{-\beta \mathcal{H}}] = \lim_{N_\epsilon \to \infty} \mathrm{Tr} \prod_{n=0}^{N_\epsilon - 1} (1 - \epsilon \mathcal{H}(\tau_n)) \tag{1.10}$$

where $\epsilon = \beta / N_\epsilon$, and $\tau_n = n\epsilon$. We now insert resolutions of the identities, composed of coherent states, between the factors.

$$\mathcal{Z} = \lim_{N_\epsilon \to \infty} \left(\prod_{\tau=\epsilon}^{\beta} \int d\hat{\Omega}(\tau) \right) \prod_{\tau=\epsilon}^{\beta} \langle \hat{\Omega}(\tau) \, | \hat{\Omega}(\tau - \epsilon) \rangle \, [1 - \epsilon H(\tau)] \tag{1.11}$$

where $\hat{\Omega} = (\hat{\Omega}_1, \hat{\Omega}_2, ..., \hat{\Omega}_{\mathcal{N}})$ and we refer to H as the "classical hamiltonian".

$$H(\tau) = \frac{\langle \hat{\Omega}(\tau) | \, \mathcal{H} \, | \hat{\Omega}(\tau - \epsilon) \rangle}{\langle \hat{\Omega}(\tau) \, | \hat{\Omega}(\tau - \epsilon) \rangle} \simeq \langle \hat{\Omega}(\tau) | \, \mathcal{H} \, | \hat{\Omega}(\tau) \rangle + O(\epsilon) \tag{1.12}$$

The quantum effect is hidden in the overlap term, and we expand the overlap between coherent states at nearby timesteps to leading order in ϵ. This gives us the *Berry phase* term for a quantum spin.

$$\langle \hat{\Omega}(\tau) \, | \hat{\Omega}(\tau - \epsilon) \rangle = \exp \left(-iS\epsilon \sum_i \dot{\phi}_i \cos[\theta_i(\tau)] \right) \tag{1.13}$$

By exponentiating the expansion, the partition function can be written as

$$\mathcal{Z} = \int \mathcal{D}\hat{\Omega}(\tau) \exp \left(-\mathcal{S}[\hat{\Omega}] \right) \tag{1.14}$$

$$\mathcal{S} = iS \sum_{i=1}^{N} \omega[\hat{\Omega}_i] + \int_0^\beta d\tau J S^2 \sum_{i=1}^{\mathcal{N}} \hat{\Omega}_i(\tau) \cdot \hat{\Omega}_{i+1}(\tau) \tag{1.15}$$

The Berry phase term measures the solid angle enclosed by the orbit parametrized by $\theta(\tau)$ and $\phi(\tau)$. We can rewrite the Berry phase term as a Wess-Zumino-Witten (WZW) term at level-$2S$.

$$iS\omega[\hat{\Omega}] = iS \int_0^\beta d\tau \dot{\phi}(1 - \cos[\theta(\tau)]) = \frac{i2\pi(2S)}{4\pi} \int_0^\beta d\tau \int_0^1 du \epsilon_{abc} \hat{\Omega}^a \partial_\tau \hat{\Omega}^b \partial_u \hat{\Omega}^c \tag{1.16}$$

where we extend the definition of $\hat{\Omega}$ to another direction u with the boundary conditions:

$$\hat{\Omega}(\tau, u = 0) = (0, 0, 1), \quad \hat{\Omega}(\tau, u = 1) = \hat{\Omega}(\tau) \tag{1.17}$$

Thus far, we have translated the Heisenberg hamiltonian into the language of coherent state path integrals. Now, let us suppose we are considering a point in parameter space where the antiferromagnetic correlation length ξ is sufficiently long that we use a *continuum approximation* of the model. In this case, we parametrize the spins in the

following way.

$$\hat{\Omega}_i(\tau) = (-1)^i \boldsymbol{n}(x_i,\tau)\sqrt{1-(\boldsymbol{m}(x_i,\tau)/S)^2} + (\boldsymbol{m}(x_i,\tau)/S) \tag{1.18}$$

where $\boldsymbol{n}$ is the unimodular Neel order parameter ($\boldsymbol{n}\cdot\boldsymbol{n}=1$) and $\boldsymbol{m} \ll 1$ is the transverse canting field with the condition $\boldsymbol{n}\cdot\boldsymbol{m}=0$. $\boldsymbol{n}$ is a slowly varying field on the scale of the correlation length ξ. The canting field $\boldsymbol{m}$ can have fluctuation at shorter scales, and eventually we want to integrate out the canting field to get an effective theory of $\boldsymbol{n}$. Expanding the action with these two fields and taking the continuum limit, for the classical piece we get

$$\begin{aligned} JS^2\sum_{i=1}^{\mathcal{N}} \hat{\Omega}_i\cdot\hat{\Omega}_{i+1} &= \frac{JS^2}{2}\sum_{i=1}^{\mathcal{N}}(a^2(\partial_x\boldsymbol{n}(x_i,\tau))^2 + 4(\boldsymbol{m}(x_i,\tau)/S)^2 + O^3(\partial,\boldsymbol{m})) \\ &\simeq \frac{1}{2}\int dx\left(\rho_s(\partial_x\boldsymbol{n})^2 + \chi_\perp \boldsymbol{m}^2\right) \end{aligned} \tag{1.19}$$

where $\rho_s = JS^2a$, and $\chi_\perp = 4Ja^{-1}$. The Berry phase piece is a staggered sum of WZW terms. After taking the continuum limit and integrating over the u coordinate, the sum becomes a topological Θ-term for the Neel order parameter.

$$\begin{aligned} iS\sum_{i=1}^{\mathcal{N}}\int_0^\beta d\tau\int_0^1 du\,\epsilon_{abc}\hat{\Omega}_i^a\partial_\tau\hat{\Omega}_i^b\partial_u\hat{\Omega}_i^c &\simeq i\frac{S}{2}\int dxd\tau\epsilon_{abc}n^a\partial_x n^b\partial_\tau n^c \\ &+ a^{-1}\int dxd\tau\epsilon_{abc}m^a n^b\partial_\tau n^c + O^3(\partial,\boldsymbol{m}) \end{aligned} \tag{1.20}$$

We can then integrate out the canting field.

$$\mathcal{Z} = \int \mathcal{D}[\boldsymbol{n}]\mathcal{D}[\boldsymbol{m}]e^{-\mathcal{S}[\boldsymbol{n},\boldsymbol{m}]} = \int \mathcal{D}[\boldsymbol{n}]e^{-\mathcal{S}_{NL\sigma M}[\boldsymbol{n}]} \tag{1.21}$$

The low energy effective field theory written in terms of the Neel parameter $\boldsymbol{n}$ is an $O(3)$

non-linear σ-model (NLσM) with topological Θ-term at $\Theta = 2\pi S$.

$$\mathcal{S}_{NL\sigma M} = \int dx d\tau \left(\frac{a^{-2}}{2\chi_\perp} (\partial_\tau \boldsymbol{n})^2 + \frac{1}{2}\rho_s (\partial_x \boldsymbol{n})^2 + \frac{i2\pi S}{4\pi} \epsilon_{abc} n^a \partial_x n^b \partial_\tau n^c \right) \tag{1.22}$$

We can read off the velocity of $\boldsymbol{n}$ field $v = (\chi_\perp \rho_s / a^{-2})^{1/2} = 2JSa$. After rescaling $\tau \to v\tau$, we get the effective field theory in a clean form

$$\mathcal{S}_{NL\sigma M} = \int dx d\tau \frac{1}{g} (\partial_\mu \boldsymbol{n})^2 + \frac{i2\pi S}{4\pi} \epsilon_{abc} n^a \partial_x n^b \partial_\tau n^c \tag{1.23}$$

where $g = 4/S$ is a dimensionless coupling constant.

Let us consider the physics behind the topological Θ-term. We want to impose the boundary condition that the action is finite after integrating over space-time. This requires that the order parameter $\boldsymbol{n}$ becomes a constant vector at space-time infinity. With this boundary condition, topologically the space-time manifold is isomorphic to a two-sphere S^2. We call the space-time manifold as the base manifold. The field configuration, $\boldsymbol{n}(x, \tau)$, is a smooth map from the base manifold, S^2, to the target manifold, $\mathcal{M} = S^2$, which is the manifold for the order parameters. The Θ-term measures the topological index, or Pontryagin index to be precise, for this mapping. Physically, it counts how many instanton configurations there are in the $2D$ Euclidean space-time. The Θ-term gives a phase additional factor of $e^{i2\pi S}$ to each instanton configuration in the path integral.

More mathmatically, the Pontryagin index is classified by the homotopy group.

$$\pi_2(S^2) = \mathbb{Z} \tag{1.24}$$

Having a non-trivial homotopy group for the target manifold is the necessary condition for having an instanton configuration. In other words, for manifolds with trivial homotopy groups, we can write down similar topological terms, but it always gives zero after

integrating over the space-time.

If we put the Θ-term with $\Theta = 2\pi S$ on a manifold with spatial boundaries, then the Θ-term can be reduced to the boundary WZW terms with level-S.

$$\begin{aligned}\int_0^L dx \int d\tau \frac{i2\pi S}{4\pi} \epsilon_{abc} n^a \partial_x n^b \partial_\tau n^c &= \int_0^1 du \int d\tau \frac{i2\pi S}{4\pi} \epsilon_{abc} n_L^a \partial_u n_L^b \partial_\tau n_L^c \\ &- \int_0^1 du \int d\tau \frac{i2\pi S}{4\pi} \epsilon_{abc} n_0^a \partial_u n_0^b \partial_\tau n_0^c \end{aligned} \quad (1.25)$$

As we derived in Eq. (1.16), a spin-S degree of freedom will have a Berry's phase of WZW terms at level-$2S$, so the boundary of the Θ-term at $\Theta = 2\pi S$ describes a spin-$S/2$. This agrees with the AKLT construction, which states that the boundary of spin-1 chain hosts a spin-$\frac{1}{2}$. Therefore, the $O(3)$ NLσM with Θ-term captures the key physics of the $1d$ SPT phase. In chapter 2 we further analyse the NLσM and their generalizations to higher dimensions, and make connections to bosonic SPT phases.

1.4 Outline

Continuous field theories are descriptions of the low energy degrees of freedom in the long wavelength limit. Many microscopic details of the system are washed out in the continuum limit, so the field theory accurately captures the universal properties of the system. Therefore, we use lots of field theoretical methods to study the properties of symmetry protected topological phases in this dissertation.

In chapter 2, we show that generalized non-linear σ-models with topological Θ-term are good field theory descriptions of bosonic symmetry protected topological phases. Based on the general formalism, we provide a new classification scheme for bosonic symmetry protected topological phases. This chapter is mostly based on *Phys. Rev. B* ***91****, 134404 (2015)* and *Phys. Rev. B* ***91****, 184404 (2015).*

In chapter 3, we investigate some bulk properties of SPT phases. The first part is about gauging the symmetry of a SPT phase. It has been shown that introducing gauge field is an effective theoretical tool to detect the SPT state. We study the gauging procedure in $2d$ and $3d$ bosonic SPT states with non-linear σ-model description and discuss various exotic statistical properties of gauge fluxes in the bulk SPT. This section is mostly based on *Phys. Rev. B* ***90****, 081110 (2014).* In the second part we propose a new numerical quantity, the strange correlator, that can distinguish topological phases by their bulk wavefunction. We test the strange correlator on a number of model systems including some strongly interacting SPT states. This section is mostly based on *Phys. Rev. Lett.* ***112****, 247202 (2014).*

In chapter 4, we discuss various surface states of SPT phases. In the first section we studied an exotic phase transition between the superfluid phase and topological order on the surface of $3d$ topological insulators. We design a new large-k expansion method, which when combined with the newly developed fermion-vortex duality enables us to perform a controlled renormalization group study of the critical point. This part is based on *Phys. Rev. B* ***94****, 024433 (2016).* The second part is about the surface state of a certain class of $3d$ bosonic SPT state. We develop techniques to carry out controlled renormalization group studies of a NLσM with WZW term in $(2+1)d$. As a result, we find a new quantum disordered fixed point that describes a new strongly interacting conformal field theory. This work is based on *arXiv:1605.05336.* In the third part, a general connection between Lieb-Schultz-Mattis (LSM) theorem and the surface of symmetry protected topological phases is pointed out. We focus on $SU(N)$ and $SO(N)$ spin system in $1d$, $2d$ and $3d$. From the SPT perspective, we are able to get new generalized LSM theorems. This part of our discussion is based on *arXiv:1705.00012.*

In chapter 5, we proposed an experimental realization of bosonic SPT states. The key observation is that bosonic SPT can be built from interacting fermionic SPTs. This

connection is discussed in the first section, and it is based on *New J. Phys.* ***17****, 075010 (2015)*. In the second section, we layout an experimental proposal to realize bosonic SPT in bilayer graphene system. Experimental signatures for bosonic SPT states are predicted in *Phys. Rev. Lett.* ***118****, 126801 (2017)*. Finally, the third part is a careful theoretical study of the bilayer model, in which we discover a multi-layer generalization to realize bosonic SPT with $Sp(N)$ symmetry (*Phys. Rev. B* ***93****, 125101 (2016)*).

Chapter 2

Nonlinear σ-Model Formalism for Bosonic Symmetry Protected Topological Phases

In this chapter, the content is reprinted with permission from Zhen Bi, Alex Rasmussen, Kevin Slagle, and Cenke Xu, authors of *Phys. Rev. B* ***91****, 134404 (2015)* [21] and *Phys. Rev. B* ***91****, 184404 (2015)* [22]. Copyright by the American Physical Society.

The concept of SPT phase was pioneered by Wen and his colleagues. A rather complete periodic table for free fermion SPTs was obtained through the method of K-theory[23] and also by mapping the boundary of the SPT state to Anderson localization problem[24]. A mathematical paradigm for bosonic SPT phases was developed by Wen's group in Ref. [25, 26] that systematically classified bosonic SPT phases based on the group cohomology of their symmetry G. But this abstract approach was unable to reveal all the physical properties of the SPT phases. In the last few years, SPT phase has rapidly developed into a very active and exciting field [25, 26, 27, 28, 29, 30, 31, 32, 33, 34, 35, 36, 37, 38, 39, 40, 41, 42], and besides the general mathematical classification, other

approaches of understanding SPT phases were also taken. In $2d$, it was demonstrated that the SPT phases can be thoroughly classified by the Chern-Simons field theory [31], although it is unclear how to generalize this approach to $3d$. Nonlinear σ-model (NLσM) field theories were also used to describe some SPT phases in $3d$ and $2d$ [33, 32, 34], but a complete classification based on this field theory is still demanded.

The goal of this chapter is to systematically classify and describe bosonic SPT phases with various continuous and discrete symmetries in *all dimensions*, using semiclassical NLσM field theories. At least in one dimensional systems, semiclassical NLσMs have been proved successful in describing SPT phases. The O(3) NLσM plus a topological $\Theta-$term describes a spin-1 Heisenberg chain when $\Theta = 2\pi$:

$$\mathcal{S}_{1d} = \int dxd\tau \frac{1}{g}(\partial_\mu \boldsymbol{n})^2 + \frac{i2\pi}{4\pi}\epsilon_{abc} n^a \partial_x n^b \partial_\tau n^c, \tag{2.1}$$

and it is well-known that the spin-1 antiferromagnetic Heisenberg model is a SPT phase with 2-fold degeneracy at each boundary [15, 16, 17, 43, 44, 45].

In this chapter we will discuss SPT phases with symmetry Z_2^T, Z_2, $Z_2 \times Z_2$, $Z_2 \times Z_2^T$, $U(1)$, $U(1) \times Z_2$, $U(1) \rtimes Z_2$, $U(1) \times Z_2^T$, $U(1) \rtimes Z_2^T$, Z_m, $Z_m \times Z_2$, $Z_m \rtimes Z_2$, $Z_m \times Z_2^T$, $Z_m \rtimes Z_2^T$, $SO(3)$, $SO(3) \times Z_2^T$, $Z_2 \times Z_2 \times Z_2$. Here we use the standard notation: Z_2^T stands for time-reversal symmetry, $G \times Z_2^T$ and $G \rtimes Z_2^T$ stand for direct and semidirect product between unitary group G and time-reversal symmetry. A semidirect product between two groups means that these two group actions do not commute with each other. More details will be explained when we discuss the classification of these states. We will demonstrate that a $d-$dimensional SPT phase with any symmetry mentioned above can always be described by an O$(d+2)$ NLσM in $(d+1)$-dimensional space-time, namely all the $1d$ SPT phases discussed in this paper can be described by Eq. (2.1), all

the $2d$ and $3d$ SPT phases can be described by the following two field theories:

$$\mathcal{S}_{2d} = \int d^2x d\tau \ \frac{1}{g}(\partial_\mu \boldsymbol{n})^2 + \frac{i2\pi k}{\Omega_3}\epsilon_{abcd} n^a \partial_\tau n^b \partial_x n^c \partial_y n^d, \tag{2.2}$$

$$\mathcal{S}_{3d} = \int d^3x d\tau \ \frac{1}{g}(\partial_\mu \boldsymbol{n})^2 + \frac{i2\pi}{\Omega_4}\epsilon_{abcde} n^a \partial_\tau n^b \partial_x n^c \partial_y n^d \partial_z n^e, \tag{2.3}$$

The $\mathrm{O}(d+2)$ vector is a Landau order parameter with a unit length constraint: $|\boldsymbol{n}| = 1$. Ω_d is the surface area of a $d-$dimensional unit sphere. The $2d$ action Eq. (2.2) has a level-k in front of its Θ-term, whose reason will be explained later. Different SPT phases in the same dimension are distinguished by the transformation of the $\mathrm{O}(d+2)$ vector under the symmetry. The classification of SPT phases on a d-dimensional lattice is given by all the *independent* symmetry transformations of $\boldsymbol{n}$ that keep the entire Lagrangian (including the Θ-term) invariant. This classification rule will be further clarified in the next section.

An $\mathrm{O}(d+2)$ NLσM can support maximally $\mathrm{O}(d+2)$ symmetry and other discrete symmetries such as time-reversal. We choose the 17 symmetries listed above, because they can all be embedded into the maximal symmetry of the field theory, and they are the most physically relevant symmetries. Of course, if we want to study an SPT phase with a large Lie group such as SU(N), the above field theories need to be generalized to NLσM defined with a symmetric space of that Lie group. But for all these physically relevant symmetries, our NLσM is already sufficient.

In principle, a NLσM describes a system with a long correlation length. Thus a NLσM plus a Θ-term most precisely describes a SPT phase tuned *close to* a critical point (but still in the SPT phase). When a SPT phase is tuned close to a critical point, the NLσM not only describes its topological properties (*e.g.* edge states *etc.*), but also describes its

dynamics, for example excitation spectrum above the energy gap (much smaller than the ultraviolet cut-off). When the system is tuned deep inside the SPT phase, namely the correlation length is comparable with the lattice constant, this NLσM can no longer describe its dynamics accurately, but since the topological properties of this SPT phase is unchanged while tuning, these topological properties (like edge states) can still be described by the NLσM. The NLσM is an effective method of describing the universal topological properties, as long as we ignore the extra nonuniversal information about dynamics, such as the exact dispersion of excitations, which depends on the details of the lattice Hamiltonian and hence is not universal.

Besides the classification, our NLσMs in all dimensions can tell us explicit physical information about this SPT phase. For example, the boundary states of $1d$ SPT phases can be obtained by explicitly solving the field theory reduced to the $0d$ boundary. The boundary of a $3d$ SPT phase could be a $2d$ topological phase, and the NLσMs can tell us the quantum number of the anyons of the boundary topological phases. The boundary topological phases of $3d$ SPT phases with $U(1)$ and time-reversal symmetry were discussed in Ref. [32]. We will analyze the boundary topological phases for some other $3d$ SPT phases in the current paper.

Our formalism not only can study each individual SPT phase, it also reveals the relation between different SPT phases. For example, using our formalism we are able to show that there is a very intriguing relation between SPT phases with $U(1) \times (\rtimes)G$ symmetry and SPT phases with $Z_m \times (\rtimes)G$ symmetry, where G is another discrete group such as Z_2, Z_2^T. Our formalism demonstrates that after breaking $U(1)$ to Z_m, whether the SPT phase survives or not depends on the parity of integer m. We also demonstrate that when m is an even number, we can construct some extra SPT phases with $Z_m \times (\rtimes)G$ symmetry that *cannot* be deduced from SPT phases with $U(1) \times (\rtimes)G$ symmetry by breaking $U(1)$ down to Z_m. Our field theory also gives many of these SPT states a

natural "decorated defect" construction, which will be discussed in more detail in the next section.

In this chapter, we first discuss SPT states within cohomology. It is now understood that the group cohomology classification is incomplete, and in each dimension there are a few examples beyond cohomology classification [46, 47, 48]. These beyond-cohomology states all involve gravitational anomalies [49] or mixed gauge-gravitational anomalies [48]. In the last section of this chapter, we will describe a generalization of our field theory to the cases that are beyond group cohomology classification.

2.1 Strategy and Clarification

2.1.1 Edge states of NLσMs with Θ-term

In d-dimensional theories Eq. (2.1),2.2 and 2.3 (d denotes the spatial dimension), when $\Theta = 2\pi$, their boundaries are described by $(d-1)+1$-dimensional O$(d+2)$ NLσMs with a Wess-Zumino-Witten (WZW) term at level-1. When $d = 1$, the boundary of Eq. (2.1) with $\Theta = 2\pi$ is a $0+1d$ O(3) NLσM with a Wess-Zumino-Witten term at level $k = 1$ [45]:

$$\mathcal{S}_b = \int d\tau \frac{1}{g}(\partial_\tau \boldsymbol{n})^2 + \int d\tau du \frac{i2\pi}{8\pi}\epsilon_{abc}\epsilon_{\mu\nu} n^a \partial_\mu n^b \partial_\nu n^c. \tag{2.4}$$

The WZW term involves an extension of $\boldsymbol{n}(\tau)$ to $\boldsymbol{n}(\tau, u)$:

$$\boldsymbol{n}(\tau, 0) = (0, 0, 1), \quad \boldsymbol{n}(\tau, 1) = \boldsymbol{n}(\tau). \tag{2.5}$$

The boundary action $\mathcal{S}_b$ describes a point particle moving on a sphere S^2, with a 2π magnetic flux through the sphere. The ground state of this single particle quantum mechanics problem is two fold degenerate. The two fold degenerate ground states have

the following wave functions on the unit sphere:

$$U = (\cos(\theta/2)e^{i\phi/2}, \ \ \sin(\theta/2)e^{-i\phi/2})^t,$$

$$\boldsymbol{n} = (\sin(\theta)\cos(\phi), \sin(\theta)\sin(\phi), \cos(\theta)) \,. \tag{2.6}$$

The boundary doublet U transforms projectively under symmetry of the SPT phase, and its transformation can be derived explicitly from the transformation of $\boldsymbol{n}$. For example if $\boldsymbol{n}$ transforms as $\boldsymbol{n} \to -\boldsymbol{n}$ under time-reversal, then this implies that under time-reversal $\phi \to \phi$, $\theta \to \pi + \theta$, and $U \to i\sigma^y U$.

When $d = 2$, the boundary is a 1+1-dimensional O(4) NLσM with a WZW term at level $k = 1$, and it is well-known that this theory is a gapless conformal field theory if the system has a full O(4) symmetry [50, 51]. The 1d boundary could be gapped but still degenerate if the symmetry of $\boldsymbol{n}$ is discrete (the degeneracy corresponds to spontaneous discrete symmetry breaking); when $d = 3$, the boundary is a $2 + 1d$ O(5) NLσM with a WZW at level $k = 1$, which can be reduced to a $2+1d$ O(4) NLσM with $\Theta = \pi$ after the fifth component of $\boldsymbol{n}$ is integrated out [32]. This $2+1d$ boundary theory should either be gapless or degenerate, and one particularly interesting possibility is that it can become a topological order, which will be discussed in more detail in section IIF. Starting with this topological order, we can prove that this $2 + 1d$ boundary system cannot be gapped without degeneracy.

All components of $\boldsymbol{n}$ in Eq. (2.1),2.2 and 2.3 must have a nontrivial transformation under the symmetry group G, namely it is not allowed to turn on a linear "Zeeman" term that polarizes any component of $\boldsymbol{n}$. Otherwise the edge states can be trivially gapped, and the bulk Θ-term plays no role.

2.1.2 Phase diagram of NLσMs with a Θ-term

In our classification, the NLσM including its Θ-term is invariant under the symmetry of the SPT phase, for arbitrary value of Θ. For special values of Θ, such as $\Theta = k\pi$ with integer k, some extra discrete symmetry may emerge, but these symmetries are *unimportant* to the SPT phase. However, these extra symmetries guarantee that $\Theta = k\pi$ is a fixed point under renormalization group (RG) flow. In $1+1d$ NLσMs, the RG flow of Θ was calculated explicitly in Ref. [52, 53] and it was shown that $\Theta = 2\pi k$ are stable fixed points, while $\Theta = (2k+1)\pi$ are instable fixed points, which correspond to phase transitions; in higher dimensions, similar explicit calculations are possible, but for our purposes, we just need to argue that $\Theta = 2\pi k$ are stable fixed points under RG flow. The bulk spectrum of the NLσM with $\Theta = 2\pi k$ is identical to the case with $\Theta = 0$: in the quantum disordered phase the bulk of the system is fully gapped without degeneracy. Now if Θ is tuned away from $2\pi k$: $\Theta = 2\pi k \pm \epsilon$, this perturbation cannot close the bulk gap, and since the essential symmetry of the SPT phase is unchanged, the SPT phase including its edge states should be stable against this perturbation. Thus a SPT phase corresponds to a finite phase $\Theta \in (2\pi k - \delta_1, 2\pi k + \delta_2)$ in the phase diagram.

There is a major difference between Θ-term in NLσM and the Θ-term in the response action of the external gauge field. In our description, a SPT phase corresponds to the entire phase whose stable fixed point is at $\Theta = 2\pi$ (or $2\pi k$ with integer k). Tuning slightly away from these stable fixed points will not break any essential symmetry that protects the SPT state, and hence it does not change the main physics. The theory will always flow back to these stable fixed points under RG (this RG flow was computed explicitly in $1+1d$ in Ref. [52, 53], and a similar RG flow was proposed for higher dimensional cases [54]). The Θ-term of the external gauge field after integrating out the matter fields is protected by the symmetry of the SPT phase to be certain discrete value. For example

$\Theta = \pi$ for the ordinary 3d topological insulator [55, 56] is protected by time-reversal symmetry. Tuning Θ away from π will necessarily break the time-reversal symmetry.

2.1.3 $\mathbb{Z}_k$ or $\mathbb{Z}$ classification?

In the classification table in Ref. [25, 26], one can see that in even dimensions, there are many SPT states with $\mathbb{Z}$ classifications, but in odd dimensions, $\mathbb{Z}$ classification never appears. This fact was a consequence of mathematical calculations in Ref. [25, 26], but in this section we will give a very simple explanation based on our field theories.

The manifold of O$(d+2)$ NLσM is S^{d+1}, which has a Θ-term in $(d+1)-$dimensional space-time due to homotopy group $\pi_{d+1}[S^{d+1}] = \mathbb{Z}$. However, this does *not* mean that the $\Theta-$term will always give us $\mathbb{Z}$ classification, because more often than not we can show that $\Theta = 0$ and $\Theta = 2\pi k$ with certain nonzero integer k can be connected to each other without any bulk transition.

For example, let us couple two Haldane phases to each other:

$$\mathcal{S}_{coupled} = \int dx d\tau \frac{1}{g}(\partial_\mu \boldsymbol{n}^{(1)})^2 + \frac{i2\pi}{8\pi}\epsilon_{abc}\epsilon_{\mu\nu} n_a^{(1)} \partial_\mu n_b^{(1)} \partial_\nu n_c^{(1)} + (1 \to 2) + A(\boldsymbol{n}^{(1)} \cdot \boldsymbol{n}^{(2)}). \quad (2.7)$$

When $A < 0$, effectively $\boldsymbol{n}^{(1)} = \boldsymbol{n}^{(2)} = \boldsymbol{n}$, then the system is effectively described by one O(3) NLσM with $\Theta = 4\pi$; while when $A > 0$, effectively $\boldsymbol{n}^{(1)} = -\boldsymbol{n}^{(2)} = \boldsymbol{n}$, the effective NL$\sigma$M for the system has $\Theta = 0$. When parameter A is tuned from negative to positive, the bulk gap does not close. The reason is that, since $\Theta = 2\pi$ in both Haldane phases, the Θ-term does not affect the bulk spectrum at all. To analyze the bulk spectrum (and bulk phase transition) while tuning A, we can just ignore the Θ-term. Without the Θ-term, both theories are just trivial gapped phases, and an inter-chain coupling can not qualitatively change the bulk spectrum unless it is strong enough to overcome the bulk gap in each chain. We have explicitly checked this phase diagram using a Monte Carlo

simulation of two coupled O(3) NLσMs, and the result is exactly the same as what we would expect from the argument above. Thus the theory with $\Theta = 4\pi$ and $\Theta = 0$ are equivalent.

By contrast, if we couple two chains with $\Theta = \pi$ each, then the cases $A > 0$ and < 0 correspond to effective $\Theta = 0$ and 2π respectively, and these two limits are separated by a bulk phase transition point $A = 0$, when the system becomes two decoupled chains with $\Theta = \pi$ each. And it is well-known that a $1 + 1d$ O(3) NLσM with $\Theta = \pi$ is the effective field theory that describes a spin-$\frac{1}{2}$ chain [15, 16], and according to the Lieb-Shultz-Matthis theorem, this theory must be either gapless or degenerate [57]. This conclusion is consistent with the RG calculation in Ref. [52, 53], and a general nonperturbative argument in Ref. [54].

In fact when $\Theta = 4\pi$ the boundary state of Eq. (2.1) is a spin-1 triplet, and by tuning A, at the boundary there is a level crossing between triplet and singlet, while there is no bulk transition. This analysis implies that with SO(3) symmetry, $1d$ spin systems have two different classes: there is a trivial class with $\Theta = 4\pi k$, and a nontrivial Haldane class with $\Theta = (4k + 2)\pi$.

If we cannot connect $\Theta = 4\pi$ to $\Theta = 0$ without closing the bulk gap, then the classification would be bigger than $\mathbb{Z}_2$. For example, let us consider the 2d SPT phase with U(1) symmetry which was first studied in Ref. [28]. This phase is described by Eq. (2.2). $B \sim n_1 + in_2$ and $B' \sim n_3 + in_4$ ($n_1 \cdots n_4$ are the four components of O(4) vector $\boldsymbol{n}$ in Eq. (2.2)) are two complex boson (rotor) fields that transform identically under the global $U(1)$ symmetry. Now suppose we couple two copies of this systems together through symmetry allowed interactions:

$$\mathcal{S}_{coupled} = \mathcal{S}_1 + \mathcal{S}_2 + A_1 B_1 B_2^\dagger + A_2 B_1 B_2'^\dagger + A_3 B_1' B_2^\dagger + A_4 B_1' B_2'^\dagger + H.c. \tag{2.8}$$

No matter how we tune the parameters A_i, the resulting effective NLσM *always* has $\Theta = 4\pi$ instead of $\Theta = 0$ (this is simply because $(-1)^2 = (-1)^4 = +1$). This implies that we cannot smoothly connect $\Theta = 4\pi$ to 0 without any bulk transition. Thus the classification of 2d SPT phases with $U(1)$ symmetry is $\mathbb{Z}$ instead of $\mathbb{Z}_2$. This is why in $2d$ (and all even dimensions), many SPT states have $\mathbb{Z}$ classification, while in odd dimensions there is no $\mathbb{Z}$ classification at all, namely all the nontrivial SPT phases in odd dimensions correspond to $\Theta = 2\pi$. Thus in Eq. (2.2) we added a level-k in the Θ-term.

2.1.4 NLσM and "decorated defect" construction of SPT states

Ref. [38] has given us a physical construction of some of the SPT states in terms of the "decorated domain wall" picture. For example, one of the $3d$ $Z_2^A \times Z_2^B$ SPT state can be constructed as follows: we first break the Z_2^B symmetry, then restore the Z_2^B symmetry by proliferating the domain wall of Z_2^B, and each Z_2^B domain wall is decorated with a $2d$ SPT state with Z_2^A symmetry. This state is described by Eq. (2.3) with transformation

$$\begin{aligned} Z_2^B &: \ n_{1,2} \to -n_{1,2}, \quad n_a \to n_a (a = 3, 4, 5); \\ Z_2^A &: \ n_1, \to n_1, \quad n_a \to -n_a (a = 2, \cdots 5). \end{aligned} \tag{2.9}$$

Here n_i is the ith component of vector $\boldsymbol{n}$. To visualize the "decorated domain" wall picture, we can literally make a domain wall of n_1, and consider the following configuration of vector $\boldsymbol{n}$: $\boldsymbol{n} = (\cos\theta, \sin\theta N_2, \sin\theta N_3, \sin\theta N_4, \sin\theta N_5)$, where $\boldsymbol{N}$ is a O(4) vector with unit length, and θ is a function of coordinate z only:

$$\theta(z = +\infty) = \pi, \quad \theta(z = -\infty) = 0. \tag{2.10}$$

Plug this parametrization of $\boldsymbol{n}$ into Eq. (2.3), and integrate along z direction, the $\Theta-$term in Eq. (2.3) precisely reduces to the $\Theta-$term in Eq. (2.2) with $k = 1$, and the O(4) vector $\boldsymbol{n} = \boldsymbol{N}$. This is precisely the $2d$ SPT with Z_2 symmetry. This implies that the Z_2^B domain wall is decorated with a $2d$ SPT state with Z_2^A symmetry.

Many SPT states can be constructed with this decorated domain wall picture. Some $3d$ SPT states can also be understood as "decorated vortex", which was first discussed in [32]. This state has $U(1) \times Z_2^T$ symmetry, and the vector $\boldsymbol{n}$ transforms as

$$\begin{aligned} U(1) \quad &: \quad (n_1 + in_2) \to (n_1 + in_2)e^{i\theta}, \quad n_{3,4,5} \to n_{3,4,5}, \\ Z_2^T \quad &: \quad \boldsymbol{n} \to -\boldsymbol{n}. \end{aligned} \tag{2.11}$$

If we make a vortex of the $U(1)$ order parameter (n_1, n_2), Eq. (2.3) reduces to Eq. (2.1) with O(3) order parameter (n_3, n_4, n_5). Thus this SPT can be viewed as decorating the $U(1)$ vortex with a $1d$ Haldane phase, and then proliferating the vortices.

2.1.5 Independent NLσMs

Let us take the example of $1d$ SPT phases with $Z_2 \times Z_2^T$ symmetry. As we claimed, all $1d$ SPT phases in this paper are described by the same NLσM Eq. (2.1). With $Z_2 \times Z_2^T$ symmetry, there seems to be three different ways of assigning transformations to $\boldsymbol{n}$ that make the entire Lagrangian invariant:

$$(1) \quad : \quad Z_2 : \boldsymbol{n} \to \boldsymbol{n}, \quad Z_2^T : \boldsymbol{n} \to -\boldsymbol{n}.$$

$$(2) \quad : \quad Z_2 : n_{1,2} \to -n_{1,2}, \quad n_3 \to n_3$$

$$Z_2^T : \boldsymbol{n} \to -\boldsymbol{n}$$

$$(3) \quad : \quad Z_2 : n_{1,2} \to -n_{1,2}, \quad n_3 \to n_3$$

$$Z_2^T : n_3 \to -n_3, \quad n_{1,2} \to n_{1,2}. \tag{2.12}$$

However the NLσMs defined with these three different transformations are not totally independent from each other. Let us parameterize the O(3) vectors $\boldsymbol{n}^{(i)}$ with transformations (1), (2) and (3) as:

$$\boldsymbol{n}^{(i)}(\boldsymbol{r}) = (n_1^{(i)}, n_2^{(i)}, n_3^{(i)}) = \left(\sin(\theta_{\boldsymbol{r}}^{(i)})\cos(\phi_{\boldsymbol{r}}^{(i)}), \sin(\theta_{\boldsymbol{r}}^{(i)})\sin(\phi_{\boldsymbol{r}}^{(i)}), \cos(\theta_{\boldsymbol{r}}^{(i)})\right), \tag{2.13}$$

$\phi_{\boldsymbol{r}}^{(i)}$ and $\theta_{\boldsymbol{r}}^{(i)}$ are functions of space-time. Under Z_2 and Z_2^T symmetry, $\theta^{(i)}$ and $\phi^{(i)}$ transform as

$$Z_2 \quad : \quad \theta^{(i)} \to \theta^{(i)},$$

$$\phi^{(1)} \to \phi^{(1)}, \quad \phi^{(i)} \to \phi^{(i)} + \pi, \ (i = 2, 3);$$

$$Z_2^T \quad : \quad \theta^{(i)} \to \pi - \theta^{(i)},$$

$$\phi^{(i)} \to \phi^{(i)} + \pi, \ (i = 1, 2), \quad \phi^{(3)} \to \phi^{(3)}. \tag{2.14}$$

First of all, since $\theta^{(i)}$ have the same transformation for all i, we can turn on strong coupling between the three NLσMs to make $\theta^{(1)} = \theta^{(2)} = \theta^{(3)} = \theta$. Now we can construct

$\boldsymbol{n}^{(3)}$ using the parametrization of $\boldsymbol{n}^{(1)}$ and $\boldsymbol{n}^{(2)}$:

$$\begin{aligned} n_1^{(3)} &= \sin(\theta)\cos(\phi^{(1)}+\phi^{(2)}), \\ n_2^{(3)} &= \sin(\theta)\sin(\phi^{(1)}+\phi^{(2)}), \\ n_3^{(3)} &= \cos(\theta). \end{aligned} \tag{2.15}$$

It is straightforward to prove that $\boldsymbol{n}^{(3)}$ defined this way transforms identically with the case (3) in Eq. (2.12), also the topological number of $\boldsymbol{n}^{(3)}$ in $1+1d$ space-time is the sum of topological numbers of $\boldsymbol{n}^{(1)}$ and $\boldsymbol{n}^{(2)}$. More explicitly, an instanton of $\boldsymbol{n}^{(a)}$ is a domain wall of $n_3^{(a)}$ decorated with a vortex of $\phi^{(a)}$. As we explained above, with appropriate coupling between these vectors, we can make $\theta^{(1)}=\theta^{(2)}=\theta^{(3)}=\theta$, and $\phi^{(3)}=\phi^{(1)}+\phi^{(2)}$. Thus a domain wall of $n_3^{(3)}$ is also a domain wall of $n_3^{(1)}$ and $n_3^{(2)}$, while the vortex number of $\phi^{(3)}$ is the sum of vortex number of $\phi^{(1)}$ and $\phi^{(2)}$. Thus the Θ-term of $\boldsymbol{n}^{(3)}$ reduces to the sum of $\Theta-$terms of $\boldsymbol{n}^{(1)}$ and $\boldsymbol{n}^{(2)}$. In this example we have shown that NLσMs (1) and (2) in Eq. (2.12) can "merge" into NLσM (3). Thus the three NLσMs defined with transformations (1), (2) and (3) are not independent from each other. [1] The consequence of this analysis is that if all three theories exist in one system, although each theory is a nontrivial SPT phase individually, we can turn on some symmetry allowed couplings between these NLσMs and cancel the bulk topological terms completely, and drive the entire coupled system to a trivial state.

Also, for either NLσM (1) or (2) in Eq. (2.12), we can show that $\Theta^{(i)}=0$ and 4π can be connected to each other without a bulk transition (using the same method as

[1] The "merging" argument is usually easy to implement for systems with simple symmetries, but we should admit that for higher dimensions and complicated symmetries, the "merging" argument can become rather involved.

the previous subsection). Then eventually the $1d$ SPT phase with $Z_2 \times Z_2^T$ symmetry is parametrized by two independent Θ-terms, the fixed point values of $\Theta^{(1)}$ and $\Theta^{(2)}$ can be either 0 or 2π, thus this SPT phase has a $(\mathbb{Z}_2)^2$ classification, which is consistent with the classification using group cohomology. NLσMs with transformations (1), (2) are two "root phases" of $1d$ SPT phases with $Z_2 \times Z_2^T$ symmetry. All the other SPT phases can be constructed with these two root phases.

For most SPT phases, we can construct the NLσMs using the smallest representation (fundamental representation) of the symmetry groups G, because usually (but not always!) NLσMs constructed using higher representations can reduce to constructions with the fundamental representation with a different Θ. For example, the $1d$ SPT phase with $U(1) \rtimes Z_2$ symmetry can be described by Eq. (2.1) with the following transformation

$$\begin{aligned} U(1) \quad &: \quad (n_1 + in_2) \to e^{i\theta}(n_1 + in_2), \quad n_3 \to n_3, \\ Z_2 \quad &: \quad n_1 \to n_1, \quad n_{2,3} \to -n_{2,3}, \end{aligned} \tag{2.16}$$

namely $B \sim (n_1 + in_2)$ is a charge-1 boson under the $U(1)$ rotation, and the edge state of this SPT phase carries charge-1/2 of boson B. We can also construct an O(3) NLσM using charge-2 boson $B' \sim (n_1' + in_2') \sim (n_1 + in_2)^2$ that transforms as $B' \to B' e^{2i\alpha}$, then mathematically we can demonstrate that the NLσM with $\Theta = 2\pi$ for order parameter $\boldsymbol{n}' = (n_1', n_2', n_3)$ reduces to a NLσM of $\boldsymbol{n}$ with $\Theta = 4\pi$, hence it is a trivial phase.

More explicitly, let us take unit vector $\boldsymbol{n} = (\sin(\theta)\cos(\phi), \sin(\theta)\sin(\phi), \cos(\theta))$, and vector $\boldsymbol{n}' = (\sin(\theta)\cos(2\phi), \sin(\theta)\sin(2\phi), \cos(\theta))$, then we can show that when $\boldsymbol{n}$ has topological number 1 in $1+1d$ space-time, $\boldsymbol{n}'$ would have topological number 2. This means that if there is a $\Theta-$term for $\boldsymbol{n}'$ with $\Theta = 2\pi$, it is equivalent to a $\Theta-$term for $\boldsymbol{n}$ with $\Theta = 4\pi$.

Physically, the edge state of NLσM of $\boldsymbol{n}'$ with $\Theta = 2\pi$ carries a half-charge of B', which is still a charge-1 object, so it can be screened by another charge-1 boson B. Hence in this case NLσM constructed using charge-2 boson B' would be trivial.

However, later we will also show that when the symmetry group involves Z_m with even integer $m > 2$, then using higher representations of Z_m we can construct SPT phases that *cannot* be obtained from the fundamental representation of Z_m.

2.1.6 Boundary topological order of 3d SPT phases

The $(d-1)$-dimensional boundary of a d-dimensional SPT phase must be either degenerate or gapless. When $d = 3$, its $2d$ boundary can spontaneously break the symmetry, or have a topological order [32]. We can use the bulk field theory Eq. (2.3) to derive the quantum numbers of the anyons at the boundary.

Let us take the $3d$ SPT phase with $Z_2 \times Z_2^T$ symmetry as an example. One of the SPT phases has the following transformations:

$$\begin{aligned} Z_2 &: \ n_a \to -n_a (a = 1, \cdots 4), \quad n_5 \to n_5; \\ Z_2^T &: \ \boldsymbol{n} \to -\boldsymbol{n}. \end{aligned} \tag{2.17}$$

The $2+1d$ boundary of the system is described by a $2+1d$ O(5) NLσM with a Wess-Zumino-Witten (WZW) term at level $k = 1$:

$$\mathcal{S}_b = \int d^2x d\tau \ \frac{1}{g}(\partial_\mu \boldsymbol{n})^2 + \int_0^1 du \ \frac{i2\pi}{\Omega_4} \epsilon_{abcde} n^a \partial_x n^b \partial_y n^c \partial_z n^d \partial_\tau n^e, \tag{2.18}$$

where $\boldsymbol{n}(x, \tau, u)$ satisfies $\boldsymbol{n}(x, \tau, 0) = (0, 0, 0, 0, 1)$ and $\boldsymbol{n}(x, \tau, 1) = \boldsymbol{n}(x, \tau)$. If the time-reversal symmetry is preserved, namely $\langle n_5 \rangle = 0$, we can integrate out n_5, and Eq. (2.18)

reduces to a 2+1d O(4) NLσM with $\Theta = \pi$:

$$\mathcal{S}_b = \int d^2x d\tau \ \frac{1}{g}(\partial_\mu \boldsymbol{n})^2 + \frac{i\pi}{\Omega_3}\epsilon_{abcd} n^a \partial_\tau n^b \partial_x n^c \partial_y n^d. \tag{2.19}$$

In Eq. (2.19) $\Theta = \pi$ is protected by time-reversal symmetry.

In the following we will argue that the topological terms in Eq. (2.18) and Eq. (2.19) guarantee that the $2d$ boundary cannot be gapped without degeneracy. One particularly interesting possibility of the boundary is a phase with $2d$ Z_2 topological order [32]. A $2d$ Z_2 topological phase has e and m excitations that have mutual semion statistics [58]. The semion statistics can be directly read off from Eq. (2.19): if we define complex boson fields $z_1 = n_1 + in_2$ and $z_2 = n_3 + in_4$, then the $\Theta-$term in Eq. (2.19) implies that a vortex of (n_3, n_4) carries half charge of z_1, while a vortex of (n_1, n_2) carries half charge of z_2, thus vortices of z_1 and z_2 are bosons with mutual semion statistics. This statistics survives after z_1 and z_2 are disordered by condensing the *double vortex* (vortex with vorticity 4π) of either z_1 or z_2 at the boundary, then the disordered phase must inherit the statistics and become a Z_2 topological phase [32]. The vortices of (n_1, n_2) and (n_3, n_4) become the e and m excitations respectively. Normally a vortex defect is discussed in systems with a $U(1)$ global symmetry. We do not assume such $U(1)$ global symmetry in our case, this symmetry reduction is unimportant in the Z_2 topological phase.

At the vortex core of (n_3, n_4), namely the m excitation, Eq. (2.18) reduces to a $0+1d$ O(3) NLσM with a WZW term at level-1 [59]:

$$\mathcal{S}_m = \int d\tau \frac{1}{g}(\partial_\tau \boldsymbol{N})^2 + \int_0^1 du \frac{i2\pi}{8\pi}\epsilon_{abc}\epsilon_{\mu\nu} N^a \partial_\mu N^b \partial_\nu N^c, \tag{2.20}$$

where $\boldsymbol{N} \sim (n_1, n_2, n_5)$. This $0+1d$ field theory describes a single particle moving on a 2d sphere with a magnetic monopole at the origin. It is well known that if there is a $SO(3)$

symmetry for $\boldsymbol{N}$, then the ground state of this $0d$ problem has two fold degeneracy, with two orthogonal solutions

$$u_m = \cos(\theta/2)e^{i\phi/2}, \quad v_m = \sin(\theta/2)e^{-i\phi/2},$$

$$\boldsymbol{N} = (\sin(\theta)\cos(\phi), \sin(\theta)\sin(\phi), \cos(\theta)) . \tag{2.21}$$

Likewise, the vortex of (n_1, n_2) (e excitation) also carries a doublet (u_e, v_e). Under the Z_2 transformation, $\phi \to \phi + \pi$, thus $u_{e,m}$ and $v_{e,m}$ carry charge $\pm 1/2$ of the Z_2 symmetry, namely under the Z_2 transformation:

$$Z_2 : U_{e,m} \to i\sigma^z U_{e,m}, \tag{2.22}$$

where $U_{e,m} = (u_{e,m}, v_{e,m})^t$.

Under time-reversal transformation $\mathcal{T}$, $\boldsymbol{N} \to -\boldsymbol{N}$, $\theta \to \theta + \pi$. Thus the e and m doublets transform as

$$Z_2^T : U_{e,m} \to i\sigma^y U_{e,m}, \tag{2.23}$$

thus the e and m anyons at the boundary carry projective representation of Z_2^T which satisfies $\mathcal{T}^2 = -1$.

Based on this Z_2 topological order, we can derive the phase diagram around the Z_2 topological order, and show that this boundary cannot be gapped without degeneracy. For example, starting with a $2d$ Z_2 topological order, one can condense either e or m excitation and kill the topological degeneracy. However, because $U_{e,m}$ transform nontrivially under the symmetry group, condensate of either e or m will always spontaneously break certain symmetry and lead to degeneracy. For example, the condensate of e excitation

has nonzero expectation value of $(n_3, n_4, n_5) \sim U_e^\dagger \boldsymbol{\sigma} U_e$, which necessarily spontaneously breaks the Z_2 or Z_2^T symmetry.

We also note that one bulk BSPT state can have different boundary states, which depends on the details of the boundary Hamiltonian. Recently a different boundary topological order of BSPT state was derived in Ref. [60], but the bulk state is the same as ours.

2.1.7 Rule of classification

With all these preparations, we are ready to lay out the rules of our classification:

1. In d-dimensional space, all the SPT phases discussed in this paper are described by a $(d+1)$-dimensional O$(d+2)$ NLσM with a Θ-term. The O$(d+2)$ vector field $\boldsymbol{n}$ is an order parameter, namely it must carry a nontrivial representation of the given symmetry. In other words, no component of the vector field transforms completely trivially under the symmetry, because otherwise it is allowed to turn on a strong linear "Zeeman" term to the trivial component, and then the system will become a trivial direct product state.

2. The classification is given by all the possible *independent* symmetry transformations on vector order parameter $\boldsymbol{n}$ that keep the Θ-term invariant, for *arbitrary* value of Θ. Independent transformations mean that any NLσM defined with one transformation cannot be obtained by "merging" two (or more) other NLσMs defined with other transformations. SPT phases constructed using independent NLσMs are called "root phases". All the other SPT phases can be constructed with these root phases.

3. With a given symmetry, and given transformation of $\boldsymbol{n}$, if $\Theta = 2\pi k$ and $\Theta = 0$ can be connected without a bulk transition, this transformation will contribute classification $\mathbb{Z}_k$; otherwise the transformation will contribute classification $\mathbb{Z}$.

Using the rule and strategy discussed in this section, we can obtain the classification

of all SPT phases in all dimensions. The final classification of the SPT phases we obtained is consistent to the classification based on group cohomology [25, 26].

2.2 Full classification of BSPT phases

Let us carefully discuss $(1+1)d$ BSPT phases with $Z_2 \times Z_2 \times Z_2^T$ symmetry as an example in the following section. And then we list our classification results for the 17 different symmetry classes in Table 2.1. The root states for each of the symmetry classes are given in the appendix.

2.2.1 Example: 1d BSPT phase with $Z_2 \times Z_2 \times Z_2^T$ symmetry

These SPT phases were discussed very thoroughly in Ref. [61]. There are in total 16 different phases (including the trivial phase). The goal of this section is to show that all these phases can be described by the *same* equation Eq. (2.1) with certain transformation of $\boldsymbol{n}$, and the projective representation of the boundary states given in Ref. [61] can be derived explicitly using Eq. (2.6).

For the consistency of notation in this paper, R_z and R_x in Ref. [61] will be labelled Z_2^A and Z_2^B here. Let us consider one example, namely Eq. (2.1) with the following transformation:

$$\begin{aligned} Z_2^A &: \quad n_{1,2} \to -n_{1,2}, \quad n_3 \to n_3; \\ Z_2^B &: \quad n_{2,3} \to -n_{2,3}, \quad n_1 \to n_1; \\ Z_2^T &: \quad n_2 \to -n_2, \quad n_{1,3} \to n_{1,3}. \end{aligned} \tag{2.24}$$

Now let us parametrize $\boldsymbol{n}$ as

$$\boldsymbol{n} = (\sin\theta\cos\phi,\ \sin\theta\sin\phi,\ \cos\theta)\,, \tag{2.25}$$

then θ and ϕ transform as

$$\begin{aligned} Z_2^A &: \ \theta \to \theta, \ \ \phi \to \phi + \pi, \\ Z_2^B &: \ \theta \to \pi - \theta, \ \ \phi \to -\phi, \\ Z_2^T &: \ \theta \to \theta, \ \ \phi \to -\phi. \end{aligned} \tag{2.26}$$

These transformations lead to the following projective transformation of edge state Eq. (2.6):

$$\begin{aligned} Z_2^A &: \ U \to i\sigma^z U, \\ Z_2^B &: \ U \to \sigma^x U, \\ Z_2^T &: \ U \to U. \end{aligned} \tag{2.27}$$

Thus this NLσM corresponds to phase E_5 in Ref. [61].

The 16 phases in Ref. [61] correspond to the following transformations of O(3) vector $\boldsymbol{n}$:

$$E_0 \ : \ \text{Trivial phase, } \Theta = 0;$$

$$E_0' \quad : \quad Z_2^A, Z_2^B : \boldsymbol{n} \to \boldsymbol{n}, \quad Z_2^T : \boldsymbol{n} \to -\boldsymbol{n};$$

$$E_1 \quad : \quad Z_2^A : \boldsymbol{n} \to \boldsymbol{n},$$

$$Z_2^B : n_{1,2} \to -n_{1,2}, \quad n_3 \to n_3,$$

$$Z_2^T : \boldsymbol{n} \to -\boldsymbol{n},$$

$$E_1' \quad : \quad Z_2^A : \boldsymbol{n} \to \boldsymbol{n},$$

$$Z_2^B : n_{1,2} \to -n_{1,2}, \quad n_3 \to n_3,$$

$$Z_2^T : n_{1,2} \to n_{1,2}, \quad n_3 \to -n_3;$$

$$E_3 \quad : \quad Z_2^B : \boldsymbol{n} \to \boldsymbol{n},$$

$$Z_2^A : n_{1,2} \to -n_{1,2}, \quad n_3 \to n_3,$$

$$Z_2^T : \boldsymbol{n} \to -\boldsymbol{n},$$

$$E_3' \quad : \quad Z_2^B : \boldsymbol{n} \to \boldsymbol{n},$$

$$Z_2^A : n_{1,2} \to -n_{1,2}, \quad n_3 \to n_3,$$

$$Z_2^T : n_{1,2} \to n_{1,2}, \quad n_3 \to -n_3;$$

$$
\begin{aligned}
E_5 \quad &: \quad Z_2^A : n_{1,2} \to -n_{1,2}, \quad n_3 \to n_3; \\
&\qquad\; Z_2^B : n_{2,3} \to -n_{2,3}, \quad n_1 \to n_1; \\
&\qquad\; Z_2^T : n_2 \to -n_2, \quad n_{1,3} \to n_{1,3}; \\
E_5' \quad &: \quad E_5 \oplus E_0'; \\
E_7 \quad &: \quad Z_2^A : n_{1,2} \to -n_{1,2}, \quad n_3 \to n_3, \\
&\qquad\; Z_2^B : n_{1,2} \to -n_{1,2}, \quad n_3 \to n_3, \\
&\qquad\; Z_2^T : n_{1,2} \to n_{1,2}, \quad n_3 \to -n_3; \\
E_7' \quad &: \quad Z_2^A : n_{1,2} \to -n_{1,2}, \quad n_3 \to n_3, \\
&\qquad\; Z_2^B : n_{1,2} \to -n_{1,2}, \quad n_3 \to n_3, \\
&\qquad\; Z_2^T : \boldsymbol{n} \to -\boldsymbol{n}; \\
E_9 \quad &: \quad Z_2^A : n_{1,2} \to -n_{1,2}, \quad n_3 \to n_3; \\
&\qquad\; Z_2^B : n_{2,3} \to -n_{2,3}, \quad n_1 \to n_1; \\
&\qquad\; Z_2^T : n_3 \to -n_3, \quad n_{1,2} \to n_{1,2};
\end{aligned}
$$

$$
\begin{aligned}
E_9' &: E_9 \oplus E_0', \\
E_{11} &: Z_2^A : n_{1,2} \to -n_{1,2}, \quad n_3 \to n_3; \\
&\quad Z_2^B : n_{2,3} \to -n_{2,3}, \quad n_1 \to n_1; \\
&\quad Z_2^T : n_1 \to -n_1, \quad n_{2,3} \to n_{2,3}; \\
E_{11}' &: E_{11} \oplus E_0'; \\
E_{13} &: Z_2^A : n_{1,2} \to -n_{1,2}, \quad n_3 \to n_3; \\
&\quad Z_2^B : n_{2,3} \to -n_{2,3}, \quad n_1 \to n_1; \\
&\quad Z_2^T : \boldsymbol{n} \to -\boldsymbol{n}; \\
E_{13}' &: E_{13} \oplus E_0'.
\end{aligned} \tag{2.28}
$$

All the phases except for the trivial phase E_0 have $\Theta = 2\pi$ in Eq. (2.1). Here $E_5 \oplus E_0'$ means it is a spin ladder with symmetry allowed weak interchain couplings, and the two chains are E_5 phase and E_0' phase respectively. For all the 16 phases above, we can compute the projective representations of the boundary states using Eq. (2.6), and they all precisely match with the results in Ref. [61].

Symmetry Group	$1+1d$	$2+1d$	$3+1d$
Z_2	$\mathbb{Z}_1$	$\mathbb{Z}_2$	$\mathbb{Z}_1$
Z_2^T	$\mathbb{Z}_2$	$\mathbb{Z}_1$	$\mathbb{Z}_2$
$U(1)$	$\mathbb{Z}_1$	$\mathbb{Z}$	$\mathbb{Z}_1$
$U(1) \rtimes Z_2$	$\mathbb{Z}_2$	$\mathbb{Z} \times \mathbb{Z}_2$	$\mathbb{Z}_2$
$U(1) \times Z_2$	$\mathbb{Z}_1$	$\mathbb{Z} \times (\mathbb{Z}_2)^2$	$\mathbb{Z}_1$
$U(1) \rtimes Z_2^T$	$\mathbb{Z}_2$	$\mathbb{Z}_2$	$(\mathbb{Z}_2)^2$
$U(1) \times Z_2^T$	$(\mathbb{Z}_2)^2$	$\mathbb{Z}_1$	$(\mathbb{Z}_2)^3$
$Z_2 \times Z_2$	$\mathbb{Z}_2$	$(\mathbb{Z}_2)^3$	$(\mathbb{Z}_2)^2$
$Z_2 \times Z_2^T$	$(\mathbb{Z}_2)^2$	$(\mathbb{Z}_2)^2$	$(\mathbb{Z}_2)^3$
Z_m	$\mathbb{Z}_1$	$\mathbb{Z}_m$	$\mathbb{Z}_1$
$Z_m \rtimes Z_2$	$\mathbb{Z}_{(2,m)}$	$\mathbb{Z}_m \times \mathbb{Z}_2 \times \mathbb{Z}_{(2,m)}$	$(\mathbb{Z}_{(2,m)})^2$
$Z_m \times Z_2$	$\mathbb{Z}_{(2,m)}$	$\mathbb{Z}_m \times \mathbb{Z}_2 \times \mathbb{Z}_{(2,m)}$	$(\mathbb{Z}_{(2,m)})^2$
$Z_m \rtimes Z_2^T$	$\mathbb{Z}_2 \times \mathbb{Z}_{(2,m)}$	$(\mathbb{Z}_{(2,m)})^2$	$\mathbb{Z}_2 \times (\mathbb{Z}_{(2,m)})^2$
$Z_m \times Z_2^T$	$\mathbb{Z}_2 \times \mathbb{Z}_{(2,m)}$	$(\mathbb{Z}_{(2,m)})^2$	$\mathbb{Z}_2 \times (\mathbb{Z}_{(2,m)})^2$
$SO(3)$	$\mathbb{Z}_2$	$\mathbb{Z}$	$\mathbb{Z}_1$
$SO(3) \times Z_2^T$	$(\mathbb{Z}_2)^2$	$\mathbb{Z}_2$	$(\mathbb{Z}_2)^3$
$Z_2 \times Z_2 \times Z_2$	$(\mathbb{Z}_2)^3$	$(\mathbb{Z}_2)^7$	$(\mathbb{Z}_2)^8$

Table 2.1: BSPT classification from NLσM method. Our results completely agree with the group cohomology classification given in Ref [25, 26]. (m, n) is the greatest common divisor of m and n.

2.2.2 Summary and comments

In this part we systematically classified and described bosonic SPT phases with a large set of physically relevant symmetries for all physical dimensions. We have demonstrated that all the SPT phases discussed in this paper can be described by three universal NLσMs Eq. (2.1), 2.2 and 2.3, and the classification of these SPT phases based on NLσMs is completely identical to the group cohomology classification [25, 26]. However, we have not built the general connection between these two classifications, and it is likely that SPT phases with some other symmetry groups (for example symmetry much larger than O($d+2$)) can no longer be described by these three NLσMs any more. In Ref. [33, 34], SPT phases that involve a large symmetry group PSU(N)= $SU(N)/Z_N$ were discussed, and in these systems it was necessary to introduce NLσMs with a larger target manifold. But it is likely that all the SPT phases with arbitrary symmetry groups (continuous or discontinuous) can be described by a NLσM with certain continuous target manifold.

Our NLσM can also be very conveniently generalized to the cases that involve lattice symmetry such as inversion, as was discussed in Ref. [62], as long as we require our order parameter $\boldsymbol{n}$ transform nontrivially under lattice symmetry. We leave a thorough study of SPT states involving lattice symmetry to future studies.

2.3 Bosonic symmetry protected topological states beyond group cohomology classification

There are roughly two types of BSPT states, their mathematical difference is whether they can be classified and described by group cohomology [25, 26] and semiclassical nonlinear sigma model field theory [63]. For example, the well-known E_8 bosonic short range

entangled (BSRE) state [2] [64, 65] in $2d$ space, and its higher dimensional generalizations [49] cannot be classified by group cohomology.

Any nontrivial SPT state's boundary state cannot exist by itself, as long as the system preserves the necessary symmetry. This means that the boundary of a SPT state must be "anomalous". The relation between boundary anomaly and bulk SPT states has been studied systematically in Ref. [66]. If a nontrivial SRE state does not need any symmetry to protect its boundary, then its boundary must have gravitational anomaly. The $2d$ $p+ip$ topological superconductor, and the $2d$ E_8 state both have chiral edge states, which lead to gravitational anomaly. Analogues of $2d$ E_8 state can be found in all even spatial dimensions. In every $(4k+2)d$ space (or equivalently $(4k+3)d$ space-time), there is a BSRE state with $\mathbb{Z}$ classification described by action [49]

$$\mathcal{S}_{(4k+3)d} = \int \frac{iK^{IJ}}{4\pi} C^I \wedge dC^J, \tag{2.29}$$

where C^I is a $2k+1$ form antisymmetric gauge field, and K^{IJ} is the Cartan matrix of the E_8 group. These states have bosonic $2k-$dimensional membrane excitations in the bulk, and perturbative gravitational anomalies at the boundary [49, 67]; In every $(4k+4)d$ space (or equivalently $(4k+5)d$ space-time), there is a BSRE state with $\mathbb{Z}_2$ classification described by action

$$\mathcal{S}_{(4k+5)d} = \int \frac{iK^{IJ}}{4\pi} B^I \wedge dB^J, \tag{2.30}$$

where B^I is a $2k+2$ form antisymmetric gauge field, and $K^{IJ} = i\sigma^y$. This theory with $k=0$ ($4d$ space) has been studied carefully in Ref. [68], and it was demonstrated that

[2] In this section, we define short range entangled state as systems with gapped and nondegenerate bulk spectrum, namely it has no topological entanglement entropy. In our definition, SRE states include SPT states as a subset.

its $3d$ boundary is an "all fermion" $3d$ QED [37] which cannot be independently realized in $3d$ space, and it has a global gravitational anomaly [48].

As was pointed out by Ref. [46, 47], the state Eq. (2.30) can also have a time-reversal symmetry. For instance, this action is invariant under $Z_2^T : i \to -i, (B^1, B^2) \to (B^2, B^1)$. But this state is also stable if the time-reversal symmetry is broken. In this section, we will only count this state as a BSRE state without any symmetry.

All these BSRE states in even spatial dimensions have their descendant BSPT states in higher dimensions. All these descendant BSPT states are also beyond the group cohomology classification. Recently, a systematic mathematical formalism for BSRE and BSPT states has been proposed in Ref. [69], which was based on cohomology of $G \times SO(\infty)$, where G is the symmetry group, and $SO(\infty)$ is supposed to describe the gravitational anomaly. The purpose of the current section is to give a physical construction and field theory description of BSPT states beyond the ordinary group cohomology classification.

2.3.1 General constructions

We will view the BSRE states without any symmetry in even spatial dimensions (Eq. (2.29) and Eq. (2.30)) as base states. Our general strategy for constructing other beyond-Group-Cohomology BSPT states, is to first break part or all of the symmetry by condensing an ordinary Landau order parameter, then proliferating/condensing the topological defects of the Landau order parameter. The nontrivial BSPT state and the trivial state are distinguished by the nature of the topological defects: nontrivial BSPT states corresponds to the case where the defects are decorated with the BSRE states in Eq. (2.29) or Eq. (2.30). The first example of such beyond-Group-Cohomology BSPT state, which is protected by Time Reversal Symmetry $\mathcal{T}$, was discovered in Ref. [32].

This state can be constructed by proliferating $\mathcal{T}$-breaking domain walls decorated with the $2d$ E_8 state. The topological term in the field theory Lagrangian density that encodes the decoration reads:

$$\mathcal{L}^{Z_2^T}_{3+1d} = \frac{i2\pi}{2\pi} n dn \wedge \frac{K^{IJ}_{E_8}}{8\pi^2} C^I \wedge dC^J = id\theta \wedge \frac{K^{IJ}_{E_8}}{8\pi^2} C^I \wedge dC^J = -i\theta \frac{K^{IJ}_{E_8}}{8\pi^2} dC^I \wedge dC^J \quad (2.31)$$

where the O(2) vector $\boldsymbol{n}$ is parametrized as $\boldsymbol{n} = (\cos\theta, \sin\theta)$. The $\mathcal{T}$-symmetry transformation is

$$\begin{aligned} Z_2^T : \quad & (n_1, n_2) \to (n_1, -n_2), \\ & \theta \to -\theta \end{aligned} \quad (2.32)$$

One can verify that the Eq. (2.31) is time-reversal invariant. Also, if we keep time-reversal invariance, then $\langle n_2 \rangle = 0$, namely $\langle \theta \rangle = 0$ or π, which precisely corresponds to the trivial and nontrivial BSPT state discussed in Ref. [32]. Meanwhile, across a $\mathcal{T}$-breaking domain wall, θ continuously changes from $-\pi + 0^+$ to $\pi + 0^-$. After integrating over the normal direction, the effective field theory left on the domain wall precisely describes a $2d$ E_8 state.

The idea of "decorated domain wall" construction of SPT states was further explored in Ref. [38]. Domain wall of Z_2 or time-reversal symmetry is the simplest kind of topological defect. In our work, we will construct beyond-group-cohomology BSPT states using more general topological defects of other symmetry groups. Here we want to clarify that in our current work the concept "topological defect" refers to a topologically stable configurations of Landau order parameter $\boldsymbol{n}$ in $d-$dimensional space $\mathbb{R}^d$ with a singularity $\mathcal{I}$, and the singularity can be viewed as the boundary of $\mathbb{R}^d - \mathcal{I}$. The Landau order parameter $\boldsymbol{n}$ has a soliton configuration on $\mathbb{R}^d - \mathcal{I}$, which has no singularity any

more. For example, in $2d$ space a vortex core is a singularity at the origin $(0,0)$, and it can be viewed as the boundary of $\mathbb{R}^2-(0,0)$, which is topologically equivalent to a ring S^1. A vortex configuration corresponds to a $1d$ soliton on S^1, based on the simple fact $\pi_1[S^1]=\mathbb{Z}$. In $3d$ space a hedgehog monopole core is again a singularity at $(0,0,0)$, and a hedgehog monopole corresponds to a soliton on space $\mathbb{R}^3-(0,0,0)$, based on the fact $\pi_2[S^2]=\mathbb{Z}$.

In general, the field theories we will discuss in this work is a combination of the Θ-term of $\boldsymbol{n}$ discussed in Ref. [63] and Chern-Simons form of C^I or B^I in Eq. (2.29),2.30. The explicitly form of the topological term in $D-$dimensional space-time is:

$$\mathcal{L}_{Dd,A}=\frac{i\Theta}{\Omega_{D-(4k+4)}}n\underbrace{dn\wedge...\wedge dn}_{D-(4k+4)}\wedge\frac{K^{IJ}}{8\pi^2}dC^I\wedge dC^J, \tag{2.33}$$

$$\mathcal{L}_{Dd,B}=\frac{i\Theta}{\Omega_{D-(4k+6)}}n\underbrace{dn\wedge...\wedge dn}_{D-(4k+6)}\wedge\frac{(i\sigma^y)^{IJ}}{8\pi^2}dB^I\wedge dB^J, \tag{2.34}$$

where $\boldsymbol{n}$ is a Landau order parameter with a unit length. $\Omega_D=V_D\times D!$, V_D is the volume of the unit D-dimensional sphere. Here we assume all components of order parameter $\boldsymbol{n}$ transform nontrivially under the symmetry group.

The equations above are also effectively equivalent to the two equations in the follows:

$$\mathcal{L}_{Dd,A}=\frac{i\Theta}{\Omega_{D-(4k+3)}}n\underbrace{dn\wedge...\wedge dn}_{D-(4k+3)}\wedge\frac{K^{IJ}}{8\pi^2}C^I\wedge dC^J. \tag{2.35}$$

$$\mathcal{L}_{Dd,B}=\frac{i\Theta}{\Omega_{D-(4k+5)}}n\underbrace{dn\wedge...\wedge dn}_{D-(4k+5)}\wedge\frac{(i\sigma^y)^{IJ}}{8\pi^2}B^I\wedge dB^J, \tag{2.36}$$

where the component n_1 does not transform under any symmetry group, but the rest of the components all transform nontrivially. The equivalence between the two descriptions

above can be made explicit by parametrizing $\boldsymbol{n}$ as: $\boldsymbol{n} = (\cos\theta, \sin\theta n_2, \sin\theta n_3, \cdots)$, then following the derivation in Eq. (2.31), because the desired BSPT state is fully symmetric, $\langle\theta\rangle$ must be either 0 or π, which corresponds to the trivial state and nontrivial BSPT state respectively. And with $\langle\theta\rangle = \pi$, Eq. (2.35),2.36 return to Eq. (2.33) and 2.34.

All the terms above are "topological" in the sense that they are invariant under local coordinate transformation, because they do not involve the metric. We only wrote down the most important topological terms explicitly, but the readers should be reminded that there are other terms that guarantee the system is in a fully gapped and nondegenerate phase. For example, we need a term $1/g(\partial_\mu \boldsymbol{n})^2$ in the field theory to control the dynamics of $\boldsymbol{n}$, and we must keep g large enough to disorder $\boldsymbol{n}$; we also need a BF theory term[32] $\sim (d\mathcal{B})^2 + \frac{1}{2\pi}\mathcal{B}\wedge dC$ to gap out all the excitations of the C^I field.

Naively, we can also write down the following field theory, with all $\boldsymbol{n}$ components transforming non-trivially under symmetry:

$$\mathcal{L} = \frac{i\Theta}{\Omega} n dn \wedge ... \wedge dn \wedge \frac{K^{IJ}}{8\pi^2} C^I \wedge dC^J.$$

For example, we can write down such field theory in $3+1d$ space-time, with $\boldsymbol{n}$ being an O(2) vector, and C^I a one form vector gauge field. Then the physical meaning of this field theory is that, the vortex core of $\boldsymbol{n}$ will host the boundary state of the $2d$ E_8 state, which must be gapless. Then this means that we can never achieve a fully gapped nondegenerate state by proliferating the vortex loops. Thus this field theory will always be gapless, unless we explicitly break the $U(1)$ symmetry of $\boldsymbol{n}$. Therefore this field theory describes the boundary of a $4d$ space, rather than a $3d$ bulk state.

For field theories in Eq. 2.33 and 2.34, in general we consider fixed points $\Theta = 2\pi p$ with $p \in \mathbb{Z}$. However, this does not mean that we have a $\mathbb{Z}$ classified state. If we can show that two field theories, $\Theta = 0$ and $\Theta = 2\pi q$ with certain $q \in \mathbb{Z}$, can be smoothly

connected without closing the bulk gap, then they must be in the same phase. In that case, the classification will be reduced to $\mathbb{Z}_q$.

Because our field theory is constructed with order parameter $\boldsymbol{n}$ and Chern-Simons form of C^I or B^I, the classification will depend on both sectors.

For pure $C \wedge dC$ theory, the classification is $\mathbb{Z}$, because its boundary state has perturbative gravitational anomaly [67, 49], which has $\mathbb{Z}$ classification. Then the classification of the mixed field theory of $\boldsymbol{n}$ and C^I only depends on the $\boldsymbol{n}$ sector.

For instance, we can take Eq. (2.31) as an example. Take two copies of the field theories and couple them to each other:

$$\mathcal{L} = \frac{i2\pi}{2\pi} n_{(1)} dn_{(1)} \wedge \frac{K^{IJ}_{E_8}}{8\pi^2} C^I_{(1)} \wedge dC^J_{(1)} + (1 \to 2) + \beta n_{2,(1)} \cdot n_{2,(2)} + \lambda dC^I_{(1)} \wedge \star dC^I_{(2)}, \quad (2.37)$$

where $\star$ is the Hodge star operator. Now we fix λ at a negative value, and tune β from negative to positive. With negative β, effectively $\boldsymbol{n}_{(1)}$ and $\boldsymbol{n}_{(2)}$ will align with each other, thus $n_{2,(1)} = n_{2,(2)}$, $C_{(1)} = C_{(2)}$, then the two theories will "constructively interfere" with each other, and the final theory effectively has $\Theta = 4\pi$; with positive β, effectively $n_{2,(1)} = -n_{2,(2)}$, $C_{(1)} = C_{(2)}$, thus the two theories will "destructively interfere" with each other, and the final theory effectively has $\Theta = 0$. Because both theories are fully gapped and nondegenerate in the bulk, tuning the coupling between them does not close the bulk gap (as long as the coupling is not too strong to overcome the bulk gap), thus the two effective coupled theories with $\Theta = 0$ and $\Theta = 4\pi$ are smoothly connected without going through a bulk phase transition. Therefore the classification for the state Eq. (2.31) is $\mathbb{Z}_2$.

By contrast, let us consider a $U(1)$ BSPT in $4d$ space with the following field theory:

$$\mathcal{L}^{U(1)}_{4+1d} = \frac{i2\pi}{2\pi} n dn \wedge \frac{K^{IJ}_{E_8}}{8\pi^2} dC^I \wedge dC^J. \quad (2.38)$$

Symmetry	$3+1d$	$4+1d$	$5+1d$	$6+1d$
$U(1)$	0	$\mathbb{Z}$	0	$\mathbb{Z}\times\mathbb{Z}_2$
Z_2	0	$\mathbb{Z}_2$	$\mathbb{Z}_2$	$\mathbb{Z}_2^2$
Z_2^T	$\mathbb{Z}_2$	0	$\mathbb{Z}_2^2$	$\mathbb{Z}_2$
$U(1)\rtimes Z_2^T$	$\mathbb{Z}_2$	$\mathbb{Z}$	$\mathbb{Z}_2^2$	$\mathbb{Z}_2^3$ ($\mathbb{Z}_2^4$)
$U(1)\times Z_2^T$	$\mathbb{Z}_2$	0	$\mathbb{Z}_2^3$	$\mathbb{Z}_2^2$ ($\mathbb{Z}_2^3$)
$U(1)\rtimes Z_2$	0	$\mathbb{Z}_2$	$\mathbb{Z}_2^2$	$\mathbb{Z}\times\mathbb{Z}_2^3$
$U(1)\times Z_2$	0	$\mathbb{Z}\times\mathbb{Z}_2$	$\mathbb{Z}_2$	$\mathbb{Z}\times\mathbb{Z}_2^4$

Table 2.2: BSPT beyond Group Cohomology constructed from decorated topological defects. Please note that the states within group cohomology classification is not listed here. The case for $U(1)\times Z_2$ symmetry was not discussed in Ref. [69]. Our results largely agree with Ref. [69]. The results in Ref. [69] that do not fully agree with ours are highlighted in red.

The $U(1)$ symmetry acts as $U(1):(n_1+in_2)\to e^{i\phi}(n_1+in_2)$. Imagine we have two copies of the theory, the only $U(1)$ symmetry allowed coupling between these two theories would be $\beta\boldsymbol{n}_{(1)}\cdot\boldsymbol{n}_{(2)}$. Then for either sign of β, *i.e.* for either $\boldsymbol{n}_{(1)}\sim\boldsymbol{n}_{(2)}$ or $\boldsymbol{n}_{(1)}\sim-\boldsymbol{n}_{(2)}$, the final effective theory always has $\Theta=4\pi$ (simply because $(-1)^2=+1$). Thus there is no symmetry allowed coupling that can continuously connect $\Theta=4\pi$ to $\Theta=0$. Therefore the classification for this $U(1)$ BSPT state is $\mathbb{Z}$.

For pure $B\wedge dB$ theory, the classification is $\mathbb{Z}_2$ [68], therefore the classification of the mixed state can only be $\mathbb{Z}_2$ or trivial depending on the classification on the $\boldsymbol{n}$ sector.

2.3.2 Classification

We study examples of beyond-group-cohomology BSPT states with various symmetries up to $6+1d$ space-time dimensions. All these states are constructed with Landau order parameters and the $2d$ E_8 state or the $4d$ BSRE state in Eq. (2.30). Our results are summarized in Table 2.2. Our results are mostly consistent with results in Ref. [69], exceptions are highlighted in red in the table. The detailed construction of field theories for each case can be found in the appendix.

Chapter 3

Bulk Properties of Symmetry Protected Topological Phases

In this chapter, the contents, excerpts and figures are reprinted with permission from Zhen Bi, Yi-Zhuang You, Alex Rasmussen, Kevin Slagle, and Cenke Xu, authors of *Phys. Rev. B* ***90****, 081110 (2014)* [70] and *Phys. Rev. Lett.* ***112****, 247202 (2014)* [71]. Copyright by the American Physical Society.

3.1 Anyon and loop braiding statistics in field theories with a topological Θ-term

One of the key properties of topological states is that, the gapped topological excitations above the ground state can have nontrivial braiding statistics. In both $2d$ and $3d$, all discrete lattice gauge theories have a deconfined topological phase [72]. $2d$ discrete gauge theories have point particle topological excitations, while $3d$ discrete gauge theories have both particle excitations and loop excitations which correspond to gauge charge and gauge flux loop respectively. The simplest lattice discrete gauge theory (which we

call "plain gauge theory") already has nontrivial braiding statistics [58]. More exotic gauge theories can be constructed by coupling the plain gauge theory to matter fields, and drive the matter fields into certain nontrivial short range entangled (SRE) state or symmetry protected topological (SPT) phase [25, 26]. For example, once we couple a $2d$ $p+\mathrm{i}p$ topological superconductor to a Z_2 gauge field, then the vison of the gauge field would acquire a Majorana fermion zero mode, which will grant the vison a nonabelian statistics [73, 64]. Also, if we couple a $2d$ bosonic SPT phase with Z_2 symmetry to a Z_2 lattice gauge theory, the lattice gauge theory will have both semion and anti-semion excitations [27], which is different from a plain lattice gauge theory.

Recently these results have been generalized to $3d$ systems. It was demonstrated that once a $3d$ lattice discrete gauge theory is coupled to a $3d$ SPT state, the loop excitations (fluctuating gauge flux loops) would acquire nontrivial multi-loop braiding statistics [74, 75, 76, 77], in addition to the standard particle-loop statistics of the plain gauge theory. For example when loop-B and loop-C are both linked to loop-A, namely none of the loops is contractible, the system wave function could acquire a universal phase angle after braiding loop-C through loop-B as shown in Fig. 3.1(a). These braiding statistics can be used as a diagnostics for SPT phases [74].

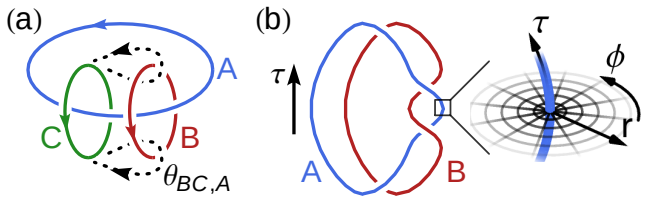

Figure 3.1: (Color online.) (a) Three-loop braiding process. The loops A, B and C are colored blue, red and green respectively. The braiding path of loop-C is indicated by the dotted arrow curve. (b) Two-loop linking in the $(2+1)d$ space-time, which corresponds to creating a pair of Z_2^A and Z_2^B visons, and annihilating them after braiding one Z_2^A and one Z_2^B visons. The time τ is along the vertical direction. The inset shows the local cylindrical coordinate system around a segment of the Z_2^A vison loop.

Besides the standard group cohomology description of SPT phases introduced in Ref. [25, 26], it was pointed out in Ref. [32, 33, 35, 63] that the bosonic SPT phases can also be described by semiclassical nonlinear sigma model (NLSM) field theories with a topological Θ-term. In this theory all the field variables are fluctuating Landau order parameters that trciteansform nontrivially under global symmetry. The goal of this section is to demonstrate that the nontrivial statistics between topological excitations after coupling the SPT phases to a discrete gauge theory can also be described and calculated using this NLSM field theory. Basically the braiding phase factor comes from the Θ−term in the field theory, as long as we carefully analyze the field configuration in the space-time which corresponds to the braiding process. The NLSM field theory with a topological term can be viewed as the continuum limit field theory description for these braiding statistics.

3.1.1 $2d$ anyon statistics

We will first look at $2d$ systems, and as an example let us start with the $2d$ SPT state with $Z_2^A \times Z_2^B$ symmetry, which can be described by the following $(2+1)d$ O(4) NLSM with a Θ-term at $\Theta = 2\pi$ [63]:

$$S = \int d^2x d\tau \ \frac{1}{g}(\partial_\mu \boldsymbol{n})^2 + \frac{\mathrm{i}\Theta}{\Omega_3}\epsilon_{abcd} n^a \partial_x n^b \partial_y n^c \partial_\tau n^d, \tag{3.1}$$

where $\boldsymbol{n}$ is a four component vector with unit length, and $\Omega_3 = 2\pi^2$ is the volume of a three dimensional sphere with unit radius. Under the $Z_2^A \times Z_2^B$ symmetry, the vector $\boldsymbol{n}$ transforms as

$$Z_2^A : n^1, n^2 \to -n^1, -n^2, \quad n^3, n^4 \to n^3, n^4;$$

$$Z_2^B : n^1, n^2 \to n^1, n^2, \quad n^3, n^4 \to -n^3, -n^4. \tag{3.2}$$

Now let us couple the vector $\boldsymbol{n}$ to a $Z_2^A \times Z_2^B$ gauge field. The excitations that will have nontrivial braiding statistics are the vison excitations (π-gauge flux) of gauge fields Z_2^A and Z_2^B. Let us consider the following braiding process: one pair of Z_2^A visons and one pair of Z_2^B visons are created in space at one instance in time, then they are annihilated at another later instance after braiding one Z_2^A vison with one Z_2^B vison. In the $(2+1)d$ space-time, this process corresponds to one linking between Z_2^A and Z_2^B vison loops, as shown in Fig. 3.1(b). Because the Z_2 gauge fields are coupled to the four-component vector $\boldsymbol{n}$, the Z_2^A vison is bound with a $\pm 1/2$-vortex of (n^1, n^2), while Z_2^B vison is bound with a $\pm 1/2$-vortex of (n^3, n^4). Then the braiding process in the space-time can be viewed as a linking configuration between (n^1, n^2) half-vortex loop and (n^3, n^4) half-vortex loop. Due to the Θ-term in Eq. (3.1), this configuration will contribute a phase factor $\exp(\pm i\pi/2) = \pm i$ to the action, which implies the mutual braiding statistics between the Z_2^A vison and Z_2^B vison.

To calculate this phase factor explicitly, let us first consider a finite segment of Z_2^A vison loop along the $\hat{\tau}$ direction. A vison is always bound with either $1/2$-vortex or $-1/2$-vortex of (n_1, n_2). Around this segment, the O(4) vector $\boldsymbol{n}$ has the following configuration with cylindrical coordinate (r, ϕ, τ) ($x = r\cos\phi$, $y = r\sin\phi$, see Fig. 3.1(b) inset):

$$\begin{aligned} n^1 &= \sin\alpha(r)\cos f(\phi), \\ n^2 &= \sin\alpha(r)\sin f(\phi), \\ n^3 &= \cos\alpha(r) N^1(\tau), \\ n^4 &= \cos\alpha(r) N^2(\tau), \end{aligned} \tag{3.3}$$

where $\boldsymbol{N} = (N_1, N_2)$ is an O(2) unit vector $|\boldsymbol{N}|^2 = 1$. $\boldsymbol{N}$ is a function of τ only. $\alpha(r)$

is a nonnegative continuous function that satisfies $\alpha(0) = 0$, $\alpha(\infty) = \pi/2$. Along the $\hat{\tau}$ axis, *i.e.* $r = 0$, we have $(n^3, n^4) = \boldsymbol{N}$. Using this configuration, we can compute the Θ-term:

$$\int d^2x d\tau \ \frac{2\pi i}{\Omega_3}\epsilon_{abcd} n^a \partial_x n^b \partial_y n^c \partial_\tau n^d = \int_0^{2\pi} d\phi \, \partial_\phi f \int d\tau \, \frac{i}{2\pi}\epsilon_{ab} N^a \partial_\tau N^b. \tag{3.4}$$

If n^1 and n^2 form a full vortex line along the $\hat{\tau}$ axis, namely $f(\phi) \sim \phi$, the O(4) Θ-term reduces to a $1d$ O(2) NLSM with $\Theta = 2\pi$. If there is a Z_2^A vison line along the $\hat{\tau}$ axis, *i.e.* n^1 and n^2 form a $\pm 1/2$-vortex line along $\hat{\tau}$ axis, namely $f(\phi) \sim \pm\phi/2$, then the $(2+1)d$ O(4) NLSM reduces to a $1d$ O(2) NLSM of vector $\boldsymbol{N}$ with $\Theta = \pm\pi$. Now let us consider two linked vison loops, and in Eq. (3.4) τ becomes the parameter along the $\mathbb{Z}_2^A$ vison loop. Since the two loops are linked, vector $\boldsymbol{N}$ will have a $\pm 1/2$-vortex winding along Z_2^A vison loop:

$$\oint \mathrm{d}\tau \ \epsilon_{ab} N^a \partial_\tau N^b = \pm\pi. \tag{3.5}$$

Combining Eq. (3.4) and Eq. (3.5) together, we conclude that this linking configuration (which corresponds to a braiding process in the space-time) would contribute factor $\pm$i to the action. In other words, the linking configuration in Fig. 3.1(b) corresponds to $\pm 1/4$-instanton of the four component vector $\boldsymbol{n}$ in the $(2+1)d$ space-time.

Now let us consider a $2d$ SPT state with Z_2 global symmetry only, and couple it to a Z_2 gauge field. This SPT state can be described by the same field theory Eq. (3.1), and under the Z_2 symmetry $\boldsymbol{n} \to -\boldsymbol{n}$. A vison of this Z_2 gauge field can be viewed as a bound state between the Z_2^A vison and Z_2^B vison discussed previously. Then the linking configuration in Fig. 3.1(b) can be interpreted as creating a pair of visons, self-twisting one vison by 2π, then annihilating them. The phase $\pm i$ corresponds to topological spin-

$\pm 1/4$ of the vison, which is consistent with the semion and anti-semion statistics of the vison proved in Ref. [27].

All the analysis above can be straightforwardly generalized to Z_N gauge theory coupled to a $2d$ Z_N SPT state. The $2d$ Z_N SPT state is described by the same field theory Eq. (3.1) [63], where $\Theta = 2\pi k$, $k = 0, 1, \cdots, (N-1)$. The same analysis above leads to the result that the topological spin of the $2\pi/N$ flux excitations can be k/N^2, namely self-twisting such excitation will grant its wave function a phase $\exp(2\pi i k/N^2)$.

3.1.2 $3d$ loop statistics

Now we consider $3d$ bosonic SPT states with $Z_2^A \times Z_2^B \times Z_2^C$ symmetry. In terms of field theory, one of these SPT states is described by the following $(3+1)d$ O(5) NLSM:

$$S = \int \mathrm{d}^3x \mathrm{d}\tau \ \frac{1}{g}(\partial_\mu \boldsymbol{n})^2 + \frac{\mathrm{i}\Theta}{\Omega_4}\epsilon_{abcde} n^a \partial_x n^b \partial_y n^c \partial_z n^d \partial_\tau n^e, \tag{3.6}$$

where $\Omega_4 = 8\pi^2/3$ is the volume of a four dimensional sphere with unit radius. Under the $Z_2^A \times Z_2^B \times Z_2^C$ symmetry, the five component vector $\boldsymbol{n}$ transforms as

$$\begin{aligned} &Z_2^A : n^1, n^2 \to -n^1, -n^2, \quad n^{3,4,5} \to n^{3,4,5}; \\ &Z_2^B : n^2, n^3 \to -n^2, -n^3, \quad n^{1,4,5} \to n^{1,4,5}; \\ &Z_2^C : n^4, n^5 \to -n^4, -n^5, \quad n^{1,2,3} \to n^{1,2,3}. \end{aligned} \tag{3.7}$$

Now let us couple this SPT state to $Z_2^A \times Z_2^B \times Z_2^C$ gauge field, and consider the statistics between the three loops in Fig. 3.1(a), in which the base loop is a vison loop of Z_2^A gauge field, and it is linked with vison loops of both Z_2^B and Z_2^C gauge fields.

A vison loop can be bound with either a $+1/2$-vortex or $-1/2$-vortex, both cases exist in the system, and they correspond to different excitations. As an example let us

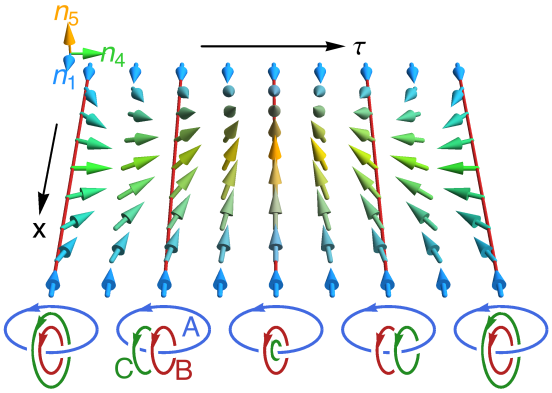

Figure 3.2: (Color online.) The space-time configuration of $\boldsymbol{N} \sim (n_1, n_4, n_5)$ on the world sheet of the Z_2^B vison loop (in red) as the Z_2^C vison loop (in green) braiding around it. Each red line is a time slice, at which moment the corresponding three-loop configuration is shown below.

study the braiding statistics of vison loops bound with $+1/2$-vortex. The choice of $+1/2$ vortex gives each vison loop an orientation, as marked out in Fig. 3.1(a). Let us first look at the Z_2^B vison loop. Following the same calculation as Eq. (3.4), because Z_2^B vison loop is bound with a half-vortex loop of (n_2, n_3), the O(5) NLSM with $\Theta = 2\pi$ is reduced to an O(3) NLSM with $\Theta = \pi$ in the $(1+1)d$ world-sheet of the Z_2^B vison loop, and the three component vector on this world sheet is $\boldsymbol{N} \sim (n_1, n_4, n_5)$:

$$S_{1d,B} = \int \mathrm{d}x\mathrm{d}\tau \ \frac{1}{g}(\partial_\mu \boldsymbol{N})^2 + \frac{i\pi}{4\pi}\epsilon_{abc} N^a \partial_x N^b \partial_\tau N^c. \tag{3.8}$$

On the $(1+1)d$ world sheet of Z_2^B vison loop, the braiding between Z_2^B and Z_2^C vison loops corresponds to the space-time configuration $\boldsymbol{N}(x, \tau)$ in Fig. 3.2, and this configuration carries $1/2$ O(3) instanton number, thus it will contribute a factor i to the action. This implies that the three-loop braiding statistics angle is $\theta_{BC,A} = \pi/2$. The statistics angle $\theta_{AC,B}$ can be calculated in the same way after interchanging n_1 and n_3 in the O(5) vector, which will lead to factor -1 due to the antisymmetrization in the Θ-term in Eq. (3.6). Thus $\theta_{AC,B} = -\pi/2$.

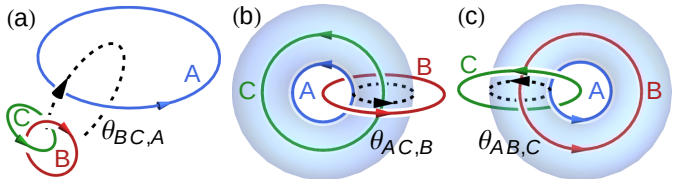

Figure 3.3: (Color online.) (a) Braiding a link of the Z_2^B and Z_2^C vison loops with the Z_2^A vison loop also accumulates the phase $\theta_{BC,A}$. (b,c) The three-loop braiding process that corresponds to the statistic angle $\theta_{AC,B}$ ($\theta_{AB,C}$). The light blue torus indicates the surface traced out by the Z_2^A vison loop through the braiding processes, which can be considered as the Gaussian surface that measures the Z_2^A charge enclosed. Small arrows on the loops mark out the loop orientation.

The loop braiding statistics can also be understood in a different way. Ref. [78] pointed out that the three-loop braiding in Fig. 3.1(a) can also be viewed as a link of the Z_2^B and Z_2^C vison loops braiding with the Z_2^A vison loop, as illustrated in Fig. 3.3(a). This link-loop braiding statistics can be described by the NLSM as well. As the vison link braid through the vison loop, the space-time configuration of the O(5) vector $\boldsymbol{n}$ around the vison link can be described as following:

$$\begin{aligned} n^1 &= \cos\alpha(\tau), \\ n^2 &= \sin\alpha(\tau) N^1(x,y,z), \\ n^3 &= \sin\alpha(\tau) N^2(x,y,z), \\ n^4 &= \sin\alpha(\tau) N^3(x,y,z), \\ n^5 &= \sin\alpha(\tau) N^4(x,y,z), \end{aligned} \tag{3.9}$$

where $\boldsymbol{N} = (N^1, N^2, N^3, N^4)$ is an O(4) unit vector $|\boldsymbol{N}|^2 = 1$ that describes the configuration of the (linked) half-vortex loops bound to the vison loops of Z_2^B and Z_2^C. The time τ (running from 0 to 1) parameterizes a full braiding of the $Z_2^B \times Z_2^C$ vison link with the Z_2^A vison loop. Suppose the n^1 component is energetically more favored, then the Z_2^A branch cut disk bordered by the Z_2^A vison loop will be bound with a n^1 domain

wall. Let the braiding of the $Z_2^B \times Z_2^C$ vison link initiates from one side of the domain wall, and ends up at the other side of the domain wall, then $\alpha(\tau)$ will be a continuous function satisfying $\alpha(0) = \pi$, $\alpha(1) = 0$. Plugging the configuration Eq. (3.9) into the NLSM Eq. (3.6), the O(5) Θ-term of $\boldsymbol{n}$ is reduced to an O(4) Θ-term of $\boldsymbol{N}$ at $\Theta = 2\pi$:

$$\begin{aligned} - & \int_0^1 \mathrm{d}\tau\, \partial_\tau \alpha \sin^3\alpha \int \mathrm{d}^3x\, \frac{2\pi \mathrm{i}}{\Omega_4} \epsilon_{abcd} N^a \partial_x N^b \partial_y N^c \partial_z N^d \\ = & \int \mathrm{d}^3x\, \frac{2\pi \mathrm{i}}{\Omega_3} \epsilon_{abcd} N^a \partial_x N^b \partial_y N^c \partial_z N^d. \end{aligned} \tag{3.10}$$

According to our previous calculation, the linking configuration between (N_1, N_2) half-vortex loop and (N_3, N_4) half-vortex loop corresponds to the 1/4 O(4) soliton in the $3d$ space, so the above O(4) Θ-term in Eq. (3.10) will result in a $\pi/2$ phase angle accumulated in the link-loop braiding, which equals to the three-loop braiding angle $\theta_{BC,A}$ calculated already in our paper.

The non-trivial link-loop braiding statistics implies that the $Z_2^B \times Z_2^C$ vison link must carry the charge of the Z_2^A gauge field. Let us denote the Z_2^A charge carried by the $Z_2^B \times Z_2^C$ vison link as q_{BC}^A. It is related to the braiding angle by $\theta_{BC,A} = -\pi q_{BC}^A$. The minus sign is due to the reversed link-loop braiding direction as shown in Fig. 3.3(a) (which corresponds to the positive three-loop braiding direction). As shown in Fig. 3.3(b), the torus traced out by the Z_2^A vison loop through braiding with the Z_2^C vison loop (in the linking with the Z_2^B vison loop) actually forms a Gaussian surface enclosing the Z_2^C vison loop. So the three-loop braiding statistics angle $\theta_{AC,B}$ measures the Z_2^A charge carried by the Z_2^C vison loop in the $Z_2^B \times \mathbb{Z}_2^C$ link, denoted q_C^A, and $\theta_{AC,B} = \pi q_C^A$. Similarly from Fig. 3.3(c), the three-loop braiding statistics angle $\theta_{AB,C}$ measures the Z_2^A charge carried by the Z_2^B vison loop in the same $Z_2^B \times \mathbb{Z}_2^C$ link, denoted q_B^A, and $\theta_{AB,C} = \pi q_B^A$. Obviously,

$q^A_{BC} = q^A_B + q^A_C$, thus

$$\theta_{AB,C} + \theta_{BC,A} + \theta_{AC,B} = 0, \tag{3.11}$$

which is precisely the cyclic relation [78, 74], and it implies that $\theta_{AB,C} = 0$ (given $\theta_{BC,A} = \pi/2$ and $\theta_{AC,B} = -\pi/2$ as previously calculated).

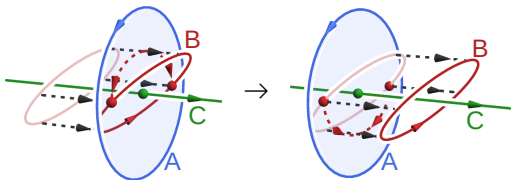

Figure 3.4: (Color online.) Illustration of moving Z_2^B vison loop through the Z_2^A vison loop. The Z_2^A vison loop borders a branch cut disk, which can be viewed as a $2d$ $Z_2^B \times Z_2^C$ SPT. When the Z_2^B vison loop pokes through this disk, a pair of Z_2^B semion-antisemion are created, braided with the Z_2^C vison, and annihilated.

$\theta_{AB,C}$ can also be computed as follows: $\theta_{AB,C}$ corresponds to braiding Z_2^A and Z_2^B vison loops, both of which are linked to a Z_2^C vison loop. This process can be divided into two steps: first moving Z_2^B vison loop through Z_2^A vison loop, then moving Z_2^A vison loop through Z_2^B vison loop. The first step (see Fig. 3.4) is equivalent to creating a pair of Z_2^B vison-antivison (vison and antivison have semion and antisemion statistics) at the $2d$ $Z_2^B \times Z_2^C$ SPT phase, then braiding the Z_2^B vison (or antivison) around the Z_2^C vison, and annihilating the vison-antivison pair. This step will contribute a phase factor i to the action. The second step is equivalent to creating and annihilating a pair of Z_2^A visons at the $2d$ $Z_2^A \times Z_2^C$ SPT phase, and braiding around the Z_2^C vison in between, which will contribute factor $-i$. The two processes together will lead to a trivial phase factor, namely $\theta_{AB,C} = 0$.

More "conventionally", $\theta_{BC,A}$ and $\theta_{AC,B}$ can be interpreted in the "decorated domain wall" picture [38]. In our NLSM Eq. (3.6), the Z_2^A vison loop is the boundary of a $2d$

disk of branch cut of coupling between n_1 components. According to Ref. [79], after integrating out n_1, the effective field theory on this $2d$ disk is the same as Eq. (3.1) with $\Theta = 2\pi$, except now the O(4) vector is (n_2, n_3, n_4, n_5), *i.e.* this $2d$ disk can be viewed as a $2d$ SPT state with $Z_2^B \times Z_2^C$ symmetry, which is precisely the decorated domain wall picture. Then after gauging the Z_2^B and Z_2^C symmetry, the vison loop statistics reduces to the anyon statistics of the $2d$ $Z_2^B \times Z_2^C$ topological order, which is what we have already computed using Eq. (3.1).

We can also consider $3d$ SPT state with $Z_2^A \times Z_2^B$ symmetry. There are in total three different nontrivial $3d$ bosonic SPT states with this symmetry [25]. The first state can be constructed using the previously discussed $Z_2^A \times Z_2^B \times Z_2^C$ SPT state, and break its subgroup $Z_2^B \times Z_2^C$ down to one diagonal Z_2 symmetry, namely now the O(5) vector $\boldsymbol{n}$ transforms as

$$\begin{aligned} &\mathbb{Z}_2^A : n_1, n_2 \to -n_1, -n_2, \quad n_{3,4,5} \to n_{3,4,5}; \\ &\mathbb{Z}_2^B : n_1 \to n_1, \quad n_{2,3,4,5} \to -n_{2,3,4,5}. \end{aligned} \tag{3.12}$$

Now a Z_2^B vison loop corresponds to a bound state between the Z_2^C and Z_2^B vison loops in the previous case. Thus [1]

$$\begin{aligned} &\theta_{BB,A} = 2\theta_{BC,A} = \pi, \\ &\theta_{AB,B} = \theta_{AC,B} + \theta_{AB,C} = \pm\pi/2. \end{aligned} \tag{3.13}$$

All the other braiding angles are zero. The second type of $3d$ SPT state corresponds to interchanging Z_2^A and Z_2^B symmetries, thus after gauging the symmetries, $\theta_{AB,A} = \pm\pi/2$, $\theta_{AA,B} = \pi$. The third type of SPT state is equivalent to the two SPT states discussed

[1] Here $\theta_{BB,A}$ stands for the full braiding statistics angle between two Z_2^B vison loops while they are both linked with a Z_2^A vison loop.

above weakly coupled together, thus

$$\theta_{AB,A} = \theta_{AB,B} = \pm\pi/2, \quad \theta_{AA,B} = \theta_{BB,A} = \pi. \tag{3.14}$$

In summary, we have computed the anyon braiding statistics, and three-loop statistics of $2d$ and $3d$ topological phases constructed by coupling plain gauge theories to bosonic SPT states. Our calculation is based on semiclassical field theories, and all the braiding phases naturally come from the topological $\Theta-$term in the field theory.

3.2 Wave function and strange correlator of short range entangled states

A short range entangled (SRE) state is a ground state of a quantum many-body system that does not have ground state degeneracy or bulk topological entanglement entropy. But a SRE state (for example the integer quantum Hall state) can still have protected stable gapless edge states. Thus it appears that the bulk of all the SRE states are identically trivial, and a nontrivial SRE state is usually characterized by its edge states. In this section, we propose a diagnosis to determine whether a given many-body wave function defined on a lattice without boundary is a nontrivial SRE state or a trivial one. This diagnosis is based on the following quantity called "strange correlator" [2]:

$$C(r, r') = \frac{\langle\Omega|\phi(r)\phi(r')|\Psi\rangle}{\langle\Omega|\Psi\rangle}. \tag{3.15}$$

[2]In the thermodynamic limit, both numerator and denominator of the strange correlator approach zero, while their ratio remains a finite constant. All the calculations in this section were based on finite system size first, the thermodynamic limit is taken *after* taking the ratio.

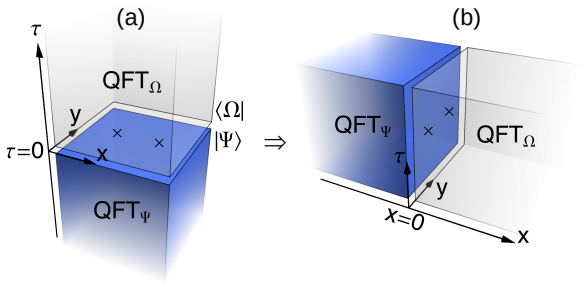

Figure 3.5: (color online). (a) $|\Psi\rangle$ and $\langle\Omega|$ are given by infinite time evolution of their quantum field theories (QFT) from below and above respectively. The strange correlator can be viewed as the correlator at the $\tau = 0$ interface. (b) Under the Lorentz rotation, the two QFT's are separated by the $x = 0$ interface, and the strange correlator can be interpreted as the correlation function on this spatial interface.

Here $|\Psi\rangle$ is the wave function that needs diagnosis, $|\Omega\rangle$ is a direct product trivial disordered state defined on the same Hilbert space. Our conclusion is that if $|\Psi\rangle$ is a nontrivial SRE state in one or two spatial dimensions, then for some local operator $\phi(r)$, $C(r, r')$ will either saturate to a *constant* or decay as a *power-law* in the limit $|r - r'| \to +\infty$, even though both $|\Omega\rangle$ and $|\Psi\rangle$ are disordered states with short-range correlation.

Another possible way of diagnosing a SRE wave function is through its entanglement spectrum [80]. If a SRE state has nontrivial edge states, an analogue of its edge states should also exist in its entanglement spectrum [81]. However, many SRE states are protected by certain symmetry, some SRE states are protected by lattice symmetries (for example the spin-2 AKLT state on the square lattice requires translation symmetry). If the cut we make to compute the entanglement spectrum breaks such lattice symmetry, then the entanglement spectrum would be trivial, even if the original state is a nontrivial SRE state. By contrast, the strange correlator in Eq. (3.15) is defined on a lattice without edge, thus it already preserves all the symmetries of the system, including all the lattice symmetries. Thus the strange correlator can reliably diagnose SRE states protected by lattice symmetries as well.

3.2.1 Field theoretical arguments

The strange correlator can be roughly understood as follows: $|\Psi\rangle$ can be viewed as a generic initial state evolved with a constant nontrivial SRE Hamiltonian from $\tau = -\infty$ to $\tau = 0$; $\langle\Omega|$ is a state evolved from $\tau = +\infty$ to $\tau = 0$ with a trivial Hamiltonian, thus the strange correlator can be viewed as a "correlation function" at a temporal domain wall of the QFT's at $\tau = 0$, see Fig. 3.5(a). If there is an approximate Lorentz invariant description of the system, a space-time rotation can transform Eq. (3.15) to a space-time correlation at a spatial interface between nontrivial and trivial SRE systems, see Fig. 3.5(b). And for one and two spatial dimensions, a spatial interface between trivial and nontrivial SRE states should have either long range or power-law correlation between certain local operators, which after Lorentz rotation will lead to the conclusion of this paper. A similar observation of Lorentz rotation was used to derive the bulk wave function of topological superconductors [82].

For bosonic SRE states that are protected by certain symmetry (so called symmetry protected topological (SPT) states [25, 26]), the argument above can be demonstrated more explicitly. In Ref. [63], it was demonstrated that a large class of $1d$ and $2d$ bosonic SPT states can be described by the following two nonlinear Sigma model (NLSM) field theories:

$$\mathcal{S}_{1d} = \int dx d\tau \frac{1}{g}(\partial_\mu \boldsymbol{n})^2 + \frac{i2\pi}{8\pi}\epsilon_{abc}\epsilon_{\mu\nu} n^a \partial_\mu n^b \partial_\nu n^c, \tag{3.16}$$

$$\mathcal{S}_{2d} = \int d^2x d\tau \frac{1}{g}(\partial_\mu \boldsymbol{n})^2 + \frac{i2\pi}{12\pi^2}\epsilon_{abcd}\epsilon_{\mu\nu\rho} n^a \partial_\mu n^b \partial_\nu n^c \partial_\rho n^d. \tag{3.17}$$

Here $\boldsymbol{n}(x)$ is an O(3) or O(4) vector order parameter with unit length constraint: $(\boldsymbol{n})^2 = 1$. Different SPT phases are distinguished from each other based on different implementa-

tions of the symmetry group on the vector order parameter $\boldsymbol{n}$. In both $1d$ and $2d$, ground state wave functions of SPT phases can be derived based on Eq. (2.1) and Eq. (2.2) (see Ref. [35]):

$$|\Psi\rangle_d \sim \int D\boldsymbol{n}(x)\ \exp^{-\int_{S^d} d^d x\ \frac{1}{G}(\nabla \boldsymbol{n})^2 + \mathrm{WZW}_d[\boldsymbol{n}]} |\boldsymbol{n}(x)\rangle, \tag{3.18}$$

where S^d is the compactified real space manifold, and $\mathrm{WZW}_d[\boldsymbol{n}]$ is a real space Wess-Zumino-Witten term:

$$\begin{aligned}
\mathrm{WZW}_1[\boldsymbol{n}] &= \int_0^1 du\ \frac{i2\pi}{8\pi}\epsilon_{\mu\nu}\epsilon_{ab} n^a \partial_\mu n^b \partial_\nu n^c,\ \mu,\nu = x,u \\
\mathrm{WZW}_2[\boldsymbol{n}] &= \int_0^1 du\ \frac{i2\pi}{12\pi^2}\epsilon_{abcd}\epsilon_{\mu\nu\rho} n^a \partial_\mu n^b \partial_\nu n^c \partial_\rho n^d, \\
\mu,\nu,\rho &= x,y,u.
\end{aligned} \tag{3.19}$$

In contrast, the trivial state wave function is a superposition of all configurations of $|\boldsymbol{n}(x)\rangle$ without a WZW term. Based on the wave functions in Eq. (3.18), the strange correlator of order parameter $\boldsymbol{n}(x)$ reads

$$C(r,r') = \frac{\int D\boldsymbol{n}(x)\ n^a(r) n^b(r') e^{-\int_{S^d} d^d x\ \frac{1}{G}(\nabla \boldsymbol{n})^2 + \mathrm{WZW}_d[\boldsymbol{n}]}}{\int D\boldsymbol{n}(x)\ e^{-\int_{S^d} d^d x\ \frac{1}{G}(\nabla \boldsymbol{n})^2 + \mathrm{WZW}_d[\boldsymbol{n}]}}. \tag{3.20}$$

Mathematically, this strange correlator can be viewed as an ordinary space-time correlation function of a $(d-1)+1$ dimensional field theory with a WZW term, as long as we view one of the spatial coordinate as the time direction. When $d=1$, this strange correlator is effectively a spin-spin correlation of one isolated free spin-1/2, and the correlation is always long range. When $d=2$, this strange correlator is effectively a space-time correlation function of a $(1+1)d$ O(4) NLSM with a WZW term, and when this model has a full $SO(4)$ symmetry, this theory is a $SU(2)_1$ conformal field theory with power-law

correlation [83, 50]; when the symmetry of the system is a subgroup of $SO(4)$, as long as the residual symmetry prohibits any linear Zeeman coupling to order parameter $\boldsymbol{n}$, this $(1+1)d$ system either remains gapless, or spontaneously breaks the symmetry and develop long range order. Thus the strange correlator is either long range or decays with a power-law.

The two arguments above both rely on a certain continuum limit description of the SRE state. However, for a fully gapped system, when the gap is comparable with the ultraviolet energy scale of the system, a continuum limit description may not be appropriate. In the rest of the section, we will compute the strange correlator for several examples of SRE states *far from* the continuum limit, *i.e.* the gap of the SRE states is comparable with UV cut-off. We will see that in some examples, the strange correlator is indeed different from the physical edge of the SRE state, but our qualitative conclusion is still valid.

3.2.2 Examples in $1d$ and $2d$

The first example we study is the AKLT state [17, 84] of the Haldane phase of spin-1 chain. In the S^z basis, the AKLT wave function is a "dilute" Néel state, namely it is an equal weight superposition of all the S^z configurations with an alternate distribution of $|+\rangle = |S^z = +1\rangle$ and $|-\rangle = |S^z = -1\rangle$, sandwiched with arbitrary numbers of $|0\rangle = |S^z = 0\rangle$ [85]:

$$|\Psi\rangle = \sum \frac{1}{N} |+0\cdots0-0\cdots0+\cdots\rangle \tag{3.21}$$

We choose the trivial state to be $|\Omega\rangle = |000\cdots\rangle$. Straightforward calculation leads to the following answer of the strange correlator:

$$C(r,r') = \frac{\langle\Omega|S_r^+ \ S_{r'}^-|\Psi\rangle}{\langle\Omega|\Psi\rangle} = 2, \tag{3.22}$$

which is the expected long range correlation.

The second example we study is the two dimensional quantum spin Hall (QSH) insulator with a Rashba spin orbit coupling. We will use the same notation as Ref. [3]. The QSH insulator Hamiltonian reads

$$H = t\sum_{\langle i,j\rangle} c_i^\dagger c_j + i\lambda_{SO}\sum_{\langle\langle i,j\rangle\rangle} \nu_{ij} c_i^\dagger s^z c_j$$

$$+\lambda_R \sum_{\langle i,j\rangle} c_i^\dagger (\mathbf{s}\times\hat{\mathbf{d}}_{ij})_z c_j + \lambda_v \sum_i \xi_i c_i^\dagger c_i. \tag{3.23}$$

λ_{SO} is the spin-orbit coupling that leads to the QSH topological band structure, λ_R is the Rashba coupling that breaks the conservation of s^z, and λ_v is a staggered potential that leads to charge density wave. The electron operator c_i carries spin and sublattice indices, thus the strange correlator $C(r,r')$ is a 4×4 matrix. For QSH state $|\Psi\rangle$, we choose $\lambda_{SO} = t$, $\lambda_R = 0.5t$, $\lambda_v = 0$; trivial state $|\Omega\rangle$ is chosen to be a strong CDW state with $\lambda_{SO} = t$, $\lambda_R = 0.5t$, $\lambda_v = 10t$. These two states are far from the continuum limit, namely the gap is comparable with the UV cut-off.

Fig. 3.6(a) shows the amplitude of strange correlator $|C_k| = |\langle\Omega|c_{A,\uparrow,k}^\dagger c_{B,\uparrow,k}|\Psi\rangle/\langle\Omega|\Psi\rangle|$ plotted in the momentum space. There is one clear singularity at the corner of the Brillouin zone, which diverges as $\sim 1/|k|$. This implies that in the real space the strange correlator decays as $|C(r,r')| \sim 1/|\boldsymbol{r}-\boldsymbol{r}'|$, which is consistent with the result obtained from Lorentz transformation, despite the large bulk gap.

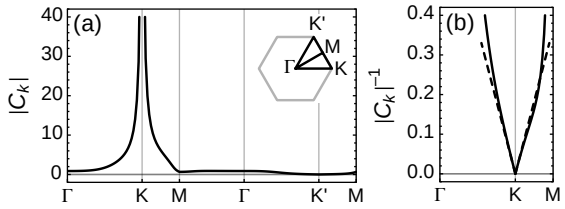

Figure 3.6: (a) The amplitude of strange correlator in the momentum space. The inset shows the Brillouin zone and the high symmetry points. (b) $|C_k|^{-1}$ exhibits nice linearity around the K point, establishing the $1/|k|$ divergence in $|C_k|$.

The third example we will study is the spin-2 AKLT state on the square lattice,[84, 86] which is a SPT state protected by the on-site $\mathbb{Z}_2 \times \mathbb{Z}_2$ and the lattice translation symmetry,[87] whose wave function has a tensor product state (TPS) representation[88, 89]

$$|\Psi\rangle = \sum_{\{m_i\}} \mathrm{tTr}(\otimes_i T^{m_i})|\{m_i\}\rangle. \tag{3.24}$$

Here $m_i = 0, \pm 1, \pm 2$ labels the S^z quantum number of the spin-2 object on site i, and $|\{m_i\}\rangle$ is the state for the configuration $\{m_i\}$ over the lattice. tTr traces out the internal legs in the tensor network shown in Fig. 3.7(a), in which the vertex tensor is given by

$$T^m_{s_1 s_2 s_3 s_4} = \begin{cases} 4 s_1 s_2 & : -s_1 - s_2 + s_3 + s_4 = m, \\ 0 & : \text{otherwise}, \end{cases} \tag{3.25}$$

with $s_j = \pm 1/2$ labeling the spin-1/2 internal degrees of freedom. While the trivial state $|\Omega\rangle = |\{\forall i : m_i = 0\}\rangle$ is chosen to be the direct product state of $S^z = 0$ on every site. We look into the strange correlator

$$C(r, r') = \frac{\langle\Omega|S^+_r S^-_{r'}|\Psi\rangle}{\langle\Omega|\Psi\rangle} = \frac{\mathrm{tTr}(T^0 \cdots T^1(r) T^{-1}(r') \cdots)}{\mathrm{tTr}(T^0 \cdots)}, \tag{3.26}$$

which can be expressed as a ratio between two tensor networks: the denominator is a

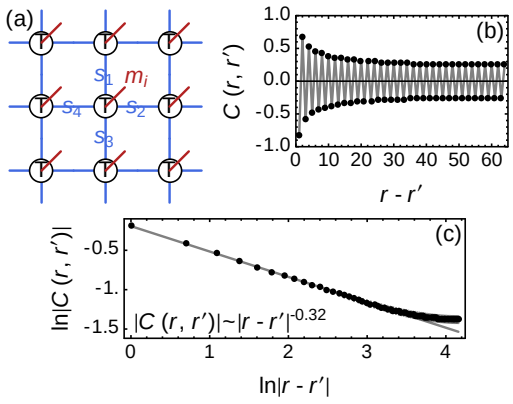

Figure 3.7: (color online). (a) Tensor network representation of the $2d$ AKLT state. The red (blue) legs represent the physical (internal) degrees of freedom. (b) Strange correlator of the $2d$ AKLT state measured along the horizontal direction. (c) The amplitude follows a power-law behavior in the log-log plot. The final deviation is due to the finite-size effect.

uniform network of the tensor T^0 on each site, and the numerator is the same network except for impurity tensors $T^{\pm 1}$ on site r and r' respectively.

The evaluation of the tensor trace in Eq. (3.26) over the $2d$ lattice can be reformulated as an (1+1) dimensional quantum mechanics problem in terms of the transfer matrix for each row, which can then be studied by the density matrix renormalization group (DMRG) method.[90, 91] The calculation is performed on an $128 \times \infty$ lattice with periodic boundary condition along both directions. We found that the strange correlator decays with oscillation (as in Fig. 3.7(b)), and its amplitude follows a power-law behavior $|C(r, r')| \sim |r - r'|^{-\eta}$ with the exponent $\eta \simeq 0.32$, see Fig. 3.7(c), which is consistent with our previous field theory argument.

The last example we will study is the two dimensional bosonic SPT phase with Z_2 symmetry which was first studied in Ref. [27]. The ground state wave function of this

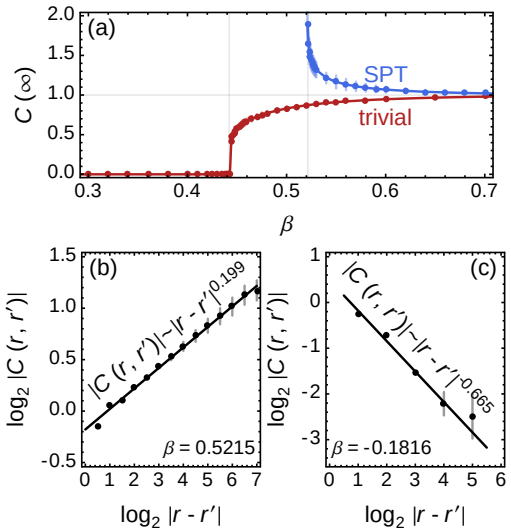

Figure 3.8: (color online). (a) The strange correlator of the SPT state (in blue) at infinite distance $|r - r'| \to \infty$, in comparison with that of the trivial state (in red). The SPT strange correlator follows the power-law behavior (b) at the critical point and (c) in the dense loop phase.

SPT phase is

$$|\Psi\rangle = \sum_{\{\sigma_i\}} (-1)^{N_d} \exp\Big(-\frac{\beta}{2} \sum_{\langle i,j\rangle} \sigma_i \sigma_j \Big) |\{\sigma_i\}\rangle, \tag{3.27}$$

which is a superposition of all the configurations of the Ising degree of freedom $|\{\sigma_i\}\rangle$ with a factor (-1) associated with each closed Ising domain wall (with N_d being the number of domain wall loops). The trivial state $|\Omega\rangle$ is simply an Ising paramagnet, whose wave function is similar to Eq. (3.27) but without the domain wall sign structure $(-1)^{N_d}$. Compared with Ref. [27], we have added a factor $\exp(-\beta/2 \sum_{\langle i,j\rangle} \sigma_i \sigma_j)$ to each Ising configuration to adjust the spin correlation length.

The strange correlator of the Z_2 bosonic SPT phase can be viewed as a correlation

function of a "classical statistical mechanics model":

$$C(r,r') = \frac{\sum_{\{\sigma_i\}} \sigma_r \sigma_{r'} (-1)^{N_d} e^{-\beta \sum_{\langle i,j\rangle} \sigma_i \sigma_j}}{\sum_{\{\sigma_i\}} (-1)^{N_d} e^{-\beta \sum_{\langle i,j\rangle} \sigma_i \sigma_j}}. \tag{3.28}$$

Our goal is to show that this is either a long range or power-law correlation for arbitrary β. In other words, Eq. 3.28 is less likely to disorder than the ordinary 2d Ising model. This result can be naively understood as follows: the ordinary 2d Ising model is disordered at high temperature (small β) due to the proliferation of Ising domain walls. But in the current model, due to the (-1) sign associated with each domain wall, the proliferation of domain walls is suppressed, thus eventually the current Ising model Eq. (3.28) is not completely disordered even for small β.

This Ising model is dual to a loop model with the following partition function:

$$Z = \sum_{\mathcal{C}} K^L n^{N_d}, \tag{3.29}$$

where loops are the domain walls of the original Ising model, $K = \exp(-2\beta)$ is the loop tension, $n = -1$ is the loop fugacity, L is the total length of loops, and N_d is the total number of closed loops. If the loops do not cross, then according to Ref. [92], by tuning K there is a phase transition between a small loop phase (which corresponds to the Ising ordered phase) for small K, and a dense loop phase for large K. The critical point and the dense loop phase are both critical with power-law correlations, and they correspond to two different conformal field theories with central charges $c = -3/5$ and $c = -7$ respectively. If the loops are allowed to cross, the dense loop phase is driven to a different conformal field theory with $c = -2$, which is described by free symplectic fermions.[93]

The Ising order parameter σ_i corresponds to the "twist" operator of the loop model,

because σ_i changes its sign when it crosses a loop. The twist operator is well-studied at the critical point of loop models, and in our case with $n = -1$, at the critical point between small and dense loop phases the scaling dimension of the twist operator is $-1/10$ [94], which is confirmed by our numerical calculation.

The tensor renormalization group (TRG) method[95, 96] has been applied to loop models in Ref. [97]. Here we use the same approach to study the twist operator correlations for the loop model in Eq. (3.29). For simplicity we forbid the loops to cross, so the model never develops antiferromagnetic order even for negative β. For positive large β, the strange correlator is long-ranged, see Fig. 3.8(a). As β decreases, the correlator grows and diverges at the critical point $\beta_c \simeq 0.521$ with a power-law $C(r, r') \sim |r - r'|^{0.199}$ as shown in Fig. 3.8(b), which confirms the theoretical prediction of scaling dimension $-1/10$ of twist operator [94]. Theoretically the entire dense loop phase (when $\beta < \beta_c$) should be controlled by one stable conformal field theory fixed point. Our numerical results suggest that this fixed point is likely around $\beta \sim -0.1816$, the power-law behavior of $C(r, r')$ at this point (Fig. 3.8) is qualitatively consistent with the conclusion of this paper. [3]

3.2.3 Subtleties in $3d$

We have checked that the ordinary free electron $3d$ topological insulator also gives us a very clear power-law decay of strange correlator. However, in general a strongly interacting SRE state in three dimensional space can be more complicated, because its two dimensional edge can be (1) a gapless $(2+1)d$ conformal field theory, (2) long range

[3] For β far away from this fixed point, the finite system size and error bar, as well as the incommensurate oscillation of the strange correlator make it more difficult to extract a conclusive scaling dimension of σ_i. But we expect $C(r, r')$ to crossover back to the same scaling behavior as the stable fixed point $\beta \sim -0.1816$ in the infrared limit for arbitrary $\beta < \beta_c$. Our result may have also been strongly affected by our choice of microscopic rules for loops close to each other. More recent studies by Scaffidi and Ringel [98] on the Levin-Gu model on a triangular lattice have successfully extracted a scaling dimension consistent with the Coulomb gas prediction of the dense loop phase [94].

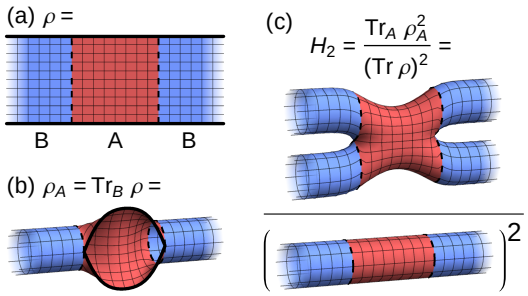

Figure 3.9: (color online). (a) Under Lorentz transformation, the density matrix of the SRE edge states is mapped to the overlap between bulk ground state wave functions on a manifold with open boundaries in one direction. The edge manifold may be partitioned into the regions A (red) and B (blue). (b) The reduced density matrix in the region A of the edge states corresponds to joining the boundaries of B together. (c) $\mathrm{Tr}\rho_A^2$ is given by doubling ρ_A and sealing the boundaries of regions A with each other, resulting in the pants (double torus) topology. $\mathrm{Tr}\rho$ is simply obtained by rolling up (a). Their ratio gives the Rényi entropy H_2.

order that spontaneously breaks symmetry, (3) two dimensional topological phase [32]. Based on our Lorentz transformation argument, it is possible that $\langle\Omega|\Psi\rangle$ is mapped to the partition function of a topological phase, then in this case the strange correlator $C(r, r')$ may also be short ranged. Thus for 3d SRE states, besides the strange correlator, we also need another method that diagnoses the situation when $\langle\Omega|\Psi\rangle$ corresponds to a topological phase partition function.

The method we propose is illustrated in Fig. 3.9, where the horizontal direction represents the XY plane, while the vertical direction is the z axis of the three dimensional space. We can first calculate the overlap between the given 3d wave function $|\Psi\rangle$ and the trivial wave function on a 3d "pants"-like manifold in Fig. 3.9c ($\langle\Omega|\Psi\rangle_{\text{pants}}$), which after Lorentz transformation becomes $\mathrm{Tr}\rho_A^2$ at the edge, where ρ_A is the reduced density matrix of subsystem A at the boundary. The following quantity after Lorentz transformation

becomes the Rényi entanglement entropy of the edge topological phase:

$$S = -\log\left(\frac{\langle\Omega|\Psi\rangle_{\text{pants}}}{(\langle\Omega|\Psi\rangle_{\text{cylinder}})^2}\right). \tag{3.30}$$

This quantity should scale as $S = \alpha L - \gamma$, where γ is the analogue of the topological entanglement entropy of the edge topological phase [99, 100]. Thus a $3d$ wave function $|\Psi\rangle$ is still a nontrivial SRE state as long as γ defined above is nonzero, even if this wave function has a short range strange correlator. We will leave the detailed study of this proposal to future work.

In summary, we have proposed a general method to diagnose $1d$ and $2d$ SRE states based on their bulk ground state wave functions. We expect our method to be useful for future numerical studies of SRE states. In Ref. [101, 102, 103, 104], it was proposed that interacting fermionic topological insulators and topological superconductors can be characterized by the full fermion Green's function; Ref. [105] proposed a method to diagnose bosonic SPT states characterized by group cohomology. The method proposed in our current paper is applicable to both fermionic and bosonic SRE states.

Chapter 4

Surface States of Symmetry Protected Topological Phases

In the first section of this chapter, the contents, excerpts and figures are reprinted with permission from Zhen Bi, Yi-Zhuang You, and Cenke Xu, authors of *Phys. Rev. B* ***94****, 024433 (2016)* [106] (Copyright by the American Physical Society). The second part is based on *arXiv:1605.05336* [107] with permissions from the authors, Zhen Bi, Alex Rasmussen, Yoni BenTov, and Cenke Xu. The third part is reprinted from *arXiv:1705.00012*[108] with permissions from Chao-Ming Jian, Zhen Bi and Cenke Xu.

4.1 Exotic Quantum Critical Point on the Surface of $3d$ Topological Insulator

Although it is well-known that the boundary state of a noninteracting $3d$ topological insulator (TI) is described by one or odd number of free $(2+1)d$ Dirac fermions [5, 6, 109], curiosity drives theorists to look for all possible boundary states of $3d$ TI under strong interaction. It was demonstrated that under strong interaction the boundary of a $3d$ TI

can have various topological orders that cannot be realized in a pure $2d$ system [110, 111, 112, 113, 13]. And the general procedure of obtaining these topological orders, is to first drive the boundary into the so-called Fu-Kane superconductor [114], then restore the U(1) symmetry by condensing a bosonic vortex of the superconductor, for example a vortex of 8 fold vorticity (or a vortex that would trap $8\frac{hc}{2e}$ flux once the fermion is coupled to the external electromagnetic field). In the condensate of the 8-fold vortex, all symmetries of the system are preserved, the boundary remains gapped, but the ground state has topological order with nonabelian anyon excitations [110, 111, 112, 113, 13].

More recent theoretical exploration has concluded that the charge neutral 4-fold vortex is a fermion, and it is doublet that transforms under time-reversal symmetry as $\mathcal{T} : \psi \to i\sigma^y\psi^\dagger$. This fermionic 4-fold vortex provides a dual description of the boundary of $3d$ TI, which is a $(2+1)d$ quantum electrodynamics (QED_3) with $N = 1$ flavor of Dirac fermion:

$$\mathcal{L}_{dual} = \bar{\psi}\gamma_\mu(\partial_\mu - ia_\mu)\psi + \frac{1}{e^2}f_{\mu\nu}^2,$$

$$\gamma^0 = \sigma^y, \quad \gamma^1 = \sigma^x, \quad \gamma^2 = \sigma^z, \tag{4.1}$$

where a_μ is the dual of the Goldstone mode of the Fu-Kane superconductor, and the flux quantum of a_μ carries half of the physical electric charge [115, 116, 117, 118], thus a_μ is a noncompact gauge field. This duality is a fermionic version of the well-known duality between the $3d$ XY model and the bosonic QED [119, 120]. And based on this duality, recently it was demonstrated that QED_3 with $N = 2$ is self-dual [121], which is a fermionic analogue of the self-duality of the noncompact CP^1 theory with easy-plane anisotropy [122, 123, 124].

Ref. [116, 117, 118] demonstrated that the dual theory Eq. (4.1) is the parent state of

many known strongly interacting boundary states of $3d$ TI, and these boundary states can also be constructed using the original physical Dirac fermion (electron). It is tempting to claim that Eq. (4.1) is exactly dual to the free Dirac fermion (or weakly interacting Dirac fermion), which is a very simple $(2+1)d$ conformal field theory (CFT). Recently a coupled wire construction of the duality further supports this idea [125]. In this paper we will assume this duality is exact: namely Eq. (4.1) is indeed a CFT in the infrared that is dual to the noninteracting $(2+1)d$ Dirac fermion, and we will use this assumption to explore other possible behaviors of the boundary.

The goal of this section is to study the quantum phase transition described by the following field theory:

$$\begin{aligned} \mathcal{L} &= \bar{\psi}\gamma_\mu(\partial_\mu - ia_\mu)\psi + \frac{1}{e^2}f_{\mu\nu}^2 \\ &+ |(\partial_\mu - ika_\mu)\phi|^2 + r|\phi|^2 + g|\phi|^4, \end{aligned} \tag{4.2}$$

with tuning parameter r, arbitrary integer k, Dirac fermion ψ and complex scalar bosonic field ϕ which both couple to the same $(2+1)d$ dynamical $U(1)$ gauge field a_μ. The boson ϕ can be viewed as the $4k$-fold vortex of the Fu-Kane superconductor *bound* with another extra degree of freedom (d.o.f). For even integer k, ϕ is the bound state of $4k$-vortex and an extra boson; while if k is odd, ϕ must contain an extra fermion that transforms in the same way as ψ under $\mathcal{T}$, but neutral under the dynamical gauge field a_μ. The tuning parameter r can be tuned by the mass gap of this extra d.o.f.

Obviously this theory has two phases: when r is sufficiently large, ϕ is gapped, and based on our assumption the boundary is described by Eq. (4.1), and it is dual to a noninteracting Dirac fermion; while when r is negative and large, ϕ condenses, and it drives the boundary into a topological order with *gapless* Dirac fermion ψ. We are

interested in the quantum phase transition between these two phases. Notice that when ϕ condenses, ψ is not automatically gapped, *i.e.* there is no Yukawa type of coupling such as $\phi^* \psi^t \gamma^0 \psi$ in the Lagrangian, which is forbidden by the gauge symmetry for $k \neq 2$. It is easy to show that there is no other obviously relevant couplings in Eq. (4.2) allowed by the gauge symmetry.

Our goal is to calculate the scaling dimension of gauge invariant order parameters and other universal quantities at the quantum critical point $r = 0$. Let us take the limit $k \to +\infty$ first. In this limit, the gauge field dynamics is completely dominated by its coupling to the scalar field, and the fermions will effectively decouple from the gauge field. More precisely, the fermion decouples from the gauge field at the energy scale below $k^2 e^2$. This effect becomes explicit after we rescale $k a_\mu = \tilde{a}_\mu$. In this case the theory becomes a standard bosonic QED with gauge field $\tilde{a}_\mu$, and it is well-known that this theory is dual to a $3d$ XY transition [119, 120]. We assume that we know *everything* about the $3d$ XY transition, including all of its critical exponents, the scaling dimension of all the composite operators, the operator product expansion, and most importantly, the universal boson conductivity $\tilde{\sigma}$ [126, 127], which we will take as a dimensionless constant, assuming the boson carries charge-1. All these information can be obtained by numerically studying the $3d$ XY transition only. For example, numerically the critical exponent ν has been confirmed to be very close to (slightly larger than) $2/3$ [128]. The universal conductivity of the $3d$ XY transition has also been studied with various methods [129, 130, 131, 132]. Recent progresses based on conformal bootstrap have determined the value of $\tilde{\sigma}$ very precisely [133], which is highly consistent with the numerical results [131, 132]

4.1.1 Scaling dimension of $\mathcal{T}$-breaking order parameter

Time-reversal symmetry $\mathcal{T}$ is the key symmetry that protects the $3d$ TI. Let us compute the scaling dimension of the time-reversal symmetry breaking order parameter $\bar{\psi}\psi = \psi^\dagger\gamma^0\psi$. In the large$-k$ limit, because ψ basically decouples from the gauge field (as we argued above), the scaling dimension of $\bar{\psi}\psi$ is the same as that of the free fermion $\Delta[\bar{\psi}\psi] = 2$. The correction to this scaling dimension comes from the gauge fluctuation a_μ, thus we need to know the photon propagator $G^a_{\mu\nu}$ in the large-k limit.

In the large$-k$ limit, since this quantum phase transition belongs to the $3d$ XY universality class, we assume that the universal conductivity of the boson degrees of freedom which carries the global $U(1)$ symmetry of the $3d$ XY transition is a known dimensionless constant $\tilde{\sigma}$. We know that in the momentum-frequency space of the Euclidean spacetime, the Kubo formula gives us the following relation between the correlation function of the boson current $J^\mu(p)$ and the universal conductivity $\tilde{\sigma}$:

$$\langle J_\mu(p)\ J_\nu(-p)\rangle = \tilde{\sigma}|p|\left(\delta_{\mu\nu} - \frac{p_\mu p_\nu}{p^2}\right). \tag{4.3}$$

Then because the boson current $J_\mu = \frac{k}{2\pi}\epsilon_{\mu\nu\rho}\partial_\nu a_\rho$, the photon propagator at the quantum critical point in the large$-k$ limit reads

$$G^a_{\mu\nu}(p) = \frac{\tilde{\sigma}(2\pi)^2}{k^2|p|}\left(\delta_{\mu\nu} - \frac{p_\mu p_\nu}{p^2}\right). \tag{4.4}$$

Or in other words Eq. (4.2) reduces to a bosonic QED in the large-k limit, and Eq. (4.4) describes the fully dressed gauge field propagator. Throughout the paper we will choose the gauge $\partial_\mu a_\mu = 0$.

The rest of the calculation is pretty standard: because the photon propagator carries a factor $1/k^2$, a systematic expansion controlled by small factor $1/k^2$ can be carried out.

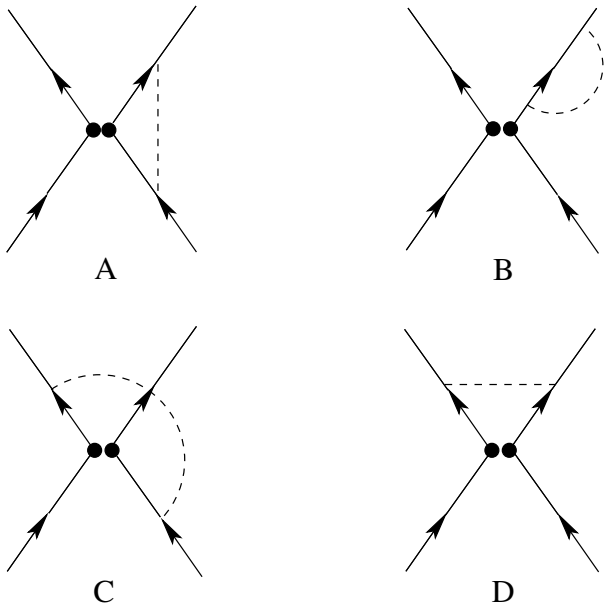

Figure 4.1: The Feynman diagrams that will contribute to the the scaling dimension of the four fermion interaction term at the $1/k^2$ order.

By combining the vertex correction and the wave function renormalization together, the scaling dimension of $\bar{\psi}\psi$ at the $1/k^2$ order reads

$$\Delta[\bar{\psi}\psi] = 2 - \frac{16\tilde{\sigma}}{3k^2}. \tag{4.5}$$

A similar calculation of scaling dimension of fermion bilinear operators of the standard QED_3 with large-N flavors of fermions can be found in Ref. [134, 135, 136]. But let us stress that in our case we only have one flavor of fermion and boson field each.

4.1.2 Scaling dimension of four-fermion interaction term

A weak short range four-fermion interaction would be irrelevant for a $(2+1)d$ gapless Dirac fermion. However, gauge fluctuation potentially could change the scaling dimension of the four-fermion interactions, and make them relevant. In our system Eq. (4.2),

because there is only one flavor of Dirac fermion ψ, there is only one allowed four fermion interaction term without spatial derivatives:

$$g(\bar{\psi}\psi)^2 = -\frac{1}{3}g(\bar{\psi}\gamma_\mu\psi)^2. \tag{4.6}$$

The scaling dimension of this four fermion interaction term can again be calculated with a $1/k^2$ expansion. All the Feynman diagrams that contribute at this $1/k^2$ order are listed in Fig. 4.1. The final result is

$$\Delta[(\bar{\psi}\psi)^2] = 4 + \frac{16\tilde{\sigma}}{3k^2}. \tag{4.7}$$

Thus the gauge fluctuation makes the four-fermion interaction term even more irrelevant than it is at the free Dirac fermion CFT. This calculation supports that Eq. (4.2) describes a continuous quantum phase transition, since the four fermion interaction is likely not rendered relevant by gauge fluctuation for any k at the quantum critical point $r = 0$.

4.1.3 Universal electrical conductivity

As was pointed out in Ref. [116, 117, 118], in Eq. (4.2), a 2π flux quantum of a_μ carries half electric charge. Thus the physical electric current density at the $2d$ surface reads $J^e_\mu = \frac{1}{4\pi}\epsilon_{\mu\nu\rho}\partial_\nu a_\rho$. The electrical conductivity σ^e is encoded in the Euclidean space-time correlation function of the current operator:

$$\langle J^e_\mu(p)\ J^e_\nu(-p)\rangle = \frac{\sigma^e}{e^2/\hbar}|p|\left(\delta_{\mu\nu} - \frac{p_\mu p_\nu}{p^2}\right). \tag{4.8}$$

When ϕ is gapped ($r > 0$), the system is described by QED with $N = 1$ flavor of Dirac fermion ψ, which by our assumption is dual to a noninteracting Dirac fermion which is

not coupled to any dynamical gauge field. Thus this phase with $r > 0$ is a semimetal with universal electrical conductivity $\sigma^e = \frac{1}{16}\frac{e^2}{\hbar}$. The quantum phase transition we are studying is a transition from an electrical semimetal to an electrical insulator, although the insulator phase is also gapless.

Right at the quantum critical point, the electrical conductivity must be a different universal value. Because we already know that in the large-k limit the photon a_μ propagator is given by Eq. (4.4), using the photon propagator, we can compute the physical electric current-current correlation function:

$$\begin{aligned} \langle J^e_\mu(p)\ J^e_\nu(-p)\rangle &= \frac{1}{(4\pi)^2} p^2 G^a_{\mu\nu}(p) \\ &= \frac{\tilde{\sigma}}{4k^2}|p|\left(\delta_{\mu\nu} - \frac{p_\mu p_\nu}{p^2}\right). \end{aligned} \tag{4.9}$$

Comparing with Eq. (4.8), we conclude that in the large$-k$ limit the universal electrical conductivity at the quantum critical point reads

$$\sigma^e = \frac{\tilde{\sigma}}{4k^2}\frac{e^2}{\hbar}. \tag{4.10}$$

The leading correction to this value must be at the $1/k^4$ order, which comes from the correction to the a_μ propagator from the Dirac fermion ψ.

If the time-reversal symmetry $\mathcal{T}$ is broken at the $2d$ boundary, *i.e.* the system develops a nonzero expectation value of $\bar{\psi}\psi$, the Hall conductivity at the quantum critical point $r = 0$ will also be at order $\sim \frac{1}{k^4}\frac{e^2}{\hbar}$.

4.1.4 Self-duality

In this subsection we will see that Eq. (4.2) has a (quasi-)self-dual structure. The duality transformation of the second line of Eq. (4.2) is rather standard, it is simply the particle-vortex duality:

$$\mathcal{L}_b = |(\partial_\mu - ib_\mu^{(1)})\Phi|^2 + \tilde{r}|\Phi|^2 + \tilde{g}|\Phi|^4 + \frac{ik}{2\pi} a \wedge db^{(1)}, \tag{4.11}$$

where Φ can be viewed as the unit vortex field of ϕ, and it is bound with $2\pi k$ flux of a_μ, because ϕ carries charge-k under a_μ. The duality of the first line of Eq. (4.2) requires the newly developed (hypothesized) duality in Ref. [116, 117, 118]:

$$\mathcal{L}_f = \bar{\chi}\gamma_\mu(\partial_\mu - ib_\mu^{(2)})\chi + \frac{i}{4\pi} a \wedge db^{(2)}, \tag{4.12}$$

where now χ transforms under time-reversal as $\mathcal{T} : \chi \to i\sigma^y\chi$. If $\mathcal{L}_b$ in Eq. (4.11) is ignored, integrating out a_μ in $\mathcal{L}_f$ will gap out $b_\mu^{(2)}$, thus $\mathcal{L}_f$ only has a free Dirac fermion χ in the infrared, which corresponds to the case studied in Ref. [116, 117, 118]

In our case, due to the existence of the bosonic matter field, integrating out a_μ induces the following constraint:

$$b_\mu^{(2)} = -2kb_\mu^{(1)} = -2kb_\mu. \tag{4.13}$$

Thus the final dual theory reads

$$\begin{aligned} \mathcal{L}_{dual} &= \bar{\chi}\gamma_\mu(\partial_\mu + i2kb_\mu)\chi + \cdots \\ &+ |(\partial_\mu - ib_\mu)\Phi|^2 + \tilde{r}|\Phi|^2 + \tilde{g}|\Phi|^4. \end{aligned} \tag{4.14}$$

Here $\tilde{r} \sim -r$: when $\tilde{r} < 0$, Φ is condensed, which is dual to the disordered phase of ϕ, and low energy physics of this phase is either described by a QED with $N = 1$ flavor of fermion ψ, or a single gapless Dirac fermion χ; When $\tilde{r} > 0$, Φ is disordered, and the low energy physics of this phase is described by either a QED with $N = 1$ flavor of fermion χ, or a single gapless Dirac fermion ψ (which is coupled to a gapped discrete gauge field). The dual theory Eq. (4.14) is very similar to the original theory Eq. (4.2), the only difference is that now it is the fermionic degree of freedom that carries a large gauge charge.

Again, in the large-k limit, Lagrangian Eq. (4.14) describes a $3d$ XY transition, because after rescaling $kb_\mu = \tilde{b}_\mu$, Φ is effectively neutral under $\tilde{b}_\mu$ in the large-k limit. Again, in the large-k limit, the propagator of gauge field b_μ can be calculated exactly, based on the observation that the fermion current $J^\psi_\mu = \bar{\psi}\gamma_\mu\psi = \frac{1}{4\pi}\epsilon_{\mu\nu\rho}\partial_\nu b^{(2)}_\mu = -\frac{k}{2\pi}\epsilon_{\mu\nu\rho}\partial_\nu b_\mu$. In the large-$k$ limit the correlation function of J^ψ_μ can be computed exactly because in this limit ψ decouples from a_μ, and the correlation function of J^ψ in this limit is well-known:

$$\langle J^\psi_\mu(p)\ J^\psi_\nu(-p)\rangle = \frac{1}{16}|p|\left(\delta_{\mu\nu} - \frac{p_\mu p_\nu}{p^2}\right), \tag{4.15}$$

this implies that photon b_μ propagator in the large-k limit reads

$$G^b_{\mu\nu} = \frac{\pi^2}{4k^2|p|}\left(\delta_{\mu\nu} - \frac{p_\mu p_\nu}{p^2}\right). \tag{4.16}$$

In this dual theory, operator $\bar{\chi}\chi$ breaks time-reversal symmetry, and hence it can be identified as $\bar{\psi}\psi$ in the original theory Eq. (4.2) [125]. Thus the scaling dimension of $\bar{\chi}\chi$ is also

$$\Delta[\bar{\chi}\chi] = 2 - \frac{16\tilde{\sigma}}{3k^2}. \tag{4.17}$$

4.1.5 Critical exponent

We would also like to calculate the scaling dimension of the tuning parameter r in Eq. (4.2), which is identified as $\tilde{r}$ in the dual theory, thus the composite operator $|\phi|^2$ is equivalent to $|\Phi|^2$.

To calculate the scaling dimension of $\tilde{r}$, one strategy is to expand Eq. (4.14) at the Gaussian fixed point of Φ and perform a combined $\epsilon = 4 - D$ and $1/k^2$ expansion. Although this calculation is straightforward, we hope to expand everything at the $3d$ XY fixed point (which we assume to know everything about) in the large-k limit. In order to carry out the renormalization group (RG) calculation, we make use of the operator product expansion (OPE) in the momentum space:

$$\begin{aligned} & \left(\frac{1}{2}\tilde{r}|\Phi|^2 J_\mu^\Phi(\boldsymbol{p}) J_\nu^\Phi(-\boldsymbol{p})\right) G_{\mu\nu}^b(\boldsymbol{p}) \\ \sim \quad & \left(\frac{1}{2}\tilde{r}|\Phi|^2 \frac{C}{p^2}\left(\delta_{\mu\nu} - \frac{p_\mu p_\nu}{p^2}\right)\right) G_{\mu\nu}^b(\boldsymbol{p}) \\ = \quad & \left(\tilde{r}|\Phi|^2 \frac{C}{|p|^3}\right) \frac{\pi^2}{4k^2}. \end{aligned} \tag{4.18}$$

$J_\mu^\Phi(\boldsymbol{p})$ is the current operator of field Φ in Eq. (4.14). The meaning of this OPE is that, when the momentum $\boldsymbol{p}$ of J_μ^Φ and the photon propagator is much larger than the momentum of $|\Phi|^2$, the correlation function between the composite operator $|\Phi|^2 J_\mu^\Phi(\boldsymbol{p}) J_\nu^\Phi(-\boldsymbol{p})$ and another operator can be approximated by the correlation between $|\Phi|^2 \frac{C}{|p|^2}\left(\delta_{\mu\nu} - \frac{p_\mu p_\nu}{p^2}\right)$ and that operator. We have checked this OPE by comparing the two Feynman diagrams in Fig. 4.2, and the correlation function $\langle |\Phi^2|_{\boldsymbol{q}} J_\mu^\Phi(\boldsymbol{p}) J_\nu^\Phi(-\boldsymbol{p}) |\Phi^2|_{-\boldsymbol{q}}\rangle$ indeed scales as $\sim \langle |\Phi^2|_{\boldsymbol{q}}\ |\Phi^2|_{-\boldsymbol{q}}\rangle \frac{1}{|p|^2}\left(\delta_{\mu\nu} - \frac{p_\mu p_\nu}{p^2}\right)$ when $|\boldsymbol{p}| \gg |\boldsymbol{q}|$.

In this OPE, the dimensionless number C only depends on the $3d$ XY universality class, and as we stated we assume that it can be determined by studying the OPE of the

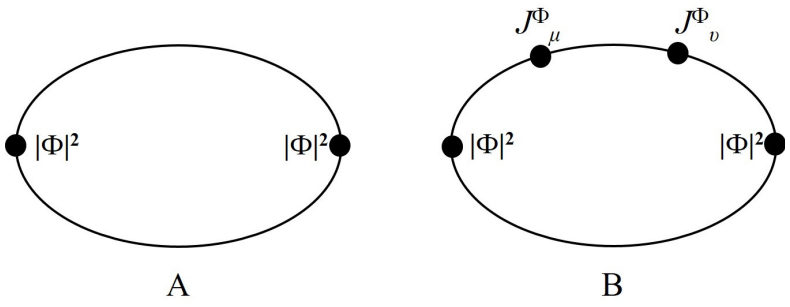

Figure 4.2: The diagram on the right hand side is the correlation function $\langle|\Phi^2|_{\boldsymbol{q}} J^{\Phi}_{\mu}(\boldsymbol{p}) J^{\Phi}_{\nu}(-\boldsymbol{p})|\Phi^2|_{-\boldsymbol{q}}\rangle$. When $|\boldsymbol{p}| \gg |\boldsymbol{q}|$ it scales as the left hand side correlation function times factor $\frac{1}{|p|^2}\left(\delta_{\mu\nu} - \frac{p_\mu p_\nu}{p^2}\right)$.

$3d$ XY transition only, through for instance the $1/N$ expansion as in Ref. [137]. Although the dimensionless number C is yet to determine, the $1/|\boldsymbol{p}|^2$ scaling of this OPE is known, because the scaling dimension of the boson current J^{Φ}_{μ} is $\Delta[J^{\Phi}_{\mu}] = 2$, which at the $3d$ XY fixed point is unrenormalized compared with the free boson theory because it is a conserved current.

After the standard momentum shell RG calculation, *i.e.* integrating out the degrees of freedom with momentum $\boldsymbol{p}$ between $b\Lambda < |p| < \Lambda$, the OPE above will contribute a correction to $\tilde{r}|\Phi|^2$ that is proportional to $\ln(1/b)$. Now we can conclude that the RG equation for $\tilde{r}$ to the $1/k^2$ order reads

$$\frac{d\tilde{r}}{d\ln(1/b)} = \left(\Delta_{xy} + \frac{C}{8k^2}\right)\tilde{r}, \tag{4.19}$$

which determines the scaling dimension of $\tilde{r}$. Here Δ_{xy} is the scaling dimension of $\tilde{r}$ at the $3d$ XY universality class, which is very close to $3/2$ [128].

4.1.6 Summary

In this work we did our best to study the the quantum phase transition described in Eq. (4.2), with its dual Lagrangian described by Eq. (4.14). The self-dual nature of this transition allows us to calculate many quantities in a controlled expansion with $1/k^2$. But it is possible that, with small enough k, the transition becomes first order.

The same techniques used in this work can be applied to other field theories as well. For instance QED_3 with two flavors of Dirac fermions, and one flavor of fermion carries gauge charge-1, while the other flavor of fermion carries a much larger gauge charge$-k$. A similar $1/k^2$ expansion can also be applied to this theory as well.

Ref. [138] has applied the mirror symmetry [139, 140, 141] (duality between supersymmetric field theories) to the half-filled Landau level [142], which is a system closely related to the boundary of $3d$ TI [116, 117, 118]. Previous study [143] also indicates that the mirror symmetry is related to the "deconfined QCP" [123, 124]. We suspect the QCP discussed here may also have an interesting supersymmetric version. We will leave this to future study.

4.2 Stable Interacting $(2+1)d$ Conformal Field Theories at the Boundary of a class of $(3+1)d$ Bosonic Symmetry Protected Topological Phases

A symmetry protected topological (SPT) phase [25, 26] must, by definition, have a boundary state with a nontrivial spectrum when the system including the boundary preserves certain global symmetries. Many $(2+1)d$ SPT states can be described with a similar Chern-Simons theory [31] as the quantum Hall states, their $(1+1)d$ boundary states are therefore relatively easy to understand. Thus it is more challenging to un-

derstand the $(3+1)d$ SPT states, whose boundary states can have much richer physics under strong interaction. The following three types of $(2+1)d$ states may exist at the boundary of a $(3+1)d$ SPT phase:

1) An ordered phase that spontaneously breaks the global symmetry and hence has degenerate ground states;

2) A $(2+1)d$ topologically ordered phase with topological degeneracy;

3) A stable gapless phase which is described by a conformal field theory (CFT).

Possibilities *1* and *2* have both been studied quite extensively in the last few years, for both fermionic and bosonic SPT states [110, 111, 112, 13, 113, 32, 63], but there is little study about the third possibility, except for the well-known simplest case of noninteracting topological insulators/superconductors. In this work we explore the third possibility of SPT phases: a stable $(2+1)d$ *interacting* conformal field theory (CFT) at the boundary of a $(3+1)d$ SPT state. This CFT should be stable against any symmetry allowed perturbations, By "stable" we mean that all perturbations allowed by symmetry should be irrelevant (in the renormalization group sense) at this fixed point.

We will take the field theory description of $(3+1)d$ bosonic SPT states, which is a nonlinear sigma model (NLσM) with a Θ-term in the $(3+1)d$ bulk spacetime. The value $\Theta = 2\pi$ corresponds to the stable fixed point of the SPT phase. This formula was used to describe and classify bosonic SPT states in Ref. [32, 35, 33, 63]. With $\Theta = 2\pi$ in the $(3+1)d$ bulk, the $(2+1)d$ boundary is described by a NLσM with a Wess-Zumino-Witten (WZW) term with level $k = 1$. In Ref. [32, 35, 63], the target space of the NLσM was the four dimensional sphere S^4, a WZW term can be defined based on the fact that the homotopy group $\pi_4[S^4] = \mathbb{Z}$. Topological phases with the same anomaly as this field theory under various anisotropies were discussed thoroughly in Ref. [32, 63].

The presence of a WZW term is known to drastically change the behavior of the NLσMs in lower dimensions. In particular, inw $(0+1)d$ a WZW term may lead to

degenerate ground states; in (1+1)d a WZW term drives the NLσM towards a conformally invariant fixed point [50, 51]. An explicit renormalization group (RG) calculation in $(1+1)d$ demonstrates that this fixed point is stable and occurs at a finite value of the NLσM coupling constant [50].

However, unlike these $(1+1)d$ analogues, it is difficult to perform a controlled calculation for NLσMs with a WZW term in $(2+1)d$. There are two standard controlled RG calculations for NLσMs in $3d$ Euclidean space-time: (1) Generalizing the space-time dimensions to $d = 2+\epsilon$, perform an expansion with "small" parameter ϵ, and then extrapolate the result to $\epsilon \to 1$; (2) Generalizing the target manifold to S^N with $N \gg 1$, and perform an expansion with small parameter $1/N$. But both of these standard approaches fail in present context because of the WZW term. The first method is questionable in this context because the topological term can only be defined in an integer number of space-time dimensions. As for the second method, the fact that $\pi_d[S^N] = 0$ for $d < N$ implies that a naive generalization from S^4 to S^N would completely miss the contribution from the WZW term. An attempt of calculating the effect of the WZW term in $(2+1)d$ was made in Ref. [144], but the calculation there was uncontrolled for precisely the reasons we mentioned above.

However, we suspect that these difficulties may be only technical in nature. We expect that the WZW term in $(2+1)d$ may still lead to a stable conformally invariant fixed point at a finite value of the coupling. This expectation is (indirectly) supported by recent quantum Monte Carlo simulation on a $2d$ lattice interacting fermion model, where a continuous quantum phase transition described by a $(2+1)d$ NLσM with a topological $\Theta-$term was found, and Θ was the tuning parameter for this transition [145, 146]. The numerical data suggest that right at $\Theta = \pi$ this theory is a $(2+1)d$ CFT with gapless bosonic excitations while no gapless fermion excitations. A field theory with $\Theta = \pi$ can be viewed as another field theory with a WZW term under symmetry breaking. Thus the

results in Ref. [145, 146] actually suggest that the disordered phase of a $(2+1)d$ NLσM with a WZW term can also be a stable CFT.

Besides these recent progresses, earlier studies of the deconfined quantum critical point [123, 124] also suggested that a WZW term in a $(2+1)d$ NLσM could lead to a stable CFT. It was conjectured that the deconfined quantum critical point corresponds to the quantum disordered phase of the $SO(5)$ NLσM with a WZW term at level-1 [147], and the $SO(5)$ symmetry could emerge at this CFT.

The goal of this work is to analytically study the effects of the WZW term on NLσMs in $(2+1)d$ space-time. In section 4.2.1 we first take a large-N generalization of the boundary field theory of $(3+1)d$ SPT states which always permits a WZW term in $(2+1)d$ space-time. This theory has a controlled large-N limit without the WZW term. In section 4.2.2 we first argue that the large-N and large-k generalization alone is insufficient to provide a reliable study of the quantum disordered phase, with presence of the WZW term. Then we demonstrate that a combined large-N, large-k and $\epsilon-$generalization enables us to identify a stable fixed point in the quantum disordered phase, which corresponds to a $(2+1)d$ interacting CFT. In section 4.2.3, we will briefly discuss the connection of this work to the "hierarchy problem" in high energy physics.

4.2.1 Lagrangian and Method

We would like to find a NLσM with a WZW term that admits a controlled approximation scheme for evaluating the RG equations (beta functions). This means that the target space $\mathcal{M}$ should have an acceptable large-N generalization that permits a WZW term in $(2+1)d$. One example that satisfies these constraints is the Grassmannian manifold:

$$\mathcal{M}(n,N) = \frac{U(N)}{U(n)\times U(N-n)}\ , \tag{4.20}$$

For any $n \geq 2$, $N \geq n+2$, $\pi_4[\mathcal{M}] = \mathbb{Z}$ while $\pi_3[\mathcal{M}] = 0$, thus a WZW term can be defined in $(2+1)d$ for $\mathcal{M}$. For $n = 1$, this manifold is the familiar CP^{N-1} manifold, and later we will argue that even for $n = 1$ a similar term in the action may also be defined.

The total dimension of $\mathcal{M}$ scales linearly with N instead of N^2 with large-N and fixed n, thus without the WZW term, a NLσM defined with target manifold $\mathcal{M}$ does not have the infinite planar diagram problem that usually occurs in matrix models. The entire action in (2+1)d Euclidean space-time that we will study is

$$\mathcal{S} = \int d^2x\, d\tau\ \frac{1}{g}\mathrm{tr}(\partial_\mu \mathcal{P}\partial^\mu \mathcal{P}) + \int_0^1 du \int d^2x\, d\tau\ \frac{i2\pi k}{256\pi^2}\varepsilon^{\mu\nu\rho\lambda}\,\mathrm{tr}(\tilde{\mathcal{P}}\partial_\mu\tilde{\mathcal{P}}\partial_\nu\tilde{\mathcal{P}}\partial_\rho\tilde{\mathcal{P}}\partial_\lambda\tilde{\mathcal{P}}). \quad (4.21)$$

The basic field $\mathcal{P} \in \mathcal{M}(n, N)$ is an $N \times N$ hermitian matrix and it can be represented in the form

$$\mathcal{P} = V\Omega V^\dagger, \ \ \Omega \equiv \begin{pmatrix} \mathbf{1}_{n\times n} & \mathbf{0}_{n\times(N-n)} \\ \\ \mathbf{0}_{(N-n)\times n} & -\mathbf{1}_{(N-n)\times(N-n)} \end{pmatrix} \quad (4.22)$$

where $V \in U(N)$. The matrix $\mathcal{P}$ satisfies $\mathcal{P}^\dagger = \mathcal{P}$, $\mathcal{P}^2 = I$, and $\mathrm{tr}(\mathcal{P}) = 2n - N$. (When $N = 2n$, $\mathrm{tr}(\mathcal{P}) = 0$, and this was the case studied in Ref. [33]). Note that when $N = 2$ and $n = 1$, $\mathcal{M}(n, N)$ is $SU(2)/U(1) = S^2$, and $\mathcal{P}$ can always be represented as $\mathcal{P} = \boldsymbol{n}\cdot\boldsymbol{\sigma}$, where $\boldsymbol{n}$ is a three component unit vector, and $\boldsymbol{\sigma}$ are the Pauli matrices.

$\tilde{\mathcal{P}}(\boldsymbol{x}, \tau, u)$ is an extension of $\mathcal{P}(\boldsymbol{x}, \tau)$ into the auxiliary fourth dimension parameterized by $u \in [0, 1]$. This extended field satisfies

$$\tilde{\mathcal{P}}(\boldsymbol{x}, \tau, 1) = \mathcal{P}(\boldsymbol{x}, \tau), \quad \tilde{\mathcal{P}}(\boldsymbol{x}, \tau, 0) = \Omega. \quad (4.23)$$

For the $(2+1)d$ boundary physics described by $\mathcal{P}(x, \tau)$ to be independent of the chosen

extension $\tilde{\mathcal{P}}(x,\tau,u)$, the coefficient k must be quantized. This action Eq. (4.21) obviously has a global $SU(N)$ symmetry: $\mathcal{P} \to U^\dagger \mathcal{P} U$, where $U \in SU(N)$ [1].

Our general theory Eq. (4.21) has the following connections with the previously studied theories:

1) In order to study $(3+1)d$ bosonic SPT states, Ref. [32, 63] introduced a NLσM with target space S^4. S^4 can also be written as a Grassmannian: $S^4 \sim \frac{Sp(4)}{Sp(2)\times Sp(2)}$. If written in terms of $\mathcal{P} = \boldsymbol{n}\cdot\boldsymbol{\Gamma}$ (where $\boldsymbol{n}$ is the five component unit vector introduced in Ref. [32, 63] and Γ^a are the five 4×4 anticommuting Gamma matrices), the topological term of Eq. (4.21) is precisely the same as the one in Ref. [32, 63]. Thus the field theory of Ref. [32, 63] can be viewed as our model with $N = 2n = 4$ after breaking the SU(4) down to smaller symmetries considered therein.

2) Ref. [148] demonstrated that for $n = 1$, the topological term discussed above can be generated by coupling the CP^{N-1} manifold to $(2+1)d$ Dirac fermions with SU(N) symmetry. Ref. [149] used this fact, and derived the effective field theory for the bosonic sector for $N = 2n = 2$, which corresponds to the boundary of the $(3+1)d$ topological superconductor with symmetry $SU(2)\times\mathcal{T}$ ($\mathcal{T}$ being time-reversal). Ref. [149] also argued that with the full $SU(2)\times\mathcal{T}$ symmetry, this boundary theory cannot be gapped out, which implies that it could be an interacting CFT. Thus our theory with large-N and $n = 1$ can also be viewed as a formal generalization of the case studied in Ref. [149] [2].

Instead of working with Eq. (4.21) directly, we will use a parametrization that is more easily amenable to a large-N analysis. This parametrization was introduced in

[1] To be more precise, the global symmetry of this system is PSU(N)=$SU(N)/Z_N = U(N)/U(1)$. This is because any configuration of $\mathcal{P}$ does not transform at all under the U(1) subgroup of U(N), or the Z_N center of $SU(N)$. For example, for $N = 2$ and $n = 1$, the manifold $\mathcal{M}$ is S^2, and a NLσM defined on S^2 should have symmetry SO(3) = SU(2)/Z_2.

[2] We do note that for $N = 2n = 2$, the space-time integral of the topological term is quantized, *i.e.* it is the Hopf term, while for larger N this term is not quantized.

Ref. [150, 151]. We define a collection of n orthonormal complex vectors

$$\{\vec{\varphi}_\alpha\}_{\alpha=1,2,...,n} \ , \quad \vec{\varphi}_\alpha^\dagger \cdot \vec{\varphi}_\beta = \delta_{\alpha\beta}. \tag{4.24}$$

The order parameter $\mathcal{P}$ can be written as

$$\mathcal{P}_{ij} = 2\sum_{\alpha=1}^{n} \varphi_\alpha^i \varphi_\alpha^{j\dagger} - \delta^{ij} \tag{4.25}$$

with $i, j = 1, ..., N$. This definition is invariant under local transformations of the form

$$\varphi_\alpha^i \to \varphi_\beta^i \, \mathrm{U}_\alpha{}^\beta(x) \tag{4.26}$$

with $\mathrm{U} \in U(n)$. Hence the action in terms of the φ_α^i will have a $U(n)$ gauge symmetry, under which each φ^i transforms as a fundamental n-dimensional representation (and $i = 1, ..., N$ serves as a flavor label).

Explicitly, we may observe that the quantity

$$a \equiv -id\varphi^\dagger \cdot \varphi = -i\sum_{i=1}^{N} d\varphi_\alpha^{i\dagger}\varphi_\beta^i \tag{4.27}$$

transforms as a $U(n)$ gauge field. If we then define the field strength 2-form $f \equiv da - ia\wedge a$, we find

$$\mathrm{tr}\left(\tilde{\mathcal{P}}\, d\tilde{\mathcal{P}} \wedge d\tilde{\mathcal{P}} \wedge d\tilde{\mathcal{P}} \wedge d\tilde{\mathcal{P}}\right) = -32 \ \mathrm{tr}\,(f \wedge f) \ . \tag{4.28}$$

The right-hand side of Eq. (4.28) is a total derivative in (3+1)d, and hence its integral can be reduced to the (2+1)d integral of a local integrand, namely a $U(n)$ Chern-Simons term.

The right hand side of Eq. (4.28) can also be defined even for $n = 1$ (which corresponds

to the case with $\mathcal{M} = \mathrm{CP}^{N-1}$), and the integral of this term on T^4 is quantized, although its integral on S^4 is trivial. This is analogous to the topological response theory $\sim \boldsymbol{E} \cdot \boldsymbol{B}$ of $3d$ topological insulator [55].

Following Ref. [150, 151], we block-decompose the φ_α^i fields as

$$\varphi_\alpha{}^i = (\Phi_\alpha^\beta \; ; \;\; \phi_\alpha^I)^t \tag{4.29}$$

where $I = n+1 \cdots N$. Then we can use local $U(n)$ transformations to make the n-by-n block Hermitian (fix the gauge [151]): $\Phi = \Phi^\dagger$, which eliminates all the continuous gauge degrees of freedom. The constraint Eq. (4.24) on φ_α^i now takes the form:

$$\Phi = (I - \phi^\dagger \cdot \phi)^{1/2} = I - \tfrac{1}{2}\phi^\dagger \cdot \phi - \tfrac{1}{8}(\phi^\dagger \cdot \phi)^2 + \mathcal{O}(\phi^6) \; . \tag{4.30}$$

Then we find $\mathrm{tr}[\tilde{\mathcal{P}}(d\tilde{\mathcal{P}})^4] = 32\,\mathrm{tr}\left[(d\phi^\dagger \cdot d\phi)(d\phi^\dagger \cdot d\phi)\right] + \mathcal{O}(\phi^6)$, where we suppress the wedge product for notational convenience.

Therefore, after carrying out this procedure (and trivially rescaling the coupling as $g \to g/8$), we obtain an alternative form of Eq. (4.21) as a local (2+1)d action in terms of unconstrained boson fields. The field ϕ is a $n \times (N-n)$ matrix, it has exactly the same number of degrees of freedom as the target manifold $\mathcal{M}$, thus it does not have any continuous gauge freedom. The Lagrangian density takes the form

$$\mathcal{L} = \mathcal{L}_{\mathrm{NL}\sigma\mathrm{M}} + \mathcal{L}_{\mathrm{WZW}}. \tag{4.31}$$

After rescaling $\phi \to \sqrt{g}\phi$, we find the Euclidean Lagrangian density $\mathcal{L}_{\mathrm{NL}\sigma\mathrm{M}}$

$$\mathcal{L}_{\mathrm{NL}\sigma\mathrm{M}} = \mathrm{tr}\left(\partial_\mu \phi^\dagger \cdot \partial_\mu \phi\right)$$

$$
\begin{aligned}
&+ \quad \tfrac{1}{4} g \mathrm{tr} \left[\left(\partial_\mu \phi^\dagger \cdot \phi + \phi^\dagger \cdot \partial_\mu \phi \right)^2 \right] \\
&+ \quad \tfrac{1}{4} g' \mathrm{tr} \left[\left(\partial_\mu \phi^\dagger \cdot \phi - \phi^\dagger \cdot \partial_\mu \phi \right)^2 \right] \\
&+ \quad \tfrac{1}{4} g^2 \mathrm{tr} \left[2 (\phi^\dagger \cdot \phi)(\partial_\mu \phi^\dagger \cdot \phi)(\phi^\dagger \cdot \partial_\mu \phi) \right] \\
&+ \quad \tfrac{1}{4} g^2 \mathrm{tr} \left[(\phi^\dagger \cdot \phi)(\partial_\mu \phi^\dagger \cdot \phi)(\partial_\mu \phi^\dagger \cdot \phi) \right] \\
&+ \quad \tfrac{1}{4} g^2 \mathrm{tr} \left[(\phi^\dagger \cdot \phi)(\phi^\dagger \cdot \partial_\mu \phi)(\phi^\dagger \cdot \partial_\mu \phi) \right] \\
&+ \quad \mathcal{O}(g^3 \phi^8). \qquad (4.32)
\end{aligned}
$$

The initial value of g' equals to g, but under renormalization group flow it will be an independent parameter from g. If we add more symmetry-allowed terms in the original theory, they will only lead to obviously irrelevant perturbations in the Lagrangian expanded in terms of ϕ.

After integrating over the u direction in Eq.(4.21), the WZW term now reads

$$
\begin{aligned}
\mathcal{L}_{\mathrm{WZW}} = i \frac{k g^2}{4\pi} \varepsilon^{\mu\nu\rho} \mathrm{tr} \left[\left(\phi^\dagger \cdot \partial_\mu \phi \right) \left(\partial_\nu \phi^\dagger \cdot \partial_\rho \phi \right) \right] - \\
i \frac{k}{4\pi} g^3 \varepsilon^{\mu\nu\rho} \frac{1}{3} \mathrm{tr} \left[\left(\partial_\mu \phi^\dagger \cdot \phi \right) \left(\partial_\nu \phi^\dagger \cdot \phi \right) \left(\partial_\rho \phi^\dagger \cdot \phi \right) + h.c. \right] \\
+ \mathcal{O}(k g^4 \phi^8) \, . \qquad (4.33)
\end{aligned}
$$

It is convenient to adopt a double-line notation for the Feynman diagrams, where a solid line represents $I = n+1, \cdots N$, and a dashed line represents $\alpha = 1, \cdots n$. We

first compute the ordinary RG equation in the large-N limit without the WZW term. We will calculate the beta function with $k = 0$ in arbitrary dimension d and insert the physical value $d = 3$. In terms of the dimensionless coupling $\tilde{g} = \Lambda^{d-2} g$ and $\tilde{g}' = \Lambda^{d-2} g'$ ($\Lambda \sim 1/l$ is the ultraviolet momentum cut-off), the beta functions in the large-N limit for the ordinary NLσM (with $k = 0$) are

$$\begin{aligned} \beta(\tilde{g})_0 = \frac{d\tilde{g}}{d\ln l} &= -(d-2)\tilde{g} + \frac{N}{2\pi^2}\tilde{g}^2, \\ \beta(\tilde{g}')_0 = \frac{d\tilde{g}'}{d\ln l} &= -(d-2)\tilde{g}' + \frac{N}{d\pi^2}\tilde{g}'^2, \end{aligned} \tag{4.34}$$

in our current case $d = 3$. As long as $n \sim N^A$ with $A < 1$, in the large-N limit we only need to keep these terms in the beta functions. Eq. (4.34) has several fixed points. If we start with the physical parameter $\tilde{g}(\Lambda) = \tilde{g}'(\Lambda)$ as the tuning parameter at the beginning of the RG flow, then increasing $\tilde{g}$ will lead to a quantum phase transition controlled by the fixed point

$$\tilde{g}_* = \frac{2\pi^2}{N}, \quad \tilde{g}'_* = 0, \tag{4.35}$$

and the critical exponent $\nu = 1$. The location of the critical point, and the critical exponent is consistent with the well-known result of the CP^{N-1} model in the large$-N$ limit [152, 153].

4.2.2 Stable fixed point in the quantum disordered phase

Now let us compute the beta functions with the WZW term. Naively one would expect that the leading order contribution from the WZW term to the beta functions is the one-loop diagram Fig. 4.3. But because the numerator of the WZW vertex is

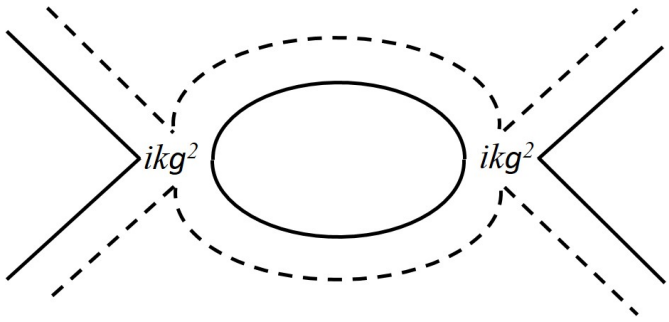

Figure 4.3: One-loop diagram which involves two WZW terms in Eq. (4.33). The numerator of the WZW vertex is completely antisymmetric in momenta, so this diagram does not renormalize g or g'.

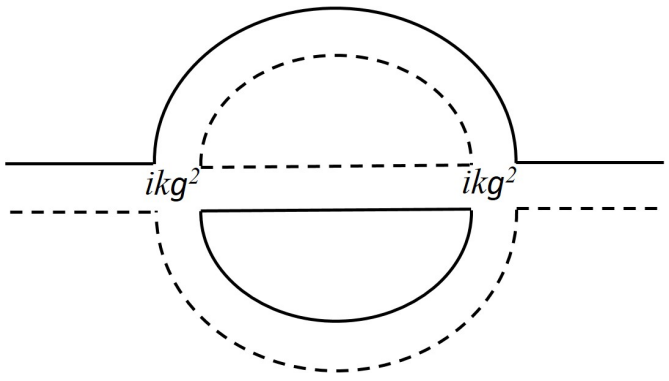

Figure 4.4: Two-loop wave function renormalization.

completely antisymmetric in momenta, this diagram does not renormalize the coupling constants g and g'. Fig. 4.4 is a two-loop planar wave function renormalization diagram that renormalizes g and g'. This diagram leads to the following corrections to the beta functions:

$$\begin{aligned} \beta(\tilde{g}) &= \beta(\tilde{g})_0 - ck^2\tilde{g}^5 Nn\frac{1}{(4\pi)^2} + \cdots \\ \beta(\tilde{g}') &= \beta(\tilde{g}')_0 - ck^2\tilde{g}'\tilde{g}^4 Nn\frac{1}{(4\pi)^2} + \cdots \end{aligned} \tag{4.36}$$

In this equation c is a positive number whose exact value is unimportant, because we are going to treat k^2 as a tuning parameter.

Our goal is to look for a stable fixed point which corresponds to a stable $(2+1)d$ CFT in the quantum disordered phase. The negative sign of the k^2 term in Eq. (4.36) suggests that this is possible. However, to make a confident conclusion, we need to choose certain adequate scaling between k and N: $k \sim N^B$. If for instance $0 < B \leq 3/2$, then the k^2 terms in Eq. (4.36) indeed lead to a new *stable* fixed point in the quantum disordered phase at $\tilde{g}_* \sim k^{-2/3} \geq 1/N$ and $\tilde{g}'_* = 0$. But around this "new fixed point", infinite number of higher loop diagrams would become nonperturbative. For example, let us examine the four-loop WZW contribution, which is shown in Fig. 4.5. This diagram has seven internal propagators, four WZW vertices, two closed solid loops, and two closed dashed loops. Therefore this diagram contributes a term $\sim g^9k^4n^2N^2$ to the beta function. Then when $B \leq 3/2$, this four-loop diagram (and infinite number of higher loop diagrams) also contributes at least at the same order as the k^2 terms in Eq. (4.36), around the "new fixed point" $\tilde{g}_* \sim k^{-2/3}$.

But on the other hand, if $B > 3/2$, then the k^2 term in Eq. (4.36) would be too large and make the entire RG equations flow to $\tilde{g} = \tilde{g}' = 0$. We stress that these difficulties

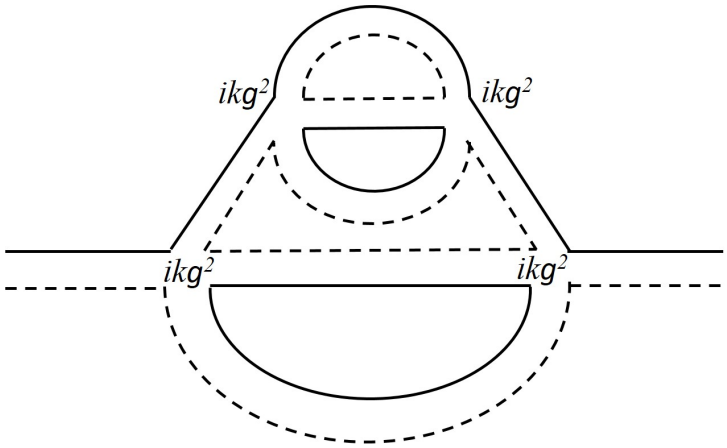

Figure 4.5: A four-loop diagram with four WZW terms. When $k \leq N^{3/2}$, in the simultaneous limit of large N and large k, this diagram contributes to the RG equation at least at the same order as the two-loop diagram in Fig. 4.4 around the "new stable fixed point" in the quantum disordered phase, so do infinite number of higher loop diagrams.

only occur with the presence of the WZW term. Without the WZW term, this theory does have a simple large-N limit.

In order to find a controlled calculation and to identify the stable fixed point in the quantum disordered phase with confidence, we need to find another small parameter to expand with. As we mentioned before we cannot rely on the ordinary $2+\epsilon$ expansion in our case. In this section we propose a possible solution to this difficulty in our current context by introducing a different $\epsilon-$generalization of our model.

We first test our approach with $n = 1$ ($\mathcal{M} = \mathrm{CP}^{N-1}$). We generalize the original action Eq. (4.31) as following:

$$\mathcal{L}_{\mathrm{NL}\sigma\mathrm{M}} = \partial_\mu \phi^\dagger \cdot \partial_\mu \phi$$

$$+ \quad \tfrac{1}{4} g \left(\partial_\mu \phi^\dagger \cdot |\bar{\partial}|^{\frac{\epsilon-1}{2}} \phi + \phi^\dagger \cdot |\bar{\partial}|^{\frac{\epsilon-1}{2}} \partial_\mu \phi \right)^2$$

$$+ \quad \tfrac{1}{4}g'\left(\phi^\dagger\cdot|\bar\partial|^{\frac{\epsilon-1}{2}}\partial_\mu\phi-\partial_\mu\phi^\dagger\cdot|\bar\partial|^{\frac{\epsilon-1}{2}}\phi\right)^2$$

$$+ \quad \tfrac{1}{4}g^2\left(\phi^\dagger\cdot|\bar\partial|^{\epsilon-1}\phi\right)\left(\partial_\mu\phi^\dagger\cdot|\bar\partial|^{\frac{\epsilon-1}{2}}\phi+\phi^\dagger\cdot|\bar\partial|^{\frac{\epsilon-1}{2}}\partial_\mu\phi\right)^2$$

$$+ \quad \mathcal{O}(g^3\phi^8). \tag{4.37}$$

Here the notation $|\bar\partial|$ is most manifest in the momentum space: $A^\dagger|\bar\partial|B$ in the momentum space corresponds to $A^\dagger(\boldsymbol{p})|\frac{1}{2}(\boldsymbol{p}+\boldsymbol{q})|B(\boldsymbol{q})$. This nonanalytic generalization can be made systematically to all higher order expansion of the Lagrangian: a singular momentum dependence $|\bar\partial|^{\frac{\epsilon-1}{2}}$ is inserted in $\phi^\dagger\cdot\partial_\mu\phi$ and $\phi\cdot\partial_\mu\phi^\dagger$, and $|\bar\partial|^{\epsilon-1}$ is inserted in $\phi^\dagger\cdot\phi$. At least in the large$-N$ limit, it can be shown that all the relevant renormalizations to this Lagrangian can still be absorbed into the RG flow of g and g'.

The nonanalytic generalization of a local field theory dated back to studies on spin systems with long range interactions [154], and the study of the Gross-Neveu model [155]. Later a generalization of the regular p^2 kinetic term to $|p|^{1+\epsilon}$ was used as a controlled calculation method for $2d$ Fermi surface coupled with a bosonic field [156, 157, 158], which without the nonanalytic generalization also suffers from the infinite diagram difficulty in the large-N limit [159]. The advantage of the nonanalytic generalization is that, now the scaling dimension of g and g' at weak interacting limit becomes $-\epsilon$, and we can treat ϵ as another small parameter to organize all the Feynman diagrams.

The WZW term is now generalized to

$$\mathcal{L}_{\text{WZW}}=i\frac{kg^2}{4\pi}\varepsilon^{\mu\nu\rho}\left(\phi^\dagger\cdot|\bar\partial|^{\epsilon-1}\partial_\mu\phi\right)\left(\partial_\nu\phi^\dagger\cdot|\bar\partial|^{\epsilon-1}\partial_\rho\phi\right). \tag{4.38}$$

When $n=1$ there is no higher order terms in the WZW term, which significantly simplifies the analysis. When $\epsilon=1$ this action returns to its original form Eq. (4.31).

This generalization keeps many of the basic properties of the original WZW term:

1) this term Eq. (4.38) is always purely imaginary;

2) like the WZW term, the parameter k is always marginal for arbitrary ϵ, which is guaranteed by the nonanalytic momentum dependence inserted in the generalized WZW term;

3) the two ϕ ($\phi^\dagger$) fields in Eq. (4.38) are equivalent to each other.

With large-N and leading order in ϵ, the RG equations of $\tilde{g}$ and $\tilde{g}'$ read (here we redefine $\tilde{g} = \Lambda^\epsilon g$ and $\tilde{g}' = \Lambda^\epsilon g'$ to make them dimensionless)

$$\begin{aligned} \frac{d\tilde{g}}{d\ln l} &= \beta(\tilde{g})_0^{(\epsilon)} - ck^2\tilde{g}^5 N\frac{1}{(4\pi)^2}, \\ \frac{d\tilde{g}'}{d\ln l} &= \beta(\tilde{g}')_0^{(\epsilon)} - ck^2\tilde{g}'\tilde{g}^4 N\frac{1}{(4\pi)^2}. \end{aligned} \tag{4.39}$$

$\beta(\tilde{g})_0^{(\epsilon)}$ and $\beta(\tilde{g}')_0^{(\epsilon)}$ are simply $\beta(\tilde{g})_0$ and $\beta(\tilde{g}')_0$ with the first term replaced by $-\epsilon\tilde{g}$ and $-\epsilon\tilde{g}'$. The wave function renormalization Fig. 4.4 is the only diagram that contributes to the last terms in Eq. (4.39) in the large$-N$ limit. Vertex corrections in Fig. 4.6 will not contribute here because under RG flow it generates an ϕ^4 term with analytic momentum dependence, which is less relevant compared with the terms in Eq. (4.37). The absence of vertex corrections here is similar to the absence of boson field wave function renormalization discussed in Ref. [157], basically because a nonanalytic momentum dependence cannot be generated by integrating out high momentum degrees of freedom in RG. This absence of vertex correction to terms with nonanalytic momentum dependence was also discussed in Ref. [160, 161].

Now we need to take $k^2 \sim (N/\epsilon)^3$ to keep all the terms in these equations at the same order, and we expect that the fixed points of these beta functions will be around $\tilde{g} \sim \epsilon/N$. With small enough ϵ, the terms we keep in Eq. (4.39) will be dominant compared with

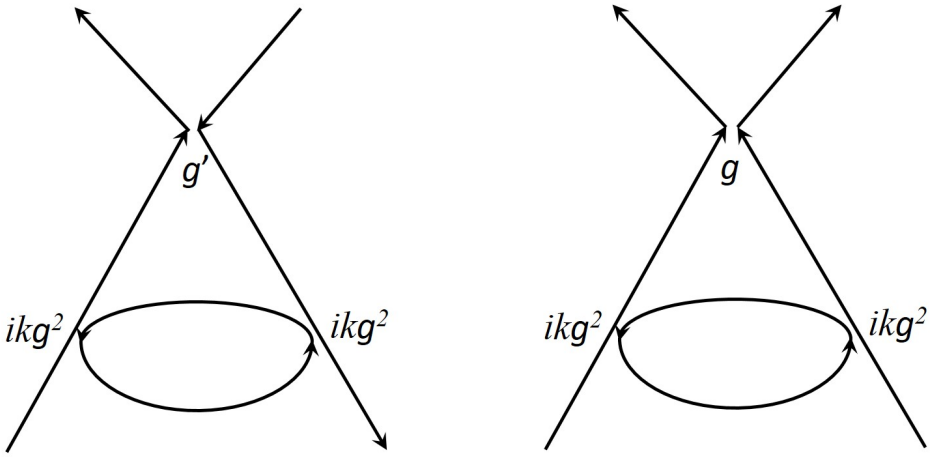

Figure 4.6: The vertex corrections from the WZW terms, which generate irrelevant interactions under RG with our nonanalytic $\epsilon-$generalization.

all higher loop diagrams.

The value of constant c is computed at $\epsilon = 0$: with large-N, large-k and $\epsilon = 0$, the wave function renormalization in Fig. 4.4 will lead to the following correction to the coupling constant g:

$$\begin{aligned} \delta\tilde{g} &= -8\tilde{g}^5 N \left(\frac{k}{4\pi}\right)^2 \int \frac{d^3p}{(2\pi)^3}\frac{d^3q}{(2\pi)^3} \\ &\times \frac{1}{3}\frac{p^2q^2-(\boldsymbol{p}\cdot\boldsymbol{q})^2}{p^2q^2|\boldsymbol{p}+\boldsymbol{q}|^2|\boldsymbol{p}-\boldsymbol{q}|^4}\times 16 \\ &\sim -\frac{1}{3\pi^2}k^2\tilde{g}^5 N\frac{1}{(4\pi)^2}\log\left(\frac{\Lambda}{\Lambda'}\right), \end{aligned} \tag{4.40}$$

where Λ and Λ' are the ultraviolet cut-off and rescaled cut-off. Thus $c = 1/(3\pi^2)$. The value of c evaluated at $\epsilon = 0$ depends on the exact form of the ϵ generalization of the WZW term.

We take $k^2 = G^3(N/\epsilon)^3$ with small coefficient G. Eq. (4.39) generates several fixed points. If we start with the physical parameters $\tilde{g}(\Lambda) = \tilde{g}'(\Lambda)$ at the beginning of the

RG, the flow of the parameters is controlled by two of these fixed points. The first fixed point is the order-disorder quantum phase transition located at

$$\tilde{g}_* \sim (2\pi^2 + 2\pi^8 c G^3 + \mathcal{O}(G^6))\frac{\epsilon}{N}, \quad \tilde{g}'_* = 0 \tag{4.41}$$

and the critical exponent $1/\nu$ is

$$\frac{1}{\nu} = \epsilon(1 - 3cG^3\pi^6 + \mathcal{O}(G^6)). \tag{4.42}$$

If we extrapolate ϵ to 1, ν will be greater than 1, which can already be expected from the negative sign of the k^2 term in the beta functions. This is qualitatively different from the critical exponent without the WZW term. For instance it is well-known that the $(2+1)d$ CP^{N-1} model has $\nu < 1$ with $1/N$ correction taken into account [153].

Most importantly, there is a stable fixed point in the quantum disordered phase:

$$\tilde{g}_* \sim \left(\frac{1}{G}\frac{2}{c^{1/3}} - \frac{2\pi^2}{3} + \mathcal{O}(G)\right)\frac{\epsilon}{N}, \quad \tilde{g}'_* = 0. \tag{4.43}$$

We need G small enough to guarantee that the coupling constant in Eq. (4.43) is larger than the one in Eq. (4.41), *i.e.* the system is in a quantum disordered phase. In the vicinity of this new stable fixed points, the beta functions give the scaling dimension of two irrelevant perturbations:

$$\begin{aligned} \Delta_1 &= \epsilon\left(-\frac{1}{G}\frac{3}{c^{1/3}\pi^2} + 5 + \mathcal{O}(G)\right), \\ \Delta_2 &= \epsilon\left(-\frac{1}{G}\frac{1}{c^{1/3}\pi^2} + \frac{1}{3} + \mathcal{O}(G)\right). \end{aligned} \tag{4.44}$$

Both scaling dimensions are negative with small enough G. The RG flow diagram for

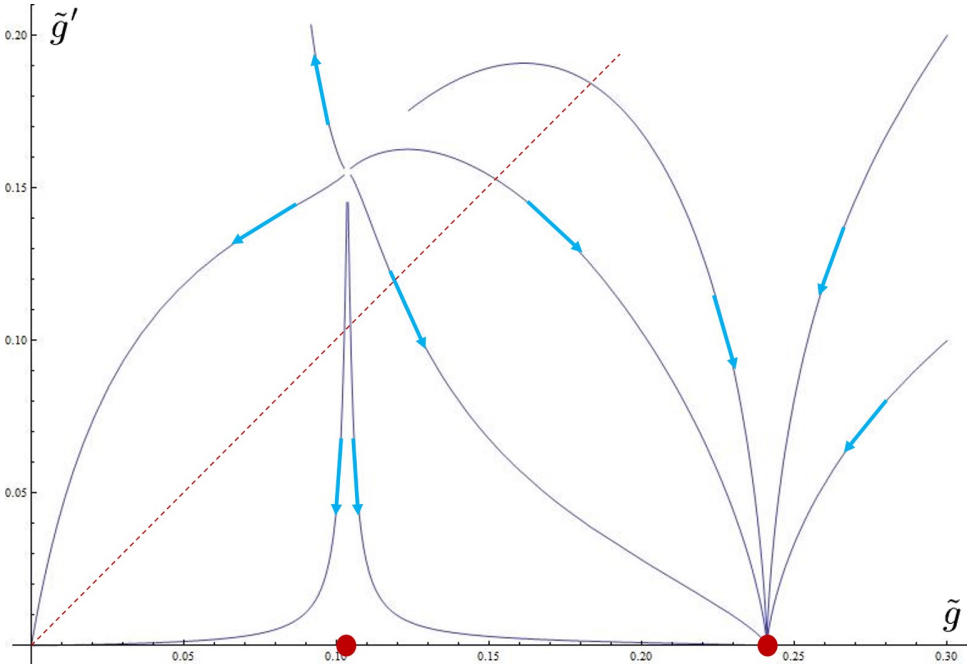

Figure 4.7: The RG flow diagram for the RG equations in Eq. (4.39). We chose parameters $\epsilon = 0.05$ $N = 10$, $ck^2n \sim 340$. The dashed line corresponds to the physical values of the tuning parameter $\tilde{g} = \tilde{g}'$ at the beginning of the RG flow. The RG flow is controlled by two fixed points, one is the order-disorder transition, the other is a stable fixed point in the quantum disordered phase.

the RG equations with parameters $\epsilon = 0.05$ $N = 10$, $ck^2n \sim 340$ is plotted in Fig. 4.7.

In order to carry out the calculation for $n > 1$, we need to include higher order terms in the expansion of the WZW term. We also need to generalize the $\mathcal{O}(\phi^6)$ order in the WZW term to a nonanalytic form. There are certainly more than one possible $\epsilon-$generations, as an example, we choose the following form for the ϕ^6 term in the momentum space:

$$\mathcal{L}_{\text{WZW}}(\phi^6) = -\sum_{\boldsymbol{w},\boldsymbol{l},\boldsymbol{p},\boldsymbol{q},\boldsymbol{t},\boldsymbol{s}} \delta(\boldsymbol{w}+\boldsymbol{p}+\boldsymbol{s}-\boldsymbol{l}-\boldsymbol{q}-\boldsymbol{r})$$

$$\times \frac{kg^3}{4\pi}\frac{1}{3}\varepsilon^{\mu\nu\rho} l_\mu q_\nu t_\rho |\boldsymbol{l}+\boldsymbol{p}|^{\epsilon-1}|\boldsymbol{q}+\boldsymbol{s}|^{\epsilon-1}|\boldsymbol{t}+\boldsymbol{w}|^{\epsilon-1}$$

$$\times \text{tr}\left(\phi^\dagger(\boldsymbol{l})\cdot\phi(\boldsymbol{w})\ \phi^\dagger(\boldsymbol{q})\cdot\phi(\boldsymbol{p})\ \phi^\dagger(\boldsymbol{t})\cdot\phi(\boldsymbol{s}) - h.c.\right). \tag{4.45}$$

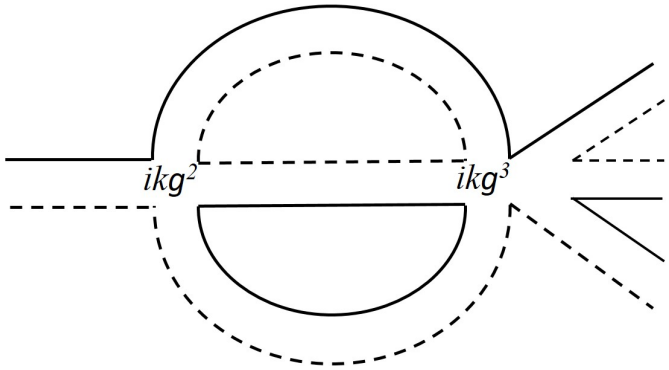

Figure 4.8: A two loop diagram that is a mixture between the ϕ^4 and ϕ^6 terms in the WZW term for $n > 1$.

This generalization still keeps the basic properties of the WZW term that we need to carry out the calculations, and when $\epsilon = 1$ it returns to the original form of the WZW term. This ϕ^6 term so designed only generates irrelevant terms in the large$-N$ limit and leading order ϵ expansion. For example, Fig. 4.8 is a leading order diagram in terms of large$-N$ and $\epsilon-$expansion counting, but it only generates an irrelevant analytic term to the Lagrangian.

4.2.3 Discussions

In this work we did our best to search for a controlled study of stable interacting conformal field theories at the boundary of $(3+1)d$ SPT states. We performed calculation in the large$-N$ limit and leading order $\epsilon-$expansion, and the desired stable fixed point is indeed found in the quantum disordered phase. But we have not proved that higher order expansions will not generate more relevant terms in the Lagrangian.

Besides exploring the exotic boundary states of $(3+1)d$ bosonic SPT phases, another motivation of this work was the "hierarchy problem" in high energy physics: why the Higgs boson is so much lighter than the Planck mass? Compared with the Planck mass, the Higgs boson, which is a space-time scalar, is almost massless. Gauge bosons, which

can emerge very naturally in condensed matter systems [162, 163, 164], indeed have zero mass. But a space-time scalar boson, unless it is a Goldstone mode, usually acquires a mass that is comparable with the ultraviolet cut-off without fine-tuning to a critical point. At least this is the case for space-time dimensions higher than $(1+1)d$ (in $(1+1)d$ space-time scalar bosons can easily form a conformal field theory). Indeed, the little Higgs theory hypothesizes that the Higgs boson itself is a pseudo Goldstone boson [165, 166, 167], which explains its small mass. The result of our current work suggests another possible route to address the hierarchy problem: the Higgs boson could be rendered massless due to a topological WZW term, even if the system is in a quantum disordered phase, *i.e.* there is no (pseudo) spontaneous symmetry breaking. But, in order to show this explicitly, one needs to first embed the Higgs boson into a larger target manifold $\mathcal{M}$ which permits a WZW term, and perform a controlled RG calculation in $(3+1)d$ [3]. We will leave this direction to future study.

At the purely technical level, although the WZW term can be formally rewritten as a Chern-Simons term, we cannot treat the gauge field a_μ (Eq. (4.27)) in the path integral as if it were an independent degree of freedom with a Chern-Simons term. For example, when $N = 2n = 2$, the topological term becomes the quantized Hopf term if written in terms of φ^i, while the Chern-Simons action of a U(1) gauge field is in general not quantized. The WZW term can only be interpreted as the Chern-Simons term if Eq. (4.27) holds rigorously. However, if a Chern-Simons term of a_μ is already included in the action, the equation of motion of the gauge field is no longer given by Eq. (4.27). In the standard path integral formalism of the CP^{N-1} model, the gauge field a_μ is introduced as an auxiliary field through the Hubbard-Stratonovich transformation. Thus one should introduce one more vector field b_μ through the Hubbard-Stratonovich transformation on

[3] $\pi_5[SU(N)] = \mathbb{Z}$ for $N > 2$, thus a matrix model whose target manifold is $SU(N)$ could have a WZW term in $(3+1)d$. But $SU(N)$ matrix model does not have a controlled large$-N$ limit even without the WZW term.

the WZW term: $\sim ik\varepsilon\varphi^{\dagger}\cdot\partial\varphi\partial b + ik\varepsilon b\partial b$ (indices and unimportant factors are omitted in this equation). Integrating out b_μ will regenerate the WZW term, for the simplest case $n = 1$. For $n > 1$ this method gets more complicated.

4.3 Generalized Lieb-Schultz-Mattis theorem and its connection to the surface states of the symmetry protected topological phase

The Lieb-Schultz-Mattis (LSM) theorem [57], and its higher dimensional generalizations [168, 169] state that if a quantum spin system defined on a lattice has odd number of spin-1/2s per unit cell, then any local spin Hamiltonian which preserves the spin and translation symmetry, cannot have a featureless (gapped and nondegenerate) ground state. This implies that any symmetry allowed Hamiltonian on the spin Hilbert space defined above can only have the following possible scenarios: *1.* its ground state spontaneously breaks either the spin symmetry or the lattice symmetry, hence leads to degenerate ground states and possible gapless Goldstone modes; *2.* it has gapped and degenerate ground states without breaking any symmetry, *i.e.* its ground state develops a topological order (the second possibility can only happen in two and higher dimensional systems); *3.* its ground state has algebraic (power-law) correlation function of physical quantities, and the spectrum is again gapless (this scenario happens most often in $1d$ spin systems, while still possible in higher dimensions).

On the other hand, there are lattice spin systems for which one can very easily construct a local Hamiltonian with a featureless ground state that preserves all the symmetry. One class of such states are called the AKLT states [17], which can be constructed for an integer spin chain in $1d$, the spin-2 antiferromagnet on the square lattice, and the

spin-3/2 antiferromagnet on the honeycomb lattice, etc. Of course, these systems violate the crucial "odd number of spin-1/2s per unit cell" assumption of the LSM theorem.

However, there are also some spin systems in the "middle ground" where the answers are not so clear. These systems do not meet the key assumption of the LSM theorems, while a simple analogue of the AKLT state mentioned above does not obviously exist. For example, the honeycomb lattice has two sites per unit cell, thus a spin-1/2 system on the honeycomb lattice has even number of spin-1/2s per unit cell, and hence there is no LSM theorem to exclude a featureless ground state. But it has been a long standing problem whether a featureless spin-1/2 state exists or not on the honeycomb lattice. Another example is the spin-1 antiferromagnet on the square lattice. Depending on the Hamiltonian, possible states of this system include the Néel state which spontaneously breaks the spin symmetry, and a nematic type of valence bond solid state which breaks the lattice rotation symmetry, etc. But the existence of a featureless state is not obvious. However, recent progresses indicate that featureless states do exist in these two "middle ground" examples mentioned above [170, 171, 172], with a more sophisticated construction compared with the AKLT state.

Another seemingly very different subject is the symmetry protected topological (SPT) state [25, 26], which is a generalization of topological insulators. By definition, the ground state of the $(d+1)-$dimensional bulk of a SPT phase must be gapped and nondegenerate, while its $d-$dimensional boundary state must be either gapless or degenerate, as long as certain symmetries are preserved. In the last few years, the classification of bosonic SPT states with on-site internal symmetries has been well understood [25, 26, 32, 63, 46, 47, 173, 174, 69, 175]. The $d-$dimensional boundary of a $(d+1)-$dimensional SPT state, just like those $d-$dimensional spin systems where the LSM theorem applies, cannot be trivially gapped. The key difference between these two systems is that, the former is (usually) protected by an on-site symmetry, while the latter is protected by the spin and

lattice symmetries together. However, the fact that neither system permits a featureless state suggests that we can potentially formulate both systems in a similar way. The connection to $3d$ bulk SPT states has been exploited in order to understand the fractional excitations of $2d$ topological orders with both spin and lattice symmetries [176].

Since we are comparing two $d-$dimensional systems with very different ultraviolet regularizations, their analogue can only be made precise when both systems are tuned close to a point where a low energy field theory description becomes available. Thus for our purpose, when we analyze a $d-$dimensional spin system, we will first tune it to a critical point described by a field theory, then interpret the lattice symmetry as an on-site symmetry, and interpret the $d-$dimensional field theory as the boundary state of a $(d+1)-$dimensional bulk. If the corresponding $(d+1)-$dimensional bulk is a trivial state instead of a nontrivial SPT state, then a featureless spin state must exist not too far from that critical point in the phase diagram; if the corresponding bulk is indeed a nontrivial SPT state, then it highly suggests that a featureless spin ground state does not exist.

However, the latter statement may not be necessarily true: if around that selected critical point of the spin system the field theory is formally equivalent to a SPT boundary state, it only rules out the featureless spin state at the vicinity of that critical point. But in principle a featureless state could be far away from the critical point in the phase diagram, and hence beyond the reach of the field theory.

In section 4.3.1 through 4.3.4, we will discuss SU(N) and SO(N) systems on a $1d$ chain, $2d$ square lattice, $2d$ honeycomb lattice, and $3d$ cubic lattice respectively, by mapping them to the boundary of $2d$, $3d$ and $4d$ bulk states. We will identify those spin systems that permit a featureless ground state. For all of these spin systems, we can explicitly construct a featureless tensor product state that is an analogue of the AKLT state. Some examples of these featureless states will be discussed in section 4.3.5. In section 4.3.5

we will also verify our conclusions by making connection with a previous study on LSM theorem based on lattice homotopy class [177].

4.3.1 $1d$ spin chain

4.3.1.1 SU(2) spin-1/2 chain

In this section we first discuss one dimensional spin chains with SU(2) symmetry. The low energy physics of the Heisenberg antiferromagnetic spin-1/2 chain with a SU(2) spin symmetry can be captured by the following nonlinear sigma model in $(1+1)d$ with a Wess-Zumino-Witten (WZW) term at level-1 [178]:

$$\mathcal{S} = \int dx d\tau \ \frac{1}{g}(\partial_\mu \boldsymbol{n})^2 + \frac{2\pi i}{\Omega_3}\int_0^1 du \ \epsilon_{abcd} n^a \partial_\tau n^b \partial_x n^c \partial_u n^d, \tag{4.46}$$

where $\boldsymbol{n}$ is a four component vector with unit length, and Ω_3 is the volume of S^3 with unit radius. The physical meaning of $\boldsymbol{n}$ is that, (n_1, n_2, n_3) are the three component Néel order parameter, while $n_4 \sim \phi$ is the valence bond solid (VBS) order parameter. If there is a SO(4) rotation symmetry of the four component vector $\boldsymbol{n}$, the coupling constant g will flow to a fixed point, which corresponds to the $\mathrm{SU}(2)_1$ conformal field theory [50, 51]. The SO(4) symmetry becomes an emergent symmetry of the spin-1/2 Heisenberg chain in the infrared: the Néel and VBS order parameter both have the same scaling dimension $[\boldsymbol{n}] = 1/2$. The key symmetry of the system, is the spin SU(2) symmetry, and the translation symmetry. (n_1, n_2, n_3) transforms as a vector under spin SU(2), and $n_4 \sim \phi$ is a SU(2) singlet; and under translation by one lattice constant, $T_x : \boldsymbol{n} \to -\boldsymbol{n}$. The physical meaning of Eq. (4.46) is the intertwinement between the Néel and VBS order parameter: the domain wall of the VBS order parameter carries a spin-1/2.

The field theory Eq. (4.46) also describes the boundary of a $2d$ bosonic SPT state

with SO(3)×Z_2 symmetry [34, 35], where Z_2 acts as $\boldsymbol{n} \to -\boldsymbol{n}$. This SPT state can be understood as the decorated domain wall construction [38]: we decorate every Z_2 symmetry breaking domain wall in the $2d$ bulk with a Haldane phase with SO(3) symmetry (Fig. 4.9a), then proliferate the Z_2 domain walls to restore the Z_2 symmetry. The so-constructed phase in the bulk is the desired SO(3)×Z_2 SPT phase. And at the $1d$ boundary of the system, there is a spin-1/2 degree of freedom localized at every Z_2 domain wall, which is also the boundary state of the Haldane phase decorated at each Z_2 domain wall in the bulk. This is consistent with the physics of the spin-1/2 chain.

This simple example demonstrates that the lattice translation symmetry, once interpreted as an on-site symmetry in a field theory, is equivalent to an "anomalous" symmetry of the boundary of a higher dimensional SPT state. And by definition the boundary of a SPT state cannot be trivially gapped without degeneracy, which is consistent with the LSM theorem of the spin-1/2 chain [57].

Here we stress that, the $1d$ SPT phase decorated at a Z_2 domain wall must have a Z_2 classification as long as the symmetry G of the $1d$ SPT phase commutes with the Z_2, *i.e.* two of the $1d$ SPT phases must fuse into a trivial state. One way to see this is that, after gauging the Z_2 symmetry, the vison ($\pi-$flux introduced by the Z_2 gauge symmetry) preserves the symmetry G as long as G commutes with Z_2, and the vison is the boundary of the $1d$ decorated SPT state [38]. Since two visons fuse into a local excitation, the $1d$ SPT state must have a Z_2 classification. But at a Z_2^T (time-reversal) domain wall one can decorate a lower-dimensional SPT phase with (for example) Z classification, because the anti-domain wall of Z_2^T is the time-reversal conjugate of a Z_2^T domain wall, which is automatically decorated with the "inverse" state of the SPT state decorated at the Z_2^T domain wall [4]. This observation is consistent with many known facts about SPT phases. For instance, in three dimensional space, there is a Z_2^T SPT which can be viewed as Z_2^T

[4]The authors thank Dung-Hai Lee for clarifying this important point for us.

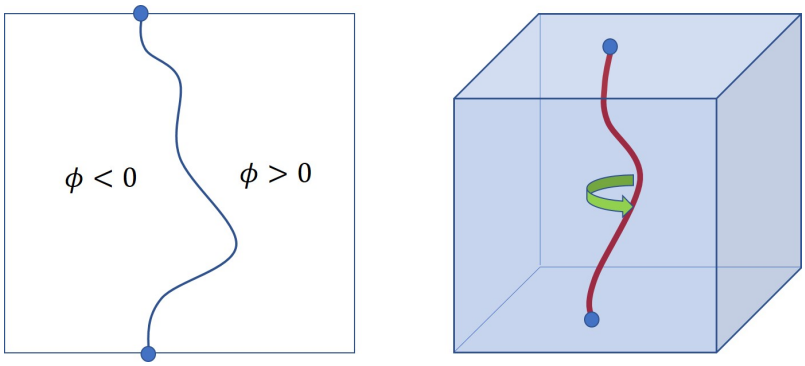

Figure 4.9: (a), the decorated domain wall construction of the $2d$ SPT state whose boundary is analogous to a SU($2N$) spin chain with a LSM theorem. A $1d$ SPT state with PSU($2N$) symmetry is decorated to each domain wall, and the domain wall terminates at the boundary with a dangling projective representation of the PSU($2N$) SPT state. (b), the decorated vortex line construction of the $3d$ SPT state whose boundary is analogous to a $2d$ spin system either on the square or honeycomb lattice. Again, we decorate each vortex line with a $1d$ SPT state. But when the $2d$ boundary is mapped to the square and honeycomb lattice spin systems, the vortex line in the bulk has a Z_4 and Z_3 conservation, which must be compatible with the classification of the $1d$ SPT state decorated on each vortex line in order to guarantee a nontrivial $3d$ SPT.

domain walls decorated with the E_8 invertible topological order [32], but there is no such decorated domain wall construction for $3d$ SPT phases with a Z_2 symmetry.

4.3.1.2 spin chain with reduced symmetry

Now one can exploit the connection between $1d$ spin chains and the boundary of $2d$ SPT states even further, and consider a spin chain with a reduced spin symmetry. For example we can start with a spin-1/2 chain, and break the SO(3) spin symmetry down to its subgroup $G \rtimes Z_2$, where Z_2 is the spin $\pi-$rotation $S^z \to -S^z$, $S^y \to -S^y$, and G is a subgroup of the inplane U(1) spin symmetry. Whether the spin chain can be featureless or not, is equivalent to the problem of whether the corresponding bulk state with $(G \rtimes Z_2) \times Z_2$ symmetry is a nontrivial SPT state or not; and based on the "decorated domain wall" picture mentioned above, this again is equivalent to the problem

of whether the $1d$ Z_2 domain wall is a nontrivial $1d$ SPT state with $G \rtimes Z_2$ symmetry or not, and if it is indeed a nontrivial SPT, whether it has a Z_2 classification.

Now we can look up the classification in Ref. [25, 26]. For example, when $G = Z_{2n+1}$ with integer n, since there is no nontrivial $1d$ SPT state with $Z_{2n+1} \rtimes Z_2$ symmetry, the bulk $\mathrm{SO}(3) \times Z_2$ SPT state discussed previously must be trivialized by reducing the SO(3) spin symmetry down to $Z_{2n+1} \rtimes Z_2$, thus its boundary can in principle be gapped and nondegenerate. This observation already gives us a meaningful conclusion:

A spin chain with translation and $(Z_{2n+1} \rtimes Z_2)$ spin symmetry can have a featureless ground state.

By contrast, for $G = U(1)$ or Z_{2n}, a nontrivial $1d$ SPT state with $G \rtimes Z_2$ does exist, and it does have a Z_2 classification. Hence the Haldane phase with SO(3) spin symmetry remains a nontrivial SPT state under the symmetry reduction to $G \rtimes Z_2$. Thus the $2d$ bulk SPT state with $(G \rtimes Z_2) \times Z_2$ remains nontrivial, and hence the $1d$ boundary cannot be trivially gapped. This observation leads to the following conclusion:

A $1d$ spin-1/2 chain cannot have a featureless ground state, even if we break the SU(2) spin symmetry down to $(Z_{2n} \rtimes Z_2)$ symmetry.

4.3.1.3 SU(2N) spin chain

Now let's consider spin chains with higher spin symmetries. A natural generalization of the spin-1/2 chain with translation symmetry, is a $\mathrm{SU}(2N)$ spin chain with self-conjugate representation on each site (Young tableau with N boxes in one column, Fig. 4.10a). The analogue of the "Néel" order parameter of this $\mathrm{SU}(2N)$ spin chain, is a

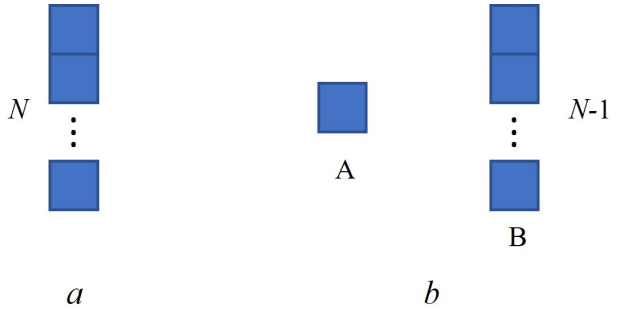

Figure 4.10: (a), the self-conjugate SU($2N$) spin representation on each site considered in section 4.3.1.3. (b), For the square, honeycomb and cubic lattice, we consider a SU(N) spin system with a fundamental representation (FR) on sublattice A, and an anti-fundamental representation (AFR) on sublattice B.

$2N \times 2N$ Hermitian matrix order parameter $\mathcal{P}$, and it can be represented in the form

$$\mathcal{P} = V\Omega V^{\dagger}, \quad \Omega \equiv \begin{pmatrix} \mathbf{1}_{N\times N} & \mathbf{0}_{N\times N} \\ \mathbf{0}_{N\times N} & -\mathbf{1}_{N\times N} \end{pmatrix} \tag{4.47}$$

where V is a SU($2N$) matrix. All the configurations of $\mathcal{P}$ belong to the Grassmanian manifold $\mathcal{M} = U(2N)/[U(N)\times U(N)]$ [179, 180]. To see that $\mathcal{P}$ is a natural generalization of the ordinary SU(2) Néel order parameter, we can take $N = 1$, then this Grassmanian is precisely S^2, which is the manifold of the ordinary SU(2) Néel order parameter. We can also define matrix order parameter $\mathcal{P} = \boldsymbol{n} \cdot \boldsymbol{\sigma}$ for the SU(2) spin chain, where $\boldsymbol{n}$ is the SU(2) Néel order parameter.

The effective field theory for the SU($2N$) spin chain described above, can be written as [179]:

$$\mathcal{S} = \int dx d\tau \ \frac{1}{g}\mathrm{tr}[\partial_\mu \mathcal{P} \partial_\mu \mathcal{P}] + \frac{\Theta}{16\pi}\epsilon_{\mu\nu}\mathrm{tr}[\mathcal{P}\partial_\mu \mathcal{P}\partial_\nu \mathcal{P}]. \tag{4.48}$$

This is the analogue of the Nonlinear sigma model for the SU(2) spin chain [15, 16],

with a $\Theta-$term which comes from the fact that for all N, the Grassmanian $\mathcal{M}$ satisfies $\pi_2[\mathcal{M}] = Z$. Under translation by one lattice constant, $\mathcal{P}$ transforms as $T_x : \mathcal{P} \to -\mathcal{P}$ ($\mathcal{P}$ and $-\mathcal{P}$ both belong to the same Grassmanian target manifold), and the coefficient Θ transforms as $T_x : \Theta \to -\Theta$, which guarantees that Θ is quantized to be multiple of π. The same field theory as Eq. (4.48) with a topological Θ term has been used to describe the phase diagram of the integer quantum Hall systems [52, 53, 181], while there the theory is written in the $2d$ real space instead of space-time. A proposed renormalization group flow for Eq. (4.48) is that, $\Theta = 2\pi k$ are stable fixed points, while $\Theta = \pi(2k+1)$ are instable fixed points which correspond to transitions between stable fixed points $\Theta = 2k\pi$ [179].

When $\Theta = \pi$, Eq. (4.48) describes the SU($2N$) spin chain with self-conjugate representation on each site; when $\Theta = 2\pi$, Eq. (4.48) describes the Haldane phase of a SU($2N$) spin-chain, or more precisely it is the Haldane phase of a PSU($2N$) spin chain, as $\mathcal{P}$ is invariant under the center of SU($2N$). The PSU($2N$) Haldane phase should have Z_{2N} classification [182], as its boundary could be $2N$ different projective representation of PSU($2N$), which are also the $2N$ different representation of the Z_{2N} center of SU($2N$). But the particular state described by Eq. (4.47) and Eq. (4.48) is the "Nth" PSU($2N$) Haldane phase, whose $0d$ boundary is a self-conjugate projective representation of PSU($2N$). This state has a Z_2 nature, namely two copies of this state will be a trivial state, *i.e.* its boundary is no longer a projective representation of PSU($2N$).

As we discussed before, the spin-1/2 SU(2) chain can also be described by Eq. (4.46), where a VBS order parameter is introduced. For the SU($2N$) spin chain with self-conjugate representation, the analogue of Eq. (4.46) is

$$\mathcal{S} = \int dx d\tau \ \frac{1}{g}\mathrm{tr}[\partial_\mu U^\dagger \partial_\mu U] + \int_0^1 du \ \frac{i2\pi}{24\pi^2}\mathrm{tr}[U^\dagger dU]^3, \tag{4.49}$$

where $U = I_{2N\times 2N}\cos(\theta) + i\sin(\theta)\mathcal{P}$ is a SU($2N$) unitary matrix. Once again, when $N = 1$, U is a SU(2) matrix, whose manifold is S^3, the same as the target manifold of Eq. (4.46). For arbitrary N, under translation, $T_x : \theta \to \pi - \theta$, $T_x : U \to -U$. Thus $\cos(\theta) \sim \phi$ is the VBS order parameter.

The same field theory Eq. (4.49) describes the boundary of a $2d$ SPT state with PSU($2N$) $\times Z_2$ symmetry, where Z_2 plays the role of T_x. And the physical picture of this $2d$ SPT is that, we decorate every Z_2 domain wall with a Haldane phase with PSU($2N$) symmetry. Thus as one would naively expect, the SU($2N$) spin chain with self-conjugate representation cannot have a featureless ground state, because it can be mapped to the boundary of a nontrivial $2d$ SPT state.

4.3.1.4 SO(N) spin chain

A SO(N) spin chain with a translation symmetry may still obey a generalization of the LSM theorem. But first let us review the current understanding of the Haldane phase of $1d$ SO(N) spin chain. When N is an odd integer, the double covering group of SO(N), *i.e.* Spin(N), has a representation which is a spinor of SO(N). Thus when N is odd, there is a Haldane phase with SO(N) symmetry with a Z_2 classification, as two spinors of SO(N) will merge into a linear representation of SO(N) [183]. Thus in $2d$ space, there is a SPT state with SO(N) $\times Z_2$ symmetry, which is constructed by decorating the $1d$ SO(N) Haldane phase in each Z_2 domain wall. Then the $1d$ boundary of this $2d$ SPT state with SO(N) $\times Z_2$ symmetry, has the feature that, at every Z_2 domain wall there must be a SO(N) spinor, and this $1d$ boundary cannot be trivially gapped without breaking the Z_2 symmetry.

Now let's consider a Spin(N) spin chain with a spinor on every site. Two Spin(N) spinors with odd N can always form a singlet, thus this spin chain naturally hosts two fold degenerate VBS states, which transform into each other through translation by one

lattice constant. The domain wall of these two VBS states is a Spin(N) spinor, which is equivalently to the domain wall of the Z_2 order parameter at the $1d$ boundary of the $2d$ SO(N) $\times$ Z_2 SPT state mentioned above. Based on these observations, we can conclude that *with odd N, a $1d$ Spin(N) spin chain with spinor representation on every site, does not permit a featureless gapped state.*

For even N, let's take $N = 2n$, then the Haldane phase has a richer structure. SO($2n$) has a Z_2 center which commutes with all the other elements, thus we can actually consider the Haldane phase with symmetry PSO($2n$) = SO($2n$)/Z_2. Then according to Ref. [182], the center of Spin($2n$) can be either Z_4 or $Z_2 \times Z_2$, for odd and even integer n respectively. But in either case, a Haldane phase with PSO($2n$) symmetry could have either spinor or vector representation at the boundary, both cases are nontrivial Haldane phase. And we can construct a $2d$ SPT with PSO($2n$)$\times Z_2$ symmetry, by decorating the Z_2 domain wall with a PSO($2n$) Haldane phase. But this PSO($2n$) Haldane phase must have a Z_2 nature, in the sense that two copies of the Haldane phase must be a trivial state, because two Z_2 domain walls will fuse into a trivial defect. Thus for both odd and even n, we can always decorate the Z_2 domain wall with the PSO($2n$) Haldane phase with a SO($2n$) vector at the boundary, which leads to the following LSM theorem:

A $1d$ SO($2n$) spin chain with vector representation on every site does not permit a featureless gapped state.

This conclusion is consistent with the result of Ref. [184].

4.3.2 spin systems on the square lattice

4.3.2.1 SU(2) spin systems

The generalized LSM theorem in higher dimensions does apply to the $2d$ spin-1/2 system on the square lattice [168, 169], *i.e.* there cannot be a featureless spin state on

the square lattice for a spin-1/2 system with SU(2) spin symmetry. This conclusion is consistent with many observations, including a generalization of Eq. (4.46) to $(2+1)d$ [147]:

$$\mathcal{S} = \int d^2x d\tau \, \frac{1}{g}(\partial_\mu \boldsymbol{n})^2 + \frac{2\pi i}{\Omega_4} \int_0^1 du \, \epsilon_{abcde} n^a \partial_\tau n^b \partial_x n^c \partial_y n^d \partial_u n^e, \tag{4.50}$$

where $\boldsymbol{n}$ is a five component unit vector, which forms the target manifold S^4 with volume Ω_4. (n_1, n_2, n_3) is still the three component Néel order parameter on the square lattice, while n_4 and n_5 are the columnar VBS states along the x and y directions respectively. The site-centered 90 degree rotation of the square lattice acts on (n_4, n_5) as a Z_4 rotation, and close to the deconfined quantum critical point [123, 124], one can usually embed the Z_4 into an enlarged U(1) group.

The physical meaning of the WZW term in Eq. (4.50) is that, the vortex of (n_4, n_5) carries a spin-1/2 excitation [28], and the Skyrmion of (n_1, n_2, n_3) carries lattice momentum. If we view $b \sim n_4 + i n_5$ as a boson annihilation operator, then the Skyrmion of (n_1, n_2, n_3) would carry nonzero boson number of b. Thus if we destroy the ordinary Néel order by condensing the Skyrmions of the Néel order parameter, the system automatically develops a columnar VBS order; and if we destroy the VBS order by condensing the (Z_4) vortex of the columnar VBS order parameter, the system automatically breaks the spin symmetry and develops the Néel order.

Eq. (4.50) can be derived explicitly by starting with the $\pi-$flux spin liquid state on the square lattice [185], and it was proposed as an effective field theory [147] that describes the deconfined quantum critical point between Néel and VBS order on the square lattice [123, 124], and this is the critical point whose vicinity we will study and map to the boundary of a $3d$ system, as we discussed in the introduction. The key physics of the intertwinement between the Néel and VBS order parameter is encoded

in the WZW term. Eq. (4.50) is capable of encapsulating a large SO(5)×Z_2^T symmetry, and it also describes the boundary state of a 3d bosonic SPT state whose symmetry can be as large as SO(5)×Z_2^T. Eq. (4.50) can also describe the boundary of 3d SPT states with a symmetry that is a subgroup of SO(5)×Z_2^T [32, 63]. According to the definition of SPT states, if the 3d bulk is a nontrivial SPT state, then the boundary cannot be a featureless state; while if the 3d bulk is a trivial direct product state after breaking the SO(5)×Z_2^T to its subgroup, then the boundary in principle can be trivially gapped without degeneracy.

It is clear that if the symmetry SO(5)×Z_2^T is reduced to SO(3)×U(1), where (n_1, n_2, n_3) rotates as a vector of SO(3) and singlet under U(1), while (n_4, n_5) transforms as a vector of U(1) and singlet of SO(3), the bulk is still a nontrivial SPT state. And this state can be understood as the "decorated vortex line" construction introduced in Ref. [32]: one first breaks the U(1) symmetry by condensing the two component vector (n_4, n_5), and decorate a Haldane phase with the SO(3) spin symmetry on each vortex loop of (n_4, n_5) with odd vorticity, then proliferate the vortex loops to restore the U(1) symmetry. The SPT state so-constructed has a Z_2 classification, which is consistent with the Z_2 classification of the Haldane phase decorated in each vortex loop, and also consistent with the Z_2 nature of the fourth Steifel-Whitney class of the SO(5) gauge bundle [185]. This implies that two copies of the 3d SPT states with SO(3)×U(1) symmetry weakly coupled together will become a trivial 3d bulk state.

The site-centered rotation symmetry of the square lattice acts on (n_4, n_5) as the Z_4 subgroup of U(1). The 3d nontrivial SPT state with SO(3)×U(1) symmetry survives under the further symmetry breaking of U(1) to Z_4, as a Z_4 vortex loop is still a well-define object in the bulk and can be decorated with a 1d Haldane phase. The same conclusion still holds if we consider a spin-1/2 system on the rectangular lattice. Now this system corresponds to the boundary of a 3d bulk SPT with SO(3)×$Z_2^x \times Z_2^y$. n_4,

n_5 each changes its sign under one of these two Z_2s, while (n_1, n_2, n_3) is odd under both Z_2s. The two Z_2s correspond to translation along x and y directions respectively. The $3d$ bulk SPT state can be viewed as decorating the Z_2^x domain wall with the $2d$ SPT with $\mathrm{SO}(3)\times Z_2^y$ symmetry, or equivalently decorating the Z_2^y domain wall with the $2d$ $\mathrm{SO}(3)\times Z_2^x$ SPT state. This observation is consistent with the generalized LSM theorem which states that a spin-1/2 system on the rectangular lattice cannot have a featureless state.

Just like the previous section, if we break the spin symmetry down to $G \rtimes Z_2$, when $G = Z_{2n+1}$ the spin system on the square lattice allows a featureless state, because the Haldane phase that we decorated in the vortex loop becomes a trivial state with only $Z_{2n+1} \rtimes Z_2$ spin symmetry.

Now suppose we consider a spin-1 system on the square lattice, then a similar deconfined quantum critical point corresponds to Eq. (4.50) with a level-2 WZW term: the coefficient of the WZW term doubles. This equation with a level-2 WZW term can be derived using the $\pi-$flux spin liquid state of a spin-1 system on the square lattice: there are twice as many Dirac fermions in the Brillouin zone compared with the case derived in Ref. [185], thus the level of the WZW term also doubles (the difference from the spin-1/2 $\pi-$flux state is that, the spin-1 $\pi-$flux state has a Sp(4) gauge fluctuation [186], while the spin-1/2 $\pi-$flux state has a SU(2) gauge fluctuation). The physical meaning of this term is that, the vortex of (n_4, n_5) now carries a spin-1 instead of spin-1/2, which is equivalent to the physics of the boundary of two weakly coupled $3d$ SPT states with $\mathrm{SO}(3)\times\mathrm{U}(1)$ symmetry, and as we discussed above, this state is generically a trivial state in the bulk. Thus its boundary could be a featureless gapped state. This observation implies that *a spin-1 system on the square lattice permits a featureless state, which is consistent with the conclusion of Ref. [171].*

4.3.2.2 SU(N) and SO(N) spin systems

Now let us consider a SU(N) spin system on the square lattice, with fundamental representation (FR) on sublattice A, and anti-fundamental representation (AFR) on sublattice B. Since the spins on two nearest neighbor sites can still form a SU(N) spin singlet, the columnar VBS order parameter and its Z_4 structure still naturally hold: the site-centered lattice rotation acts as a Z_4 rotation of the columnar VBS order parameter in this system. The Z_4 vortex (antivortex) of the VBS order parameter always has a vacant sublattice A (B) in the core, hence it always carries SU(N) FR (AFR). This is consistent with the fact that a vortex-antivortex pair can always annihilate, hence the quantum spin they carry must together form a spin singlet. An analogous effect on the honeycomb lattice is depicted in Fig. 4.11,4.12.

With large enough N, a Heisenberg model with the representation described above should have the four fold degenerate VBS state [187, 188]. Now we ask whether a featureless ground state of this spin system is in principle allowed or not. Once again, we first view the Z_4 lattice rotation as an onsite internal symmetry, and enlarge it to U(1). Then the $2d$ spin system on the square lattice can be *potentially* viewed as the boundary of a $3d$ bosonic SPT state with PSU(N) $\times$ $U(1)$ symmetry.

The bosonic SPT states with PSU(N) $\times$ $U(1)$ symmetry do exist in $3d$, and they can be interpreted as the decorated vortex loop construction, *i.e.* we decorate every U(1) unit vortex loop with a $1d$ PSU(N) Haldane phase, whose boundary is a projective representation of the PSU(N), or a faithful representation of SU(N). As we have discussed, $1d$ PSU(N) Haldane phase has a Z_N classification, which corresponds to N different projective representations of the PSU(N) group, or N different representation of the Z_N center of SU(N).

In general, the $N-1$ different nontrivial Haldane phases of PSU(N) can be described

by Eq. (4.48) with $\Theta = 2\pi$, and $\mathcal{P}$ replaced by [179]

$$\mathcal{P} = V\Omega V^{\dagger}, \;\; \Omega \equiv \begin{pmatrix} \mathbf{1}_{m\times m} & \mathbf{0}_{m\times N-m} \\ \\ \mathbf{0}_{N-m\times m} & -\mathbf{1}_{N-m\times N-m} \end{pmatrix} \tag{4.51}$$

with $m = 1, \cdots N-1$, and V is a SU(N) matrix. All the configurations of $\mathcal{P}$ belong to the Grassmanian manifold $U(N)/[U(m)\times U(N-m)]$. In our case, when the vortex line terminates at the boundary, the vortex at the boundary will carry a FR of SU(N), hence for our case we need to choose $m = 1$, and $\mathcal{P}$ becomes the CP^{N-1} manifold.

However, let us not forget that eventually we need to break the U(1) symmetry down to Z_4. Then for the $3d$ SPT state to survive under this symmetry breaking, the Z_N classification of the PSU(N) Haldane phase must be compatible with the Z_4 vortex. If N and 4 are coprime, then this bulk state definitely becomes trivial after breaking the U(1) to Z_4. For example, when $N = 3$, there is no consistent way we can decorate the Z_4 vortex with a PSU(3) Haldane phase. Because four Z_4 vortex loops merge together will no longer be a well-defined defect, while four PSU(3) Haldane phases merge together is still a nontrivial Haldane phase. Thus for odd integer N, the $3d$ SPT phase with PSU(N)×U(1) symmetry becomes a trivial phase once U(1) is broken down to Z_4.

To further demonstrate that for odd integer N, the $3d$ SPT phase with PSU(N)× U(1) symmetry is trivialized with U(1) broken down to Z_4, we need to show that its $2d$ boundary can be trivially gapped out when U(1) is broken down to Z_4. One of the $2d$ boundary states of the $3d$ PSU(N)×U(1) SPT phase, is a Z_N topological order, which can be constructed by starting with a superfluid order with spontaneous U(1) symmetry breaking at the $2d$ boundary, and then condense the $N-$fold vortex (a vortex with $2\pi N$ vorticity) of the superfluid order. The single vortex of the superfuid phase carries a FR

of SU(N), hence a $N-$fold vortex can carry a SU(N) singlet, and its condensate is a Z_N topological order which preserves all the symmetries. A $2d$ Z_N topological order has bosonic e and m excitations, while e and m have mutual statistics with statistical angle $\theta_{e,m} = 2\pi/N$. In our construction, the e excitation carries $1/N$ charge of the U(1) symmetry, and the m excitation carries a FR of SU(N).

Once U(1) is broken down to Z_4, In order to gap out the Z_N topological order, we can condense the bound state of a e particle and $3N$ Z_4 charges. This bound state carries $\frac{3N^2+1}{N}$ Z_4 charges. Under the Z_4 transformation, it acquires a phase $\exp\left(\frac{2\pi(3N^2+1)}{4N}i\right)$, which can always be cancelled/compensated by a gauge transformation with odd integer N (the numerator of the phase angle is always a multiple of 8π with odd integer N). Thus the condensate of this bound state will drive the Z_N topological order into a completely featureless gapped state without any anyons, and all the global symmetries are preserved. This is only possible when N is odd.

As a contrast, for even integer N, we can always construct a nontrivial $3d$ SPT by decorating the Z_4 vortex loop with the $1d$ SPT state with SU(N)/Z_2 symmetry, which has a Z_2 classification.

Now we can make the following conclusion:

A SU(N) spin system on the square lattice with fundamental and anti-fundamental representation on the two sublattices, permit a featureless gapped ground state for odd integer N.

We can also consider SO(N) spin systems on the square lattice. The analysis is very similar to the previous case. We can make the following conclusion:

A SO($2n$) spin system with vector representation on every site does not permit a featureless gapped state on the square lattice.

A SO($2n+1$) spin system with spinor representation on every site does not permit a featureless gapped state on the square lattice.

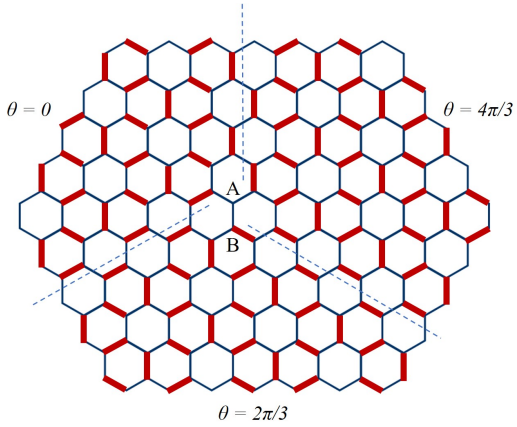

Figure 4.11: A Z_3 vortex of the VBS order parameter on the honeycomb lattice has a vacant site on the sublattice A, and hence carries a fundamental representation of the SU(N) spin.

On the other hand, A SO($2n+1$) spin system with vector representation on every site does permit a featureless gapped state.

4.3.3 spin systems on the honeycomb lattice

4.3.3.1 SU(2) spin systems

A spin-1/2 system on the honeycomb lattice, when tuned close to certain point, can also be described by Eq. (4.50). Eq. (4.50) can be derived with the SU(2) spin liquid on the honeycomb lattice, like the one discussed in Ref. [189]. Now the lattice symmetry, both the translation T_x and a site-centered 120 degree rotation, acts as a Z_3 subgroup of the U(1) transformation on (n_4, n_5).

Once again, the question of whether a featureless spin-1/2 state exists on the honeycomb lattice is equivalent to whether the $3d$ SPT state with SO(3)×U(1) symmetry is stable against breaking the U(1) down to Z_3. It turns out that this time the $3d$ bulk becomes a trivial state. The vortex loop decoration picture fails with a Z_3 symmetry. Suppose we decorate a Haldane phase on each Z_3 vortex loop, then three of the Z_3 vortex

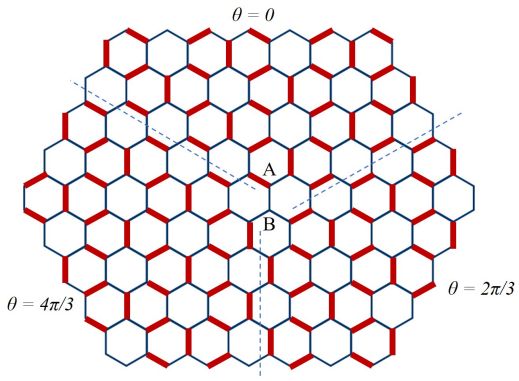

Figure 4.12: An antivortex of the VBS order parameter on the honeycomb lattice has a vacant site on the sublattice B, and hence carries a anti-fundamental representation of the SU(N) spin.

loops would be decorated with three Haldane phases, and due to the Z_2 classification of the $1d$ Haldane phase, three Haldane phases is still a nontrivial $1d$ SPT state. However, a three fold Z_3 vortex loop is no longer a well-defined defect any more. Thus the decorated vortex loop picture is incompatible with the Z_3 symmetry. Thus the bulk becomes a trivial state once we break the U(1) down to Z_3. This implies that the $2d$ boundary, which corresponds to the spin-1/2 system on the honeycomb lattice, permits a featureless spin state. This is consistent with the previous result on the honeycomb lattice [171, 172].

We can also add other symmetries of the honeycomb lattice, such as reflection P_x : $y \to -y$. Under this reflection, $P_x : (n_1, n_2, n_3) \to -(n_1, n_2, n_3)$, while (n_4, n_5) is unchanged. In the Euclidean space-time, a reflection symmetry can be treated equivalently as the time-reversal symmetry. Thus with both translation T_x and reflection P_x, we need to study whether the $3d$ SPT state with SO(3)$\times Z_2^T \times$U(1) symmetry is stable against symmetry breaking down to SO(3)$\times Z_2^T \times Z_3$. The analysis is the same as before: the $3d$ SPT state with SO(3)$\times Z_2^T \times$U(1) symmetry is constructed with proliferated vortex loops decorated with a $1d$ Haldane phase with SO(3)$\times Z_2^T$ symmetry. However, this construction is still incompatible with the Z_3 vortex loops, because the classification of the

Haldane phase with SO(3)$\times Z_2^T$ symmetry is $Z_2 \times Z_2$.

4.3.3.2 SU(N) and SO(N) spin systems

Now let us consider a SU(N) spin system on the honeycomb lattice, again with FR on sublattice A, and AFR on sublattice B. This system can still form the three fold degenerate VBS states, and the vortex (antivortex) of the VBS order parameter has a vacant site in sublattice A (B), which carries a FR (AFR) of SU(N) (Fig. 4.11,4.12).

Now we want to ask whether the $3d$ SPT state with PSU(N)$\times U(1)$ symmetry is stable against breaking the U(1) down to Z_3. This depends on whether the PSU(N) SPT state decorated on the vortex line is compatible with the Z_3 nature of the vortex line, *i.e.* N at least cannot be coprime with 3. Thus when N is coprime with 3, the $3d$ SPT state PSU(N)$\times U(1)$ symmetry is trivialized by breaking U(1) down to Z_3.

Just like the case in the previous section, the boundary of a $3d$ SPT with PSU(N)$\times U(1)$ symmetry could be a $2d$ Z_N topological order, whose e particle carries $1/N$ charge of U(1), and m particle carries a FR of SU(N). Once U(1) is broken down to Z_3, if N is coprime with 3, by condensing a bound state of e and certain number of Z_3 charges, this $2d$ boundary Z_N topological order is driven into a featureless gapped state.

We can now make the following conclusion:

SU(N) spin systems on the honeycomb lattice with fundamental and anti-fundamental representation on the two sublattices, permit a featureless gapped ground state when N is not a multiple of 3.

Also, similar conclusions can be made for SO(N) spin systems:

A SO($2n$) spin system with vector representation on every site permits a featureless state on the honeycomb lattice.

A SO($2n+1$) spin system with spinor or vector representation on every site also permits a featureless state on the honeycomb lattice.

4.3.4 $3d$ spin systems on the cubic lattice

A spin-1/2 system on the cubic lattice is subject to the generalized LSM theorem, thus it cannot have a featureless state. Besides the common Néel ordered state, another natural spin-1/2 state on the cubic lattice is the columnar VBS state. And the "hedgehog monopole" of the VBS order parameter carries a spin-1/2, and the monopole of the Néel order parameter carries lattice momentum [190], whose condensate is precisely the VBS order. This system enjoys a nice self-duality structure. We can introduce the vector Néel order parameter $\boldsymbol{n}^e$ and vector VBS order parameter $\boldsymbol{n}^m$, as well as their CP^1 fields [190, 191]:

$$\boldsymbol{n}^e \sim \frac{1}{2} z^{e\dagger} \boldsymbol{\sigma} z^e, \quad \boldsymbol{n}^m \sim \frac{1}{2} z^{m\dagger} \boldsymbol{\sigma} z^m. \tag{4.52}$$

When the spin system is driven into a photon phase, which is stable in $(3+1)d$, z^e and z^m are the gauge charge and the Dirac monopole of the dynamical U(1) gauge field a_μ respectively.

The cubic lattice symmetry acts on $\boldsymbol{n}^m$ as the octahedral subgroup of SO(3) [5], and z^e, z^m carry projective representation of the SO(3) spin and (enlarged) SO(3) lattice symmetry respectively. The intertwinement between the Néel and VBS order is captured by a $(3+1)d$ WZW term of a six component vector which contains both $\boldsymbol{n}^e$ and $\boldsymbol{n}^m$ [192].

The same physics can be realized at the boundary of a $4d$ SPT state with $\mathrm{SO}(3)^e \times \mathrm{SO}(3)^m$ symmetry. This state can be understood as the "decorated monopole line" construction. In the $4d$ space, a $\mathrm{SO}(3)^e$ hedgehog monopole is a line defect, and we can decorate it with a $1d$ Haldane phase with $\mathrm{SO}(3)^m$ symmetry. The CP^1 field z^m can be viewed as the

[5] The octahedral group O does not include the spatial mirror (reflection) symmetry. The mirror symmetry is equivalent to time-reversal symmetry in the analysis of SPT states, as we explained previously. Including the mirror symmetry does not change our conclusions, because the SO(3) Haldane phase with or without an extra time-reversal symmetry always has a Z_2 nature, *i.e.* two of these Haldane phases coupled together becomes a trivial state.

termination of the $\mathrm{SO}(3)^e$ hedgehog monopole line at the $3d$ boundary, which is also the boundary state of the $1d$ $\mathrm{SO}(3)^m$ Haldane phase. The self-duality of the boundary QED implies that the decoration construction is necessarily mutual, *i.e.* we must simultaneously decorate the $\mathrm{SO}(3)^m$ hedgehog monopole with a Haldane phase with the $\mathrm{SO}(3)^e$ symmetry.

The "mutual decoration" construction can also be perceived as follows. In the $4d$ space, we can discuss the braiding process of two loops. Imagine we create two loops L^e and L^m from vacuum, and annihilate them at a later time, then the world sheets of both loops are topologically two dimensional spheres, labelled as S^2_e and S^2_m. If these two loops are braided, their world sheets are linked in the five dimensional space-time. This linking can be interpreted as the intersection of S^2_e with the interior of S^2_m (which is a three dimensional ball) at one point in the space time. Now suppose S^2_e and S^2_m are the world sheets of the $\mathrm{SO}(3)^e$ and $\mathrm{SO}(3)^m$ monopole lines respectively, if the $\mathrm{SO}(3)^m$ monopole line is decorated with the $\mathrm{SO}(3)^e$ Haldane phase, then this linking will accumulate phase 2π, which comes from the $\Theta-$term of the $\mathrm{SO}(3)^e$ Haldane phase.

The linking mentioned above is also symmetric under interchanging e and m, namely it can be viewed as the intersection of S^2_m with the interior of S^2_e at another point in the space-time. Thus if this linking accumulates phase 2π, then consistency demands that the $\mathrm{SO}(3)^e$ monopole line be decorated with the $\mathrm{SO}(3)^m$ Haldane phase too.

The $4d$ SPT state so constructed obviously has a Z_2 classification, as both the $\mathrm{SO}(3)^e$ and $\mathrm{SO}(3)^m$ SPT phases have Z_2 classification. To make an explicit connection with the $(3+1)d$ QED state discussed in Ref. [190], one can first start with fractionalizing $\boldsymbol{n}^e$ in the bulk, and introduce a $(4+1)d$ U(1) gauge field a_μ. The hedgehog monopole line of $\boldsymbol{n}^e$ becomes the Dirac monopole line of a_μ, which is decorated with the $\mathrm{SO}(3)^m$ Haldane phase. Now we condense the Dirac monopole line in the bulk, but do not condense the termination of the Dirac monopole line at the $3d$ boundary, which becomes the Dirac

monopoles (point like defects) at the $3d$ boundary. This will lead to a gapped $4d$ bulk state, while the $3d$ boundary is the QED state discussed in Ref. [190] with z^e and z^m being the gauge charge and Dirac monopole respectively.

The picture above can again be generalized to the PSU(N) spin system with FR and AFR on the two sublattices. Whether this spin system permits a featureless gapped state or not, is equivalent to whether the corresponding $4d$ bulk state is a trivial state or a SPT state. The CP^{N-1} manifold, *i.e.* the SU(N) generalization of the Néel order parameter, has $\pi_2[\mathrm{CP}^{N-1}] = Z$, and hence also has a "hedgehog monopole" line in the $4d$ space. Thus we can again decorate the $\mathrm{SO}(3)^m$ monopole line with the PSU(N) Haldane phase, and simultaneously decorate the PSU(N) monopole line with the $\mathrm{SO}(3)^m$ Haldane phase. But now this $4d$ state is *not* always a nontrivial SPT state. Because the $\mathrm{SO}(3)^m$ Haldane phase has a Z_2 classification, hence even-number copies of the $4d$ state must be a trivial state, while odd-number copies of the states is equivalent to the state itself. On the other hand, the PSU(N) Haldane phase has a Z_N classification, namely N copies of the states must be trivial. Thus the $4d$ bulk state so constructed has a $Z_{(2,N)}$ classification: the "mutual monopole line decoration" gives us a nontrivial $4d$ SPT state only with even N.

The natural $3d$ boundary state of the $4d$ bulk based on the "mutual" monopole line decoration construction, is a U(1) photon phase whose e excitations carry SU(N) fundamental, and m carries a spin-1/2 of SO(3). When N is odd, we can drive the $3d$ boundary into a featureless state by condensing the dyon which is a bound state of N e particles and two m particles. We label this dyon as the $(N, 2)$ dyon. This $(N, 2)$ dyon is a boson, and its condensate will gap out the photons, while confining all the point particles, because there is no point particle that is mutual bosonic with this dyon, except for the dyon itself. Also, the $(N, 2)$ dyon could be a singlet of SU(N), and singlet of SO(3), thus its condensate does not break any global symmetry. This means that for odd integer N, the $3d$ boundary of the $4d$ bulk state can be driven into a featureless gapped state, which

again demonstrates that the $4d$ bulk state constructed above is trivial when N is odd.

By contrast, if N is even, then the $(N/2, 1)$ dyon (with nontrivial representation of $\mathrm{SU}(N)$ and $\mathrm{SO}(3)$) is still deconfined in the condensate of $(N, 2)$ dyon, and this condensate has topological order.

Now we can conclude that:

For odd N, the SU(N) spin system on the cubic lattice with FR and AFR spins on two sublattices permits a featureless spin state.

Here we propose a low energy effective field theory for the $4d$ SPT state that captures the "mutual decorated monopole line" construction. We first define a $\mathrm{U}(2N)$ matrix field U as

$$U = \cos(\theta)\mathcal{P} \otimes I_{2\times 2} + i\sin(\theta) I_{N\times N} \otimes \boldsymbol{n}\cdot\boldsymbol{\tau}, \tag{4.53}$$

where $\mathcal{P}$ is the CP^{N-1} matrix field given by Eq. (4.51). The "mutual decoration" picture is captured by a topological term in the nonlinear sigma model of U which reads

$$\mathcal{L}_{5d}^{topo} = \int d^4x d\tau \ \frac{2\pi}{480\pi^3}\mathrm{Tr}\left[(U^\dagger dU)^5\right]. \tag{4.54}$$

We will show that if we manually create a monopole line of $\boldsymbol{n}$, the topological term Eq. (4.54) precisely reduces to the topological term of the $(1+1)d$ $\mathrm{PSU}(N)$ SPT. Let us parametrize the $(4+1)d$ space-time by Cartesian coordinates (x, y, z, w, τ) and consider a static monopole line of $\boldsymbol{n}$ whose core line lies on the w-axis. For any fixed w and τ, we will see a monopole configuration of $\boldsymbol{n}$ centered at origin in the xyz space. For a monopole configuration in the xyz space, we have

$$\theta(r = 0) = 0,$$

$$\theta(r \to \infty) = \pi/2$$

$$\int_{r=r_0>0} d^2\Omega \ \frac{1}{8\pi}\epsilon_{ijk}\epsilon_{\alpha\beta}n^i\partial_\alpha n^j\partial_\beta n^k = 1 \tag{4.55}$$

where $r = \sqrt{x^2+y^2+z^2}$. We also assume $\mathcal{P}$ is a function of w and τ. Now we plug in this configuration of $\boldsymbol{n}$ in to Eq. (4.54) and integrate over x, y and z directions. This topological term reduces to the following $(1+1)d$ topological term in the (w, τ) space:

$$\mathcal{L}_{2d}^{topo} = \int dwd\tau \ \frac{2\pi}{16\pi}\epsilon_{\mu\nu}\mathrm{Tr}\left(\mathcal{P}\partial_\mu\mathcal{P}\partial_\nu\mathcal{P}\right), \tag{4.56}$$

which is precisely the topological Θ-term for the PSU(N) Haldane phase. This indicates that Eq. (4.54) implies there is a PSU(N) SPT decorated on the monopole line of $\boldsymbol{n}$.

If we consider a monopole line of $\mathcal{P}$ along w-axis, then in the xyz directions we have

$$\theta(r = 0) = \pi/2,$$

$$\theta(r \to \infty) = 0$$

$$\int_{r=r_0>0} d^2\Omega \ \frac{i}{16\pi}\epsilon_{\mu\nu}\mathrm{Tr}\left(\mathcal{P}\partial_\mu\mathcal{P}\partial_\nu\mathcal{P}\right) = 1 \tag{4.57}$$

Now integrating over x, y and z directions will give us the following topological term in the $(1+1)d$ space-time of the monopole line world sheet:

$$\mathcal{L}_{2d}^{topo} = \int dwd\tau \ \frac{2\pi i}{8\pi}\epsilon_{abc}\epsilon_{\mu\nu}n^a\partial_\mu n^b\partial_\nu n^c, \tag{4.58}$$

which exactly corresponds to the topological term of the $(1+1)d$ SO(3) Haldane phase.

Therefore, the topological term in Eq. (4.54) captures the "mutual decoration" construction of the $(4+1)d$ SPT phase with PSU(N)×SO(3) symmetry.

4.3.5 Further proof of our conclusions

4.3.5.1 Explicit construction of featureless spin states

Let us first restate our main conclusions about SU(N) spin systems on the square, honeycomb, and cubic lattices:

1. A SU(N) spin system on the square lattice with fundamental (FR) and anti-fundamental representation (AFR) on the two different sublattices respectively, permits a featureless gapped ground state when N is an odd integer;

2. A SU(N) spin system on the honeycomb lattice with FR and AFR on two different sublattices, permits a featureless gapped ground state when N is coprime with 3.

3. A SU(N) spin system on the cubic lattice with FR and AFR spins on two different sublattices, permits a featureless spin state when N is odd.

For all the spin systems listed above, we can construct explicit featureless tensor product spin states similar to the AKLT states. All these states will be discussed in a future work [193]. Here we discuss some of the examples of this construction.

On the honeycomb lattice, in the case of $N = 3k+1$, we introduce $3k$ auxiliary spins on each site. We also introduce a tensor on each site:

$$T^{\alpha}_{i_1 i_2 \cdots i_{3k}} = \varepsilon_{\alpha i_1 i_2 \ldots i_{3k}}, \tag{4.59}$$

where $\varepsilon_{\alpha i_1 i_2 \ldots i_{3k}}$ is the total anti-symmetric tensor with $N = 3k + 1$ indices. Here, the $i_1, i_2, \cdots i_{3k}$ labels the $3k$ auxiliary FR (or AFR) spin degrees of freedom on each site in sublattice B (or A) before the projection. Each label i_n takes value in $1, 2, \cdots N$ representing the N states in each FR (or AFR). The label α, which also takes value $1, 2, \cdots N$, represents the physical states in AFR (or FR) spin degrees of freedom on each site in sublattice B (or A). Physically, on each site of sublattice A, the tensor in Eq. (4.59) projects the $3k$ auxiliary AFR spins into a totally anti-symmetric channel which, due to the nature of SU$(3k + 1)$, becomes the physical FR spin. The analysis for sites in the sublattice B is similar. Now we can use the auxiliary spins to construct a featureless gapped state on the honeycomb lattice with k SU(N) singlet bonds along each link of the lattice, which is reminiscent of the AKLT state.

Obviously, the so constructed tensor product state respects the translation symmetry of the lattice. Now we analyze the compatibility between the point group C_{3v} and the site tensor in Eq. (4.59). Here, notice that we include not only the C_3 rotation symmetry but also the mirror reflection symmetry of the honeycomb lattice into consideration. We notice that the point group only induces a permutation of the singlet bonds before the projection. Therefore, the action of the point group permutes the $3k$ spins on each site. Since we project the $3k$ spins into a totally anti-symmetric channel using the site tensor, the point group induced permutation keeps the site tensor invariant up to a global sign which is unimportant for the global tensor network wave function. Therefore, we can conclude that the choice of projection tensor in Eq. (4.59) preserves the space symmetries.

On the square lattice, in the case of $N = 4k + 1$, we introduce $4k$ auxiliary spins on each site and let the auxiliary spins form a state with k SU(N) singlet bonds along each link of the square lattice. We can choose the site tensors to be

$$T^{\alpha}_{i_1 i_2 \cdots i_{4k}} = \varepsilon_{\alpha i_1 i_2 \cdots i_{4k}}, \tag{4.60}$$

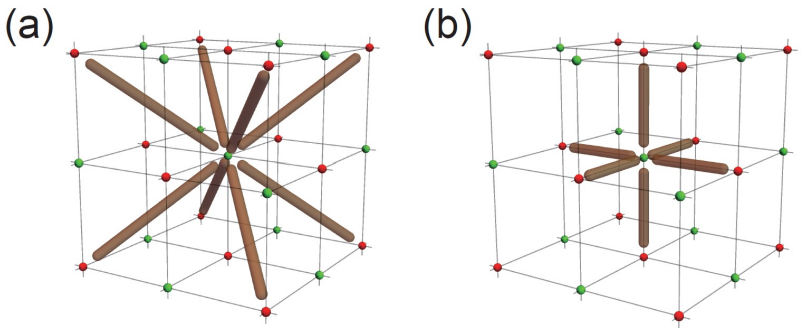

Figure 4.13: (a) The schematic featureless SU(N) spin state on the cubic lattice when $N = 8p+1$; (b), the schematic featureless SU(N) spin state on the cubic lattice when $N = 6q+1$. More general spin systems with $N = 8p+6q+1$ have valence bonds extended along both the link and diagonal directions of the cubic lattice.

where $\varepsilon_{\alpha i_1 i_2 \cdots i_{4k}}$ is the total anti-symmetric tensor with $N = 4k+1$ indices. Based on analysis completely in parallel with the honeycomb lattice, we conclude that the physical spin carries AFR (FR) under SU(N) if the auxiliary spins transform as FR (AFR). Also, we can conclude that the tensors in Eq. 4.60 are invariant under the C_{4v} point group action up to an unimportant sign because the actions of the C_{4v} point group on the site tensor are only permutation of the tensor indices. Now we can use the $4k$ auxiliary spins on each site to construct a featureless spin state on the square lattice.

On the cubic lattice, for any odd integer N that is not $3, 5$ or 11, we can write N as $N = 8p+6q+1$ with p and q non-negative integers. Again we introduce $N-1$ auxiliary spins, and an on-site tensor $T^{\alpha}_{i_1 i_2 \ldots i_{N-1}} = \varepsilon_{\alpha i_1 i_2 \ldots i_{N-1}}$. Namely on sublattice B, we represent the AFR with $N-1$ auxiliary FRs, and on sublattice A we represent the FR with $N-1$ AFRs. Now these auxiliary spins can form a featureless states with valence bonds extended either along the link (for $N = 6q+1$) or the diagonal directions (for $N = 8p+1$), or both directions (when p and q are both nonzero) on the cubic lattice (Fig. 4.13).

The point group O_h of the cubic lattice will induce a permutation among the $N-1$ auxiliary spins on each site which at most leads to an unimportant sign change of the

site tensor. Therefore, this site tensor is compatible with the point group O_h symmetry. In fact, the O_h point group is isomorphic to $S_4 \times Z_2$. The Z_2 part is the spatial inversion which takes the point (x, y, z) to $(-x, -y, -z)$. S_4 is the permutation group of 4 elements, which can be generated by a Z_3 cyclic permutation and a Z_4 cyclic permutation. In the language of the point group, the S_4 part is the part of O_h that preserves the spatial orientation. It can be generated by a C_3 rotation about the $(1, 1, 1)$-axis and a C_4 rotation about the z-axis. This S_4 part alone (without the spatial inversion) is usually referred to the point group O.

The construction of these featureless tensor product wave functions does provide strong evidence to our conclusions in previous sections. Nevertheless, we need to comment that, to eventually confirm the featureless-ness of these tensor product wave functions, numerical simulation of these states is demanded, in order to rule out possible spontaneous symmetry breaking, etc. For instance, it is known that the AKLT wave function on a three dimensional lattice could have long range spin order.

4.3.5.2 Connection to "lattice homotogy class"

In fact, we can also simplify all the discussions by just considering a $Z_N \times Z_N$ subgroup of PSU(N) and analyzing how the FR and AFR of SU(N) transform under this $Z_N \times Z_N$ subgroup. To specify this $Z_N \times Z_N$ subgroup, we first consider two SU(N) matrices in

the FR:

$$g_1 = e^{i\pi(N-1)} \begin{pmatrix} 0 & 1 & 0 & ... & 0 & 0 \\ 0 & 0 & 1 & \ddots & & 0 \\ 0 & 0 & \ddots & \ddots & \ddots & \vdots \\ \vdots & \ddots & \ddots & \ddots & 1 & 0 \\ 0 & & \ddots & 0 & 0 & 1 \\ 1 & 0 & ... & 0 & 0 & 0 \end{pmatrix}$$

$$g_2 = e^{i\pi(N-1)} \begin{pmatrix} e^{\frac{i2\pi}{N}} & & & & & \\ & e^{\frac{i4\pi}{N}} & & & & \\ & & \ddots & & & \\ & & & e^{\frac{i2\pi(N-1)}{N}} & & \\ & & & & 1 \end{pmatrix}, \tag{4.61}$$

where g_1 only has non-zero entries on a subdiagonal and the bottom left corner, and g_2 is a diagonal matrix. It is straightforward to check that

$$g_1^N = g_2^N = 1_{N\times N}, \quad g_1 g_2 = e^{-i2\pi/N} g_2 g_1. \tag{4.62}$$

We denote the elements of PSU(N) corresponding to g_1 and g_2 as $\tilde{g}_1$ and $\tilde{g}_2$. Obviously, $\tilde{g}_{1,2}$ are elements of order N. Since the phase factor $e^{-i2\pi/N}$ in the commutation relation between g_1 and g_2 is one of the center elements in SU(N), $\tilde{g}_1$ and $\tilde{g}_2$ should commute in PSU(N). Therefore, $\tilde{g}_1$ and $\tilde{g}_2$ generate a $Z_N \times Z_N$ subgroup of PSU(N). We will focus on this subgroup in the following. Notice that, a physical FR spin, which transforms according to $g_{1,2}$ under this $Z_N \times Z_N$ subgroup of PSU(N), can be viewed as a projective representation of $Z_N \times Z_N$. In the classification of the projective representation $H^2(Z_N \times$

$Z_N, \mathrm{U}(1)) = Z_N$, the FR spins actually correspond to the generating element in $H^2(Z_N \times Z_N, \mathrm{U}(1))$. The AFR spins then correspond to the conjugate of the FR spins in terms of projective representations of $Z_N \times Z_N$.

When we restrict to the global internal symmetry $Z_N \times Z_N$ (which is a subgroup of $\mathrm{PSU}(N)$), we can apply the lattice homotopy classification introduced in Ref. [177]. It was proven for $1d$ and $2d$, partially proven for $3d$, and conjectured for general dimensions that the generalized Lieb-Schultz-Mattis (LSM) theorems will forbid the existence of any featureless states on lattices of "non-trivial lattice homotopy class". In fact, the lattice homotopy classification proposed in Ref. [177] also covers the cases with continuous internal symmetry group. However, the proof of the relations between non-trivial lattice homotopy classes and the existence of generalized LSM theorems is less comprehensive for the most general continuous symmetry group than for the general Abelian finite group. Therefore, we will focus on the lattice homotopy classification with Abelian finite group in this section.

For a lattice with n FR spins on each site of the sublattice A and n AFR spins on each site of the sublattice B, we will refer to it as the (n, n)-lattice. The fundamental-anti-fundamental lattices can then also be referred to as the $(1, 1)$-lattice. In addition to the global internal symmetry, the lattice homotopy classification depends on the choice of space group symmetry. Let's specify the minimal space group symmetry for the $(1, 1)$-honeycomb, $(1, 1)$-square and $(1, 1)$-cubic lattices we want to consider. For the $(1, 1)$-honeycomb lattice, we want to at least include the C_3 spatial rotation symmetry into consideration. Therefore, the minimal choice of space group is the wallpaper group $p3$ (No. 13). For the $(1, 1)$-square lattice, we want to at least consider the C_4 spatial rotation symmetry. Therefore, the minimal choice of space group is the wallpaper group $p4$ (No. 10). For the $(1, 1)$-cubic lattice, we want to at least consider the symmetry of the point group O. Therefore, the minimal choice of the 3D space group is $F432$ (No. 209). The

wallpaper group and 3D space group numbers can be found in Ref. [194].

With the global $Z_N \times Z_N$ internal symmetry and the minimal space groups symmetry given above, the $(1,1)$-honeycomb lattice belongs to a non-trivial lattice homotopy class when N is a multiple of 3. Similarly, $(1,1)$-square and $(1,1)$-cubic lattices are also non-trivial when N is even. Therefore, according to Ref. [177], there are generalized LSM theorems obstructing any featureless state compatible with the global and space group symmetries on these lattices. Of course, when we enlarge the $Z_N \times Z_N$ symmetry back to PSU(N), such obstructions still exist.

Hence the analysis of lattice homotopy class also indicates that *there is no featureless state with* PSU(N) *global symmetry on the* $(1,1)$*-honeycomb lattice with* N *being a multiple of 3, or on* $(1,1)$*-square or cubic lattices with even integer* N. These conclusions are completely consistent with those obtained from the analysis in the previous sections.

One can perform a similar lattice homotopy analysis for SO($2N$) spin systems with spins carrying the vector representation with $N \geq 1$. We focus on a $Z_2 \times Z_2$ subgroup of PSO($2N$). When $N = 4k$, we construct the SO($4k$) matrices

$$g_1 = i\sigma^y \otimes I_{2k\times 2k}, \qquad g_2 = \sigma^z \otimes I_{2k\times 2k}, \tag{4.63}$$

and notice that

$$g_1^2 = -1, \quad g_2^2 = 1, \quad g_1 g_2 = -g_2 g_1. \tag{4.64}$$

We denote the elements of PSO($4k$) that correspond to g_1 and g_2 as $\tilde{g}_1$ and $\tilde{g}_2$. Since $-I_{4k\times 4k}$ is a non-trivial center element of $SO(4k)$, the elements $\tilde{g}_{1,2}$ generate a $Z_2 \times Z_2$ subgroup of PSO($4k$). The vector representation, which transforms according to $g_{1,2}$ under this $Z_2 \times Z_2$ subgroup, can be viewed as a non-trivial projective representation of

$Z_2 \times Z_2$. If we restrict our attention to this $Z_2 \times Z_2$ subgroup of PSO($4k$), we notice that a square lattice with a SO($4k$) spin in the vector representation per site and with the space group $p4$ belongs to a non-trivial lattice homotopy class.

When $N = 4k + 2$, we construct the SO($4k + 2$) matrices

$$g_1 = \begin{pmatrix} \sigma^z & & & & \\ & \sigma^z & & & \\ & & i\sigma^y & & \\ & & & i\sigma^y \otimes I_{2(k-1)\times 2(k-1)} & \end{pmatrix},$$
$$g_2 = \begin{pmatrix} \sigma^x & & & & \\ & i\sigma^y & & & \\ & & \sigma^x & & \\ & & & \sigma^z \otimes I_{2(k-1)\times 2(k-1)} & \end{pmatrix} \tag{4.65}$$

which satisfy

$$g_1^4 = g_2^4 = 1, \quad g_1 g_2 = -g_2 g_1. \tag{4.66}$$

By similar reasoning in the SO($4k$) case, we find that the vector presentation of SO($4k+2$) can be viewed as a non-trivial projective representation of a $Z_4 \times Z_4$ subgroup in PSO($4k + 2$). In fact, the classification of projective representation of $Z_4 \times Z_4$ is given by $H^2(Z_4 \times Z_4, U(1)) = Z_4$ in which the vector representation belongs to the "second" non-trivial class. When we consider the space group $p4$ and the $Z_4 \times Z_4$ subgroup of PSO($4k + 2$) given above, we notice that the square lattice with a spin in the vector representation on each site also belongs to a non-trivial lattice homotopy class, just like that case of SO($4k$).

Hence, we can conclude that *A SO(2N) spin system with vector representation on*

every site does not permit a featureless gapped state on the square lattice. This result completely agrees with the analysis in the previous sections.

Lastly, we consider $\mathrm{SO}(2N+1)$ spin systems with spinor representations. $\mathrm{SO}(2N+1)$ is the group of rotations in $\mathbb{R}^{2N+1}$. Let $x_{1,2,\ldots,2N+1}$ denote the $2N+1$ axes of $\mathbb{R}^{2N+1}$. We'd like to focus on a $Z_2 \times Z_2$ subgroup of $\mathrm{SO}(2N+1)$ generated by the π-rotation in the x_1-x_2 plane and the π-rotation in the x_1-x_3 plane. The spinor representation of $\mathrm{SO}(2N+1)$ can be viewed as a non-trivial projective representation of this $Z_2 \times Z_2$ subgroup. When we consider the space group $p4$ and the $Z_2 \times Z_2$ subgroup of $\mathrm{SO}(2N+1)$ given above, we notice that the square lattice with a spin in the spinor representation on each site belongs to a non-trivial lattice homotopy class. Therefore, *a SO(*$2N+1$*) spin system with spinor representation on every site does not permit a featureless gapped state on the square lattice.* Again, this statement is consistent with the analysis given in the previous sections.

Chapter 5

Experimental Proposals for Symmetry Protected Topological Phases

The first section of this chapter is reprinted with permission from Yi-Zhuang You, Zhen Bi, Alex Rasmussen, Meng Cheng, and Cenke Xu, authors of *New J. Phys.* ***17****, 075010 (2015)* [195]. The second section is reprinted from *Phys. Rev. Lett.* ***118****, 126801 (2017)* [196] with permission from Zhen Bi, Ruixing Zhang, Yi-Zhuang You, Andrea Young, Leon Balents, Chao-Xing Liu, and Cenke Xu. The third part is based on *Phys. Rev. B* ***93****, 125101 (2016)*[197], with permission from Yi-Zhuang You, Zhen Bi, Dan Mao, and Cenke Xu.

In this chapter, we propose an experimental realization of bosonic SPT states. The key observation is that bosonic SPT can be built from interacting fermionic SPTs. This connection is discussed in the first section. In the second section, we layout an experimental proposal to realize bosonic SPT in bilayer graphene system. Experimental signatures for bosonic SPT states are also predicted. Finally, the third part is a careful theoretical

study of the bilayer model, in which we discover a multi-layer generalization to realize bosonic SPT with $Sp(N)$ symmetry.

5.1 Bridging fermionic and bosonic short range entangled states

A short range entangled (SRE) state is the ground state of a quantum many-body system that does not have bulk ground state degeneracy or topological entanglement entropy. However, these states can still have stable nontrivial edge states. Some of the SRE states need certain symmetry to protect the edge states, and these SRE states are also called symmetry protected topological (SPT) states. The most well-known SPT states include the Haldane phase of spin-1 chain [15, 16], quantum spin Hall insulator [2, 3], topological insulator [5, 6, 7], and topological superconductor such as Helium^3-B phase [109, 198]. All the free fermion SPT states have been well understood and classified in Ref. [24, 199, 23], and recent studies suggest that interaction may not lead to new SRE states, but it can reduce the classification of fermionic SRE states [200, 201, 202, 203, 204, 205, 110, 149]. Unlike fermionic systems, bosonic SPT states do need strong interaction. Most bosonic SRE states can be classified by symmetry group cohomology [25, 26], Chern-Simons theory [31] and semiclassical nonlinear sigma model [63].

In this work we demonstrate that there is a close relation between fermionic and bosonic SRE states, more precisely many bosonic SRE states can be constructed from fermionic SRE states with the same symmetry. All fermion systems have at least a $\mathbb{Z}_2$ symmetry $c_i \to -c_i$, where c_i is a local fermion annihilation operator, thus we can couple all fermion Hamiltonians to a dynamical $\mathbb{Z}_2$ gauge field, and microscopically this $\mathbb{Z}_2$ gauge field commutes with the actual physical symmetry of the fermion system. Once the $\mathbb{Z}_2$

gauge field is in its confined phase, the fermionic degree of freedom no longer exists in the spectrum of the Hamiltonian, and the system becomes a bosonic system. However, in many cases, confinement of a gauge field necessarily breaks certain symmetry of the system, thus we have to be very careful. In both $2d$ and $3d$, a $\mathbb{Z}_2$ gauge field has a confined phase and a deconfined phase. The deconfined phase is characterized by topological excitations of the $\mathbb{Z}_2$ gauge field. In $2d$, the $\mathbb{Z}_2$ gauge field has a "vison" excitation, which corresponds to a π-flux seen by the matter fields. In $3d$, the topological excitation is a "vison loop", which is a closed ring of π-flux. In $2d/3d$, when the visons/vison loops proliferate (condense), the system enters the confined phase, *i.e.* fermions carrying $\mathbb{Z}_2$ gauge charge cannot propagate freely in the bulk due to the phase fluctuations induced by the vison/vison loop condensation.

However, when the $\mathbb{Z}_2$ gauge field is coupled to a fermionic SRE state, the vison and vison loop often carry nontrivial quantum numbers, or degenerate low-energy spectrum. In these cases, when visons and vison loops condense, the condensate would not be a fully gapped nondegenerate state that does not break any symmetry. Also, sometimes visons in $2d$ would have a nontrivial statistics, thus it cannot trivially condense. Thus only in certain specific cases can we confine the fermionic SRE states and obtain a fully gapped and symmetric bosonic state. Thus analysis of spectrum and quantum number carried by the vison and vison loop is the key of our study.

Our approach can also be viewed as a slave fermion construction of bosonic SRE states, which has been considered in Ref. [40, 41, 206, 207, 34]. However, in all these previous studies the gauge group associated with the slave fermion is bigger than $\mathbb{Z}_2$, which means that when the gauge fluctuation is ignored, at the mean field level the slave fermion has a much larger symmetry than the boson system, and the analysis of gauge confined phase is much more complicated. In our case the gauge group is $\mathbb{Z}_2$, and since any fermion system has this $\mathbb{Z}_2$ symmetry, the fermion SRE states would have the same

symmetry as the bosonic states after gauge confinement. Thus in our case the nature of the confined phase can be analyzed reliably, and it only depends on the properties of visons and vison loops.

5.1.1 Construction of $3d$ bosonic SPT phases

Let us take the 3d topological superconductor (TSC) phase with time-reversal symmetry as an example. One example of such TSC is the ^{3}He-B phase. Here instead of focusing on the real ^{3}He system, we are discussing a more general family of TSC phases defined on a lattice that are topologically equivalent to ^{3}He-B. One typical Hamiltonian of such TSC defined on the cubic lattice reads

$$H = \sum_{\boldsymbol{k}} \chi_{-\boldsymbol{k}} \Big[\sum_{i=1}^{3} \Gamma^i \sin k_i - \Gamma^4 \big(3 - m - \sum_{i=1}^{3} \cos k_i\big) \Big] \chi_{\boldsymbol{k}}. \tag{5.1}$$

Here m plays the same role as the chemical potential in real ^{3}He system: $m = 0$ is the trivial-TSC transition critical point. The time-reversal symmetry acts as $\chi_{\boldsymbol{k}} \to \mathrm{i}\Gamma^5 \chi_{-\boldsymbol{k}}$. Close to the trivial-TSC phase transition, in the continuum limit this TSC phase can be described by the following universal real space Hamiltonian:

$$H_0 = \int d^3x \sum_{a=1}^{n} \chi_a^\intercal \left(\mathrm{i}\Gamma^1 \partial_x + \mathrm{i}\Gamma^2 \partial_y + \mathrm{i}\Gamma^3 \partial_z + m\Gamma^4 \right) \chi_a,$$

$$\Gamma^1 = \sigma^{30},\ \Gamma^2 = \sigma^{10},\ \Gamma^3 = \sigma^{22},\ \Gamma^4 = \sigma^{21},\ \Gamma^5 = \sigma^{23}, \tag{5.2}$$

where $\sigma^{ij} = \sigma^i \otimes \sigma^j$ denotes the tensor product of Pauli matrices, and $a = 1 \cdots n$ is the flavor index. This is a widely used approximate form for this class of TSC (For example, Ref. [208, 209]). For each flavor index a, χ_a is a four component Majorana fermion. In this Hamiltonian $m > 0$ and $m < 0$ correspond to the TSC phase and the trivial phase

respectively. The time-reversal symmetry acts as $\mathbb{Z}_2^T : \chi \to \mathrm{i}\Gamma^5\chi$. Our conclusion is that, when we couple n-copies of this TSC to the same $\mathbb{Z}_2$ gauge field, the $\mathbb{Z}_2$ gauge field can have a fully gapped nondegenerate confined phase *when and only when* n is an integer multiple of 8. And when $n = 8$, the confined phase is the $3d$ bosonic SPT state with time-reversal symmetry first characterized in Ref. [32].

First of all, when $n = 1$, the vison loop must be gapless, and the gaplessness is protected by time-reversal symmetry [198]. On a vison line along x direction, there will be a pair of counter-propagating Majorana modes, so the effective $1d$ Hamiltonian along the vison line reads (see Appendix B for derivation):

$$H_{1d,x} = \int \mathrm{d}x \ \chi^\intercal \mathrm{i}\sigma^3 \partial_x \chi. \tag{5.3}$$

In this reduced $1d$ theory, time-reversal symmetry acts as $\mathbb{Z}_2^T : \chi \to \mathrm{i}\sigma^2\chi$. The only mass term $\chi^\intercal\sigma^2\chi$ in this vison line would break time-reversal symmetry, thus as long as time-reversal is preserved, the vison line is always gapless. This implies that when $n = 1$ the vison line definitely cannot drive the system into a fully gapped state by proliferation without breaking time-reversal.

For $n > 1$, the effective theory along the vison line becomes

$$H_{1d,x} = \int \mathrm{d}x \sum_{a=1}^{n} \chi_a^\intercal \mathrm{i}\sigma^3 \partial_x \chi_a. \tag{5.4}$$

Then for even integer n, it appears that there is a time-reversal symmetric mass term $\chi_a^\intercal\sigma^1 A_{ab}\chi_b$, where A is an antisymmetric matrix in the flavor space. In the bulk theory Eq. (5.2), this mass term can correspond to several terms such as $\chi_a^\intercal\sigma^{13}A_{ab}\chi_b$ (see Appendix B). However, none of these terms can gap out vison lines along all directions. For example, for vison loops along y direction, the modes moving along $+y$ is an eigenstate

of Γ^2 with $\Gamma^2 = +1$, and modes moving along $-y$ direction have eigenvalue $\Gamma^2 = -1$. Because σ^{13} commutes with $\Gamma^2 = \sigma^{10}$, $\chi_a^\intercal \sigma^{13} A_{ab} \chi_b$ can never back-scatter modes in the y vison line. In fact no flavor mixing time-reversal invariant fermion *bilinear* terms in the bulk would gap out the vison lines along all directions, while a $\mathbb{Z}_2$ gauge confined phase requires dynamically condensing vison lines in all directions. Therefore the fermion bilinear flavor mixing terms in the bulk do not allow us to condense the vison lines in order to generate a fully gapped symmetric bosonic state.

Since no fermion bilinear term can gap out all the vison loops, we need to consider interaction effects. In Ref. [200, 201], the authors studied the interaction effect on Eq. (5.4), and the conclusion is that for $n = 8$ there is an SO(7) invariant interaction term $H_{1d,\text{int}} = \int dx\, V_{abcd} \chi_a^\intercal \sigma^2 \chi_b \chi_c^\intercal \sigma^2 \chi_d$ that can gap out the $1d$ theory Eq. (5.4) without generating nonzero expectation value of any fermion bilinear operator, where V_{abcd} is some coefficient tensor specified in Ref. [200, 201]. The same field theory analysis applies here: the effective interaction $H_{1d,\text{int}}$ can gap out the $1d$ theory Eq. (5.4) along the vison loop without degeneracy. $H_{1d,\text{int}}$ corresponds[1] to the following term in the bulk:

$$H_{\text{int}} = \int \mathrm{d}^3 x\, V_{abcd} \chi_a^\intercal \Gamma^5 \chi_b \chi_c^\intercal \Gamma^5 \chi_d. \tag{5.5}$$

Since this term is rotationally invariant, it will gap out vison lines along all directions. Thus with $n = 8$, and with the interaction term H_{int} in the bulk, all vison loops can be gapped out without breaking time-reversal symmetry, thus we can safely condense the vison loops and drive the system into a fully gapped, time-reversal invariant bosonic state. But this is only possible when n is an integral multiple of 8. In the following paragraphs we will argue that when $n = 8$ the confined bosonic state is a bosonic SPT state.

[1] The fact that σ^2 on the vison line is extended to Γ^5 in the bulk is explained in Appendix B.

Ref. [32, 63] pointed out that this $3d$ bosonic SPT state can be described by a O(5) NLSM field theory with a topological $\Theta-$term. Let us couple the 8 copies of ^{3}He B to a five-component unit vector $\boldsymbol{n}$:

$$H = H_0 + \int d^3x \ \sum_{j=1}^{5} n^j \chi_a^\intercal \Gamma^5 \gamma_{ab}^j \chi_b, \tag{5.6}$$

where γ^j are five 8×8 symmetric matrices in the flavor space that satisfy $\{\gamma^i, \gamma^j\} = 2\delta_{ij}$ (e.g. a particular choice could be $\gamma^i = \sigma^{100}, \sigma^{310}, \sigma^{331}, \sigma^{333}, \sigma^{212}$). Under time-reversal transformation, $\boldsymbol{n} \to -\boldsymbol{n}$. Following the calculation in Ref. [210], we can show that for the ^{3}He B phase with $m > 0$, after integrating out the fermions, the effective field theory for the vector $\boldsymbol{n}$ contains a topological Θ-term at $\Theta = 2\pi$:

$$S = \int \mathrm{d}^3x \mathrm{d}\tau \ \frac{1}{g}(\partial_\mu \boldsymbol{n})^2 + \frac{\mathrm{i}\Theta}{\Omega_4} \epsilon_{abcde} n^a \partial_x n^b \partial_y n^c \partial_z n^d \partial_\tau n^e, \tag{5.7}$$

where Ω_4 is the volume of a four dimensional sphere with unit radius. Eq. (5.7) is precisely the field theory introduced in Ref. [32, 63] to describe the $3d$ bosonic topological SC with time-reversal symmetry.

Using the field theory Eq. (5.7), we can demonstrate that the $2d$ boundary of this $3d$ bosonic SPT state could be a $2d$ $\mathbb{Z}_2$ topological order, whose mutually semionic excitations e and m are both Kramers' doublet [32] (The so called $eTmT$ state)[2]. Ref. [110, 149, 211] argued that the boundary of 8 copies of ^{3}He B is the (fermionized) $eTmT$ state. For the sake of completeness, we will repeat this argument. Based on the field theory Eq. (5.7), the e and m excitations at the $2d$ boundary of the $3d$ bosonic SPT phase correspond to the vortex of boson field $b_1 \sim n_1 + \mathrm{i}n_2$, and vortex of $b_2 \sim n_3 + \mathrm{i}n_4$ respec-

[2]The $\mathbb{Z}_2$ topological order at the $2d$ boundary has nothing to do with the bulk $\mathbb{Z}_2$ gauge field that we will confine by proliferating the vison loops.

tively [3], which can be considered as surface terminations of bulk vortex lines. By solving the Bogoliubov-de Gennes equation with a vortex at the boundary, we can demonstrate that there are four Majorana fermion zero modes located at each vortex core. These four Majorana fermion zero modes can in total generate four different states. Under interaction, time-reversal symmetry [4] guarantees that these four states split into two degenerate doublets with opposite fermion number parity. Thus in the bulk each vortex line is effectively four copies of 1d Kitaev's Majorana chain. Since we are in a $\mathbb{Z}_2$ gauge confined phase, we are only allowed to consider states with even number of fermions, thus after gauge projection, only one of the two doublets survives, which according to the supplementary material and Ref. [149] is a Kramers doublet. Also the vortex of b_1 carries charge $\pm 1/2$ of b_2, and vortex of b_2 carries $\pm 1/2$ charge of b_1, thus these two vortices are both Kramers doublet, and they have mutual semion statistics. This means that boundary of the confined phase is really the $eTmT$ state.

Combining all the results together, we conclude that the $\mathbb{Z}_2$ confined phase of 8 copies of ^{3}He B is really the bosonic SPT phase with time-reversal symmetry. Furthermore, since this bosonic SPT state has $\mathbb{Z}_2$ classification, it implies that two copies of the bosonic state is trivial (which can be shown in our NLSM field theory by directly coupling two copies of Eq. (5.7) together [63]), which then implies that 16 multiples of the ^{3}He-B TSC is trivial under interaction. This conclusions is consistent with the well-known $\mathbb{Z}_{16}$ classification of DIII class fermionic SPT states[110, 149, 62].

We can also give the 8 copies of ^{3}He B phase various flavor symmetries, and we can construct many $3d$ bosonic SPT phases with symmetry that contains $\mathbb{Z}_2^T$ as a normal subgroup by confining the bulk $\mathbb{Z}_2$ gauge field. Since all the free fermion SPT states in

[3] assuming tentatively an enlarged $U(1) \times U(1)$ symmetry for rotation of (n_1, n_2) and (n_3, n_4) respectively

[4] Here the time-reversal symmetry is a modified time-reversal symmetry defined in Ref. [149], which is a product of ordinary time-reversal and a $\pi-$rotation of boson field b_1 or b_2.

$3d$ require the time-reversal symmetry, thus so far our approach does not allow us to construct $3d$ bosonic SPT phases without $\mathbb{Z}_2^T$.

5.1.2 Construction of $2d$ bosonic SPT phases

Now let us look at $2d$ examples. In $2d$ the simplest fermionic SRE state is the $p+\mathrm{i}p$ topological superconductor (TSC) that does not require any symmetry, and the simplest bosonic SRE state is the so called "E_8" state with chiral central charge $c_- = 8$ at its boundary [64, 65]. In the following we will prove that if we couple n copies of $p+\mathrm{i}p$ TSC to a $\mathbb{Z}_2$ gauge field, the $\mathbb{Z}_2$ gauge field can confine to a gapped bosonic state when and only when n is a integral multiple of 16. And when $n = 16$, the confined phase is precisely the bosonic E_8 SRE state [212]. First of all, when $n = 1$, the vison of the $\mathbb{Z}_2$ gauge field carries a Majorana fermion zero mode, which grants the vison a nonabelian statistics, thus when $n = 1$ (and generally for odd integer n) the $\mathbb{Z}_2$ gauge field cannot enter its confined phase by condensing the vison. When n is even, n-copies of $p+\mathrm{i}p$ TSC is equivalent to an integer quantum Hall (IQH) state with Hall conductivity $\nu = n/2$, thus a vison (half flux quantum) would carry charge $n/4$, and has statistics angle $\pi n/8$ under exchange. Thus the smallest n that makes vison a boson is 16, and when $n = 16$, the $\mathbb{Z}_2$ gauge field can enter a confined phase by condensing the bosonic vison.

The vison condensation can be formulated by the Chern-Simons theory.[213] Let us start from the Chern-Simons description for n-copies of $p+\mathrm{i}p$ TSC with even $n = 2\nu$ (*i.e.* ν layers of IQH), and couple the fermion currents da^I $(I = 1, \cdots, \nu)$ to the $\mathbb{Z}_2$ gauge field. The Lagrangian density can be written as

$$\mathcal{L} = \sum_I \frac{1}{4\pi} a^I \wedge da^I + \sum_I \frac{1}{2\pi} A \wedge da^I + \frac{1}{\pi} A \wedge d\tilde{A}. \tag{5.8}$$

Here the $\mathbb{Z}_2$ gauge theory is described by the mutual Chern-Simon theory of two gauge

fields A and $\tilde{A}$ with the K-matrix $\left[\begin{smallmatrix} 0 & 2 \\ 2 & 0 \end{smallmatrix}\right]$. $\tilde{A}$ can be considered as a Higgs field that Higgs the U(1) gauge structure of A down to $\mathbb{Z}_2$. The field A couples to the fermion current $j^I = \star \mathrm{d}a^I$ with equal charge, and the field $\tilde{A}$ couples to the vison current in the $\mathbb{Z}_2$ gauge theory. The field A can be treated as a Lagrangian multiplier and integrated out first, which leads to the constraint $\sum_I a^I + 2\tilde{A} = 0$. This constraint can be solved by the following reparameterization

$$\begin{aligned} &a^1 = \tilde{a}^1, a^{\nu-1} = \tilde{a}^\nu + \tilde{a}^{\nu-1} - \tilde{a}^{\nu-2}, a^\nu = \tilde{a}^\nu - \tilde{a}^{\nu-1}, \\ &a^I = \tilde{a}^I - \tilde{a}^{I-1} (\text{for } I = 2, \cdots, \nu-2), \tilde{A} = -\tilde{a}^\nu. \end{aligned} \tag{5.9}$$

Substituting Eq. (5.9) into Eq. (5.8), we arrive at a bosonic theory in terms of the new set of gauge fields $\tilde{a}^I$, as $\mathcal{L} = \sum_{I,J} \frac{1}{4\pi} K^{SO(n)}_{IJ} \tilde{a}^I \wedge d\tilde{a}^J$, where $K^{SO(n)}$ is the Cartan matrix of the $\mathfrak{so}(n)$ Lie algebra(for even $n > 2$). For $n = 16$, the K-matrix reads

$$K^{SO(16)} = \begin{bmatrix} 2 & -1 & 0 & 0 & 0 & 0 & 0 & 0 \\ -1 & 2 & -1 & 0 & 0 & 0 & 0 & 0 \\ 0 & -1 & 2 & -1 & 0 & 0 & 0 & 0 \\ 0 & 0 & -1 & 2 & -1 & 0 & 0 & 0 \\ 0 & 0 & 0 & -1 & 2 & -1 & 0 & 0 \\ 0 & 0 & 0 & 0 & -1 & 2 & -1 & -1 \\ 0 & 0 & 0 & 0 & 0 & -1 & 2 & 0 \\ 0 & 0 & 0 & 0 & 0 & -1 & 0 & 2 \end{bmatrix}, \tag{5.10}$$

which gives the $SO(16)_1$ Chern-Simons theory. We now extend $K^{SO(16)}$ by a block of trivial boson, given by the K-matrix σ^1 [214], and define $K^{\text{ext}} = K^{SO(16)} \oplus \sigma^1$. One finds a transform W, with $\det W = 1$, given by

$$W^{-1} = \begin{bmatrix} 1 & 0 & 0 & 0 & 0 & 0 & 1 & -1 & 0 & 0 \\ 0 & 1 & 0 & 0 & 0 & 0 & 2 & -2 & 0 & 0 \\ 0 & 0 & 1 & 0 & 0 & 0 & 3 & -3 & 0 & 0 \\ 0 & 0 & 0 & 1 & 0 & 0 & 4 & -4 & 0 & 0 \\ 0 & 0 & 0 & 0 & 1 & 0 & 5 & -5 & 0 & 0 \\ 0 & 0 & 0 & 0 & 1 & 0 & 3 & -4 & -1 & 0 \\ 0 & 0 & 0 & 0 & 1 & 0 & 1 & -2 & 0 & 0 \\ 0 & 0 & 0 & 0 & 1 & -1 & 3 & -2 & 0 & 0 \\ 0 & 0 & 0 & 0 & 1 & -1 & 0 & 0 & -1 & 0 \\ 0 & 0 & 0 & 0 & 0 & 0 & 0 & 1 & 1 & -1 \end{bmatrix}, \tag{5.11}$$

such that

$$W^{\intercal}K^{\text{ext}}W = \begin{bmatrix} 2 & -1 & 0 & 0 & 0 & 0 & 0 & 0 & 0 & 0 \\ -1 & 2 & -1 & 0 & 0 & 0 & 0 & 0 & 0 & 0 \\ 0 & -1 & 2 & -1 & 0 & 0 & 0 & 0 & 0 & 0 \\ 0 & 0 & -1 & 2 & -1 & 0 & 0 & 0 & 0 & 0 \\ 0 & 0 & 0 & -1 & 2 & -1 & 0 & -1 & 0 & 2 \\ 0 & 0 & 0 & 0 & -1 & 2 & -1 & 0 & 0 & -1 \\ 0 & 0 & 0 & 0 & 0 & -1 & 2 & 0 & 0 & -1 \\ 0 & 0 & 0 & 0 & -1 & 0 & 0 & 2 & 0 & -2 \\ 0 & 0 & 0 & 0 & 0 & 0 & 0 & 0 & 0 & 2 \\ 0 & 0 & 0 & 0 & 2 & -1 & -1 & -2 & 2 & 0 \end{bmatrix}, \tag{5.12}$$

The last 2×2 block describes a $\mathbb{Z}_2$ topological order. The fermion excitations of this K-matrix corresponds to the original fermion in the $p+\mathrm{i}p$ TSC. The vison couples to the last gauge field, *i.e.* it corresponds to the charge vector $(0,0,0,0,0,0,0,0,0,1)$, and is a boson ready to condense. Thus after the vison condensation, the $\mathbb{Z}_2$ topological order is destroyed and the original fermion is confined. The K-matrix is left with the upper 8×8 block, which is exactly the Cartan matrix of the E_8 Lie algebra. Since all the charge vectors of the upper 8×8 block are self-bosons, and they are bosons relative to the vison, these charge vectors are unaffected by the vison condensate. Thus we have shown by explicit calculation that confining the fermions in 16-copies of $p+\mathrm{i}p$ TSC leads to the E_8 bosonic SRE state.

Now let us investigate the $p\pm\mathrm{i}p$ TSC with a $\mathbb{Z}_2$ symmetry discussed in Ref. [204]. In this system the fermions with zero $\mathbb{Z}_2$ charge form a $p+\mathrm{i}p$ TSC, while fermions carrying $\mathbb{Z}_2$ charge form a $p-\mathrm{i}p$ TSC. This $\mathbb{Z}_2$ global symmetry is different from the $\mathbb{Z}_2$ gauge symmetry, since all the fermions in our system carry $\mathbb{Z}_2$ gauge charge. For one copy of the $p\pm\mathrm{i}p$ TSC coupled to the $\mathbb{Z}_2$ gauge field, the vison carries two independent Majorana fermion zero modes χ_1 and χ_2, and the global $\mathbb{Z}_2$ symmetry acts $\mathbb{Z}_2 : \chi \to \sigma^z\chi$. There is no nontrivial Hamiltonian for these two Majorana fermion modes that preserves the $\mathbb{Z}_2$ symmetry, thus the spectrum of the vison is always two fold degenerate, and hence condensing the vison will not lead to a nondegenerate state.

Two copies of the $p\pm\mathrm{i}p$ TSC is formally equivalent to a quantum spin Hall (QSH) insulator: fermions that carry global $\mathbb{Z}_2$ charge 0 and 1 form $\nu = 1$ and -1 integer quantum Hall states respectively. Then after coupling to the $\mathbb{Z}_2$ gauge field, the vison would

carry two complex localized fermion modes c_1 and c_2, and a vison would carry charge $\pm 1/2$ of the $\mathbb{Z}_2$ global symmetry, which corresponds to $n_2 = c_2^\dagger c_2 = 1,\ 0$ respectively. Thus the condensate of the vison always spontaneously breaks the $\mathbb{Z}_2$ symmetry. This situation is very similar to the case discussed in Ref. [215]. The universality class of the confinement transition is the so-called $3d$ XY* transition, namely at the quantum critical point the $\mathbb{Z}_2$ symmetry order parameter has an anomalous dimension $\eta \sim 1.49$ [216, 217].

Eventually for four copies of this $p \pm \mathrm{i}p$ TSC, a vison carries four complex fermion modes $c_{1A},\ c_{1B},\ c_{2A},\ c_{2B}$. The vison now can be a boson that does not carry any $\mathbb{Z}_2$ global charge, for example the state with $n_{2A} = 1$ and $n_{2B} = 0$ is a $\mathbb{Z}_2$ charge neutral boson. Thus condensing this vison would lead to a fully gapped nondegenerate bosonic state that preserves the global $\mathbb{Z}_2$ symmetry.

Now let us couple four copies of the $p \pm \mathrm{i}p$ TSC to a four-component unit vector $\boldsymbol{n}$:

$$\begin{aligned} H = \int \mathrm{d}^2x\ \chi^\intercal(\mathrm{i}\sigma^{3000}\partial_x + \mathrm{i}\sigma^{1000}\partial_y + m\sigma^{2300})\chi \\ + \sum_{j=1}^{4} n^j \chi^\intercal \gamma^j \chi, \end{aligned} \tag{5.13}$$

with $\gamma^1 = \sigma^{2100}$, $\gamma^2 = \sigma^{2221}$, $\gamma^3 = \sigma^{2223}$, $\gamma^4 = \sigma^{2202}$. The global $\mathbb{Z}_2$ symmetry acts as $\mathbb{Z}_2 : \chi \to \sigma^{0300}\chi$, and $\boldsymbol{n} \to -\boldsymbol{n}$. After integrating out the fermions, the resulting theory is a $(2+1)d$ O(4) NLSM with a topological Θ-term at $\Theta = 2\pi$:

$$S = \int \mathrm{d}^2x \mathrm{d}\tau \frac{1}{g}(\partial_\mu \boldsymbol{n})^2 + \frac{\mathrm{i}\Theta}{\Omega_3}\epsilon_{abcd} n^a \partial_x n^b \partial_y n^c \partial_\tau n^d, \tag{5.14}$$

where $\Omega_3 = 2\pi^2$ is the volume of a three dimensional sphere with unit radius, and this is precisely the field theory describing the $2d$ bosonic SPT phase with $\mathbb{Z}_2$ symmetry, which was first studied in Ref. [27]. This field theory was studied in Ref. [35, 63].

Finally we condense the vison in this system to confine the fermions. Similar to our

previous K-matrix calculation, we couple the four copies of $p \pm \mathrm{i}p$ TSC to the $\mathbb{Z}_2$ gauge field, as described by the Lagrangian density

$$\mathcal{L} = \sum_{I,J} \frac{K^{\mathrm{QSH}}_{IJ}}{4\pi} a^I \wedge \mathrm{d}a^J + \sum_I \frac{1}{2\pi} A \wedge \mathrm{d}a^I + \frac{1}{\pi} A \wedge \mathrm{d}\tilde{A}, \tag{5.15}$$

where the matrix K^{QSH} is diagonal with the diagonal elements $(1, 1, -1, -1)$. In the theory, the global $\mathbb{Z}_2$ symmetry charge is given by the charge vector $q_{\mathbb{Z}_2} = (0, 0, 1, 1)$. Integrating out A leads to the constraint $\sum_I a^I + 2\tilde{A} = 0$, which can be solved by

$$\begin{bmatrix} a^1 \\ a^2 \\ a^3 \\ a^4 \\ \tilde{A} \end{bmatrix} = \begin{bmatrix} 1 & 1 & -1 & 1 \\ 0 & 0 & 1 & 1 \\ 1 & 0 & -1 & 1 \\ 0 & -1 & 1 & -1 \\ -1 & 0 & 0 & -1 \end{bmatrix} \begin{bmatrix} \tilde{a}^1 \\ \tilde{a}^2 \\ \tilde{a}^3 \\ \tilde{a}^4 \end{bmatrix}. \tag{5.16}$$

Substituting Eq. (5.16) into Eq. (5.15) yields a Chern-Simons theory $\mathcal{L} = \sum_{I,J} \frac{1}{4\pi} K^{\mathrm{SPT}^*}_{IJ} \tilde{a}^I \wedge d\tilde{a}^J$ with

$$K^{\mathrm{SPT}^*} = \begin{bmatrix} 0 & 1 & 0 & 0 \\ 1 & 0 & 0 & 0 \\ 0 & 0 & 0 & 2 \\ 0 & 0 & 2 & 0 \end{bmatrix}. \tag{5.17}$$

Correspondingly, the global $\mathbb{Z}_2$ charge is transformed to $\tilde{q}_{\mathbb{Z}_2} = W^{\intercal} q_{\mathbb{Z}_2} = (1, -1, 0, 0)$, with the transformation matrix W taken from the first 4 rows of the matrix in Eq. (5.16). In K^{SPT^*}, the lower 2×2 block describes the $\mathbb{Z}_2$ topological order, which contains the bosonic vison with neutral global $\mathbb{Z}_2$ charge (as seen from $\tilde{q}_{\mathbb{Z}_2}$). As the vison condenses, the $\mathbb{Z}_2$ topological order is removed, leaving the upper 2×2 block, *i.e.* the σ^1 matrix, as the K-matrix describing a SRE bosonic state, with the global $\mathbb{Z}_2$ charge $q = (1, -1)$

(as taken from $\tilde{q}_{\mathbb{Z}_2}$). Such a K-matrix equipped with the $\mathbb{Z}_2$ symmetry matches [31] the Chern-Simons description of the $\mathbb{Z}_2$ SPT state. Therefore after confining the fermions in four copies of $p\pm \mathrm{i}p$ TSC, we obtain the bosonic SPT state with $\mathbb{Z}_2$ global symmetry. This bosonic SPT state has $\mathbb{Z}_2$ classification [25, 27, 63], which implies that 8 copies of the $p \pm \mathrm{i}p$ TSC with $\mathbb{Z}_2$ symmetry is a trivial state, which is consistent with the well-known $\mathbb{Z}_8$ classification of such $p \pm \mathrm{i}p$ TSC under interaction [202, 205, 203, 204, 62]

Extra symmetries can be added to the four copies of $p \pm \mathrm{i}p$ TSC discussed above, and other $2d$ bosonic TSC can be constructed in the same way. Construction of $1d$ bosonic SPT phases is much more obvious, which will be discussed in the supplementary material.

5.1.3 Construction of $1d$ Bosonic SPT phases

In this part, we construct the $1d$ Haldane phase using four copies of Kitaev's chains with the time-reversal symmetry$\mathbb{Z}_2^T$. Let us start from the fermionic SPT phase composed of four copies of Kitaev's chains coupled to a fluctuating three-component unit vector $\boldsymbol{n}$:

$$H = \chi^\intercal(\mathrm{i}\sigma^{100}\partial_x + m\sigma^{200})\chi + \sum_{j=1}^{3} n^j \chi^\intercal \gamma^j \chi, \tag{5.18}$$

with $\gamma^1 = \sigma^{332}$, $\gamma^2 = \sigma^{320}$, $\gamma^3 = \sigma^{312}$. The time reversal symmetry acts as $\mathbb{Z}_2^T : \chi \to \sigma^{300}\chi$ and $\boldsymbol{n} \to -\boldsymbol{n}$ followed by the complex conjugation (denoted $\mathcal{K}$). Note that the time reversal operator $\mathcal{T} = \mathcal{K}\sigma^{300}$ behaves as $\mathcal{T}^2 = 1$ on the Majorana fermions χ. After integrating out the fermions, the resulting theory is a $(1+1)d$ O(3) NLSM with a topological Θ-term at $\Theta = 2\pi$:

$$S = \int \mathrm{d}x\mathrm{d}\tau \frac{1}{g}(\partial_\mu \boldsymbol{n})^2 + \frac{\mathrm{i}\Theta}{\Omega_2}\epsilon_{abc} n^a \partial_x n^b \partial_\tau n^c, \tag{5.19}$$

where $\Omega_2 = 4\pi$ is the volume of a two dimensional sphere with unit radius, and this is precisely the field theory describing the $1d$ bosonic SPT phase with $\mathbb{Z}_2^T$ symmetry, *i.e.* the Haldane phase of $1d$ spin chain [15, 16].

Then we can couple the fermions to a $\mathbb{Z}_2$ gauge field, namely we impose the following gauge constraint on every site: $\chi_{i0}\chi_{i1}\chi_{i2}\chi_{i3} = 1$. The same gauge constraint is imposed on the edge Majorana fermion zero modes. The edge Majorana fermion zero modes may be arranged in a matrix as[189]

$$F = \frac{1}{2}(\chi_0\sigma^0 + \mathrm{i}\chi_1\sigma^1 + \mathrm{i}\chi_2\sigma^2 + \mathrm{i}\chi_3\sigma^3). \tag{5.20}$$

Under time-reversal transformation, $\mathbb{Z}_2^T : F \to F^* = (i\sigma^2)F(-i\sigma^2)$.

Two three-component vector operators can be conveniently constructed with these edge Majorana operators ($a = 1, 2, 3$):

$$S^a = \frac{1}{2}\mathrm{Tr}F^\dagger\sigma^a F, \qquad K^a = \frac{1}{2}\mathrm{Tr}F\sigma^a F^\dagger. \tag{5.21}$$

In fact, the boundary Majorana fermions have an emergent SO(4) symmetry, and the two vectors correspond to the two independent SU(2) subgroups of the SO(4). The full SO(4) rotational symmetry among the four flavors of Majorana fermions is decomposed to $\mathrm{SU}(2)_{\mathrm{spin}}\times\mathrm{SU}(2)_{\mathrm{gauge}}$, generated by $\boldsymbol{S}$ and $\boldsymbol{K}$ respectively. For the fermions in F, the $\mathrm{SU}(2)_{\mathrm{spin}}$ rotation corresponds to a left rotation $F \to U^\dagger F$ with $U \in \mathrm{SU}(2)_{\mathrm{spin}}$, while the $\mathrm{SU}(2)_{\mathrm{gauge}}$ rotation corresponds to a right rotation $F \to FG$ with $G \in \mathrm{SU}(2)_{\mathrm{gauge}}$.

Under the constraint $\chi_0\chi_1\chi_2\chi_3 = 1$, which is equivalent to the requirement of gauge neutrality, *i.e.* $\boldsymbol{K} = 0$. Therefore under the gauge constraint, the physical state of the boundary is only two fold degenerate, and these states are invariant under $\mathrm{SU}(2)_{\mathrm{gauge}}$. This means that we are free to combine time-reversal symmetry with a $\mathrm{SU}(2)_{\mathrm{gauge}}$ trans-

formation. For example, we can define a new time-reversal transformation $\mathcal{T} : F \to F^*(i\sigma^2) = -i\sigma^2 F$, this new time-reversal transformation satisfies $\mathcal{T}^2 = -1$, and it is exactly the same time-reversal transformation for spin-1/2 object. Thus we conclude that under gauge constraint, four copies of Kitaev's chain is equivalent to the Haldane's phase.

5.2 Bilayer graphene as a platform for bosonic symmetry protected topological states

A symmetry protected topological (SPT) state, first defined in Ref. [25, 26], is the ground state of a local quantum many-body Hamiltonian whose bulk is gapped and nondegenerate, but whose boundary remains either gapless or degenerate as long as the entire system including the boundary preserves certain symmetries. Fermionic SPT states include the familiar quantum spin Hall (QSH) insulator [2, 3], the three-dimensional ($3d$) topological insulator (TI) [5, 6, 7], and topological superconductors. Noninteracting fermionic SPT states have been fully classified and understood [24, 23]. Unlike fermionic systems, bosonic SPT (BSPT) states require strong interaction to overcome the tendency to form Bose-Einstein condensates. The simplest and most well-known BSPT state is the $1d$ Haldane phase, which can be realized in the simplest nearest-neighbor spin-1 Heisenberg chain [15, 16]. However, higher dimensional generalizations of BSPT states have not been found. The only even *potentially feasible* experimental proposal is for a bosonic integer quantum Hall state in ultracold atoms [218], but even this seems far away, since as yet experiments with both rotating traps and artificial magnetic fields are still far from the quantum Hall regime. The exactly soluble parent Hamiltonians constructed in Ref. [25, 26] in dimensions higher than one all involve high order multiple

spin interactions, and are thus unlikely to exist in realistic materials. Up to now, all approaches to classifying and characterizing BSPT states [25, 26, 32, 31, 63, 219] rely on mathematical or effective field theory descriptions, which shed little light on how to identify a realistic candidate BSPT state.

5.2.1 The experimental proposal

In the current section, we hope to bridge the gap between theoretical studies and experimental realizations of BSPT states. We propose that bilayer graphene in magnetic field (with both inplane and out-of-plane components) provides a platform of realizing and probing the $2d$ BSPT state with $U(1)_s \times U(1)_c$ symmetry, where $U(1)_s$ and $U(1)_c$ correspond to the total spin$-S^z$ and total electric charge conservation respectively. Based on the formalism developed in Ref. [31, 63], this state has a $\mathbb{Z}$ classification, *i.e.* with these symmetries there is an infinite set of non-trivial $2d$ BSPT classes, which are indexed by an integer k. Effective field theory descriptions of these BSPT states have been given in terms of Chern-Simon field theory [31] and a non-linear sigma model (NLSM) with a Θ-term [35, 63]. The action for the latter is

$$\mathcal{S} = \int d^2x d\tau \ \frac{1}{g}(\partial_\mu \boldsymbol{n})^2 + \frac{i\Theta}{\Omega_3}\epsilon_{abcd} n^a \partial_x n^b \partial_y n^c \partial_\tau n^d, \tag{5.22}$$

where $\boldsymbol{n} = (n_1, n_2, n_3, n_4)$ is a four component vector with unit length [35, 63], and Ω_3 is the volume of a $3d$ sphere with unit radius. In Eq. (5.22), the BSPT phases correspond to the strongly interacting fixed point $g \to \infty$, and $\Theta \to 2k\pi$ with nonzero integer k, while the trivial phase corresponds to the fixed point $\Theta \to 0$. The quantum phase transition between different BSPT phases is driven by tuning Θ in Eq. (5.22), and the critical point is at $\Theta = (2k+1)\pi$. A similar phase diagram and renormalization group flow for NLSMs in one lower dimension was studied thoroughly in Ref. [52, 53].

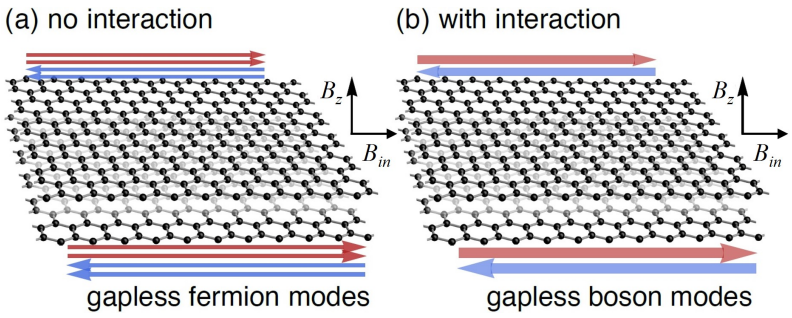

Figure 5.1: Schematic of bilayer graphene in the presence of a magnetic field with both inplane and out-of-plane components. (a) Without interactions, the boundary hosts two channels of fermionic edge states with total central charge $c = 2$. (b) Including the Coulomb interactions, there is only one gapless channel of bosonic edge state with $c = 1$.

Let us elaborate on our claim. It was proposed that an out-of-plane magnetic field drives undoped graphene into a "quantum spin Hall insulator"[220] (it is also called the ferromagnetic quantum Hall state, since the bulk is fully spin polarized. In order to avoid a canted antiferromagnetic phase, one also needs an inplane magnetic field to increase the Zeeman coupling [221, 222], which will be discussed in detail in the supplementary material [5]). In a bilayer, this possesses at the Hartree-Fock level two channels of counter-propagating spin-filtered helical fermionic edge states [229, 222]. However, when the Coulomb interaction is included, we will demonstrate that (as illustrated in Fig. 5.1), the behavior is qualitatively modified to correspond precisely to that of the BSPT theories, Eq. (5.22) with $k = 1$, so that, although it is built from electrons, it is a proper BSPT state in the following senses:

1. the Coulomb interaction, which is expected to play an important role in this system, induces a gap for all fermionic excitations at the boundary, while bosonic charge and spin excitations remain gapless and protected by the two $U(1)$ symmetries (Fig. 5.1*b*);

2. after the fermions are gapped out at the boundary by the Coulomb interaction, using the correlation functions of the boundary states, and following the procedure in

[5]Please see the supplementary material, which includes Ref. [223, 224, 225, 226, 227, 228].

Ref. [230], one can derive the bulk wave function for the bosonic charge and spin, which takes exactly the form as the BSPT wave function constructed using the mutual flux attachment picture in Ref. [28].

3. Using the Chalker-Coddington picture, the bulk quantum phase transition between the nontrivial SPT phase ($k = 1$) and trivial ($k = 0$) phase (hereafter phrased as "topological to trivial transition") can be described by percolation of domains and the corresponding network of interface/boundary states. Because the boundary only has gapless bosonic modes, such a topological quantum phase transition can occur while preserving the bulk gap for fermionic quasiparticles. The topological to trivial transition can be driven by varying competing magnetic and electric fields, and we propose that the bosonic scenario for this quantum phase transition could occur with sufficiently strong interactions. This is a qualitatively different situation from the well-known topological to trivial transitions in weakly correlated systems, such as the plateau transition between integer quantum Hall states, or the transition between normal and topological band insulators – these transitions have a free fermion description which involves the fermion gap closing in the bulk. The above statement is supported by recent numerical studies of a similar model on the bilayer honeycomb lattice [145, 146].

5.2.2 Boundary analysis

We now proceed to an exposition of these results. In this work we will focus on the boundary states and the bulk wave function of the BSPT state, we will defer the detailed analysis of the bulk topological transition to future study. For non-interacting bilayer graphene, there are two channels of helical edge states, described by the Hamiltonian

$$H_0 = \int dx \sum_{l=1}^{2} \psi_{l,L}^{\dagger} iv\partial_x \psi_{l,L} - \psi_{l,R}^{\dagger} iv\partial_x \psi_{l,R}, \tag{5.23}$$

where $l = 1, 2$ labels the channels, L, R denote the left and right moving fermions respectively, which also correspond to electrons with spin-up and down, and v is the Fermi velocity [6]. The presence of *some* counter-propagating edge states was deduced experimentally from non-local transport signatures [222]. When the Coulomb interaction is ignored, the boundary is a free fermion conformal field theory (CFT) with central charge $c = 2$.

The free fermion edge states can be bosonized into two flavors of free bosons:

$$H_0 = \int dx \sum_{l=1}^{2} \frac{v}{2K}(\partial_x \theta_l)^2 + \frac{vK}{2}(\partial_x \phi_l)^2, \tag{5.24}$$

where $[\theta_l(x),\ \partial_{x'}\phi_{l'}(x')] = i\delta(x - x')\delta_{ll'}$, and $\psi_{l,L/R} \sim e^{i\theta_l \pm i\pi\phi_l}$. For free $1d$ fermions without interaction, the Luttinger parameter $K = \pi$.

Coulomb interactions H_{int} are conveniently handled in the bosonization framework. Using the representation of the fermion density $n_l \sim \partial_x \phi_l$, one obtains:

$$H_{int} = \int dx \sum_{l=1}^{2} \frac{U_{\text{intra}}}{2}(\partial_x \phi_l)^2 + U_{\text{inter}} \partial_x \phi_1 \partial_x \phi_2 + H_v, \tag{5.25}$$

where U_{intra} and U_{inter} represent intralayer and interlayer forward-scattering interactions, respectively. H_v is an anharmonic vertex term, and will play a central role here [7]:

$$H_v \sim \alpha \cos(2\pi\phi_1 - 2\pi\phi_2). \tag{5.26}$$

Here we have assumed that the long range Coulomb interaction is screened to a short range one, but this is not essential. Physically H_v describes the backscattering between

[6] In principle the velocity of the two channels of edge states could be different, but this velocity difference would be unimportant for the rest of the analysis.

[7] Interaction can induce another anharmonic term: $\cos(2\theta_1 - 2\theta_2)$, but this term is irrelevant in our system.

two channels of edge states: $H_v \sim \psi^\dagger_{1,L}\psi_{1,R}\psi^\dagger_{2,R}\psi_{2,L}$. The anharmonic H_v is relevant in the renormalization group sense, as long as $U_{\text{intra}} > U_{\text{inter}}$. This condition is naturally satisfied because U_{inter} is suppressed by the square of the wave function overlap between the two channels of edge states.

When it is relevant, H_v will "pin" the bosonic mode $\phi_- = (\phi_1 - \phi_2)/2$, causing large fluctuations of $\theta_- = \theta_1 - \theta_2$, leading to a gap in this antisymmetric sector, and also a gap for all fermions at the boundary. The symmetric edge modes $\phi = (\phi_1 + \phi_2)/2$ and $\theta = \theta_1 + \theta_2$, however, remain gapless, because θ transforms under symmetry $U(1)_c$, while ϕ transforms under $U(1)_s$. It is straightforward to show – see below – that only physical operators which create bosonic excitations can be built from the gapless ϕ, θ fields, consistent with the statement that the boundary has symmetry protected gapless bosonic modes. The size of the fermion gap at the boundary state is estimated in detail in the supplementary material.

The effective low energy theory that describes the canonical conjugate modes ϕ and θ reads

$$\tilde{H} = \int dx \, \frac{\tilde{v}}{2\tilde{K}}(\partial_x\theta)^2 + \frac{\tilde{v}\tilde{K}}{2}(\partial_x\phi)^2. \tag{5.27}$$

Hence interaction reduces the central charge of the system from $c = 2$ to $c = 1$. Because θ and ϕ transform nontrivially (i.e. shift under $U(1)_c$ and $U(1)_s$ symmetries respectively), there are no anharmonic vertex operators allowed by symmetry in Eq. (5.27). Because θ and ϕ are "dual" to each other, a unit soliton of ϕ at the $1d$ boundary carries charge-$2e$, and a unit soliton of θ carries spin $S^z = 1$. The gaplessness of the boundary state is protected by the $U(1)_c \times U(1)_s$ symmetry alone: even if the translation symmetry of the boundary is broken by disorder (which is inevitable in any real system), as long as the $U(1)_c \times U(1)_s$ symmetry is preserved, the boundary must still remain gapless. The edge state in our system is also very different from the cases studied in Ref. [231, 232], since

in those systems the states localized at the domain wall is unstable to disorder.

Here we note that although the bosonization of the edge states of bilayer graphene in a magnetic field was also studied in Ref. [233, 234], in these works only the spin symmetry was considered in the bosonization, and the conclusion of Ref. [233, 234] was that the system is equivalent to a $1d$ spin model. Here we stress that, both the $U(1)_s$ and $U(1)_c$ symmetries are crucial to define the BSPT state: *i.e.* if either of the U(1) symmetries is broken (for example if the bulk forms a canted antiferromagnetic order), the system will become a trivial state. With both $U(1)$ symmetries in our system, the boundary theory Eq. (5.27) must remain gapless, and it can never be realized as a $1d$ system, but rather only as the boundary of a $2d$ system, which is an essential property of all SPT states.

Let us discuss the operator content further. Assuming ϕ_- is pinned and θ_- fluctuates strongly, one can obtain the low energy components of the four component vector $\boldsymbol{n}$ in Eq. (5.22):

$$\begin{aligned} n_1 + in_2 \quad &\sim \epsilon_{\alpha\beta}\psi_{1,\alpha}\psi_{2,\beta} \qquad \sim e^{i\theta}, \\ n_3 + in_4 \quad &\sim \sum_l (-1)^l \psi_l^\dagger \sigma^+ \psi_l \sim e^{i2\pi\phi}. \end{aligned} \tag{5.28}$$

Here $n_1 + in_2$ corresponds to an interlayer spin-singlet ($S^z = 0$) Cooper pair, while n_3 and n_4 correspond to in-plane magnetic order. All components of the vector $\boldsymbol{n}$ have power-law correlations at the boundary, and their scaling dimensions are $\Delta[\epsilon_{\alpha\beta}\psi_{1,\alpha}\psi_{2,\beta}] = \frac{\tilde{K}}{4\pi}$, $\Delta[\sum_l (-1)^l \psi_l^\dagger \sigma^+ \psi_l] = \frac{\pi}{\tilde{K}}$. Thus we see that indeed the low energy correlations at the edge all correspond to bosonic fields, which could be built from elementary bosons of even charge and integer spin. The presence of four distinct "primary fields" is characteristic of the Wess-Zumino-Witten (WZW) $SU(2)_1$ CFT, which is well-known to be expressable in terms of a single gapless boson and has $c = 1$[50, 51]. The model in Eq. (5.27) is a deformation of the usual $SU(2)_1$ theory which reduces the symmetry to $U(1)_c \times U(1)_s$. It

is also equivalent to a (deformed) O(4) NLSM with $k = 1$ WZW term – see e.g. Ref. [197].

Eq. (5.28) identified the effective bosonic degrees of freedom that form a bosonic SPT state in the bulk. There are two flavors of bosons carrying charge and spin quantum numbers respectively. Following the method of Ref. [230], we can derive the wave function of the bosons in the bulk, by calculating the following correlation function of the boundary conformal field theory:

$$\Psi(z_1, z_2 \cdots w_1, w_2 \cdots) \sim \langle \prod_j e^{i\theta(z_j)} \prod_k e^{2\pi i \phi(w_k)} \mathcal{O}_{bg} \rangle, \tag{5.29}$$

where z_j and w_k are the complex coordinates in the $2d$ plane for the two flavors of bosons. This is equivalent to calculating the partition function of a $2d$ Coulomb gas with both electric and magnetic charges [235, 236], and $\mathcal{O}_{bg}$ represents a neutralizing background charge operator. The correlation function in Eq. (5.29) can be evaluated with either Eq. (5.24) or Eq. (5.27), and the result will be qualitatively the same:

$$\Psi(z_1, z_2 \cdots w_1, w_2 \cdots) \sim \mathrm{Norm}(z_j, w_k) \prod_{j,k} (z_j - w_k), \tag{5.30}$$

where $\mathrm{Norm}(z_j, w_k)$ only depends on the norm of $z_j - w_k$, $z_i - z_j$ and $w_i - w_j$, and contains all the dependence upon the Luttinger parameters in Eq. (5.24) and Eq. (5.27). This wave function indeed represents a bosonic SPT state: it is symmetric under interchange of identical z_i or w_j bosons, and the two flavors of bosons view each other as a $2\pi-$flux. This mutual "flux attachment" picture is the very essence of the BSPT state [28].

Knowing the effective field theory at the boundary is the $(1+1)d$ NLSM for $\boldsymbol{n}$ with a Wess-Zumino-Witten term at level $k = 1$, the bulk theory can be constructed with the Chalker-Coddington network model [237], and as was shown in Ref. [32, 54], the bulk theory obtained by this construction is precisely Eq. (5.22) with $\Theta = 2\pi$. The physical

meaning of this topological $\Theta-$term is that, a vortex of (n_1, n_2), *i.e.* a vortex of the superconductor order parameter, which traps magnetic flux $\frac{hc}{2e}$, would carry spin $S^z = 1$, which is perfectly consistent with the physics of the bilayer QSH state.

It is worth contrasting with the case of a single layer QSH insulator, in which the boundary *cannot* be driven into a state with gapped fermions but gapless bosonic modes, as long as the $U(1)_c$ and time-reversal (or $U(1)_s$) symmetry of the QSH insulator are preserved [8, 9]. The mapping between fermionic QSH insulator and BSPT is only valid for two copies of QSH insulators (which mathematically is equivalent to four copies of $p \pm ip$ topological superconductors), as was shown in Ref. [238].

By varying competing electric and magnetic fields normal to the layer, a quantum phase transition can occur between the BSPT and the trivial state in the $2d$ bulk. Using the Chalker-Coddington network picture, one may construct a theory for the 2d bulk phase transition which involves only gapless bosonic modes and retains the single-fermion gap. In the field theory Eq. (5.22) this transition occurs when Θ is tuned to π. Although directly analyzing the bulk field theory at $\Theta = \pi$ is difficult, recent unbiased determinant quantum Monte Carlo simulation on a similar bilayer honeycomb lattice interacting fermion model confirms that this purely bosonic topological-trivial quantum phase transition can indeed happen [145, 146], which is fundamentally different from the ordinary topological to trivial transition in any free fermion system. Maintaining the single particle gap requires strong interactions, and other less interesting possibilities are possible in experiment, such as other intermediate phases between the BSPT phase and the trivial phase. Nevertheless, a direct second order "bosonic" transition like the one found in Ref. [145, 146] seems allowed and a quite interesting prospect.

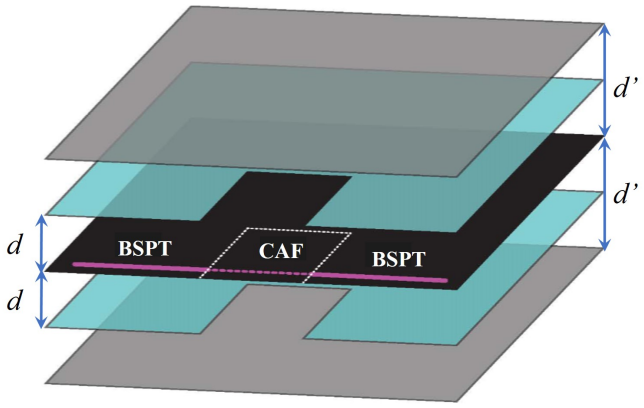

Figure 5.2: Our proposed set-up for measuring the carrier charge at the boundary of our system. Most of the sample are screened by the inner symmetric gates, while the unscreened region has a stronger interaction which leads to a CAF order, and induces backscattering of the edge states. We also add a pair of outer gates to control the strength of interaction in the CAF region.

5.2.3 Experimental Implications

The central prediction of our theory is that in a bilayer graphene in the quantum spin Hall phase [222], the gapless boundary modes are bosonic rather than fermionic. The low energy charge carriers on the edge are Cooper pairs $\epsilon_{\alpha\beta}c_{1,\alpha}c_{2,\beta}$, with charge $2e$. Tunnelling from a normal metal electrode or tip is predicted to show a hard gap, despite ballistic, dissipationless in-plane resistance. Conversely, tunnelling from a superconducting tip should show zero gap.

A purely transport measurement is also possible using shot noise, which has previously been used to probe fractional charges in quantum Hall edge states [239, 240, 241, 242]. By introducing a quantum point contact, either using electrostatic gates or a nano-constriction, edge-to-edge backscattering is possible at that contact, with a finite transmission probability [242]. Individual tunneling events will carry charge $\pm 2e$, which is directly observable in the noise spectrum. The detailed calculation about the shot noise in a quantum point contact geometry has been presented in a follow-up paper by some

of the current authors [243].

Here we propose a different method to measure the carrier charge at the boundary. Compared with the point-contact geometry, our current proposal is easier to implement experimentally, and more convenient to analyze theoretically, as it only involves one edge instead of two opposite edges. Our proposal is based on the dual-gated geometry that has been used in experiments Ref. [222]. The screened Coulomb interaction in our system can be tuned by its distance d to the gates due to screening. The competition between interaction and the Zeeman energy can lead to a rich phase diagram, and when the interaction is dominant, the system develops a canted antiferromagnetic (CAF) order [222]. The size of the fermion gap at the boundary, as well as the magnetic field required to realize the BSPT state in this set up will be discussed in detail in the supplementary material.

The stability of the edge states of our system relies on the conservation of S^z, and if locally the S^z conservation is broken, the edge modes encounters backscattering, and hence leads to noise of the current. We propose to screen the Coulomb interaction for most of the sample, while leaving a region close to the edge unscreened, in order to develop a local CAF order, which serves as a local "magnetic impurity" that breaks the S^z conservation. We calculate the quantum shot noise in the supplementary material with the proposed set-up Fig. 5.2, and recover the expected result:

$$\tilde{S}(\omega = 0) = 2e^* \langle I \rangle \coth \frac{e^* V}{2k_B T}. \tag{5.31}$$

$e^* = 2e$ is the smoking gun signature of the BSPT state proposed in our work.

If a direct second order quantum phase transition between the BSPT and trivial phase found in Ref. [145, 146] indeed happens in a real system, then at the transition, which corresponds to a $(2+1)d$ CFT, the bulk conductivity should be a universal value

$\sigma = De^2/h$, where D is an order-1 universal constant [126, 127]. Moreover the transition should be accompanied by a closing of the spin gap, with observable consequences for spin susceptibility as well as thermal transport measurements.

5.3 Quantum phase transitions between bosonic symmetry protected topological states without sign problem: a generalization of the bilayer quantum spin hall model

Unlike fermionic symmetry protected topological (SPT) states (or equivalently called topological insulators and topological superconductors), bosonic SPT states all require strong interaction, which makes it very difficult to analyze any generic model of bosonic SPT states. The original general Hamiltonians for bosonic SPT states proposed in Ref. [25, 26] and the lattice models that describe the Z_2 SPT state [27, 244] are exactly soluble, but they are artificial and only describe the fixed points of the SPT states. Most discussions of bosonic SPT states so far are based on effective field theories [31, 30, 63], and their exact relation to lattice models was not carefully explored yet.

Besides their special symmetry protected edge states, SPT states must also have special quantum phase transitions between each other (or from the trivial state). These transitions are clearly beyond the Ginzburg-Landau paradigm because no symmetry is spontaneously broken across the transition. In order to study bosonic SPT states more quantitatively, especially at the quantum phase transitions between bosonic SPT states, we need lattice models that can be tuned away from their fixed points, namely they are not soluble, but can be simulated reliably without sign problem. Several lattice

models of bosons with statistical interactions[245, 246, 247, 248] has been proposed and studied by various numerical techniques. In this paper, we propose a series of $2d$ lattice models built with interacting fermions instead of bosons. However, we argue that in the entire phase diagram the fermions never have to show up at low energy. First of all, we demonstrate that the edge states (interface between SPT and trivial states) at the $(1+1)d$ boundary only contain gapless boson modes, while fermions are gapped by interaction. Then it is expected that at the bulk quantum phase transition between the SPT and the trivial states the fermions are also gapped while bosons are gapless, which can be understood in a simple Chalker-Coddington network construction of the bulk quantum phase transition [237]. Indeed, it was shown in an interacting bilayer quantum spin Hall model [145, 146] that the quantum phase transition between the SPT and trivial states only involve gapless bosonic modes. Especially, the data in Ref. [146] strongly suggests that along a special SO(4) symmetric line of the model, the SPT-trivial quantum phase transition (which is described the O(4) nonlinear sigma model (NLSM) with $\Theta = \pi$) is a special $(2 + 1)d$ conformal field theory (CFT) that only involves bosonic fields, which is consistent with the conjectured renormalization group flow diagram in Ref. [54].

In this work, we will first review and further analyze the model used in Ref. [145, 146]. Then we demonstrate that this model can be generalized to a whole series of models with N times of fermion flavors, and we argue that the bulk is described by a $\mathrm{Sp}(N)$ principal chiral model with a topological $\Theta-$term, and by tuning one parameter this model can have a quantum phase transition between SPT and trivial state, which in the field theory occurs precisely at $\Theta = \pi$. In the SPT phase the boundary of this model is described by the $\mathrm{Sp}(N)_1$ CFT. Again all the fermion modes at the boundary are gapped out by interaction, and hence we expect the same happens at the SPT-trivial transition in the bulk (based on the Chalk-Coddington construction [237]), which awaits further numerical confirmation. Implication of our results on the $2d$ boundary of $3d$ fermionic and bosonic

SPT states will also be discussed.

5.3.1 Bilayer Quantum Spin Hall Insulator

5.3.1.1 Bulk Theory

Model and Symmetry In this section let us first review and also further analyze the model used in Ref. [145, 146], which is an interacting bilayer quantum spin Hall insulator without sign problem. Let $c_{i\ell} = (c_{i\ell\uparrow}, c_{i\ell\downarrow})^\intercal$ be the spin-1/2 fermion doublet on site-i layer-ℓ. The free fermion part of the Hamiltonian for the bilayer QSH model is given by

$$H_{\text{band}} = -t \sum_{\langle ij\rangle,\ell} c^\dagger_{i\ell} c_{j\ell} + \sum_{\langle\langle ij\rangle\rangle,\ell} \mathrm{i}\lambda_{ij} c^\dagger_{i\ell}\sigma^z c_{j\ell} + H.c., \tag{5.32}$$

where t is the nearest neighbor hopping and $\lambda_{ij} = -\lambda_{ji}$ is the Kane-Mele spin-orbit coupling, as illustrated in Fig. 5.3. The layer index $\ell = 1, 2$ labels the two layers of QSH systems. Without any interaction, the free-fermion Hamiltonian H_{band} has a pretty high symmetry SO(4) $\times$ SO(3).[146] The symmetry will be most evident, if we rewrite the model in a new set of fermion basis (roughly by a particle-hole transformation of fermions in the second layer), defined by

$$\begin{aligned} f_{i\uparrow} \equiv \begin{pmatrix} f_{i\uparrow 1} \\ f_{i\uparrow 2} \end{pmatrix} &= \begin{pmatrix} c_{i1\uparrow} \\ (-)^i c^\dagger_{i2\uparrow} \end{pmatrix}, \\ f_{i\downarrow} \equiv \begin{pmatrix} f_{i\downarrow 1} \\ f_{i\downarrow 2} \end{pmatrix} &= \begin{pmatrix} (-)^i c_{i1\downarrow} \\ c^\dagger_{i2\downarrow} \end{pmatrix}, \end{aligned} \tag{5.33}$$

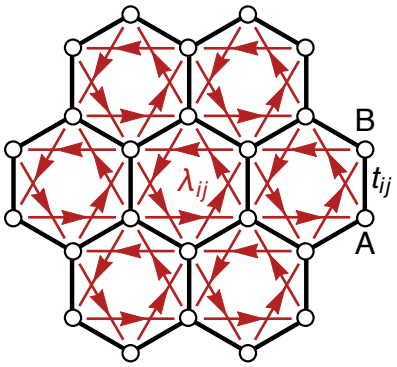

Figure 5.3: Honeycomb lattice with the nearest neighboring hopping t_{ij} and the 2nd nearest neighboring hopping λ_{ij}. $\lambda_{ij} = -\lambda_{ji} = \lambda$ if i follows the bound orientation to j. The lattice can be divided into A and B sublattices.

where $(-)^i = +/-$ on sublattice A/B respectively. In the new basis, the Hamiltonian H_{band} reads

$$H_{\text{band}} = \sum_{i,j,\sigma} (-)^\sigma f^\dagger_{i\sigma}(-t_{ij} + \mathrm{i}\lambda_{ij}) f_{j\sigma} + h.c., \tag{5.34}$$

where $(-)^\sigma = +/-$ for spin $\uparrow / \downarrow$ respectively. Here $t_{ij} = t$ for nearest neighboring sites i, j and $t_{ij} = 0$ otherwise.

The SO(4) symmetry rotates the following fermion bilinear operators $\boldsymbol{N}_i$ as an O(4) vector:

$$\boldsymbol{N}_i = (N^0_i, N^1_i, N^2_i, N^3_i) = f^\dagger_{i\downarrow}(\tau^0, \mathrm{i}\tau^1, \mathrm{i}\tau^2, \mathrm{i}\tau^3) f_{i\uparrow} + h.c., \tag{5.35}$$

where $\tau^{0,1,2,3}$ are Pauli matrices acting on the f-fermion doublets. The SO(4) group is naturally factorized to $\mathrm{SU}(2)_\uparrow \times \mathrm{SU}(2)_\downarrow$ as right and left isoclinic rotations, under which the fermions transform as $f_{i\sigma} \to U_\sigma f_{i\sigma}$ with $U_\sigma \in \mathrm{SU}(2)_\sigma$ for $\sigma = \uparrow, \downarrow$. It is straightforward to see the band Hamiltonian H_{band} in Eq. (5.34) is invariant under both $\mathrm{SU}(2)_\uparrow$ and $\mathrm{SU}(2)_\downarrow$, and hence SO(4) symmetric. On the other hand, the SO(3) symmetry rotates another set of fermion bilinear operators $\boldsymbol{M}_i = (M^1_i, M^2_i, M^3_i)$ as an O(3) vector. Let

$M_i^{\pm} = M_i^1 \pm \mathrm{i}M_i^2$, the definition of $\boldsymbol{M}_i$ follows from

$$M_i^- = \sum_\sigma f_{i\sigma}^\intercal \mathrm{i}\tau^2 f_{i\sigma},\ M_i^3 = (-)^i \sum_\sigma (-)^\sigma f_{i\sigma}^\dagger f_{i\sigma}, \tag{5.36}$$

and $M_i^+ = (M_i^-)^\dagger$. This also defines an SU(2) symmetry of the f-fermions, denoted as $\mathrm{SU}(2)_M$. The SU(2) generators are given by $\boldsymbol{Q} = \sum_i \boldsymbol{Q}_i$ with $Q_i^a = \frac{1}{2\mathrm{i}}\epsilon_{abc} M_i^b M_i^c$. Let $Q_i^{\pm} = Q_i^1 \pm \mathrm{i}Q_i^2$, the $\mathrm{SU}(2)_M$ generators can be explicitly written as

$$\begin{aligned} Q_i^- &= (-)^i \sum_\sigma (-)^\sigma f_{i\sigma}^\intercal \mathrm{i}\tau^2 f_{i\sigma}, \\ Q_i^3 &= \sum_\sigma (f_{i\sigma}^\dagger f_{i\sigma} - 1). \end{aligned} \tag{5.37}$$

The physical meaning of Q^3 is the total number of f-fermions away from half-filling, which is obviously conserved. It can be further checked that $[H_{\mathrm{band}}, \boldsymbol{Q}] = 0$, so the model is indeed $\mathrm{SU}(2)_M \simeq \mathrm{SO}(3)$ symmetric. Therefore on the free-fermion level, the bilayer QSH model has the $\mathrm{SO}(4) \times \mathrm{SO}(3) \simeq \mathrm{SU}(2)_\uparrow \times \mathrm{SU}(2)_\downarrow \times \mathrm{SU}(2)_M$ symmetry.

In terms of the original fermion $c_{i\ell} = (c_{i\ell\uparrow}, c_{i\ell\downarrow})^\intercal$, the O(4) vector $\boldsymbol{N}_i$ and the O(3) vector $\boldsymbol{M}_i$ have simple physical interpretations. They correspond to the following fermion bilinear orders,[145, 146]

$$\begin{aligned} \text{SDW: } \boldsymbol{S}_i = (N_i^0, N_i^3, M_i^3) &= \sum_\ell (-)^{i+\ell} c_{i\ell}^\dagger \boldsymbol{\sigma} c_{i\ell}, \\ \text{SC: } \Delta_i = N_i^2 + \mathrm{i}N_i^1 &= 2c_{i1}^\intercal \mathrm{i}\sigma^y c_{i2}, \\ \text{Exciton: } D_i = M_i^1 + \mathrm{i}M_i^2 &= -2(-)^i c_{i1}^\dagger c_{i2}. \end{aligned} \tag{5.38}$$

The spin density wave (SDW) is an antiferromagnet both between the sublattices and across the layers, the superconductivity (SC) is an inter-layer spin-singlet s-wave pairing, and the exciton condensation is an inter-layer particle-hole pairing with opposite

phase between the sublattices. The SO(4) symmetry rotates the SDW-XY and the SC order parameters, and the SO(3) symmetry rotates the exciton and the SDW-Z order parameters. In the original fermion basis, the $\mathrm{SO}(3) \simeq \mathrm{SU}(2)_M$ generators read

$$Q_i^- = -2c_{i2}^\dagger \sigma^z c_{i1},\ Q_i^3 = \sum_\ell (-)^\ell c_{i\ell}^\dagger c_{i\ell}. \tag{5.39}$$

So the $\mathrm{SU}(2)_M$ symmetry rotates the original c-fermions across the layers, and Q^3 is the charge difference between the layers. Because the layers are identical to each other in the bilayer QSH model Eq. (5.32), the $\mathrm{SU}(2)_M$ symmetry is manifest.

Phase Diagram A generic four-fermion interaction that preserves the $\mathrm{SO}(4) \times \mathrm{SO}(3)$ symmetry takes the form of

$$H_{\mathrm{int}} = -\sum_{i,j} \left(J_{ij} \boldsymbol{N}_i \cdot \boldsymbol{N}_j + U_{ij} \boldsymbol{M}_i \cdot \boldsymbol{M}_j \right), \tag{5.40}$$

where $\boldsymbol{N}_i$ and $\boldsymbol{M}_i$ are fermion bilinear operators defined in Eq. (5.35) and Eq. (5.36) respectively. To simplify, we consider the nearest neighboring coupling $J_{ij} = J\delta_{\langle ij \rangle}$ of O(4) vectors, and the on-site interaction $U_{ij} = U\delta_{ij}$ of O(3) vectors. Then the full Hamiltonian of the interacting bilayer QSH model reads

$$H = \sum_{i,j,\sigma} (-)^\sigma f_{i\sigma}^\dagger (-t_{ij} + \mathrm{i}\lambda_{ij}) f_{j\sigma} + h.c. - J \sum_{\langle ij \rangle} \boldsymbol{N}_i \cdot \boldsymbol{N}_j - U \sum_i \boldsymbol{M}_i \cdot \boldsymbol{M}_i. \tag{5.41}$$

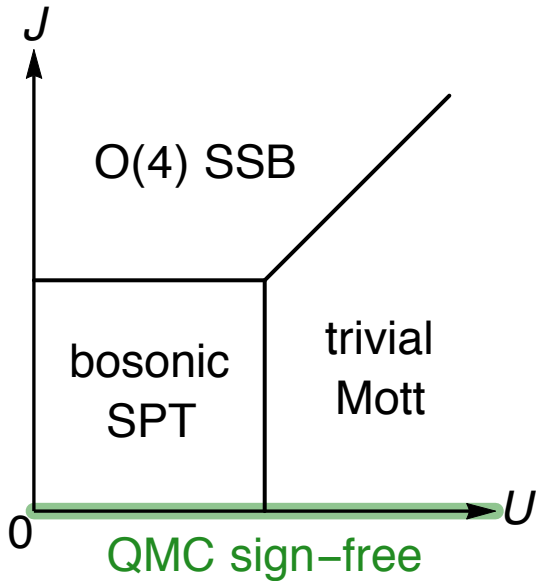

Figure 5.4: A schematic phase diagram of the interacting bilayer QSH model.

Or in terms of the original c-fermion,

$$\begin{aligned} H =& H_{\text{band}} + H_{\text{int}}, \\ H_{\text{band}} =& -t \sum_{\langle ij\rangle,\ell} c^\dagger_{i\ell} c_{j\ell} + \sum_{\langle\langle ij\rangle\rangle,\ell} \mathrm{i}\lambda_{ij} c^\dagger_{i\ell}\sigma^z c_{j\ell} + H.c., \\ H_{\text{int}} =& -J \sum_{\langle ij\rangle} \tfrac{1}{2}(S^+_i S^-_j + \Delta^\dagger_i \Delta_j + h.c.) \\ & - U \sum_i \left(\tfrac{1}{2}(D^\dagger_i D_i + D_i D^\dagger_i) + S^z_i S^z_i\right), \end{aligned} \tag{5.42}$$

where $S^\pm_i = S^x_i \pm \mathrm{i} S^y_i$ and $\boldsymbol{S}_i$, Δ_i, D_i are c-fermion bilinear operators defined in Eq. (5.38).

A schematic phase diagram of the model is shown in Fig. 5.4. In the weak interaction limit when both J and U are small, the model is an SO(4) bosonic SPT phase. In the next subsection we will demonstrate that the interaction gaps out the fermion modes of the boundary states of the quantum spin Hall insulator, which leaves the boundary only a CFT with central charge $c = 1$ and exact SO(4) symmetry. The boundary precisely

corresponds an $(1+1)d$ O(4) NLSM with a Wess-Zumino-Witten (WZW) term at level $k=1$.

$$S=\int \mathrm{d}\tau\mathrm{d}x\mathrm{d}u\,\frac{1}{2g}(\partial_\mu \boldsymbol{n})^2+\frac{\mathrm{i}k}{2\pi}\epsilon_{abcd}n^a\partial_\tau n^b\partial_x n^c\partial_u n^d, \tag{5.43}$$

where $\boldsymbol{n}=(n^0,n^1,n^2,n^3)$ transforms like a vector under O(4). Based on this boundary theory, we can conclude that the bulk theory is a $(2+1)d$ O(4) NLSM with a Θ-term at $\Theta=2\pi$:

$$S=\int \mathrm{d}\tau\mathrm{d}^2x\,\frac{1}{2g}(\partial_\mu \boldsymbol{n})^2+\frac{\mathrm{i}\Theta}{2\pi^2}\epsilon_{abcd}n^a\partial_\tau n^b\partial_x n^c\partial_y n^d, \tag{5.44}$$

where the coupling strength g is controlled by J. The relation between g and J is indirectly inferred from their physical consequences. A large J in Eq. (5.41) will favor the ferromagnetic long-range order of $\boldsymbol{N}_i$, which breaks the O(4) symmetry spontaneously. A small g in Eq. (5.44) will suppress the fluctuation of $\partial_\nu \boldsymbol{n}$ and stabilize the long-range order of $\boldsymbol{n}$, which also breaks the O(4) symmetry. Thus we identify the small g limit with the large J limit, which both correspond to the spontaneous symmetry broken (SSB) phase. Reversely in the large g (small J) limit, the model Eq. (5.44) is in the O(4) symmetric disordered phase with a topological Θ-term, which describes the $2d$ bosonic SPT phase.[30, 34, 63] The field theories, either on the boundary Eq. (5.43) or in the bulk Eq. (5.44), can also be derive by coupling the fermions to a bosonic O(4) vector field $\boldsymbol{n}_i$ via

$$H_{\mathrm{cp}}=-\sum_i \boldsymbol{n}_i\cdot\boldsymbol{N}_i, \tag{5.45}$$

where $\boldsymbol{N}_i$ are fermion bilinear operators in Eq. (5.35). Integrating out the fermions,[210] will generate the bosonic theories mentioned above.

Another way to connect the bilayer QSH insulator to the bosonic SPT state is to consider the fermions as partons of the O(4) vector field $\boldsymbol{N}_i$ under the constraint $\boldsymbol{Q}_i=0$, which amounts to gauging the $\mathrm{SU}(2)_M$ symmetry. After the fermions are confined by the

$\mathrm{SU}(2)_M$ gauge field, the remaining bulk degrees of freedom will be purely bosonic. The gauge theory argument along this line has been discussed in Ref. [238], arriving at the conclusion that the bilayer QSH state precisely becomes a bosonic SPT state under gauge confinement. After coupling the fermions to dynamical gauge fields, it is equivalent to view the fermions as "slave fermions", which is an approach taken in Ref. [34, 249, 40]. However in this work, we will use interactions to gap out the fermions instead of confining the fermions by gauge fluctuations.

Now we consider the effect of the on-site interaction U. Large enough U will drive the system to a featureless Mott insulator (no symmetry breaking and topologically trivial) as indicated in Fig. 5.4. At first glance, this seems counterintuitive because one may expect the interaction Hamiltonian $H_U = -U\boldsymbol{M}_i \cdot \boldsymbol{M}_i$ to favor a mean-field ground state with $\langle \boldsymbol{M}_i \rangle \neq 0$ on each site, which would then break the SO(3) symmetry spontaneously. However such mean-field state is not an eigenstate of the Hamiltonian H_U and hence not the true ground state. Take the mean-field states $|M_i^3 = \pm 2\rangle$ for example (where ± 2 are the maximal/minimal eigenvalues of the M_i^3 operator). Because $(M_i^1)^2 + (M_i^2)^2$ does not commute with M_i^3, the states $|M_i^3 = \pm 2\rangle$ must be mixed to produce the true on-site ground state: $|M_i^3 = +2\rangle + |M_i^3 = -2\rangle$, which is actually an $\mathrm{SO}(4) \times \mathrm{SO}(3)$ *singlet state*. Although the expectation value of the O(3) vector $\langle \boldsymbol{M}_i \rangle = 0$ vanishes in the singlet state, $\langle \boldsymbol{M}_i \cdot \boldsymbol{M}_i \rangle$ is not zero, so that the Hamiltonian H_U does gain energy from the singlet state. The singlet state has the energy $-12U$ (per site), which is lower than the energy of any mean-field state. By exact diagonalization of the on-site interaction H_U, it can be verified that the singlet state is the unique on-site ground state and is gapped from all excited states by the energy of the order $\sim U$.

Therefore in the large U limit, the model has an unique and fully-gapped ground

state, which is the direct product state of on-site SO(4) × SO(3) singlets

$$|\mathrm{GS}\rangle = \prod_i M_i^+ |0\rangle_f = \prod_i (f_{i\uparrow 2}^\dagger f_{i\uparrow 1}^\dagger + f_{i\downarrow 2}^\dagger f_{i\downarrow 1}^\dagger) |0\rangle_f , \tag{5.46}$$

where $|0\rangle_f$ denotes the zero fermion state of f-fermions. One can see $M_i^+ |0\rangle_f$ is just another way of writing the singlet state $|M_i^3 = +2\rangle + |M_i^3 = -2\rangle$, given $M_i^3 \sim f_{i\uparrow}^\dagger f_{i\uparrow} - f_{i\downarrow}^\dagger f_{i\downarrow}$. In the original c-fermion basis, the ground state reads

$$|\mathrm{GS}\rangle = \prod_i \Delta_i^\dagger |0\rangle_c = \prod_i (c_{i1\downarrow}^\dagger c_{i2\uparrow}^\dagger - c_{i1\uparrow}^\dagger c_{i2\downarrow}^\dagger) |0\rangle_c , \tag{5.47}$$

where $|0\rangle_c$ denotes the zero fermion state of c-fermions. Because the ground state is unique and fully gapped, it should be stable against all local perturbations, and can be considered as a representative state that controls the whole trivial Mott phase.

The symmetry property of the ground state is most obvious in the f-fermion basis. It is easy to see that the ground state $|\mathrm{GS}\rangle$ in Eq. (5.46) is invariant under $\mathrm{SU}(2)_\uparrow \times \mathrm{SU}(2)_\downarrow$, because $f_{i\sigma 2}^\dagger f_{i\sigma 1}^\dagger$ is the $\mathrm{SU}(2)_\sigma$ singlet operator and $|0\rangle_f$ is also $\mathrm{SU}(2)_\sigma$ invariant (for both $\sigma = \uparrow, \downarrow$). The $\mathrm{SU}(2)_M$ symmetry can be verified by showing $\boldsymbol{Q} |\mathrm{GS}\rangle = 0$. Since $|\mathrm{GS}\rangle$ is at half-filling, $Q^3 |\mathrm{GS}\rangle = 0$. Then by definition, $[Q_i^a, M_j^b] = 2\mathrm{i}\epsilon^{abc}\delta_{ij} M_i^c$, thus $Q_i^- M_i^+ = M_i^+ Q_i^- - 4M_i^3$, so

$$Q_i^- |\mathrm{GS}\rangle = \prod_{j\neq i} M_j^+ (M_i^+ Q_i^- - 4M_i^3) |0\rangle_f = 0. \tag{5.48}$$

Because $Q_i^- \sim (-)^\sigma f_{i\sigma}^\intercal \mathrm{i}\tau^2 f_{i\sigma}$ only contains fermion annihilation operators and $M_i^3 \sim (-)^\sigma f_{i\sigma}^\dagger f_{i\sigma}$ is a sum of number operators, both of them quench the fermion vacuum state $|0\rangle_f$, therefore $Q^- |\mathrm{GS}\rangle = \sum_i Q_i^- |\mathrm{GS}\rangle = 0$. In conclusion, the large-U ground state preserves the full $\mathrm{SU}(2)_\uparrow \times \mathrm{SU}(2)_\downarrow \times \mathrm{SU}(2)_M \simeq \mathrm{SO}(4) \times \mathrm{SO}(3)$ symmetry.

In the trivial Mott phase, both the fermionic and bosonic excitations are gapped. In the large U limit, the single particle gap is $9U$, the O(3) vector gap is $8U$ and the O(4) vector gap is $12U$. The O(4) vector gap can be soften by the inter-site coupling J. When the gap is soften to zero, the O(4) boson will condense and the system will enter the SSB phase. So we expect the order-disorder transition to happen at $J \sim U$ in the strong interaction limit.

The most interesting feature of this model is the topological transition between the bosonic SPT phase and the trivial Mott phase. Previous numerical study[146] shows that with the exact SO(4) symmetry described in this section, there can be a direct continuous transition between the bosonic SPT phase and the trivial Mott phase, where the gap of bosonic modes $\boldsymbol{N}$ closes, while the fermion gap remains open. Thus we expect this phase transition can be described by Eq. (5.44). The phase diagram and the renormalization group flow of Eq. (5.44) was studied in Ref. [54]. In the large g (small J) regime, the bosonic SPT phase corresponds to $\pi < \Theta \leq 2\pi$ controlled by the stable fixed point $\Theta = 2\pi$, and the trivial Mott phase corresponds to $0 \leq \Theta < \pi$ controlled by the stable fixed point $\Theta = 0$. The two phases are separated by the quantum phase transition at $\Theta = \pi$, which in general can be either first order or continuous, while numerical results in Ref. [146] demonstrates that this transition is continuous, which implies that the disordered phase of Eq. (5.44) with $\Theta = \pi$ is a $(2+1)d$ CFT. The stability of this CFT against perturbations that break the SO(4) symmetry needs further studies.

Sign-Free QMC Simulation In this subsection we show that the whole $J = 0$ line in the phase diagram Fig. 5.4 can be simulated by determinant QMC without fermion sign problem. Along the $J = 0$ line, the interacting bilayer QSH model in Eq. (5.41) admits sign-free QMC simulations. We perform Hubbard-Stratonovich (HS) decomposition of the on-site interaction in the O(3) vector channel by introducing the O(3) auxiliary field

$\boldsymbol{m}_i$, such that $-U\boldsymbol{M}_i^2 \to -\boldsymbol{m}_i \cdot \boldsymbol{M}_i + \frac{1}{4U}\boldsymbol{m}_i^2$. The partition function is a sum of the Boltzmann weight $W[\boldsymbol{m}_i(\tau)]$ over spacetime configurations of the auxiliary field $\boldsymbol{m}_i(\tau)$,

$$\begin{aligned} Z &= \sum_{[\boldsymbol{m}_i(\tau)]} W[\boldsymbol{m}_i(\tau)], \\ W[\boldsymbol{m}_i(\tau)] &= \mathrm{Tr} \prod_{\tau} e^{-\Delta\tau H[\boldsymbol{m}_i(\tau)]}, \end{aligned} \tag{5.49}$$

where $H[\boldsymbol{m}_i]$ is a fermion bilinear Hamiltonian as a functional of $\boldsymbol{m}_i$,

$$H[\boldsymbol{m}_i] = H_{\text{band}} + \sum_i \Big(-\boldsymbol{m}_i \cdot \boldsymbol{M}_i + \frac{1}{4U}\boldsymbol{m}_i^2 \Big). \tag{5.50}$$

It can be verified that the Hamiltonian $H[\boldsymbol{m}_i]$ has the following time-reversal symmetry $\mathcal{T}$ for all configurations of $\boldsymbol{m}_i$.

$$\mathcal{T} : \begin{cases} f_{i\uparrow} \to \mathcal{K}\mathrm{i} f_{i\downarrow}^\dagger \\ f_{i\downarrow} \to \mathcal{K}\mathrm{i} f_{i\uparrow}^\dagger \end{cases}, \quad \begin{cases} f_{i\uparrow}^\dagger \to \mathcal{K}(-\mathrm{i}) f_{i\downarrow} \\ f_{i\downarrow}^\dagger \to \mathcal{K}(-\mathrm{i}) f_{i\uparrow} \end{cases}, \tag{5.51}$$

where $\mathcal{K}$ is the complex conjugation operator. According to Ref. [250, 251, 252], the time-reversal symmetry ensures the weight $W[\boldsymbol{m}_i]$ to be positive definite, which allows QMC simulations without the fermion sign problem.

However when $J \neq 0$, we are not aware of any sign-free QMC simulation scheme that also preserves the SO(4) symmetry. The most straight-forward HS decomposition of the J-term interaction is in the O(4) vector channel, as done in Eq. (5.45). However it suffers from the fermion sign problem. Because the fermion sign structure of the weight $W[\boldsymbol{n}_i(\tau)]$ must match the bosonic SPT sign structure described by the topological Θ-term in Eq. (5.44), which requires each O(4) skyrmion in the spacetime configuration of $\boldsymbol{n}$ to be associated with a minus sign. Such sign structure is a defining feature of the bosonic SPT phase, and can not be avoided. It turns out that other HS decompositions

in the fermion hopping/pairing channels do not eliminate the sign problem either.

Nevertheless if we are allowed to break the SO(4) symmetry, we can introduce the inter-site correlation of $\boldsymbol{N}$ field without spoiling the sign-free QMC. Because as long as the time reversal symmetry in Eq. (5.51) is preserved, the Boltzmann weight will be positive definite. Among the four components of the vector $\boldsymbol{N}$, only N^0 is time-reversal odd (i.e. $\mathcal{T} : N^0 \to -N^0$), and the remaining components $N^{1,2,3}$ are time-reversal even (i.e. $\mathcal{T} : N^{1,2,3} \to N^{1,2,3}$). Hence the following decomposition is time reversal symmetric,

$$H[\boldsymbol{m}_i, \boldsymbol{n}_i] = H[\boldsymbol{m}_i] + \sum_i \sum_{a=1,2,3} n_i^a N_i^a + \cdots , \tag{5.52}$$

which will result in positive definite weight $W[\boldsymbol{m}_i, \boldsymbol{n}_i]$. Therefore it is possible to explore the entire J-U phase diagram like Fig. 5.4, if we lower the SO(4) symmetry to its SO(3), U(1) or Z_2 subgroups.

5.3.1.2 Boundary Theory

One-Loop RG On the free-fermion level, the helical edge modes of the bilayer QSH model is described by

$$H_{\text{bdy}} = \int \mathrm{d}x (\psi_L^\dagger \mathrm{i}\partial_x \psi_L - \psi_R^\dagger \mathrm{i}\partial_x \psi_R), \tag{5.53}$$

where ψ_L (ψ_R) is the left (right) moving edge mode associated to $f_\uparrow$ ($f_\downarrow$). Both of them are complex fermion doublets,

$$\psi_L = \begin{pmatrix} \psi_{L1} \\ \psi_{L2} \end{pmatrix}, \psi_R = \begin{pmatrix} \psi_{R1} \\ \psi_{R2} \end{pmatrix}. \tag{5.54}$$

The SO(4) symmetry is factorized to $\mathrm{SU}(2)_L \times \mathrm{SU}(2)_R$ acting on ψ_L and ψ_R respectively. On symmetry ground, the most generic $\mathrm{SO}(4) \times \mathrm{SO}(3)$ invariant interaction that can be induced on the boundary takes the form of

$$H_{\text{int}} = \int \mathrm{d}x(\lambda_J \boldsymbol{N} \cdot \boldsymbol{N} + \lambda_U \boldsymbol{M} \cdot \boldsymbol{M}), \tag{5.55}$$

where the O(4) vector $\boldsymbol{N}$ follows from Eq. (5.35) as

$$\boldsymbol{N} = \psi_R^\dagger(\tau^0, \mathrm{i}\tau^1, \mathrm{i}\tau^2, \mathrm{i}\tau^3)\psi_L + h.c., \tag{5.56}$$

and the O(3) vector $\boldsymbol{M}$ follows from Eq. (5.36) as

$$M^- = \sum_{\sigma=L,R} \psi_\sigma^{\mathrm{T}} \mathrm{i}\tau^2 \psi_\sigma, M^3 = \sum_{\sigma=L,R} (-)^\sigma \psi_\sigma^\dagger \psi_\sigma. \tag{5.57}$$

Along the $J = 0$ line, we expect $\lambda_J \to 0$ and $\lambda_U < 0$ at the UV scale. To facilitate the analysis, we split the $\lambda_U \boldsymbol{M} \cdot \boldsymbol{M}$ interaction into the in-plane $H_\pm$ and out-of-plane H_3 terms, and rearrange the interaction as

$$\begin{aligned} H_{\text{int}} &= \int \mathrm{d}x(\lambda_\pm H_\pm + \lambda_3 H_3 + \lambda_0 H_0), \\ H_\pm &= \tfrac{1}{2}(M^+ M^- + M^- M^+), \\ H_3 &= M^3 M^3, \\ H_0 &= \tfrac{1}{3}\boldsymbol{M} \cdot \boldsymbol{M} - \tfrac{1}{6}\boldsymbol{N} \cdot \boldsymbol{N} + \tfrac{2}{3} \\ &= \sum_{\sigma=L,R} (\psi_\sigma^\dagger \psi_\sigma - 1)^2. \end{aligned} \tag{5.58}$$

Here the SO(3) symmetry is allowed to be broken if $\lambda_\pm \neq \lambda_3$. However we will show that the anisotropy is irrelevant under RG. The one-loop RG equations are

$$\begin{aligned} \tfrac{\mathrm{d}}{\mathrm{d}\ell}\lambda_\pm &= -\tfrac{4}{3}\lambda_\pm\lambda_3, \\ \tfrac{\mathrm{d}}{\mathrm{d}\ell}\lambda_3 &= -\tfrac{4}{3}\lambda_\pm^2, \\ \tfrac{\mathrm{d}}{\mathrm{d}\ell}\lambda_0 &= \tfrac{4}{3}\lambda_\pm^2 + \tfrac{8}{3}\lambda_\pm\lambda_3. \end{aligned} \tag{5.59}$$

At the free-fermion fixed point, $\lambda_\pm$ is always a marginally relevant perturbation, regardless of its initial sign. The interaction will flow towards the $(\lambda_\pm, \lambda_3, \lambda_0) \to (-1, -1, +3)$ direction if $\lambda_\pm < 0$, or towards the $(\lambda_\pm, \lambda_3, \lambda_0) \to (+1, -1, -1)$ direction if $\lambda_\pm > 0$. The fixed-point interaction will take the following form

$$\begin{aligned} H_{\text{int}} = \int \mathrm{d}x\big(&- 4\lambda_\pm(\psi_{R1}^\dagger\psi_{R2}^\dagger\psi_{L1}\psi_{L2} + h.c.) \\ &- 2\lambda_3(\psi_R^\dagger\psi_R - 1)(\psi_L^\dagger\psi_L - 1)\big). \end{aligned} \tag{5.60}$$

with $\lambda_3 < 0$ and $\lambda_\pm = \pm\lambda_3$. In both cases, the SO(3) symmetry is restored under the RG flow. At the RG fixed point, the interaction is expected to gap out fluctuations of the O(3) vector $\boldsymbol{M}$ on the boundary. Since $\boldsymbol{M}$ is a collective mode of fermions, so the fermions must also be gapped out by the interaction on the boundary.

Abelian Bonsonization In the following, we will use the Abelian bosonization to show that the interaction indeed gaps out the fermion mode, and drive the boundary into a $\mathrm{SU}(2)_1$ CFT. The boundary fermions in Eq. (5.54) can be written as

$$\psi_{\sigma\alpha} = \frac{\kappa_{\sigma\alpha}}{\sqrt{2\pi a}} e^{\mathrm{i}\phi_{\sigma\alpha}} \quad \sigma = L, R,\ \alpha = 1, 2, \tag{5.61}$$

where a is a short distance cut-off and $\kappa_{\sigma\alpha}$ is the Klein factor that ensures the anticommutation of the fermion operators. The helical edge modes in Eq. (5.53) can be bosonized to a Luttinger liquid (LL)

$$S_{\rm LL} = \int \mathrm{d}\tau \mathrm{d}x \, \frac{1}{4\pi} (\partial_x \phi^\intercal K \partial_\tau \phi + \partial_x \phi^\intercal V \partial_x \phi), \tag{5.62}$$

where $\phi = (\phi_{L1}, \phi_{L2}, \phi_{R1}, \phi_{R2})^\intercal$, and the density fluctuations are given by $\psi^\dagger_{\sigma\alpha}\psi_{\sigma\alpha} = \frac{1}{2\pi}(-)^\sigma \partial_x \phi_{\sigma\alpha}$. The K matrix reads

$$K = \begin{pmatrix} +1 & & & \\ & +1 & & \\ & & -1 & \\ & & & -1 \end{pmatrix}. \tag{5.63}$$

The V matrix is an identity matrix at the free-fermion fixed point, and will be modified under interactions.

Under the RG flow, forward scatterings become irrelevant, and the fixed point interaction only contains umklapp and backward scatterings as in Eq. (5.60). In terms of the bonsonized degrees of freedom ϕ,

$$H_{\rm int} = \int \mathrm{d}x \, \frac{g_3}{2\pi} \sum_{\alpha,\beta} \partial_x \phi_{L\alpha} \partial_x \phi_{R\beta} - 8\lambda_\pm \cos(l_0^\intercal \phi), \tag{5.64}$$

where $g_3 = \lambda_3/\pi$ and the vector $l_0 = (1, 1, -1, -1)^\intercal$. So the full boundary theory reads

$$S = S_{\rm LL} - 8\lambda_\pm \int \mathrm{d}\tau \mathrm{d}x \cos(l_0^\intercal \phi), \tag{5.65}$$

with the V matrix given by

$$V = \begin{pmatrix} 1 & 0 & g_3 & g_3 \\ 0 & 1 & g_3 & g_3 \\ g_3 & g_3 & 1 & 0 \\ g_3 & g_3 & 0 & 1 \end{pmatrix}. \tag{5.66}$$

So the scaling dimension of $\cos(l_0^{\intercal}\phi)$ is

$$\Delta_0 = 2\sqrt{\frac{1+2g_3}{1-2g_3}}. \tag{5.67}$$

For small λ_3, $\Delta_0 \simeq 2 + 4\lambda_3/\pi$ (recall that $g_3 = \lambda_3/\pi$). The gapping term $\cos(l_0^{\intercal}\phi)$ is marginal ($\Delta_0 = 2$) at the free-fermion fixed point $\lambda_3 = 0$, and will become relevant ($\Delta_0 < 2$) if $\lambda_3 < 0$.

Although we started from a rather specific fixed point interaction in Eq. (5.60), the resulting boundary theory in Eq. (5.65) is of the generic form which is compatible with symmetry requirements. The $\mathrm{SO}(4) \times \mathrm{SO}(3) \simeq \mathrm{SU}(2)_L \times \mathrm{SU}(2)_R \times \mathrm{SU}(2)_M$ symmetry action is not transparent in the Abelian bosonization, nevertheless its $\mathrm{U}(1)_L \times \mathrm{U}(1)_R \times \mathrm{U}(1)_M$ subgroup is clear:

$$\begin{aligned} \mathrm{U}(1)_L &: \psi_L \to e^{\mathrm{i}\alpha_L \tau^3}\psi_L, \\ \mathrm{U}(1)_R &: \psi_R \to e^{\mathrm{i}\alpha_R \tau^3}\psi_R, \\ \mathrm{U}(1)_M &: \psi_{L/R} \to e^{\mathrm{i}\alpha_M}\psi_{L/R}. \end{aligned} \tag{5.68}$$

Correspondingly the ϕ field is transformed as follows

$$\phi \to \phi + \begin{pmatrix} 1 & 0 & 1 \\ -1 & 0 & 1 \\ 0 & 1 & 1 \\ 0 & -1 & 1 \end{pmatrix} \begin{pmatrix} \alpha_L \\ \alpha_R \\ \alpha_M \end{pmatrix}. \tag{5.69}$$

Therefore $-8\lambda_\pm \cos(l_0^\intercal \phi)$ is the most relevant symmetry-preserving cosine term that can be added to the action. The O(4) vector $\boldsymbol{N}$ are linearly recombinations of the following fermion bilinear operators (and their conjugates)

$$\begin{aligned} &\psi_{R1}^\dagger \psi_{L1} = e^{\mathrm{i} l_1^\intercal \phi}, \quad l_1^\intercal = (1,0,-1,0); \\ &\psi_{R1}^\dagger \psi_{L2} = e^{\mathrm{i} l_2^\intercal \phi}, \quad l_2^\intercal = (0,1,-1,0); \\ &\psi_{R2}^\dagger \psi_{L1} = e^{\mathrm{i} l_3^\intercal \phi}, \quad l_3^\intercal = (1,0,0,-1); \\ &\psi_{R2}^\dagger \psi_{L2} = e^{\mathrm{i} l_4^\intercal \phi}, \quad l_4^\intercal = (0,1,0,-1). \end{aligned} \tag{5.70}$$

They transform under $\mathrm{U}(1)_L \times \mathrm{U}(1)_R$ but not $\mathrm{U}(1)_M$. These operators $e^{\mathrm{i} l_a^\intercal \phi}$ $(a = 1,2,3,4)$ all have the same scaling dimension

$$\Delta_a = \frac{-2g_3}{1 - 2g_3 - \sqrt{1 - 4g_3^2}}. \tag{5.71}$$

At the free-fermion fixed point, $-8\lambda_\pm \cos(l_0^\intercal \phi)$ is a marginal perturbation, meaning that it is sitting right at a KT transition point. So any finite $\lambda_\pm$ will render the cosine term relevant, regardless of the sign of $\lambda_\pm$, as shown in Fig. 5.5. The RG equation near

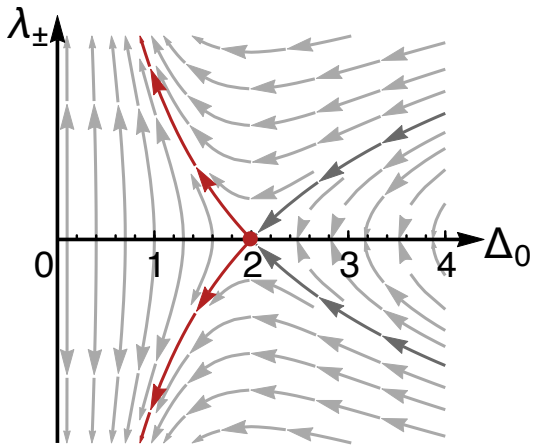

Figure 5.5: RG flow near the KT transition point. The free-fermion fixed point $(\Delta_0, \lambda_\pm) = (2, 0)$ is marked out by a red point. The red arrows illustrate the RG flow after small $\lambda_\pm$ perturbation.

KT transition is given by

$$\begin{aligned} \tfrac{\mathrm{d}}{\mathrm{d}\ell}\lambda_\pm &\sim (2-\Delta_0)\lambda_\pm, \\ \tfrac{\mathrm{d}}{\mathrm{d}\ell}\Delta_0^{-1} &\sim \lambda_\pm^2. \end{aligned} \tag{5.72}$$

Plugging in Eq. (5.67) for Δ_0 and expanding around $\lambda_3 \to 0$, we arrive at $\frac{\mathrm{d}}{\mathrm{d}\ell}\lambda_\pm \sim -\lambda_\pm\lambda_3$, $\frac{\mathrm{d}}{\mathrm{d}\ell}\lambda_3 \sim -\lambda_\pm^2$, consistent with Eq. (5.59), therefore the $\lambda_\pm$ term is marginally relevant.

From $l_0^\intercal K^{-1} l_0 = 0$, we know that $\cos(l_0^\intercal\phi)$ is a bosonic operator. So as $\lambda_\pm$ flows to infinity under RG, the field ϕ will be pinned by the cosine term to $l_0^\intercal\phi = 0 \mod 2\pi$. Any operator $O_l = e^{\mathrm{i}l^\intercal\phi}$ that does not commute with $\cos(l_0^\intercal\phi)$ (i.e. $l^\intercal K^{-1} l_0 \neq 0$) will be gapped out. Using this criterion, it is easy to check that all fermions are gapped out, and the O(4) vector operators $\boldsymbol{N}$ as in Eq. (5.70) remain gapless. Further more, $l_0^\intercal\phi = 0 \mod 2\pi$ implies that any charge vector l_a will be equivalent to $l_a + nl_0$ ($n \in \mathbb{Z}$). As a result, we establish the equivalences $l_1 \sim -l_4$ and $l_2 \sim -l_3$ among the O(4) operators. So under interactions, there are only two independent bosonic modes left on the boundary. Let us choose $l_1^\intercal\phi$ and $l_2^\intercal\phi$ as the bosonic boundary modes, the effective K matrix can be

obtained from the projection $K_{\text{eff}}^{-1} = P^{\intercal} K^{-1} P$ with $P = (l_1, l_2)$. The result is

$$K_{\text{eff}} = \begin{pmatrix} 0 & 1 \\ 1 & 0 \end{pmatrix}, \tag{5.73}$$

which exactly describes the bosonic SPT boundary. [31] According to Eq. (5.70), the physical meaning of the bosonic boundary modes are simply the SDW-XY and SC fluctuations on the boundary,

$$\begin{aligned} e^{\mathrm{i} l_1^{\intercal}\phi} &= \psi_{R1}^{\dagger}\psi_{L1} \sim N^0 - \mathrm{i}N^3 = S^-, \\ e^{\mathrm{i} l_2^{\intercal}\phi} &= \psi_{R1}^{\dagger}\psi_{L2} \sim N^2 - \mathrm{i}N^1 = \Delta^{\dagger}. \end{aligned} \tag{5.74}$$

Then the K_{eff} matrix describes the effect that each 2π vortex of the pairing field $\Delta^{\dagger}$ will trap a spin-1 excitation S^-. This corresponds to the spin Hall conductance $\sigma_{\text{sH}} = 2$, consistent with the bilayer QSH state in the free-fermion limit.

As the gapping term $\cos(l_0^{\intercal}\phi)$ becomes relevant, its scaling dimension Δ_0 will flow to 0 as shown in Fig. 5.5. From Eq. (5.67), $\Delta_0 \to 0$ corresponds to $g_3 \to -1/2$. Substitute the fixed point $g_3 = -1/2$ to Eq. (5.71), we find $\Delta_a = 1/2$, meaning that the scaling dimensions of both the SDW-XY and SC boundary modes are modified to 1/2 under the RG flow, which is consistent with the $\mathrm{SU}(2)_1$ CFT, and it is also described by the IR fixed point of the O(4) NLSM with WZW term at level $k = 1$,[50, 51] as we have claimed in Eq. (5.43),

$$S = \int \mathrm{d}\tau \mathrm{d}x \mathrm{d}u \, \frac{1}{2g}(\partial_\mu \boldsymbol{n})^2 + \frac{\mathrm{i}k}{2\pi}\epsilon_{abcd} n^a \partial_\tau n^b \partial_x n^c \partial_u n^d. \tag{5.75}$$

The O(4) vector field $\boldsymbol{n}$ couples to the fermion bilinear terms $\boldsymbol{N}$ via $H_{\text{cp}} = -\sum_i \boldsymbol{n}_i \cdot \boldsymbol{N}_i$ as mentioned in Eq. (5.45), such that $\boldsymbol{n} \sim \boldsymbol{N}$ in terms of symmetry properties. Therefore according to Eq. (5.74), $\boldsymbol{n}$ is related to the bonsonization field ϕ via $n^0 - \mathrm{i}n^3 \sim e^{\mathrm{i} l_1^{\intercal}\phi}$ and

$n^2 - \mathrm{i}n^1 \sim e^{\mathrm{i}l_2^{\mathrm{T}}\phi}$. Such a connection becomes more evident if we note that the WZW term requires each 2π soliton of $n^2 - \mathrm{i}n^1$ (winding of the complex field $n^2 - \mathrm{i}n^1$ along x by 2π phase) should carry one unite of charge that is conjugate to $n^0 - \mathrm{i}n^3$. This topological response is nothing but the commutation relation $[l_1^{\mathrm{T}}\phi(x_1), \partial_x l_2^{\mathrm{T}}\phi(x_2)] = 2\pi\mathrm{i}\delta(x_1 - x_2)$ in the canonical quantization language, as required by the K_{eff} matrix in Eq. (5.73). So the K_{eff} matrix and the WZW term describe the same topological phenomenon.

Similar Luttinger liquid analysis for the helical edge modes was carried out in Ref. [253] under a lower symmetry, where the boundary can be unstable towards spontaneous symmetry breaking. In that case, the boundary bosonic modes are gapped out by symmetry breaking, however the bulk state still corresponds to a bosonic SPT state.

In conclusion, the interaction we designed can gap out all the fermions on the boundary and change the scaling dimension of the bosonic modes to that of the CFT $\mathrm{SU}(2)_1$, so that the interacting bilayer QSH model has no low-energy fermion both in the bulk and on the boundary, i.e. it becomes a real bosonic SPT state. More importantly, the interaction $-U\sum_i \boldsymbol{M}_i \cdot \boldsymbol{M}_i$ admits sign-free QMC simulations, providing us powerful numerical tools to study the O(4) bosonic SPT phase and its transition to the trivial SPT phase. The fate of the boundary modes can also be investigated by QMC.

5.3.2 Large-N Generalization

5.3.2.1 Bulk Theory

Model and Symmetry The bilayer QSH model can be generalized to $2N$ layers by simply making more identical copies. On each site i, we define $4N$ fermions $c_{i\ell\sigma}$ with the layer index $\ell = 1, 2, \cdots, 2N$ and the spin index $\sigma = \uparrow, \downarrow$. Consider the following

interacting fermion model,

$$\begin{aligned} H =& H_{\text{band}} + H_{\text{int}} \\ H_{\text{band}} =& -t \sum_{\langle ij\rangle,\ell} c^\dagger_{i\ell} c_{j\ell} + \sum_{\langle\langle ij\rangle\rangle,\ell} \mathrm{i}\lambda_{ij} c^\dagger_{i\ell}\sigma^z c_{j\ell} + H.c. \\ H_{\text{int}} =& -U \sum_i \boldsymbol{M}_i \cdot \boldsymbol{M}_i, \end{aligned} \tag{5.76}$$

where $\boldsymbol{M}_i$ follows the similar definitions in Eq. (5.38) as

$$M_i^- = 2(-)^i \sum_{\ell\in\text{odd}} c_{i,\ell} c^\dagger_{i,\ell+1},\ M_i^3 = \sum_\ell (-)^{i+\ell} c^\dagger_{i\ell}\sigma^z c_{i\ell}. \tag{5.77}$$

Following a similar transformation as in Eq. (5.33), we can switch to the more convenient f-fermion basis. The band Hamiltonian still takes the same form as Eq. (5.34)

$$H_{\text{band}} = \sum_{i,j,\sigma} (-)^\sigma f^\dagger_{i\sigma}(-t_{ij} + \mathrm{i}\lambda_{ij}) f_{j\sigma} + h.c., \tag{5.78}$$

but $f_{i\sigma}$ are now $\mathrm{Sp}(N)$ multiplets. The model has a $\mathrm{Sp}(N)_\uparrow \times \mathrm{Sp}(N)_\downarrow \times \mathrm{SU}(2)$ symmetry. The fermions transform as $f_{i\sigma} \to S_\sigma f_{i\sigma}$ with $S_\sigma \in \mathrm{Sp}(N)_\sigma$ for $\sigma = \uparrow, \downarrow$. For each spin σ, the symplectic form is defined by an antisymmetric real matrix J_σ, such that

$$S_\sigma^\intercal J_\sigma S_\sigma = J_\sigma \text{ with } J_\sigma^\intercal = -J_\sigma. \tag{5.79}$$

The $\mathrm{SU}(2) \simeq \mathrm{SO}(3)$ symmetry rotates the fermion bilinear operators $\boldsymbol{M}_i = (M_i^1, M_i^2, M_i^3)$ as an O(3) vector. Let $M_i^\pm = M_i^1 \pm \mathrm{i} M_i^2$, the definition of $\boldsymbol{M}_i$ follows form

$$M_i^- = \sum_\sigma f^\intercal_{i\sigma} J_\sigma f_{i\sigma},\ M_i^3 = (-)^i \sum_\sigma (-)^\sigma f^\dagger_{i\sigma} f_{i\sigma}, \tag{5.80}$$

and $M_i^+ = (M_i^-)^\dagger$. The SU(2) generators are therefore defined as $\boldsymbol{Q} = \sum_i \boldsymbol{Q}_i$ with

$Q_i^a = \frac{1}{2\mathrm{i}}\epsilon_{abc}M_i^b M_i^c$. Let $Q_i^{\pm} = Q_i^1 \pm \mathrm{i}Q_i^2$, we can write down the SU(2) charges on each site explicitly

$$\begin{aligned} Q_i^- &= (-)^i \sum_\sigma (-)^\sigma f_{i\sigma}^\intercal J_\sigma f_{i\sigma}, \\ Q_i^3 &= \sum_\sigma (f_{i\sigma}^\dagger f_{i\sigma} - N), \end{aligned} \tag{5.81}$$

and $Q_i^+ = (Q_i^-)^\dagger$. The 3rd component of the global SU(2) charge $Q^3 = \sum_i Q_i^3$ is the total number of f-fermions in the system (counted with respect to half-filling), which is obviously conserved by the Hamiltonian H_{band} in Eq. (5.78). It can be further verified that $Q^{\pm}$ are also conserved, as $[H_{\text{band}}, \boldsymbol{Q}] = 0$. Therefore the free fermion model H_{band} has the $\mathrm{Sp}(N)_\uparrow \times \mathrm{Sp}(N)_\downarrow \times \mathrm{SU}(2)$ symmetry.

Realizing Bosonic SPT Phases We propose that the following on-site interaction can turn the $2N$-layer QSH system into a $\mathrm{Sp}(N) \times \mathrm{Sp}(N)$ bosonic SPT state,

$$H_{\text{int}} = -U \sum_i \boldsymbol{M}_i \cdot \boldsymbol{M}_i. \tag{5.82}$$

This interaction preserves the $\mathrm{Sp}(N)_\uparrow \times \mathrm{Sp}(N)_\downarrow \times \mathrm{SU}(2)$ symmetry. Tuned by the interaction strength U, the model has two phases: in the weak interaction regime, the model is in a $\mathrm{Sp}(N)_\uparrow \times \mathrm{Sp}(N)_\downarrow$ (bosonic) SPT phase. In the strong interaction regime, the model is in a trivial Mott phase.

In the next subsection we will show that the boundary states at the weakly interacting regime is the CFT $\mathrm{Sp}(N)_1$, without any gapless fermion mode. Thus the bulk theory is a $\mathrm{Sp}(N)$ principal chiral model with a $\Theta-$term at $\Theta = 2\pi$,

$$S = \int \mathrm{d}\tau \mathrm{d}^2x \frac{1}{g} \mathrm{Tr}' \partial_\mu S^{-1} \partial_\mu S + \frac{\mathrm{i}\Theta}{24\pi^2} \epsilon^{\mu\nu\lambda} \mathrm{Tr}' \mathcal{A}_\mu \mathcal{A}_\nu \mathcal{A}_\lambda, \tag{5.83}$$

with $\mathcal{A}_\mu = S^{-1}\partial_\mu S$ for $S \in \mathrm{Sp}(N)$, which describes the $\mathrm{Sp}(N)_\uparrow \times \mathrm{Sp}(N)_\downarrow$ bosonic SPT phase.

In the strong interaction limit $U \to \infty$, the Hamiltonian is decoupled on each site. The on-site interaction $-U\boldsymbol{M}_i \cdot \boldsymbol{M}_i$ can be exact diagonalized. We found that the on-site ground state is unique. Its energy is $E_{\mathrm{GS}} = -4N(N+2)U$ (per site), and its wave function is

$$|\mathrm{GS}_i\rangle = \sum_{q=0}^{N} \alpha_q (Q_i^+)^q (M_i^+)^{N-q} |0\rangle_f ,$$
$$\text{with } \alpha_q = \begin{cases} \frac{1}{q+1}\binom{N}{q} & q \in \text{even}, \\ 0 & q \in \text{odd}, \end{cases} \tag{5.84}$$

where $\binom{N}{q} \equiv \frac{N!}{q!(N-q)!}$ is the binomial coefficient and $|0\rangle_f$ denotes the zero fermion state of f-fermions. So the ground state of the whole system is simply a direct product state of on-site ground states

$$|\mathrm{GS}\rangle = \prod_i |\mathrm{GS}_i\rangle . \tag{5.85}$$

It is easy to see that $|\mathrm{GS}_i\rangle$ is $\mathrm{Sp}(N)_\uparrow \times \mathrm{Sp}(N)_\downarrow$ symmetric, because Q_i^+, M_i^+ and $|0\rangle_f$ are all invariant under $\mathrm{Sp}(N)_\uparrow \times \mathrm{Sp}(N)_\downarrow$ transformations. One can further verify that $|\mathrm{GS}_i\rangle$ also preserves the SU(2) symmetry by checking that $\boldsymbol{Q}_i |\mathrm{GS}_i\rangle = 0$. Thus the ground state is fully symmetric. Upon the ground state, the single particle excitation energy is $(4N+5)U$, the O(3) excitation energy is $8U$ and the $\mathrm{Sp}(N)$ excitation energy is $(8N+4)U$. All the fermionic and bosonic excitations are gapped from the ground state. Therefore the ground state describes a trivial (featureless) Mott insulator. Because the ground state is unique and fully gapped, it should be stable against any local perturbation. So we expect a stable phase of the trivial Mott insulator in the large U regime.

On the field theory level, the trivial Mott phase corresponds to the $\Theta = 0$ fixed point

of the Sp(N) principal chiral model in Eq. (5.83). If there is a single continuous transition between the small-U SPT phase and the large-U trivial Mott phase, it must be described by the Sp(N) principal chiral model at $\Theta = \pi$. The phase diagram and the possible criticality can be numerically studied by QMC without fermion sign problem. Because the interaction term can still be decoupled in the O(3) vector channel by introducing the auxiliary field $\boldsymbol{m}_i$ as in Eq. (5.50). The resulting Hamiltonian $H[\boldsymbol{m}_i]$ still has the time-reversal symmetry in Eq. (5.51), which ensures the Boltzmann weight $W[\boldsymbol{m}_i(\tau)]$ to be positive definite for any configurations of the auxiliary field $\boldsymbol{m}_i(\tau)$.

5.3.2.2 Boundary Theory

One-Loop RG Without interaction, the boundary of the $2N$-layer QSH insulator hosts $2N$ pairs of counter-propagating fermion modes. The edge mode chirality is locked to the fermion spin: all the $2N$ left (right) moving fermions are of $\uparrow$ ($\downarrow$) spin, forming a Sp$(N)_{L(R)}$ multiplet, denoted by $\psi_{L(R)}$. Thus bulk operators can be mapped to the boundary simply by rewriting $\uparrow \to L$ and $\downarrow \to R$. The boundary theory takes the same form as Eq. (5.53), and is repeated here

$$H_{\text{bdy}} = \int \mathrm{d}x (\psi_L^\dagger \mathrm{i}\partial_x \psi_L - \psi_R^\dagger \mathrm{i}\partial_x \psi_R). \tag{5.86}$$

On the boundary, the O(3) vector $\boldsymbol{M}$ follows from Eq. (5.80) as

$$M^- = \sum_\sigma \psi_\sigma^\intercal J_\sigma \psi_\sigma,\ M^3 = \sum_\sigma (-)^\sigma \psi_\sigma^\dagger \psi_\sigma; \tag{5.87}$$

and the SU(2) charge $\boldsymbol{Q}$ follows from Eq. (5.81) as

$$Q^- = \sum_\sigma (-)^\sigma \psi_\sigma^\intercal J_\sigma \psi_\sigma,\ Q^3 = \sum_\sigma (\psi_\sigma^\dagger \psi_\sigma - N). \tag{5.88}$$

The bulk interaction H_{int} in Eq. (5.82) will induce a short range interaction $H_{\text{int}} = -U' \int \mathrm{d}x \boldsymbol{M}\cdot\boldsymbol{M}$ on the boundary at the UV scale. However under the RG flow, $\int \mathrm{d}x \boldsymbol{Q}\cdot\boldsymbol{Q}$ will be generated. In the $N = 1$ case, the $\boldsymbol{Q}\cdot\boldsymbol{Q}$ term reduces to a linear combination of the $\boldsymbol{M}\cdot\boldsymbol{M}$ and $\boldsymbol{N}\cdot\boldsymbol{N}$ terms, i.e. $\boldsymbol{Q}\cdot\boldsymbol{Q} = \boldsymbol{M}\cdot\boldsymbol{M} - \boldsymbol{N}\cdot\boldsymbol{N} + 4$, which has been included in Eq. (5.55). The one-loop RG analysis is similar for $N > 1$ cases. For the purpose of RG analysis, we start with the most generic $\mathrm{Sp}(N)_L \times \mathrm{Sp}(N)_R \times \mathrm{SU}(2)$ symmetric interaction as follows

$$H_{\text{int}} = \int \mathrm{d}x (\lambda_M \boldsymbol{M}\cdot\boldsymbol{M} + \lambda_Q \boldsymbol{Q}\cdot\boldsymbol{Q}). \tag{5.89}$$

The one-loop RG equations are

$$\begin{aligned} \tfrac{\mathrm{d}}{\mathrm{d}\ell}\lambda_M &= -\tfrac{2}{3}(\lambda_M - \lambda_Q)^2, \\ \tfrac{\mathrm{d}}{\mathrm{d}\ell}\lambda_Q &= \tfrac{2}{3}(\lambda_M - \lambda_Q)^2. \end{aligned} \tag{5.90}$$

Therefore the interaction is marginally relevant when $\lambda_M < \lambda_Q$, and will follow towards the $(\lambda_M, \lambda_Q) \to (-1, +1)$ direction. The fixed point interaction is given by $\lambda_Q = -\lambda_M$ and $\lambda_M \to -\infty$,

$$\begin{aligned} H_{\text{int}} =& \lambda_M (\boldsymbol{M}\cdot\boldsymbol{M} - \boldsymbol{Q}\cdot\boldsymbol{Q}) \\ =& 2\lambda_M \big((\psi_R^\intercal J_R \psi_R)^\dagger (\psi_L^\intercal J_L \psi_L) + h.c. \big) \\ & - 4\lambda_M (\psi_R^\dagger \psi_R - N)(\psi_L^\dagger \psi_L - N). \end{aligned} \tag{5.91}$$

The fixed point interaction only contains the left-right mixing terms. The interactions within the same chiral sector (forward scatterings) will only renormalize the mode velocity, and can be ignored. In the $N = 1$ case, Eq. (5.91) reduces to Eq. (5.60) by $\lambda_\pm = \lambda_3 = 2\lambda_M$ (at the fixed point).

CFT Analysis For each chiral sector, we have the following decomposition of CFT:[254]

$$\mathrm{U}(2N)_1 \simeq \mathrm{O}(4N)_1 \simeq \mathrm{Sp}(N)_1 + \mathrm{SU}(2)_N. \tag{5.92}$$

This means the $\mathrm{U}(2N)_1$ or $\mathrm{O}(4N)_1$ CFT, which is described by $2N$ copies of free complex fermions or $4N$ copies of free Majorana fermions, can be decomposed into the direct sum of two interacting CFT: $\mathrm{Sp}(N)_1$ and $\mathrm{SU}(2)_N$. The validity of this equation can be seen from the central charges of these CFT:

$$c_{\mathrm{Sp}(N)_1} = \frac{N(2N+1)}{N+2}, \quad c_{\mathrm{SU}(2)_N} = \frac{3N}{N+2}, \tag{5.93}$$

the sum of these two gives $2N$, which is the central charge of $\mathrm{U}(2N)_1$ or $\mathrm{O}(4N)_1$.

Therefore the helical fermion CFT can be written in terms of $\mathrm{Sp}(N)$ and $\mathrm{SU}(2)$ current operators as

$$\begin{aligned} H_{\mathrm{bdy}} &= \int \mathrm{d}x\ (T_L + T_R), \\ T_\sigma &= :\psi_\sigma^\dagger \mathrm{i}\partial_x \psi_\sigma: \\ &= \frac{2\pi}{N+2}\big(J^a_{\mathrm{Sp}(N)_\sigma} J^a_{\mathrm{Sp}(N)_\sigma} + J^a_{\mathrm{SU}(2)_\sigma} J^a_{\mathrm{SU}(2)_\sigma}\big), \end{aligned} \tag{5.94}$$

where $\sigma = L, R$. The $\mathrm{Sp}(N)_\sigma$ current operators are given by

$$J^a_{\mathrm{Sp}(N)_\sigma} = :\psi_\sigma^\dagger A^a_\sigma \psi_\sigma:, \tag{5.95}$$

where A^a_σ $(a = 1, 2, \cdots, N(2N+1))$ are the $\mathrm{Sp}(N)_\sigma$ generators, which are properly normalized according to $\mathrm{Tr} A^a_\sigma A^b_\sigma = \frac{1}{2}\delta^{ab}$. The $\mathrm{SU}(2)_\sigma$ current operators are defined as

$$J^-_{\mathrm{SU}(2)_\sigma} = \tfrac{1}{2}(-)^\sigma :\psi_\sigma^\intercal J_\sigma \psi_\sigma:, J^3_{\mathrm{SU}(2)_\sigma} = \tfrac{1}{2} :\psi_\sigma^\dagger \psi_\sigma:, \tag{5.96}$$

such that $J^{1(2)}_{\mathrm{SU}(2)_\sigma} = \mathrm{Re}(\mathrm{Im})J^{-}_{\mathrm{SU}(2)_\sigma}$. The current operators satisfy the Kac-Moody algebra

$$\begin{aligned}
[J^a_{\mathrm{Sp}(N)_\sigma}(x), J^b_{\mathrm{Sp}(N)_\sigma}(y)] =& \mathrm{i} f^{abc}_{\mathrm{Sp}(N)} J^c_{\mathrm{Sp}(N)_\sigma}(x)\delta(x-y) \\
&+ (-)^\sigma \frac{\mathrm{i}\delta^{ab}}{4\pi}\delta'(x-y), \\
[J^a_{\mathrm{SU}(2)_\sigma}(x), J^b_{\mathrm{SU}(2)_\sigma}(y)] =& \mathrm{i} f^{abc}_{\mathrm{SU}(2)} J^c_{\mathrm{SU}(2)_\sigma}(x)\delta(x-y) \\
&+ N(-)^\sigma \frac{\mathrm{i}\delta^{ab}}{4\pi}\delta'(x-y),
\end{aligned} \tag{5.97}$$

where $f_{\mathrm{Sp}(N)}$ and $f_{\mathrm{SU}(2)}$ are $\mathrm{Sp}(N)$ and $\mathrm{SU}(2)$ structure factors respectively.

The fixed point interaction H_{int} in Eq. (5.91) can be written exactly as a back-scattering term of the SU(2) currents

$$H_{\mathrm{int}} = -16\lambda_M J^a_{\mathrm{SU}(2)_R} J^a_{\mathrm{SU}(2)_L}, \tag{5.98}$$

because this term is marginally relevant, it will gap out the $\mathrm{SU}(2)_N \times \mathrm{SU}(2)_{-N}$ sector completely [178]. The boundary is left with the $\mathrm{Sp}(N)_1 \times \mathrm{Sp}(N)_{-1}$ modes only. The fermion modes at the boundary must also be gapped because the $\mathrm{SU}(2)_N$ sector as collective modes of the fermions are gapped. Hence indeed the interaction we design will drive the boundary of this system to a $\mathrm{Sp}(N)_1$ CFT, and the bulk of the SPT is described by Eq. (5.83).

5.3.3 Summary and Discussion

In this work, we designed a series of interacting fermion model with short-range interaction, and we demonstrated that these models can describe the quantum phase transition between a bosonic SPT state and a trivial Mott insulator state. These bosonic SPT states are described by a $\mathrm{Sp}(N)$ principal chiral model with a $\Theta-$term. These models

can be reliably simulated using determinant QMC algorithm without sign problem. Our previous results [145, 146] already suggest that this SPT-trivial transition is continuous, which corresponds to the case with $N = 1$.

The Sp(N) principal chiral model with $N = 1$, which is also an O(4) NLSM was also used to describe the boundary of $3d$ bosonic SPT states [32, 63]. But in those cases Θ is no longer a tuning parameter, because $\Theta = \pi$ is protected by the symmetry of the system, for instance time-reversal symmetry. Our results also suggest that if there is an exact SO(4) symmetry, the boundary of this SPT state could be a stable $(2 + 1)d$ CFT. But if the SO(4) symmetry is strongly broken down its subgroups, this CFT can be further driven into various topological orders as was discussed in Ref. [32, 63].

Another interesting direction is to design a series of fermion models that would generate the SU(N) principal chiral model with a topological $\Theta-$term. This is a little difficult (though not impossible) to achieve using our method, because the interaction we designed in this paper is based on the Sp(N) $\times$ Sp(N) singlet vector $\boldsymbol{M}$, and because of the properties of the Sp(N) group, its singlet can still be a fermion bilinear operator, thus the interactions in our models are all four-fermion short range interaction. But if we want to generalize our idea to the SU(N) groups, it seems much higher order fermion interaction must be involved because two SU(N) fundamental fermions cannot form a SU(N) singlet in general. We will leave this to future study.

Appendix A

NLσM classifications

A.1 NLσM classification of BSPT phase within group cohomology

A.1.1 Z_2 symmetry

In 1d and 3d, there is no Z_2 symmetry transformation that we can assign vector $\boldsymbol{n}$ that makes the actions Eq. 2.1 and Eq. 2.3 invariant, thus there is no SPT phase in 1d and 3d with Z_2 symmetry. However, in 2d there is obviously one and only one way to assign the Z_2 symmetry:

$$Z_2 : (n_1, n_2, n_3, n_4) \to -(n_1, n_2, n_3, n_4). \tag{A.1}$$

Then when $\Theta = 2\pi$ this 2+1d O(4) NLσM describes the Z_2 SPT phase studied in Ref. [27]. Using the method in section IIC, one can show that with the transformation Eq. A.1, the 2+1d O(4) NLσM Eq. 2.2 with $\Theta = 4\pi$ is equivalent to $\Theta = 0$, thus the classification in 2d is $\mathbb{Z}_2$.

In Ref. [35], the authors also used this NLσM to derive the ground state wave function of the SPT phase:

$$|\Psi\rangle = \sum (-1)^{dw} |C\rangle, \tag{A.2}$$

where $|C\rangle$ standards for an arbitrary Ising field configuration, while dw is the number of Ising domain walls of this configuration. This wave function was also derived in Ref. [27] with an exactly soluble model for this SPT phase.

The classification of SPT phases with Z_2 symmetry is:

$$1d : \mathbb{Z}_1, \quad 2d : \mathbb{Z}_2, \quad 3d : \mathbb{Z}_1. \tag{A.3}$$

Here $\mathbb{Z}_1$ means there is only one trivial state, and $\mathbb{Z}_2$ means there is one trivial state and one nontrivial SPT state.

A.1.2 Z_2^T symmetry

In 2d, there is no way to assign Z_2^T symmetry to the O(4) NLσM order parameter in Eq. 2.2 to make the $\Theta-$term invariant, thus there is no bosonic SPT phase in 2d with Z_2^T symmetry. In 1d and 3d, there is only one way to assign the Z_2^T symmetry to vector $\boldsymbol{n}$:

$$Z_2^T : \boldsymbol{n} \to -\boldsymbol{n}, \tag{A.4}$$

and $\Theta = 0$ and $\Theta = 4\pi$ are equivalent. Thus in both 1d and 3d, the classification is $\mathbb{Z}_2$. Notice that time-reversal is an antiunitary transformation, thus $i \to -i$ under Z_2^T; also since our NLσMs are defined in Euclidean space-time, the Euclidean time $\tau = it$ is

invariant under Z_2^T.

Using the method in section II.F, one can demonstrate that the boundary of the $3d$ SPT state with Z_2^T symmetry is a $2d$ Z_2 topological order, whose both e and m excitations are Kramers doublet, i.e. the so called $eTmT$ state.

The classification of SPT phases with Z_2^T symmetry is:

$$1d : \mathbb{Z}_2, \quad 2d : \mathbb{Z}_1, \quad 3d : \mathbb{Z}_2. \tag{A.5}$$

Now it is understood that in $3d$ there is bosonic SPT state with Z_2^T symmetry that is beyond the group cohomology classification [32], and there is a explicit lattice construction for such state [255]. This state is also beyond our current NLσM description. However, a generalized field theory which involves both the NLσM and Chern-Simons theory can describe at least a large class of BSPT states beyond group cohomology. This will be discussed in a different paper [175].

A.1.3 $U(1)$ symmetry

In 1d and 3d, there is no way to assign U(1) symmetry to vector $\boldsymbol{n}$ that keeps the entire Lagrangian invariant. But in 2d, bosonic SPT phase with U(1) symmetry was discussed in Ref. [28], and its field theory is given by Eq. 2.2. And since in this case we cannot connect $\Theta = 2\pi k$ and $\Theta = 0$ without a bulk transition, the classification is $\mathbb{Z}$.

The classification of SPT phases with $U(1)$ symmetry is:

$$1d : \mathbb{Z}_1, \quad 2d : \mathbb{Z}, \quad 3d : \mathbb{Z}_1. \tag{A.6}$$

A.1.4 SPT phases with $U(1) \rtimes Z_2$ symmetry

$U(1) \rtimes Z_2$ is a subgroup of SO(3). In 1d, there is only one way of assigning the symmetry to vector $\boldsymbol{n}$ that keeps the entire Lagrangian invariant:

$$\begin{aligned} U(1) \quad &: \quad (n_1 + in_2) \to e^{i\theta}(n_1 + in_2), \quad n_3 \to n_3, \\ Z_2 \quad &: \quad n_1 \to n_1, \quad n_{2,3} \to -n_{2,3}. \end{aligned} \tag{A.7}$$

Here Z_2 is a particle-hole transformation of rotor/boson field $b \sim n_1 + in_2$. n_3 can be viewed as the boson density, which changes sign under particle-hole transformation. One can check that the U(1) and Z_2 symmetry defined above do not commute with each other. The boundary state of this 1d SPT phase is given in Eq. 2.6. Under U(1) and Z_2 transformation, the boundary doublet U transforms as

$$U(1) : U \to e^{i\theta\sigma^z/2}U, \quad Z_2 : U \to \sigma^x U. \tag{A.8}$$

In 3d, there is also only one way of assigning the symmetry to the O(5) vector:

$$\begin{aligned} U(1) \quad &: \quad (n_1 + in_2) \to e^{i\theta}(n_1 + in_2), \quad n_b \to n_b, \ b = 3, 4, 5; \\ Z_2 \quad &: \quad n_1 \to n_1, \quad n_b, \to -n_b, \quad b = 2, \cdots 5. \end{aligned} \tag{A.9}$$

In both 1d and 3d, $\Theta = 4\pi$ is equivalent to $\Theta = 0$, thus in both 1d and 3d the classification is $\mathbb{Z}_2$.

In 2d, there are two independent ways of assigning $U(1) \rtimes Z_2$ transformations to the

O(4) vector $\boldsymbol{n}$:

$$\begin{aligned}(1) \quad &: \quad U(1): (n_1+in_2)\to e^{i\theta}(n_1+in_2),\\ &\qquad (n_3+in_4)\to e^{i\theta}(n_3+in_4);\\ &\qquad Z_2: n_1,n_3\to n_1,n_3, \quad n_2,n_4\to -n_2,-n_4;\\ (2) \quad &: \quad U(1): \boldsymbol{n}\to\boldsymbol{n}, \quad Z_2:\boldsymbol{n}\to-\boldsymbol{n}.\end{aligned} \tag{A.10}$$

The transformation (1) contributes $\mathbb{Z}$ classification, while transformation (2) contributes $\mathbb{Z}_2$ classification, *i.e.* in 2d the classification is $\mathbb{Z}\times\mathbb{Z}_2$. *The final classification of SPT phases with* $U(1)\rtimes Z_2$ *symmetry is*:

$$1d:\mathbb{Z}_2, \quad 2d:\mathbb{Z}\times\mathbb{Z}_2, \quad 3d:\mathbb{Z}_2. \tag{A.11}$$

A.1.5 $U(1)\times Z_2$ symmetry

In both 1d and 3d, there is no way of assigning $U(1)\times Z_2$ transformations to vector $\boldsymbol{n}$ that keeps the Θ term invariant. But in 2d, we can construct three root phases:

$$\begin{aligned}(1) \quad &: \quad U(1): (n_1+in_2)\to e^{i\theta}(n_1+in_2),\\ &\qquad (n_3+in_4)\to e^{i\theta}(n_3+in_4);\\ &\qquad Z_2:\boldsymbol{n}\to\boldsymbol{n};\end{aligned}$$

$$
\begin{aligned}
(2) \quad &: \quad U(1) : \boldsymbol{n} \to \boldsymbol{n}, \quad Z_2 : \boldsymbol{n} \to -\boldsymbol{n}; \\
(3) \quad &: \quad U(1) : (n_1 + i n_2) \to e^{i\theta}(n_1 + i n_2), \\
&\qquad\quad n_{3,4} \to n_{3,4}; \\
&\qquad\quad Z_2 : n_{1,2} \to n_{1,2}, \quad n_{3,4} \to -n_{3,4}.
\end{aligned} \tag{A.12}
$$

The first transformation contributes classification $\mathbb{Z}$, while transformations (2) and (3) both contribute classification $\mathbb{Z}_2$, *thus the final classification of SPT phases with* $U(1) \times Z_2$ *symmetry is*:

$$
1d : \mathbb{Z}_1, \quad 2d : \mathbb{Z} \times (\mathbb{Z}_2)^2, \quad 3d : \mathbb{Z}_1. \tag{A.13}
$$

A.1.6 $U(1) \rtimes Z_2^T$ symmetry

A boson operator b with $U(1) \rtimes Z_2^T$ symmetry transforms as $b \to b$ under Z_2^T. In 1d, the only $U(1) \rtimes Z_2^T$ symmetry transformation that keeps Eq. 2.1 invariant is the same transformation as Z_2^T SPT phase, namely vector $\boldsymbol{n}$ does not transform under $U(1)$, but changes sign under Z_2^T.

In 2d, the only transformation that keeps Eq. 2.2 invariant is

$$
\begin{aligned}
U(1) \quad &: \quad (n_1 + i n_2) \to e^{i\theta}(n_1 + i n_2), \ n_{3,4} \to n_{3,4}; \\
Z_2^T \quad &: \quad n_1 \to n_1, \quad n_a \to -n_a (a = 2, 3, 4),
\end{aligned} \tag{A.14}
$$

and this NLσM gives classification $\mathbb{Z}_2$.

The NLσMs for $U(1) \rtimes Z_2^T$ SPT phases in 3d have been discussed in Ref. [32], and in 3d the classification is $(\mathbb{Z}_2)^2$. *Thus the final classification of SPT phases with* $U(1) \rtimes Z_2^T$ *symmetry is*:

$$1d : \mathbb{Z}_2, \quad 2d : \mathbb{Z}_2, \quad 3d : (\mathbb{Z}_2)^2. \tag{A.15}$$

A.1.7 $U(1) \times Z_2^T$ symmetry

In 1d, there are two independent transformations that keep Eq. 2.1 invariant:

$$\begin{aligned}
(1) \quad &: \quad U(1) : (n_1 + in_2) \to e^{i\theta}(n_1 + in_2), \quad n_3 \to n_3; \\
&\qquad Z_2^T : n_{1,2} \to n_{1,2}, \quad n_3 \to -n_3, \\
(2) \quad &: \quad U(1) : \boldsymbol{n} \to \boldsymbol{n}, \\
&\qquad Z_2^T : \boldsymbol{n} \to -\boldsymbol{n}.
\end{aligned} \tag{A.16}$$

In 2d there is no $U(1) \times Z_2^T$ transformation that keeps Eq. 2.2 invariant. In 3d the NLσMs for $U(1) \times Z_2^T$ SPT phases were discussed in Ref. [32]. *The final classification of SPT phases with* $U(1) \times Z_2^T$ *symmetry is*:

$$1d : (\mathbb{Z}_2)^2, \quad 2d : \mathbb{Z}_1, \quad 3d : (\mathbb{Z}_2)^3. \tag{A.17}$$

A.1.8 $Z_2 \times Z_2$ symmetry

In 1d, there is only one $Z_2 \times Z_2$ transformation that keeps Eq. 2.1 invariant:

$$\begin{aligned} Z_2^A &: n_{1,2} \to -n_{1,2}, \quad n_3 \to n_3, \\ Z_2^B &: n_1 \to n_1, \quad n_{2,3} \to -n_{2,3}. \end{aligned} \tag{A.18}$$

The boundary state U defined in Eq. 2.6 transforms as

$$Z_2^A : U \to i\sigma^z U, \quad Z_2^B : U \to \sigma^x U. \tag{A.19}$$

Thus Z_2^A and Z_2^B no longer commute with each other at the boundary.

In 2d, there are three independent $Z_2 \times Z_2$ transformations (three different root phases):

$$\begin{aligned} (1) &: Z_2^A : \boldsymbol{n} \to -\boldsymbol{n}, \quad Z_2^B : \boldsymbol{n} \to \boldsymbol{n}; \\ (2) &: Z_2^A : \boldsymbol{n} \to \boldsymbol{n}, \quad Z_2^B : \boldsymbol{n} \to -\boldsymbol{n}; \\ (3) &: Z_2^A : n_{1,2} \to -n_{1,2}, \quad n_{3,4} \to n_{3,4}; \\ & \quad Z_2^B : n_{1,2} \to n_{1,2}, \quad n_{3,4} \to -n_{3,4}. \end{aligned} \tag{A.20}$$

In 3d, there are also two independent $Z_2 \times Z_2$ transformations that keep Eq. 2.3

invariant (two root phases):

$$\begin{aligned}
(1) \quad : \quad & Z_2^A : n_{1,2} \to -n_{1,2}, \quad n_a \to n_a (a = 3, 4, 5); \\
& Z_2^B : n_1, \to n_1, \quad n_a \to -n_a (a = 2, \cdots 5); \\
(2) \quad : \quad & Z_2^B : n_{1,2} \to -n_{1,2}, \quad n_a \to n_a (a = 3, 4, 5); \\
& Z_2^A : n_1, \to n_1, \quad n_a \to -n_a (a = 2, \cdots 5).
\end{aligned} \tag{A.21}$$

As we discussed in section II.F, the boundary of these 3d SPT phases can have 2d Z_2 topological order. A 2d Z_2 topological phase has e and m anyon excitations, and these anyons correspond to vortices of certain components of order parameter $\boldsymbol{n}$. If the e and m anyons correspond to vortices of (n_3, n_4) and (n_1, n_2) respectively, then according to Eq. 2.20, the e excitation corresponds to a $0+1d$ O(3) WZW model for vector (n_1, n_2, n_5), and the m excitation corresponds to a $0 + 1d$ WZW model for vector (n_3, n_4, n_5). The boundary anyons of phase (1) transform as:

$$\begin{aligned}
(1) \quad : \quad & Z_2^A : U_e \to i\sigma^z U_e, \quad U_m \to U_m; \\
& Z_2^B : U_e \to \sigma^x U_e, \quad U_m \to i\sigma^y U_m^*.
\end{aligned} \tag{A.22}$$

Notice that under Z_2^B, a vortex of (n_1, n_2) becomes an antivortex, thus the transformation of U_m under Z_2^B involves a complex conjugation. The transformation of boundary anyons of phase (2) is the same as Eq. A.22 after interchanging Z_2^A and Z_2^B.

The final classification of SPT phases with $Z_2 \times Z_2$ symmetry is:

$$1d : \mathbb{Z}_2, \quad 2d : (\mathbb{Z}_2)^3, \quad 3d : (\mathbb{Z}_2)^2. \tag{A.23}$$

A.1.9 $Z_2 \times Z_2^T$ symmetry

In 1d and 3d, the SPT phases with $Z_2 \times Z_2^T$ symmetry are simply SPT phases with $U(1) \times Z_2^T$ symmetry after reducing U(1) to its subgroup Z_2. The classification is the same as the $U(1) \times Z_2^T$ SPT phases discussed in the previous subsection. In 2d, there are two different root phases that correspond to the following transformations:

$$\begin{aligned}
(1) \quad : \quad & Z_2 : n_{1,2} \to -n_{1,2}, \quad n_{3,4} \to n_{3,4}, \\
& Z_2^T : n_1 \to n_1, \quad n_a \to -n_a (a = 2, 3, 4); \\
(2) \quad : \quad & Z_2 : \boldsymbol{n} \to -\boldsymbol{n}, \\
& Z_2^T : n_1 \to n_1, \quad n_a \to -n_a (a = 2, 3, 4).
\end{aligned} \tag{A.24}$$

The final classification of SPT phases with $Z_2 \times Z_2^T$ symmetry is:

$$1d : (\mathbb{Z}_2)^2, \quad 2d : (\mathbb{Z}_2)^2, \quad 3d : (\mathbb{Z}_2)^3. \tag{A.25}$$

A.1.10 Z_m symmetry

In 1d and 3d, there are no nontrivial Z_m transformations that can keep Eq. 2.1 and Eq. 2.3 invariant. In 2d, we can construct the following root phase:

$$\begin{aligned} Z_m \quad : \quad & (n_1 + in_2) \to e^{i2\pi k/m}(n_1 + in_2); \\ & (n_3 + in_4) \to e^{i2\pi k/m}(n_3 + in_4), \\ & k = 0, \cdots m-1 \end{aligned} \tag{A.26}$$

Using the method in section II, we can demonstrate that with these transformations, Eq. 2.2 with $\Theta = 2\pi m$ and $\Theta = 0$ are equivalent to each other, thus the classification is $\mathbb{Z}_m$ in 2d.

The final classification of SPT phases with Z_m symmetry is:

$$1d : \mathbb{Z}_1, \quad 2d : \mathbb{Z}_m, \quad 3d : \mathbb{Z}_1. \tag{A.27}$$

A.1.11 $Z_m \rtimes Z_2$ symmetry

In 1d, there is one SPT phase with $U(1) \rtimes Z_2$ symmetry. Naively one would expect that when U(1) is broken down to Z_m, this SPT phase survives and becomes a SPT phase with $Z_m \rtimes Z_2$ symmetry. However, this statement is only true for even m, and when m is odd the $U(1) \rtimes Z_2$ SPT phase becomes trivial once U(1) is broken down to Z_m.

The 1d $U(1) \rtimes Z_2$ SPT phase is described by a 1d O(3) NLσM of vector $\boldsymbol{n}$ with $\Theta = 2\pi$, and $B \sim (n_1 + in_2)$ is a charge-1 boson under the U(1) rotation. Because the classification of 1d $U(1) \rtimes Z_2$ SPT phase is $\mathbb{Z}_2$, $\Theta = 2\pi$ is equivalent to $\Theta = 2\pi m$ for odd

m. As we discussed in section IID, this NLσM with $\Theta = 2\pi m$ is equivalent to another NLσM defined with $\boldsymbol{n}'$ and $\Theta = 2\pi$, where $B' \sim (n_1' + in_2') \sim (n_1 + in_2)^m$ is a charge-m boson. Under Z_2 transformation, $n_1' \to n_1'$, $n_2' \to -n_2'$.

Now let us break U(1) down to its subgroup Z_m. B' transforms trivially under Z_m, thus we are allowed to turn on a Zeeman term $\mathrm{Re}[B'] \sim n_1'$ which fully polarizes n_1' and kills the SPT phase. Thus the original $U(1) \rtimes Z_2$ SPT phase is instable under U(1) to Z_m breaking with odd m.

The discussion above is very abstract, let us understand this result physically, and we will take $m = 3$ as an example. With a full SO(3) symmetry and $\Theta = 2\pi$ in the bulk, the ground state of the boundary is a spin-1/2 doublet in Eq. 2.6. The excited states of the boundary include a spin-3/2 quartet. When $\Theta = 6\pi$ in the bulk, the boundary ground state is a spin-3/2 quartet. The spin-3/2 and spin-1/2 states can have a boundary transition (level crossing at the boundary) without closing the bulk gap, thus $\Theta = 2\pi$ and 6π are equivalent in the bulk. Now let us take $\Theta = 6\pi$ in the bulk, and break the SO(3) down to $Z_3 \rtimes Z_2$. Then we are allowed to turn on a perturbation $\cos(3\phi)$ at the boundary (which precisely corresponds to the Zeeman coupling $\mathrm{Re}[B'] \sim n_1'$ discussed in the previous paragraph), which will mix and split the two states $S^z = \pm 3/2$ at the boundary, and the boundary ground state can become nondegenerate. Thus when m is odd, the $U(1) \rtimes Z_2$ SPT phase does not survive the symmetry breaking from U(1) to Z_m.

The same situation occurs in 2d and 3d. There is a 3d SPT phase with $U(1) \rtimes Z_2$ symmetry, but once we break the U(1) down to Z_m, this SPT phase does not survive when m is odd. When m is even, besides the phase deduced from $U(1) \rtimes Z_2$ SPT phase, one can construct another root phase:

$$Z_2 \quad : \quad n_{1,2} \to -n_{1,2}, \quad n_a \to n_a \ (a = 3, 4, 5);$$

$$Z_m \;:\; n_1, \to n_1, \;\; n_a \to (-1)^k n_a \; (a = 2, \cdots 5),$$

$$k = 0, \cdots m-1. \tag{A.28}$$

Here $n_a (a = 2, \cdots 5)$ still carries a nontrivial representation of Z_m for even integer m. n_a with $a = 3, 4, 5$ can be viewed as the real parts of charge-$m/2$ bosons, while n_2 is the imaginary part of such charge-$m/2$ boson. This construction does not apply for odd m.

In 2d, for arbitrary $m > 1$, the $U(1) \rtimes Z_2$ SPT phases survive under $U(1)$ to Z_m symmetry breaking. With even m, another root phase can be constructed

$$Z_m \;:\; n_{1,2} \to (-1)^k n_{1,2}, \;\; n_{3,4} \to n_{3,4};$$

$$Z_2 \;:\; n_{1,2} \to n_{1,2}, \;\; n_{3,4} \to -n_{3,4},$$

$$k = 0, \cdots m-1. \tag{A.29}$$

Here n_1 and n_2 are both the real parts of the charge-$m/2$ bosons.

The final classification of SPT phases with $Z_m \rtimes Z_2$ symmetry is:

$$1d : \mathbb{Z}_{(2,m)}, \quad 2d : \mathbb{Z}_m \times \mathbb{Z}_2 \times \mathbb{Z}_{(2,m)}, \quad 3d : (\mathbb{Z}_{(2,m)})^2. \tag{A.30}$$

A.1.12 $Z_m \times Z_2$ symmetry

The case $m = 2$ has already been discussed. When $m > 2$, one would naively expect these SPT phases can be interpreted as $U(1) \times Z_2$ SPT phases after breaking U(1) to its Z_m subgroup, but again this is not entirely correct. In 1d there is no SPT phase with $U(1) \times Z_2$ symmetry, simply because we cannot find a nontrivial transformation of $\boldsymbol{n}$

under $U(1) \times Z_2$ that keeps Eq. 2.1 invariant. But when m is an even number, we can construct one SPT phase with $Z_m \times Z_2$ symmetry using Eq. 2.1:

$$\begin{aligned} Z_m \quad &: \quad n_{1,2} \to (-1)^k n_{1,2}, \quad n_3 \to n_3, \\ Z_2 \quad &: \quad n_1 \to n_1, \quad n_{2,3} \to -n_{2,3}, \\ & k = 0, \cdots m-1. \end{aligned} \tag{A.31}$$

The Z_m and Z_2 transformations on $\boldsymbol{n}$ commute with each other.

Again this construction applies to even integer m only. The boundary states of this 1d SPT phase have the following transformations:

$$\begin{aligned} Z_m \quad &: \quad U \to (i\sigma^z)^k U, \quad Z_2 : U \to \sigma^x U; \\ & k = 0, \cdots m-1. \end{aligned} \tag{A.32}$$

Thus the boundary states carry projective representations of $Z_m \times Z_2$, and the transformations of Z_m and Z_2 do not commute.

Similar situations occur in 3d. In 3d, we can construct two root phases for even m, even though there is no SPT phase with $U(1) \times Z_2$ symmetry in 3d :

$$\begin{aligned} (1) \quad &: \quad Z_m : n_{1,2} \to (-1)^k n_{1,2}, \quad n_a \to n_a (a = 3,4,5); \\ & Z_2 : n_1, \to n_1, \quad n_a \to -n_a \ (a = 2, \cdots 5); \end{aligned}$$

$$
\begin{aligned}
(2) \quad : \quad & Z_2 : n_{1,2} \to -n_{1,2}, \quad n_a \to n_a (a = 3, 4, 5); \\
& Z_m : n_1, \to n_1, \quad n_a \to (-1)^k n_a (a = 2, \cdots 5); \\
& k = 0, \cdots m - 1.
\end{aligned} \tag{A.33}
$$

The boundary of these 3d SPT phases can have 2d Z_2 topological order. If the e and m anyons correspond to vortices of (n_3, n_4) and (n_1, n_2) respectively, then the boundary anyons of phase (1) transform as:

$$
\begin{aligned}
(1) \quad : \quad & Z_m : U_e \to (i\sigma^z)^k U_e, \quad U_m \to U_m; \\
& Z_2 : U_e \to \sigma^x U_e, \quad U_m \to i\sigma^y U_m^*.
\end{aligned} \tag{A.34}
$$

The transformation of boundary anyons of phase (2) can be derived in the same way.

In 2d all the $Z_m \times Z_2$ SPT phases can be deduced from $U(1) \times Z_2$ SPT phases, by breaking U(1) down to its Z_m subgroup. Thus cases (1), (2) and (3) in Eq. A.12 seem to reduce to SPT phases with $Z_m \times Z_2$ symmetry after breaking U(1) down to Z_m. However, case (3) in Eq. A.12 becomes the trivial phase when m is odd. In case (3) of $U(1) \times Z_2$ SPT phase (Eq. A.12), the NLσM is constructed with a charge-1 boson $B \sim (n_1 + in_2)$, and because case (3) contributes classification $\mathbb{Z}_2$, $\Theta = 2\pi m$ is equivalent to $\Theta = 2\pi$ for odd m. Also, the NLσM with $\Theta = 2\pi m$ is equivalent to the NLσM with $\Theta = 2\pi$ constructed using a charge-m boson $B' \sim (n_1' + in_2') \sim (n_1 + in_2)^m$. Now let us break the U(1) symmetry down to Z_m. Because B' is invariant under Z_m and Z_2, we can turn on a linear Zeeman term that polarizes $\mathrm{Re}[B'] \sim n_1'$, and destroy the boundary states. Thus the NLσM constructed with the charge-m boson B' is trivial once we break U(1) down

to Z_m. This implies that when m is odd, case (3) in Eq. A.12 becomes a trivial phase once U(1) is broken down to Z_m.

The final classification of SPT phases with $Z_m \times Z_2$ symmetry is:

$$1d : \mathbb{Z}_{(2,m)}, \quad 2d : \mathbb{Z}_m \times \mathbb{Z}_2 \times \mathbb{Z}_{(2,m)}, \quad 3d : (\mathbb{Z}_{(2,m)})^2. \tag{A.35}$$

A.1.13 SPT phases with $Z_m \rtimes Z_2^T$ symmetry

Again, the situation depends on the parity of m. If m is odd, then in 1d and 3d the only SPT phase is the SPT phase with Z_2^T only. In 2d and 3d the $U(1) \rtimes Z_2^T$ SPT phases (except for the one with Z_2^T symmetry only) do not survive when U(1) is broken down to Z_m with odd m. The reason is similar to what we discussed in the previous two subsections.

When m is even, then in 1d besides the Haldane phase with Z_2^T symmetry, we can construct another SPT phase:

$$\begin{aligned} Z_m \quad &: \quad n_{1,2} \to (-1)^k n_{1,2}, \quad n_3 \to n_3, \\ & \\ & k = 0, \cdots m-1; \\ & \\ Z_2^T \quad &: \quad \boldsymbol{n} \to -\boldsymbol{n}. \end{aligned} \tag{A.36}$$

Here n_1 and n_2 are both imaginary parts of charge-$m/2$ bosons. The boundary state is a Kramers doublet and transforms as

$$Z_m \quad : \quad U \to (i\sigma^z)^k U, \quad Z_2^T : U \to i\sigma^y U;$$

$$k = 0, \cdots m-1. \tag{A.37}$$

In 2d, we can construct two different root phases:

$$\begin{aligned}
(1) \qquad & Z_m : (n_1 + in_2) \to (n_1 + in_2) e^{i2\pi k/m}, \\
& n_3, n_4 \to n_3, n_4; \\
& Z_2^T : n_1 \to n_1, \quad n_a \to -n_a (a = 2, 3, 4); \\
(2) \qquad & Z_m : \boldsymbol{n} \to (-1)^k \boldsymbol{n}; \\
& Z_2^T : n_1 \to n_1, \quad n_a \to -n_a (a = 2, 3, 4); \\
& k = 0, \cdots m-1.
\end{aligned} \tag{A.38}$$

Phase (1) is the same phase as the 2d $U(1) \rtimes Z_2^T$ SPT phase, after breaking U(1) to Z_m; phase (2) is a new phase, where n_1 is the real part of a charge-$m/2$ boson, while $n_{2,3,4}$ are the imaginary parts of such charge-$m/2$ bosons.

Using similar methods, we can construct three root phases in 3d for even m. Two of the phases can be deduced from the 3d $U(1) \rtimes Z_2^T$ SPT phases. The third root phase has the following transformation:

$$\begin{aligned}
Z_m \quad &: \quad n_{1,2} \to (-1)^k n_{1,2}, \quad n_a \to n_a (a = 3, 4, 5); \\
Z_2^T \quad &: \quad \boldsymbol{n} \to -\boldsymbol{n};
\end{aligned}$$

$$k = 0, \cdots m-1. \tag{A.39}$$

Both n_1 and n_2 are imaginary parts of charge-$m/2$ bosons.

Just like the 3d SPT phase with $U(1) \rtimes Z_2^T$ symmetry, the 2d boundary of the 3d $Z_m \rtimes Z_2^T$ SPT phase described by Eq. A.39 can have a Z_2 topological order with electric and magnetic anyons. The electric and magnetic anyons are both Kramers doublet, and only one of them has a nontrivial transformation under Z_m: $Z_m : U \to (i\sigma^z)^k U$, $(k = 0, \cdots m-1)$.

The final classification of SPT phases with $Z_m \rtimes Z_2^T$ symmetry is:

$$1d : \mathbb{Z}_2 \times \mathbb{Z}_{(2,m)}, \quad 2d : (\mathbb{Z}_{(2,m)})^2, \quad 3d : \mathbb{Z}_2 \times (\mathbb{Z}_{(2,m)})^2. \tag{A.40}$$

A.1.14 $Z_m \times Z_2^T$ symmetry

In 1d and 3d, the SPT phases with $Z_m \times Z_2^T$ symmetry can all be deduced from $U(1) \times Z_2^T$ symmetry by breaking U(1) down to Z_m. Again, when m is odd, some of the SPT phases become trivial, for the same reason as what we discussed before.

In 2d there is no SPT phase with $U(1) \times Z_2^T$ symmetry, but when m is even we can construct two root phases, which *cannot* be deduced from $U(1) \times Z_2^T$ SPT phases:

$$(1) \quad : \quad Z_m : \boldsymbol{n} \to (-1)^k \boldsymbol{n};$$

$$Z_2^T : n_1 \to n_1, \quad n_a \to -n_a (a = 2, 3, 4);$$

$$(2) \quad : \quad Z_m : n_{1,2} \to (-1)^k n_{1,2}, \quad n_{3,4} \to n_{3,4};$$

$$Z_2^T : n_1 \to n_1, \quad n_a \to -n_a (a = 2, 3, 4);$$

$$k = 0, \cdots m - 1. \tag{A.41}$$

The final classification of SPT phases with $Z_m \times Z_2^T$ symmetry is:

$$1d : \mathbb{Z}_2 \times \mathbb{Z}_{(2,m)}, \quad 2d : (\mathbb{Z}_{(2,m)})^2, \quad 3d : \mathbb{Z}_2 \times (\mathbb{Z}_{(2,m)})^2. \tag{A.42}$$

A.1.15 $SO(3)$ symmetry

In 1d, the SO(3) symmetry leads to the Haldane phase, which is described by Eq. 2.1 with $\Theta = 2\pi$. In 3d, there is no way to assign SO(3) symmetry to the five-component vector $\boldsymbol{n}$ which makes the $\Theta-$term invariant, thus there is no 3d SPT phase with SO(3) symmetry.

In 2d, Ref. [30] has given a nice way of describing SPT phase with SO(3) symmetry, which is a principal chiral model defined with group elements $SO(3)$. We will argue that the SO(3) principal chiral model in Ref. [30] can be formally rewritten as the O(4) NLσM Eq. 2.2, because we can represent every group element G_{ab} (3×3 orthogonal matrix) as a SU(2) matrix $\mathcal{Z}$:

$$G_{ab} = \frac{1}{2}\mathrm{tr}[\mathcal{Z}^\dagger \sigma^a \mathcal{Z} \sigma^b], \tag{A.43}$$

and the SU(2) matrix $\mathcal{Z}$ is equivalent to an O(4) vector $\boldsymbol{n}$ with unit length: $\mathcal{Z} = n^4 I_{2\times 2} + i\boldsymbol{n} \cdot \boldsymbol{\sigma}$. We propose that the minimal SO(3) SPT phase discussed in Ref. [30] can be effectively described by Eq. 2.2 with $\Theta = 8\pi$:

$$\mathcal{S}_{2d} = \int d^2x d\tau \, \frac{1}{g}(\partial_\mu \boldsymbol{n})^2 + \frac{i8\pi}{12\pi^2}\epsilon_{abcd}\epsilon_{\mu\nu\rho} n^a \partial_\mu n^b \partial_\nu n^c \partial_\rho n^d$$

$$= \int d^2x d\tau \ \frac{1}{g}\mathrm{tr}[\partial_\mu \mathcal{Z}^\dagger \partial_\mu \mathcal{Z}] + \frac{i8\pi}{24\pi^2}\mathrm{tr}[(\mathcal{Z}^\dagger d\mathcal{Z})^3]. \tag{A.44}$$

Physically, Eq. A.44 with $\Theta = 8\pi$ gives SU(2) Hall conductivity $\sigma_{SU(2)} = 8$, or equivalently SO(3) Hall conductivity $\sigma_{SO(3)} = 2$, which is the same as the principal chiral model in Ref. [30]. Mathematically, when field $\mathcal{Z}$ has a instanton number $\int d^3x \ \mathrm{tr}[(\mathcal{Z}^\dagger d\mathcal{Z})^3]/(24\pi^2) = +1$ in the 2+1d space-time, the SO(3) matrix field G_{ab} defined in Eq. A.43 will have instanton number $\int d^3x \ \mathrm{tr}[(G^{-1}dG)^3]/(24\pi^2) = +4$. This factor of 4 is precisely why $\Theta = 8\pi$ in Eq. A.44.

In order to represent G_{ab} as $\mathcal{Z}$, we need to introduce a Z_2 gauge field that couples to $\mathcal{Z}$, because $\mathcal{Z}$ is a "fractional" representation of G_{ab}, and G_{ab} is invariant under gauge transformation $\mathcal{Z} \to -\mathcal{Z}$. In the language of lattice gauge theory, our statement in the previous paragraph implies that one of the possible confined phases of this Z_2 gauge field is trivial in the bulk without any extra symmetry breaking or topological degeneracy, namely the vison (a dynamical Z_2 $\pi-$flux coupled to $\mathcal{Z}$) in the bulk can condensed without breaking any symmetry. This is indeed possible, because if we weakly break the SU(2) symmetry down to U(1), Eq. A.44 describes a bosonic integer quantum Hall state with Hall conductivity 8. A $\pi-$flux in this system carries charge 4, which can be fully screened by four bosons, while maintaining its bosonic statistics. Thus a vison can safely condense in the bulk, confine the field $\mathcal{Z}$, and drive the system into a SO(3) SPT phase.

The final classification of SPT phases with SO(3) symmetry is:

$$1d : \mathbb{Z}_2, \quad 2d : \mathbb{Z}, \quad 3d : \mathbb{Z}_1. \tag{A.45}$$

A.1.16 $SO(3) \times Z_2^T$ symmetry

In 1d, there are two different SPT root phases with $SO(3) \times Z_2^T$ symmetry, which correspond to the following transformations of O(3) vector $\boldsymbol{n}$:

$$\begin{aligned} (1) \quad &: \quad SO(3) : n_a \to G_{ab} n_b, \quad Z_2^T : \boldsymbol{n} \to -\boldsymbol{n}; \\ (2) \quad &: \quad SO(3) : \boldsymbol{n} \to \boldsymbol{n}, \quad Z_2^T : \boldsymbol{n} \to -\boldsymbol{n}. \end{aligned} \tag{A.46}$$

In 2d, the SPT phases with $SO(3) \times Z_2^T$ symmetry were discussed in Ref. [34], and it is described by Eq. 2.2 with transformation

$$\begin{aligned} SO(3) \quad &: \quad n_a \to G_{ab} n_b (a, b = 1, 2, 3), \quad n_4 \to n_4; \\ Z_2^T \quad &: \quad n_a \to n_a (a = 1, 2, 3), \quad n_4 \to -n_4. \end{aligned} \tag{A.47}$$

In 3d, there are three root phases for $SO(3) \times Z_2^T$ SPT phases, two of which have the following field theory:

$$\begin{aligned} (1) \quad &: \quad SO(3) : \boldsymbol{n} \to \boldsymbol{n}, \quad Z_2^T : \boldsymbol{n} \to -\boldsymbol{n}; \\ (2) \quad &: \quad SO(3) : n_a \to G_{ab} n_b (a, b = 1, 2, 3), \quad n_{4,5} \to n_{4,5} \\ & \quad Z_2^T : \boldsymbol{n} \to -\boldsymbol{n}; \end{aligned} \tag{A.48}$$

phase (1) is simply the SPT phase with Z_2^T symmetry only. After we break the SO(3) symmetry down to its inplane O(2) subgroup, phase (2) will reduce to a SPT phase with

$U(1) \times Z_2^T$ symmetry discussed in Ref. [32], which is a phase whose bulk vortex line is a 1d Haldane phase with Z_2^T symmetry.

Besides the two phases discussed above, there should be another root phase (3) that will reduce to the $U(1) \times Z_2^T$ SPT phase whose boundary is a bosonic quantum Hall state with Hall conductivity ± 1, when time-reversal symmetry is broken at the boundary [32]. In the next two paragraphs we will argue *without* proof that this third root phase can be described by Eq. 2.3 with the following definition and transformation of O(5) vector order parameter $\boldsymbol{n}$:

$$\begin{aligned} (3) \quad : \quad & \mathcal{Z} = n^4 I_{2\times 2} + \sum_{a=1}^{3} i n_a \sigma^a, \\ & Z_2^T : \mathcal{Z} \to i\sigma^y \mathcal{Z}, \quad n_5 \to -n_5; \\ & \Theta = 8\pi \text{ in bulk.} \end{aligned} \tag{A.49}$$

Here $\mathcal{Z}$ is still the "fractional" representation of SO(3) matrix G_{ab} introduced in Eq. A.43. If we break the Z_2^T symmetry at the boundary of phase (3), the boundary becomes a 2d SO(3) SPT phase with SO(3) Hall conductivity ± 1 (when SO(3) is broken to U(1), the boundary becomes a bosonic integer quantum Hall state with Hall conductivity ± 1), thus it cannot be realized in a pure 2d bosonic system without degeneracy.

In principle $\mathcal{Z}$ is still coupled to a Z_2 gauge field. We propose that the confined phase of this Z_2 gauge field is the desired $SO(3) \times Z_2^T$ SPT phase. In the confined phase of a 3d Z_2 gauge field, the vison loops of the Z_2 gauge field proliferate. Since the Z_2 gauge field is coupled to the fractional field $\mathcal{Z}$, a vison loop of this Z_2 gauge field is bound with a vortex loop of SO(3) matrix field G_{ab} [136], which is defined based on homotopy group $\pi_1[SO(3)] = \mathbb{Z}_2$, thus the confined phase of the Z_2 gauge field is a phase where

the SO(3) vortex loops proliferate. If we reduce the SO(3) symmetry down to its inplane U(1) symmetry, the vison loop reduces to the vortex loop of the U(1) phase. When a bulk vortex (vison) loop ends at the boundary, it becomes a 2d vortex (vison). This 2d vortex is a fermion, because according to the previous paragraph, once the Z_2^T is broken at the boundary, the boundary becomes a boson quantum Hall state with Hall conductivity ± 1. This is consistent with the results for $U(1) \times Z_2^T$ SPT phase discussed in Ref. [32, 35, 39]. Thus the SPT phase described by Eq. A.49 is a phase where SO(3) vortex loops proliferate, and the SO(3) vortices at the boundary are fermions.

The final classification of SPT phases with $SO(3) \times Z_2^T$ symmetry is:

$$1d : (\mathbb{Z}_2)^2, \quad 2d : \mathbb{Z}_2, \quad 3d : (\mathbb{Z}_2)^3. \tag{A.50}$$

A.1.17 $Z_2 \times Z_2 \times Z_2$ symmetry

In 1d, we can construct three different root phases:

$$\begin{aligned}
(1) \quad : \quad & Z_2^A : n_{1,2} \to -n_{1,2}, \quad n_3 \to n_3; \\
& Z_2^B : n_1 \to n_1, \quad n_{2,3} \to -n_{2,3}; \\
& Z_2^C : \boldsymbol{n} \to \boldsymbol{n}; \\
(2) \quad : \quad & Z_2^B : n_{1,2} \to -n_{1,2}, \quad n_3 \to n_3; \\
& Z_2^C : n_1 \to n_1, \quad n_{2,3} \to -n_{2,3}; \\
& Z_2^A : \boldsymbol{n} \to \boldsymbol{n};
\end{aligned}$$

$$
\begin{aligned}
(3) \quad : \quad & Z_2^C : n_{1,2} \to -n_{1,2}, \quad n_3 \to n_3; \\
& Z_2^A : n_1 \to n_1, \quad n_{2,3} \to -n_{2,3}; \\
& Z_2^B : \boldsymbol{n} \to \boldsymbol{n}.
\end{aligned} \tag{A.51}
$$

In 2d there are seven different root phases:

$$
\begin{aligned}
(1) \quad : \quad & Z_2^A : \boldsymbol{n} \to -\boldsymbol{n}, \quad Z_2^B, Z_2^C : \boldsymbol{n} \to \boldsymbol{n}; \\
(2) \quad : \quad & Z_2^B : \boldsymbol{n} \to -\boldsymbol{n}, \quad Z_2^C, Z_2^A : \boldsymbol{n} \to \boldsymbol{n}; \\
(3) \quad : \quad & Z_2^C : \boldsymbol{n} \to -\boldsymbol{n}, \quad Z_2^A, Z_2^B : \boldsymbol{n} \to \boldsymbol{n}; \\
(4) \quad : \quad & Z_2^A : n_{1,2} \to -n_{1,2}, \quad n_{3,4} \to n_{3,4}; \\
& Z_2^B : n_{1,2} \to n_{1,2}, \quad n_{3,4} \to -n_{3,4}; \\
& Z_2^C : \boldsymbol{n} \to \boldsymbol{n}; \\
(5) \quad : \quad & Z_2^A : n_{1,2} \to -n_{1,2}, \quad n_{3,4} \to n_{3,4}; \\
& Z_2^C : n_{1,2} \to n_{1,2}, \quad n_{3,4} \to -n_{3,4}; \\
& Z_2^B : \boldsymbol{n} \to \boldsymbol{n};
\end{aligned}
$$

$$
\begin{aligned}
(6) \quad : \quad & Z_2^A : n_{1,2} \to -n_{1,2}, \quad n_{3,4} \to n_{3,4}; \\
& Z_2^B : n_{1,3} \to -n_{1,3}, \quad n_{2,4} \to n_{2,4}; \\
& Z_2^C : n_{1,4} \to -n_{1,4}, \quad n_{2,3} \to n_{2,3}; \\
(7) \quad : \quad & Z_2^A : n_{2,3} \to -n_{2,3}, \quad n_{1,4} \to n_{1,4} \\
& Z_2^B : n_{1,2} \to -n_{1,2}, \quad n_{3,4} \to n_{3,4}, \\
& Z_2^C : n_{1,2} \to n_{1,2}, \quad n_{3,4} \to -n_{3,4}.
\end{aligned} \tag{A.52}
$$

In 3d there are six different root phases:

$$
\begin{aligned}
(1) \quad : \quad & Z_2^A : n_{1,2} \to -n_{1,2}, \quad n_a \to n_a, (a = 3, 4, 5); \\
& Z_2^B : n_1 \to n_1, \quad n_a \to -n_a, (a = 2, \cdots 5); \\
& Z_2^C : \boldsymbol{n} \to \boldsymbol{n}; \\
(2) \quad : \quad & Z_2^B : n_{1,2} \to -n_{1,2}, \quad n_a \to n_a, (a = 3, 4, 5); \\
& Z_2^A : n_1 \to n_1, \quad n_a \to -n_a, (a = 2, \cdots 5); \\
& Z_2^C : \boldsymbol{n} \to \boldsymbol{n};
\end{aligned}
$$

$$(3) \quad : \quad Z_2^B : n_{1,2} \to -n_{1,2}, \quad n_a \to n_a, (a = 3, 4, 5);$$

$$Z_2^C : n_1 \to n_1, \quad n_a \to -n_a, (a = 2, \cdots 5);$$

$$Z_2^A : \boldsymbol{n} \to \boldsymbol{n};$$

$$(4) \quad : \quad Z_2^C : n_{1,2} \to -n_{1,2}, \quad n_a \to n_a, (a = 3, 4, 5);$$

$$Z_2^B : n_1 \to n_1, \quad n_a \to -n_a, (a = 2, \cdots 5);$$

$$Z_2^A : \boldsymbol{n} \to \boldsymbol{n};$$

$$(5) \quad : \quad Z_2^A : n_{1,2} \to -n_{1,2}, \quad n_a \to n_a, (a = 3, 4, 5);$$

$$Z_2^C : n_1 \to n_1, \quad n_a \to -n_a, (a = 2, \cdots 5);$$

$$Z_2^B : \boldsymbol{n} \to \boldsymbol{n};$$

$$(6) \quad : \quad Z_2^C : n_{1,2} \to -n_{1,2}, \quad n_a \to n_a, (a = 3, 4, 5);$$

$$Z_2^A : n_1 \to n_1, \quad n_a \to -n_a, (a = 2, \cdots 5);$$

$$Z_2^B : \boldsymbol{n} \to \boldsymbol{n};$$

$$(7) \quad : \quad Z_2^A : n_{1,2} \to -n_{1,2}, \quad n_{3,4,5} \to n_{3,4,5};$$

$$Z_2^B : n_{2,3} \to -n_{2,3}, \quad n_{1,4,5} \to n_{1,4,5};$$

$$Z_2^C : n_{4,5} \to -n_{4,5}, \quad n_{1,2,3} \to n_{1,2,3};$$

$$(8) \quad : \quad Z_2^A : n_{1,2} \to -n_{1,2}, \quad n_{3,4,5} \to n_{3,4,5};$$

$$Z_2^C : n_{2,3} \to -n_{2,3}, \quad n_{1,4,5} \to n_{1,4,5};$$

$$Z_2^B : n_{4,5} \to -n_{4,5}, \quad n_{1,2,3} \to n_{1,2,3}. \tag{A.53}$$

All the other SPT phases can be constructed with these root phases above. Here we will show one construction explicitly. For example, one may think the following state should also exist in $3d$:

$$Z_2^B : n_{1,2} \to -n_{1,2}, \quad n_{3,4,5} \to n_{3,4,5},$$

$$Z_2^C : n_{2,3} \to -n_{2,3}, \quad n_{1,4,5} \to n_{1,4,5},$$

$$Z_2^A : n_{4,5} \to -n_{4,5}, \quad n_{1,2,3} \to n_{1,2,3}. \tag{A.54}$$

But this state can be obtained by "merging" state (7) and (8) in Eq. A.53. First of all, since $n^{(7)}_{1,3,5}$ transform exactly equivalently to $n^{(8)}_{1,5,3}$ under all symmetries, we can turn on coupling between $\boldsymbol{n}^{(7)}$ and $\boldsymbol{n}^{(8)}$ to make $n^{(7)}_{1,3,5} = n^{(8)}_{1,5,3}$. Now without loss of generality

these two vectors can be written as

$$\begin{aligned} \boldsymbol{n}^{(7)} &= (\cos\theta N_1,\ \sin\theta\cos\alpha^{(7)},\ \cos\theta N_2, \\ &\quad \sin\theta\sin\alpha^{(7)},\ \cos\theta N_3); \\ \boldsymbol{n}^{(8)} &= (\cos\theta N_1,\ \sin\theta\cos\alpha^{(8)},\ \cos\theta N_3, \\ &\quad \sin\theta\sin\alpha^{(8)},\ \cos\theta N_2); \end{aligned} \tag{A.55}$$

where $\boldsymbol{N}$ is a unit three-component vector. All the symmetries transformations act on $\boldsymbol{N}$ and $\alpha^{(7)}$, $\alpha^{(8)}$, while θ is invariant under all symmetries.

Now let us define a new vector $\boldsymbol{n}^{(9)}$ using the parametrization of $\boldsymbol{n}^{(7)}$ and $\boldsymbol{n}^{(8)}$:

$$\begin{aligned} \boldsymbol{n}^{(9)} &= (\cos\theta N_2,\ \sin\theta\cos(\alpha^{(7)}+\alpha^{(8)}),\ \cos\theta N_3, \\ &\quad \sin\theta\sin(\alpha^{(7)}+\alpha^{(8)}),\ \cos\theta N_1); \end{aligned} \tag{A.56}$$

Obviously, the O(5) instanton number of $\boldsymbol{n}^{(9)}$ is exactly the sum of instantons of $\boldsymbol{n}^{(7)}$ and $\boldsymbol{n}^{(8)}$. More importantly, $\boldsymbol{n}^{(9)}$ transforms under all the symmetries as Eq. A.54, and since it can be "merged" from phase (7) and (8), it should not be viewed as an independent root phase.

The final classification of SPT phases with $Z_2 \times Z_2 \times Z_2$ symmetry is:

$$1d : (\mathbb{Z}_2)^3, \quad 2d : (\mathbb{Z}_2)^7, \quad 3d : (\mathbb{Z}_2)^8. \tag{A.57}$$

A.2 Examples of BSPT beyond group cohomology

A.2.1 $U(1)$ Symmetry

• In $4d$ space, there is a series of BSPT states with $U(1)$ symmetry that is beyond the group cohomology, their field theory is given by:

$$\mathcal{L}^{U(1)}_{4+1d} = \frac{i2\pi k}{2\pi} n dn \wedge \frac{K^{IJ}_{E_8}}{8\pi^2} dC^I \wedge dC^J, \tag{A.58}$$

where C^I's are rank-1 gauge field, and k can take arbitrary integer value. Physically this state can be viewed as decorating the 2π vortex of $U(1)$ order parameter $\vec{n} = (n_1, n_2)$ (which is a $2d$ membrane in this dimension) with the E_8 state, and then proliferating the vortices. As we have shown in the previous section, this phase has $\mathbb{Z}$ classification.

The $3+1d$ boundary of this state can be a superfluid phase with spontaneously U(1) symmetry breaking, whose vortex line hosts the edge states of the $2d$ E_8 state, *i.e.* a chiral conformal field theory with central charge $c = 8$. If we couple $\vec{n}$ to a $U(1)$ gauge field, then after we integrate out the gapped matter field $\vec{n}$, the boundary of the system will have a mixed $U(1)$-gravitational anomaly, namely the stress tensor of the system is no longer conserved inside the $U(1)$ flux at the boundary. A similar mixed gauge-gravity anomaly was also studied in Ref. [219].

• In $6+1d$ space-time, there are two root states for $U(1)$ BSPT states beyond group cohomology, the first state is described by the following field theory:

$$\mathcal{L}^{U(1)}_{6+1d,A} = \frac{i2\pi k}{12\pi^2} n dn \wedge dn \wedge dn \wedge \frac{K^{IJ}_{E_8}}{8\pi^2} dC^I \wedge dC^J \tag{A.59}$$

with

$$\begin{aligned} U(1): \quad & (n_1 + in_2) \to e^{i\phi}(n_1 + in_2), \\ & (n_3 + in_4) \to e^{i\phi}(n_3 + in_4). \end{aligned} \tag{A.60}$$

This state has $\mathbb{Z}$ classification. The state is constructed by decorating the E_8 states on the intersection of two $U(1)$ vortices, and then proliferate the vortices (the two-vortex intersection is now a $2d$ brane in $6d$ space).

The field theory of the second root phase is

$$\mathcal{L}^{U(1)}_{6+1d,B} = \frac{i2\pi}{2\pi} ndn \wedge \frac{(i\sigma^y)^{IJ}}{8\pi^2} dB^I \wedge dB^J \tag{A.61}$$

where

$$U(1) : (n_1 + in_2) \to e^{i\phi}(n_1 + in_2) \tag{A.62}$$

and B's are 2-form fields. The state has $\mathbb{Z}_2$ classification according to our rules. And physically this field theory corresponds to decorating the $U(1)$ vortex with the $4d$ BSRE state in Eq. 2.30.

A.2.2 Z_2 Symmetry

• In $4+1d$ space-time, there is one nontrivial beyond-cohomology BSPT state with Z_2 symmetry, and this state is the descendant of the $U(1)$ beyond Group Cohomology state in the same dimension in the sense that it can be obtained by breaking the $U(1)$ symmetry to its subgroup Z_2 from Eq. A.58:

$$\mathcal{L}^{Z_2}_{4+1d} = \frac{i2\pi}{2\pi} ndn \wedge \frac{K^{IJ}_{E_8}}{8\pi^2} dC^I \wedge dC^J \tag{A.63}$$

with

$$Z_2 : (n_1, n_2) \to -(n_1, n_2) \tag{A.64}$$

while the classification of the state is now reduced to $\mathbb{Z}_2$ because the n-sector is now $\mathbb{Z}_2$ classified.

• In $5+1d$ space-time, there is a $\mathbb{Z}_2$ classified new state which is not a descendant of any $U(1)$ state discussed in the previous subsection. Physically this state is constructed by decorating the Z_2 domain wall with $4d$ BSRE state:

$$\begin{aligned} \mathcal{L}^{Z_2}_{5+1d} &= \frac{i2\pi}{2\pi} n dn \wedge \frac{(i\sigma^y)^{IJ}}{8\pi^2} B^I \wedge dB^J \\ &= id\theta \wedge \frac{(i\sigma^y)^{IJ}}{8\pi^2} B^I \wedge dB^J \\ &= -i\theta \frac{(i\sigma^y)^{IJ}}{8\pi^2} dB^I \wedge dB^J \end{aligned} \tag{A.65}$$

Here we parametrize $\vec{n}$ as $\vec{n} = (\cos\theta, \sin\theta)$. The symmetry transformation is:

$$\begin{aligned} Z_2 : \quad & (n_1, n_2) \to (n_1, -n_2) \\ & (B^1, B^2) \to (B^2, B^1) \\ & \theta \to -\theta. \end{aligned} \tag{A.66}$$

Notice that B^I must transform nontrivially under Z_2 symmetry, in order to guarantee that the field theory is Z_2 invariant. We can also choose a different transformation for B^I: $Z_2 : B \to \sigma^z B$, but this transformation is equivalent to the previous after a basis change. In a Z_2 invariant state, $\langle n_2 \rangle = 0$, *i.e.* $\langle \theta \rangle = 0$ or π, which corresponds to the trivial and BSPT state respectively.

• In $6+1d$ space-time, there are two root states, both of which are descendants of

$U(1)$ BSPT states, and both have $\mathbb{Z}_2$ classification:

$$\mathcal{L}^{Z_2}_{6+1d,A} = \frac{i2\pi}{12\pi^2} ndn \wedge dn \wedge dn \wedge \frac{K^{IJ}_{E_8}}{8\pi^2} dC^I \wedge dC^J \tag{A.67}$$

with

$$Z_2 : (n_1, n_2, n_3, n_4) \to -(n_1, n_2, n_3, n_4). \tag{A.68}$$

$$\mathcal{L}^{Z_2}_{6+1d,B} = \frac{i2\pi}{2\pi} ndn \wedge \frac{(i\sigma^y)^{IJ}}{8\pi^2} dB^I \wedge dB^J \tag{A.69}$$

with

$$Z_2 : (n_1, n_2) \to -(n_1, n_2). \tag{A.70}$$

A.2.3 Z_2^T Symmetry

• In $3+1d$ space-time, it is well-known that there is a BSPT state beyond Group Cohomology [32]. The state can be understood by decorating Z_2^T domain walls with the $2d$ E_8 state:

$$\begin{aligned} \mathcal{L}^{Z_2^T}_{3+1d} &= \frac{i2\pi}{2\pi} ndn \wedge \frac{K^{IJ}_{E_8}}{8\pi^2} C^I \wedge dC^J \\ &= -i\theta \frac{K^{IJ}_{E_8}}{8\pi^2} dC^I \wedge dC^J \end{aligned} \tag{A.71}$$

with

$$\begin{aligned} Z_2^T : \quad & (n_1, n_2) \to (n_1, -n_2) \\ & \theta \to -\theta. \end{aligned} \tag{A.72}$$

θ is defined as before, $\langle\theta\rangle = 0$ and π correspond to the trivial and BSPT state respectively. This state has $\mathbb{Z}_2$ classification.

• In $5+1d$ space-time, there are two root states, both have $\mathbb{Z}_2$ classification. The field theory for the first state reads:

$$\mathcal{L}^{Z_2^T}_{5+1d,A} = \frac{i2\pi}{8\pi} n dn \wedge dn \wedge \frac{K^{IJ}_{E_8}}{8\pi^2} dC^I \wedge dC^J \tag{A.73}$$

with

$$Z_2^T : (n_1, n_2, n_3) \to -(n_1, n_2, n_3). \tag{A.74}$$

The physical meaning of this state is most transparent if we start with a system with an enlarged SO(3)$\times Z_2^T$ symmetry, and $\vec{n}$ forms a vector under the SO(3) symmetry. Then Eq. A.73 can be viewed as decoration of the hedgehog monopole of $\vec{n}$ with the $2d$ E_8 state. Weakly breaking the SO(3) symmetry while preserving the Z_2^T symmetry does not change the nature of this state. Alternatively, we can view the hedgehog monopole as the intersection of three Z_2^T domain walls.

The field theory for the second root state is

$$\begin{aligned} \mathcal{L}^{Z_2^T}_{5+1d,B} &= \frac{i2\pi}{2\pi} n dn \wedge \frac{(i\sigma^y)^{IJ}}{8\pi^2} B^I \wedge dB^J \\ &= -i\theta \frac{(i\sigma^y)^{IJ}}{8\pi^2} dB^I \wedge dB^J \end{aligned} \tag{A.75}$$

with

$$\begin{aligned} Z_2^T : \quad & (n_1, n_2) \to (n_1, -n_2) \\ & \theta \to -\theta. \end{aligned} \tag{A.76}$$

This state can be viewed as decoration of Z_2^T domain wall with the $4d$ BSRE state.

• In $6+1d$ space-time, there is one new state with $\mathbb{Z}_2$ classification:

$$\mathcal{L}_{6+1d}^{Z_2^T} = \frac{i2\pi}{2\pi} ndn \wedge \frac{(i\sigma^y)^{IJ}}{8\pi^2} dB^I \wedge dB^J \tag{A.77}$$

with

$$\begin{aligned} Z_2^T : \quad & (n_1, n_2) \to -(n_1, n_2) \\ & (B^1, B^2) \to (B^2, B^1). \end{aligned} \tag{A.78}$$

The state is constructed by decorating the vortex of $\vec{n}$ (or the intersection of two Z_2^T domain walls) with the $4d$ BSRE state.

A.2.4 $U(1) \rtimes Z_2^T$ Symmetry

• In $3+1d$ space-time, there is one nontrivial beyond-cohomology BSPT state with $U(1) \rtimes Z_2^T$ symmetry, but it is identical to the Z_2^T state in the same dimension, $U(1)$ symmetry simply acts trivially.

• In $4+1d$ space-time, there is one root state with $\mathbb{Z}$ classification:

$$\mathcal{L}_{4+1d}^{U(1)\rtimes Z_2^T} = \frac{i2\pi k}{2\pi} ndn \wedge \frac{K_{E_8}^{IJ}}{8\pi^2} dC^I \wedge dC^J. \tag{A.79}$$

with

$$\begin{aligned} U(1) : \quad & (n_1 + in_2) \to e^{i\phi}(n_1 + in_2) \\ Z_2^T : \quad & (n_1, n_2) \to (n_1, -n_2). \end{aligned} \tag{A.80}$$

• In $5+1d$ space-time, there are two root states, both are identical to the Z_2^T state in the same dimension with trivial $U(1)$ symmetry transformation, and both are $\mathbb{Z}_2$

classified.

• In $6+1d$ space-time, in Ref. [69] there are *four* root states, all $\mathbb{Z}_2$ classified. However, we can only find *three* $\mathbb{Z}_2$ classified root states by our construction. The first one is identical to the Z_2^T state in $6+1d$. The other two root states are given by:

$$\mathcal{L}_{6+1d,A}^{U(1)\rtimes Z_2^T} = \frac{i2\pi}{12\pi^2} ndn\wedge dn\wedge dn\wedge \frac{K_{E_8}^{IJ}}{8\pi^2} dC^I\wedge dC^J \tag{A.81}$$

with

$$\begin{aligned} U(1): &\quad (n_1+in_2)\to e^{i\phi}(n_1+in_2),\\ Z_2^T: &\quad (n_1,n_2,n_3,n_4)\to (n_1,-n_2,-n_3,-n_4) \end{aligned} \tag{A.82}$$

and

$$\mathcal{L}_{6+1d,B}^{U(1)\rtimes Z_2^T} = \frac{i2\pi}{2\pi} ndn\wedge \frac{(i\sigma^y)^{IJ}}{8\pi^2} dB^I\wedge dB^J \tag{A.83}$$

with

$$\begin{aligned} U(1): &\quad (n_1+in_2)\to e^{i\phi}(n_1+in_2),\\ Z_2^T: &\quad (n_1,n_2)\to (n_1,-n_2) \end{aligned} \tag{A.84}$$

We suspect the state we missed here is the mixed SPT state described by $E^d(G)$ in Ref. [69].

A.2.5 $U(1)\times Z_2^T$ Symmetry

• In $3+1d$ space-time, there is a state identical to the pure Z_2^T state with trivial $U(1)$ symmetry transformation.

• In $5+1d$ space-time, we find three $\mathbb{Z}_2$ classified root states. Two of them are identical

to the Z_2^T states in $5+1d$ space-time, with trivial $U(1)$ symmetry transformation. The third state is given by:

$$\mathcal{L}_{5+1d}^{U(1)\times Z_2^T} = \frac{i2\pi}{8\pi} n dn \wedge dn \wedge \frac{K_{E_8}^{IJ}}{8\pi^2} dC^I \wedge dC^J \tag{A.85}$$

with

$$\begin{aligned} U(1): &\quad (n_1 + in_2) \to e^{i\phi}(n_1 + in_2), \\ Z_2^T: &\quad (n_1, n_2, n_3) \to (n_1, n_2, -n_3). \end{aligned} \tag{A.86}$$

This state can be viewed as decorating the $2d$ E_8 state on the intersection of a Z_2^T domain wall and a $U(1)$ vortex (it can also be viewed as the hedgehog monopole of $\vec{n}$), then proliferating both the domain walls and vortices.

• In $6+1d$ space-time, in Ref. [69] there are *three* $\mathbb{Z}_2$ classified root states. However, using our method we can only construct *two* $\mathbb{Z}_2$ classified root states. The first one is identical to the Z_2^T state with trivial $U(1)$ symmetry transformation. The other one is:

$$\mathcal{L}_{6+1d}^{U(1)\times Z_2^T} = \frac{i2\pi}{2\pi} n dn \wedge \frac{(i\sigma^y)^{IJ}}{8\pi^2} dB^I \wedge dB^J \tag{A.87}$$

with

$$\begin{aligned} U(1): &\quad (n_1 + in_2) \to e^{i\phi}(n_1 + in_2), \\ Z_2^T: &\quad (n_1, n_2) \to -(n_1, n_2), \quad B^{1(2)} \to B^{2(1)}. \end{aligned} \tag{A.88}$$

One may ask whether field theory like Eq. A.81 could correspond to a new root state. However, there is no consistent way to assign the U(1)$\times Z_2^T$ symmetry transformations on Eq. A.81, namely Eq. A.81 cannot be invariant under U(1)$\times Z_2^T$ symmetry, although

it is invariant under $\mathrm{U}(1)\rtimes Z_2^T$ symmetry.

A.2.6 $U(1)\rtimes Z_2 = O_2$ Symmetry

• In $4+1d$ space-time, there is one root state identical to the BSPT state with Z_2 symmetry in the same dimension, the $U(1)$ symmetry simply acts trivially.

• In $5+1d$ space-time, there are two root states, both $\mathbb{Z}_2$ classified. One is the same Z_2 state with trivial $U(1)$ action. The other one is given by:

$$\mathcal{L}^{U(1)\rtimes Z_2}_{5+1d} = \frac{i2\pi}{8\pi} n dn\wedge dn\wedge \frac{K^{IJ}_{E_8}}{8\pi^2} dC^I\wedge dC^J \tag{A.89}$$

with

$$\begin{aligned} U(1): &\quad (n_1+in_2)\to e^{i\phi}(n_1+in_2),\\ Z_2: &\quad (n_1,n_2,n_3)\to(n_1,-n_2,-n_3). \end{aligned} \tag{A.90}$$

This state can be viewed as decorating the $2d$ E_8 state on the intersection of $U(1)$ vortex and Z_2 domain wall. Also, the O_2 symmetry is a subgroup of $SO(3)$ symmetry, thus the vortex-domain wall intersection is simply the hedgehog monopole of the $SO(3)$ vector $\vec{n}$.

• In $6+1d$ space-time, we find $four$ root states, which is *more* than the results in Ref. [69]. Two of them are the same as the BSPT states with Z_2 symmetry, both of which are $\mathbb{Z}_2$ classified. The third root state is described by

$$\mathcal{L}^{U(1)\rtimes Z_2}_{6+1d,A} = \frac{i2\pi k}{12\pi^2} n dn\wedge dn\wedge dn\wedge \frac{K^{IJ}_{E_8}}{8\pi^2} dC^I\wedge dC^J \tag{A.91}$$

with

$$\begin{aligned} U(1): \quad & (n_1+in_2)\to e^{i\phi}(n_1+in_2), \\ & (n_3+in_4)\to e^{i\phi}(n_3+in_4), \\ Z_2: \quad & (n_1,n_2,n_3,n_4)\to(n_1,-n_2,n_3,-n_4) \end{aligned} \tag{A.92}$$

This state is $\mathbb{Z}$ classified. This state can be viewed as decorating the $2d$ E_8 state on the intersection of two vortices, then proliferate the vortices afterwards.

The last root state in $6+1d$ space-time is described by

$$\mathcal{L}^{U(1)\rtimes Z_2}_{6+1d,B}=\frac{i2\pi}{2\pi}ndn\wedge\frac{(i\sigma^y)^{IJ}}{8\pi^2}dB^I\wedge dB^J \tag{A.93}$$

with

$$\begin{aligned} U(1): \quad & (n_1+in_2)\to e^{i\phi}(n_1+in_2), \\ Z_2: \quad & (n_1,n_2)\to(n_1,-n_2), \\ & (B^1,B^2)\to(B^2,B^1). \end{aligned} \tag{A.94}$$

This state has $\mathbb{Z}_2$ classification.

A.2.7 $U(1)\times Z_2$ Symmetry

• In $4+1d$ space-time, we have two root states, both of which are descendants from pure $U(1)$ state and pure Z_2 state respectively.

• In $5+1d$ space-time, there is only one root state, which is the same as the state with Z_2 symmetry only.

• In $6+1d$ space-time, there are five root states. The first three states can all be

described by the same field theory:

$$\mathcal{L}^{U(1)\times Z_2}_{6+1d,A} = \frac{i2\pi k}{12\pi^2} n dn \wedge dn \wedge dn \wedge \frac{K^{IJ}_{E_8}}{8\pi^2} dC^I \wedge dC^J \tag{A.95}$$

These three different states have the same form of Lagrangian, but they are distinguished from each other by their symmetry transformations:

$$\begin{aligned} (1)\ U(1): &\quad trivial, \\ Z_2: &\quad (n_1, n_2, n_3, n_4) \to -(n_1, n_2, n_3, n_4). \end{aligned} \tag{A.96}$$

$$\begin{aligned} (2)\ U(1): &\quad (n_1 + in_2) \to e^{i\phi}(n_1 + in_2), \\ Z_2: &\quad (n_1, n_2, n_3, n_4) \to -(n_1, n_2, n_3, n_4). \end{aligned} \tag{A.97}$$

$$\begin{aligned} (3)\ U(1): &\quad (n_1 + in_2) \to e^{i\phi}(n_1 + in_2), \\ &\quad (n_3 + in_4) \to e^{i\phi}(n_3 + in_4), \\ Z_2: &\quad (n_1, n_2, n_3, n_4) \to -(n_1, n_2, n_3, n_4). \end{aligned} \tag{A.98}$$

The classification of the three states are $\mathbb{Z}_2$, $\mathbb{Z}_2$ and $\mathbb{Z}$ respectively.

The other two states are described by the following field theory:

$$\mathcal{L}^{U(1)\times Z_2}_{6+1d,B} = \frac{i2\pi}{2\pi} n dn \wedge \frac{(i\sigma^y)^{IJ}}{8\pi^2} dB^I \wedge dB^J \tag{A.99}$$

again, these two states have different transformations under symmetry groups:

$$\begin{aligned} (4)\ U(1): &\quad \textit{trivial}, \\ Z_2: &\quad (n_1, n_2) \to -(n_1, n_2). \end{aligned} \tag{A.100}$$

$$\begin{aligned} (5)\ U(1): &\quad (n_1 + in_2) \to e^{i\phi}(n_1 + in_2), \\ Z_2: &\quad \textit{trivial}. \end{aligned} \tag{A.101}$$

The classification of the two states are both $\mathbb{Z}_2$.

Appendix B

Fermion σ-model

B.1 Vison Loops in ^{3}He B TSC

In this appendix, we derive the effective theory along the vison loop in the ^{3}He B TSC. Let us start with Eq. (5.2), and first consider a straight vison line along the x-direction. The vison line can be considered as a thin hollow cylinder through the bulk of the TSC with a $\mathbb{Z}_2$ flux (π-flux) threading through the hole of the tube. For this configuration, it could be convenient to use the cylindrical coordinate defined as $(x, y, z) = (x, \rho\cos\theta, \rho\sin\theta)$. Applying the coordinate transform to Eq. (5.2), the Schördinger equation reads

$$\big(\mathrm{i}\Gamma^1\partial_x + \mathrm{i}\Gamma^2 e^{\Gamma^2\Gamma^3\theta}\partial_\rho + \mathrm{i}\Gamma^3 e^{\Gamma^2\Gamma^3\theta}\rho^{-1}(\partial_\theta - \mathrm{i}\omega_\theta) + m\Gamma^4\big)\chi = E\chi, \tag{B.1}$$

where $\omega_\theta = \mathrm{i}\Gamma^2\Gamma^3\theta/2$ is the spin connection that corresponds to threading the π-flux (as $e^{\oint \mathrm{i}\omega_\theta \mathrm{d}\theta} = -1$). The low-energy fermion modes around the vison line are given by the

following ansatz in the asymptotic limit,

$$\chi_a(x,\rho,\theta) \simeq e^{-m\rho}e^{-\Gamma^2\Gamma^3\theta/2}\chi_a(x). \tag{B.2}$$

Substitute Eq. (B.2) to Eq. (B.1), one can see $\chi_a(x)$ must satisfy $\mathrm{i}\Gamma^4\Gamma^2\chi_a(x) = \chi_a(x)$ in order to obtain the low-energy modes (whose energy $E \to 0$ as the x-direction momentum $\mathrm{i}\partial_x \to 0$). The matrix $\mathrm{i}\Gamma^4\Gamma^2 = \sigma^{31}$ has two eigenvectors of the $+1$ eigenvalue:

$$\chi_1 = \frac{1}{\sqrt{2}}(1,1,0,0)^\intercal, \quad \chi_2 = \frac{1}{\sqrt{2}}(0,0,1,-1)^\intercal, \tag{B.3}$$

corresponding to the two counter-propagating Majorana modes along the vison line. It is straight forward to see that the 4×4 matrix $\Gamma^1 = \sigma^{30}$ represented on the basis (χ_1,χ_2) becomes the 2×2 matrix σ^3, so the effective $1d$ Hamiltonian should be $H_{1d,x} = \int \mathrm{d}x\chi^\intercal(x)\mathrm{i}\sigma^3\partial_x\chi(x)$ as shown in Eq. (5.3).

In general, any operator O (as a 4×4 matrix) defined in the $3d$ bulk can be thus projected to the subspace of the fermion modes along the vison line, as the corresponding 2×2 matrix $\tilde{O}$ by $(a,b=1,2)$

$$\begin{aligned}\tilde{O}_{ab} &= \int \mathrm{d}\rho\,\mathrm{d}\theta\,\chi_a^\intercal(x,\rho,\theta)O\chi_b(x,\rho,\theta)\\ &\simeq \int \frac{\mathrm{d}\theta}{2\pi}\,\chi_a^\intercal e^{\Gamma^2\Gamma^3\theta/2}Oe^{-\Gamma^2\Gamma^3\theta/2}\chi_b.\end{aligned} \tag{B.4}$$

In Tab. B.1, we conclude the projection of all 4×4 Hermitian matrices (16 complete basis) to the 2-dimensional subspace of counter propagating Majorana modes along the vison line. This establishes the correspondence between the operators in the bulk and that on the vison line. One can see Γ^5 in the bulk would correspond to σ^2 on the vison line. So the action of the time-reversal symmetry $\mathbb{Z}_2^T$ is reduced to $\chi \to \mathrm{i}\sigma^2\chi$ on the vison line.

Given the effective Hamiltonian Eq. (5.3) and the above $\mathbb{Z}_2^T$ symmetry on the vison line, it seems that if we make even copies of the system, the vison line can be gapped out by a bilinear mass term of the form $\chi^\intercal \sigma^1 \otimes A\chi$ (with $A = -A^\intercal$) which does not breaks the time-reversal symmetry. However, this is only true for our analysis of the straight vison line along the x-direction. Because according to Tab. B.1, the mass term $\chi^\intercal \sigma^1 \otimes A\chi$ would extend to the bulk as $\chi^\intercal \sigma^{13} \otimes A\chi$, which can not gap out the vison lines along any other directions, as σ^{13} commutes with both $\Gamma^2 = \sigma^{10}$ and $\Gamma^3 = \sigma^{22}$. Therefore it is impossible to fully gap out the vison loop by any fermion bilinear term.

Table B.1: Projection of bulk operators to the vison line (x-direction)

O	$\to$	$\tilde{O}$
σ^{00}	$\int \frac{\mathrm{d}\theta}{2\pi} \sigma^0$	$= \sigma^0$
σ^{31}	$\int \frac{\mathrm{d}\theta}{2\pi} \cos\theta \, \sigma^0$	$= 0$
σ^{03}	$-\int \frac{\mathrm{d}\theta}{2\pi} \sin\theta \, \sigma^0$	$= 0$
σ^{13}	$\int \frac{\mathrm{d}\theta}{2\pi} \sigma^1$	$= \sigma^1$
$\Gamma^3 = \sigma^{22}$	$\int \frac{\mathrm{d}\theta}{2\pi} \cos\theta \, \sigma^1$	$= 0$
$\Gamma^2 = \sigma^{10}$	$-\int \frac{\mathrm{d}\theta}{2\pi} \sin\theta \, \sigma^1$	$= 0$
$\Gamma^5 = \sigma^{23}$	$\int \frac{\mathrm{d}\theta}{2\pi} \sigma^2$	$= \sigma^2$
σ^{12}	$-\int \frac{\mathrm{d}\theta}{2\pi} \cos\theta \, \sigma^2$	$= 0$
σ^{20}	$-\int \frac{\mathrm{d}\theta}{2\pi} \sin\theta \, \sigma^2$	$= 0$
$\Gamma^1 = \sigma^{30}$	$\int \frac{\mathrm{d}\theta}{2\pi} \sigma^3$	$= \sigma^3$
σ^{01}	$\int \frac{\mathrm{d}\theta}{2\pi} \cos\theta \, \sigma^3$	$= 0$
σ^{33}	$-\int \frac{\mathrm{d}\theta}{2\pi} \sin\theta \, \sigma^3$	$= 0$
$\Gamma^4 = \sigma^{21}$		0
σ^{02}		0
σ^{11}		0
σ^{32}		0

Bibliography

[1] Y.-C. He, M. P. Zaletel, M. Oshikawa, and F. Pollmann, *Signatures of Dirac cones in a DMRG study of the Kagome Heisenberg model*, *ArXiv e-prints* (Nov., 2016) [arXiv:1611.0623].

[2] C. L. Kane and E. J. Mele, *Quantum spin hall effect in graphene*, *Physical Review Letter* **95** (2005) 226801.

[3] C. L. Kane and E. J. Mele, Z_2 *topological order and the quantum spin hall effect*, *Physical Review Letter* **95** (2005) 146802.

[4] B. A. Bernevig, T. L. Hughes, and S.-C. Zhang, *Quantum spin* Hall *effect and topological phase transition in* HgTe *quantum wells*, *Science* **314** (2006) 1757–1761.

[5] L. Fu, C. L. Kane, and E. J. Mele, *Topological insulators in three dimensions*, *Phys. Rev. Lett.* **98** (2008) 106803.

[6] J. E. Moore and L. Balents, *Topological invariants of time-reversal-invariant band structures*, *Phys. Rev. B* **75** (2007) 121306(R).

[7] R. Roy, *Topological phases and the quantum spin hall effect in three dimensions*, *Phys. Rev. B* **79** (May, 2009) 195322.

[8] C. Xu and J. E. Moore, *Stability of the quantum spin hall effect: Effects of interactions, disorder, and* F_2 *topology*, *Phys. Rev. B* **73** (Jan, 2006) 045322.

[9] C. Wu, B. A. Bernevig, and S.-C. Zhang, *Helical liquid and the edge of quantum spin hall systems*, *Phys. Rev. Lett.* **96** (Mar, 2006) 106401.

[10] C. Xu, *Time-reversal symmetry breaking at the edge states of a three-dimensional topological band insulator*, *Phys. Rev. B* **81** (Jan, 2010) 020411.

[11] C. Wang, A. C. Potter, and T. Senthil, *Gapped symmetry preserving surface state for the electron topological insulator*, *Phys. Rev. B* **88** (Sep, 2013) 115137.

[12] P. Bonderson, C. Nayak, and X.-L. Qi, *A time-reversal invariant topological phase at the surface of a 3d topological insulator*, *Journal of Statistical Mechanics: Theory and Experiment* **2013** (2013), no. 09 P09016.

[13] M. A. Metlitski, C. L. Kane, and M. P. A. Fisher, *Symmetry-respecting topologically ordered surface phase of three-dimensional electron topological insulators*, *Phys. Rev. B* **92** (Sep, 2015) 125111.

[14] X. Chen, L. Fidkowski, and A. Vishwanath, *Symmetry enforced non-abelian topological order at the surface of a topological insulator*, *Phys. Rev. B* **89** (Apr, 2014) 165132.

[15] F. Haldane, *Continuum dynamics of the 1-d heisenberg antiferromagnet: Identification with the o(3) nonlinear sigma model*, *Physics Letters A* **93** (1983), no. 9 464 – 468.

[16] F. D. M. Haldane, *Nonlinear field theory of large-spin heisenberg antiferromagnets: Semiclassically quantized solitons of the one-dimensional easy-axis néel state*, *Phys. Rev. Lett.* **50** (Apr, 1983) 1153–1156.

[17] I. Affleck, T. Kennedy, E. H. Lieb, and H. Tasaki, *Rigorous results on valence-bond ground states in antiferromagnets*, *Phys. Rev. Lett.* **59** (Aug, 1987) 799–802.

[18] A. Läuchli, G. Schmid, and S. Trebst, *Spin nematics correlations in bilinear-biquadratic $s = 1$ spin chains*, *Phys. Rev. B* **74** (Oct, 2006) 144426.

[19] A. Auerbach, *Interacting electrons and quantum magnetism*. Springer, 1994.

[20] E. Fradkin, *Field Theories of Condensed Matter Physics*. Cambridge University Press, 2013.

[21] Z. Bi, A. Rasmussen, K. Slagle, and C. Xu, *Classification and description of bosonic symmetry protected topological phases with semiclassical nonlinear sigma models*, *Phys. Rev. B* **91** (Apr, 2015) 134404.

[22] Z. Bi and C. Xu, *Construction and field theory of bosonic-symmetry-protected topological states beyond group cohomology*, *Phys. Rev. B* **91** (May, 2015) 184404.

[23] A. Kitaev, *Periodic table for topological insulators and superconductors*, *AIP Conference Proceedings* **1134** (2009), no. 1 22–30, [http://aip.scitation.org/doi/pdf/10.1063/1.3149495].

[24] A. P. Schnyder, S. Ryu, A. Furusaki, and A. W. W. Ludwig, *Classification of topological insulators and superconductors*, *AIP Conference Proceedings* **1134** (2009), no. 1 10–21, [http://aip.scitation.org/doi/pdf/10.1063/1.3149481].

[25] X. Chen, Z.-C. Gu, Z.-X. Liu, and X.-G. Wen, *Symmetry protected topological orders and the group cohomology of their symmetry group*, *Phys. Rev. B* **87** (Apr, 2013) 155114.

[26] X. Chen, Z.-C. Gu, Z.-X. Liu, and X.-G. Wen, *Symmetry-protected topological orders in interacting bosonic systems*, *Science* **338** (2012), no. 6114 1604–1606, [http://science.sciencemag.org/content/338/6114/1604.full.pdf].

[27] M. Levin and Z.-C. Gu, *Braiding statistics approach to symmetry-protected topological phases*, *Phys. Rev. B* **86** (Sep, 2012) 115109.

[28] T. Senthil and M. Levin, *Integer quantum hall effect for bosons*, *Phys. Rev. Lett.* **110** (Jan, 2013) 046801.

[29] M. Levin and A. Stern, *Classification and analysis of two-dimensional abelian fractional topological insulators*, *Phys. Rev. B* **86** (Sep, 2012) 115131.

[30] Z.-X. Liu and X.-G. Wen, *Symmetry-protected quantum spin hall phases in two dimensions*, *Phys. Rev. Lett.* **110** (Feb, 2013) 067205.

[31] Y.-M. Lu and A. Vishwanath, *Theory and classification of interacting integer topological phases in two dimensions: A chern-simons approach*, *Phys. Rev. B* **86** (Sep, 2012) 125119.

[32] A. Vishwanath and T. Senthil, *Physics of three-dimensional bosonic topological insulators: Surface-deconfined criticality and quantized magnetoelectric effect*, *Phys. Rev. X* **3** (Feb, 2013) 011016.

[33] C. Xu, *Three-dimensional symmetry-protected topological phase close to antiferromagnetic néel order*, *Phys. Rev. B* **87** (Apr, 2013) 144421.

[34] J. Oon, G. Y. Cho, and C. Xu, *Two-dimensional symmetry-protected topological phases with* $\mathbf{PSU}(n)$ *and time-reversal symmetry*, *Phys. Rev. B* **88** (Jul, 2013) 014425.

[35] C. Xu and T. Senthil, *Wave functions of bosonic symmetry protected topological phases*, *Phys. Rev. B* **87** (May, 2013) 174412.

[36] C. Wang and T. Senthil, *Boson topological insulators: A window into highly entangled quantum phases*, *Phys. Rev. B* **87** (Jun, 2013) 235122.

[37] C. Wang, A. C. Potter, and T. Senthil, *Classification of interacting electronic topological insulators in three dimensions*, *Science* **343** (2014), no. 6171 629–631, [http://science.sciencemag.org/content/343/6171/629.full.pdf].

[38] X. Chen, Y.-M. Lu, and A. Vishwanath, *Symmetry-protected topological phases from decorated domain walls*, *Nature Communications* **5** (2014) 3507.

[39] M. A. Metlitski, C. L. Kane, and M. P. A. Fisher, *Bosonic topological insulator in three dimensions and the statistical witten effect*, *Phys. Rev. B* **88** (Jul, 2013) 035131.

[40] P. Ye and X.-G. Wen, *Projective construction of two-dimensional symmetry-protected topological phases with u(1), so(3), or su(2) symmetries*, *Phys. Rev. B* **87** (May, 2013) 195128.

[41] P. Ye and X.-G. Wen, *Constructing symmetric topological phases of bosons in three dimensions via fermionic projective construction and dyon condensation*, *Phys. Rev. B* **89** (Jan, 2014) 045127.

[42] M. Cheng and Z.-C. Gu, *Topological response theory of abelian symmetry-protected topological phases in two dimensions*, *Phys. Rev. Lett.* **112** (Apr, 2014) 141602.

[43] T. Kennedy, *Exact diagonalisations of open spin-1 chains*, *Journal of Physics: Condensed Matter* **2** (1990), no. 26 5737.

[44] M. Hagiwara, K. Katsumata, I. Affleck, B. I. Halperin, and J. P. Renard, *Observation of s=1/2 degrees of freedom in an s=1 linear-chain heisenberg antiferromagnet*, *Phys. Rev. Lett.* **65** (Dec, 1990) 3181–3184.

[45] T.-K. Ng, *Edge states in antiferromagnetic quantum spin chains*, *Phys. Rev. B* **50** (Jul, 1994) 555–558.

[46] A. Kapustin, *Bosonic Topological Insulators and Paramagnets: a view from cobordisms*, arXiv:1404.6659.

[47] A. Kapustin, *Symmetry Protected Topological Phases, Anomalies, and Cobordisms: Beyond Group Cohomology*, arXiv:1403.1467.

[48] L. Kong and X.-G. Wen, *Braided fusion categories, gravitational anomalies, and the mathematical framework for topological orders in any dimensions*, arXiv:1405.5858.

[49] C. Xu and Y.-Z. You, *Bosonic short-range entangled states beyond group cohomology classification*, *Phys. Rev. B* **91** (Feb, 2015) 054406.

[50] E. Witten, *Nonabelian bosonization in two dimensions*, *Comm. Math. Phys.* **92** (1984), no. 4 455–472.

[51] V. Knizhnik and A. Zamolodchikov, *Current algebra and wess-zumino model in two dimensions*, *Nuclear Physics B* **247** (1984), no. 1 83 – 103.

[52] H. Levine, S. B. Libby, and A. M. M. Pruisken, *Electron delocalization by a magnetic field in two dimensions*, *Phys. Rev. Lett.* **51** (Nov, 1983) 1915–1918.

[53] H. Levine, S. B. Libby, and A. M. M. Pruisken, *Theory of the quantized hall effect*, *Nucl. Phys. B* **240** (1984) 30, 49, 71.

[54] C. Xu and A. W. W. Ludwig, *Nonperturbative effects of a topological theta term on principal chiral nonlinear sigma models in* $2+1$ *dimensions*, *Phys. Rev. Lett.* **110** (May, 2013) 200405.

[55] X.-L. Qi, T. L. Hughes, and S.-C. Zhang, *Topological field theory of time-reversal invariant insulators*, *Phys. Rev. B* **78** (Nov, 2008) 195424.

[56] A. M. Essin, J. E. Moore, and D. Vanderbilt, *Magnetoelectric polarizability and axion electrodynamics in crystalline insulators*, *Phys. Rev. Lett.* **102** (Apr, 2009) 146805.

[57] E. Lieb, T. Schultz, and D. Mattis, *Two soluble models of an antiferromagnetic chain*, *Annals of Physics* **16** (1961), no. 3 407 – 466.

[58] A. Kitaev, *Fault-tolerant quantum computation by anyons*, *Annals of Physics* **303** (2003), no. 1 2 – 30.

[59] T. Grover and T. Senthil, *Topological spin hall states, charged skyrmions, and superconductivity in two dimensions*, *Phys. Rev. Lett.* **100** (Apr, 2008) 156804.

[60] X. Chen, F. J. Burnell, A. Vishwanath, and L. Fidkowski, *Anomalous symmetry fractionalization and surface topological order*, *Phys. Rev. X* **5** (Oct, 2015) 041013.

[61] Z.-X. Liu, X. Chen, and X.-G. Wen, *Symmetry-protected topological orders of one-dimensional spin systems with* $D_2 + t$ *symmetry*, *Phys. Rev. B* **84** (Nov, 2011) 195145.

[62] Y.-Z. You and C. Xu, *Symmetry-protected topological states of interacting fermions and bosons*, *Phys. Rev. B* **90** (Dec, 2014) 245120.

[63] Z. Bi, A. Rasmussen, K. Slagle, and C. Xu, *Classification and description of bosonic symmetry protected topological phases with semiclassical nonlinear sigma models*, *Phys. Rev. B* **91** (Apr, 2015) 134404.

[64] A. Kitaev, *Anyons in an exactly solved model and beyond*, *Annals of Physics* **321** (2006), no. 1 2 – 111. January Special Issue.

[65] A. Kitaev. http://online.kitp.ucsb.edu/online/topomat11/kitaev.

[66] X.-G. Wen, *Classifying gauge anomalies through symmetry-protected trivial orders and classifying gravitational anomalies through topological orders*, *Phys. Rev. D* **88** (Aug, 2013) 045013.

[67] L. Alvarez-Gaume and E. Witten, *Gravitational anomalies*, *Nucl. Phys. B* **234** (1983) 269–330.

[68] S. Kravec, J. McGreevy, and B. Swingle, *All-fermion electrodynamics and fermion number anomaly inflow*, *Phys. Rev. D* **92** (Oct, 2015) 085024.

[69] X.-G. Wen, *Construction of bosonic symmetry-protected-trivial states and their topological invariants via $g \times so(\infty)$ nonlinear σ models*, *Phys. Rev. B* **91** (May, 2015) 205101.

[70] Z. Bi, Y.-Z. You, and C. Xu, *Anyon and loop braiding statistics in field theories with a topological Θ term*, *Phys. Rev. B* **90** (Aug, 2014) 081110.

[71] Y.-Z. You, Z. Bi, A. Rasmussen, K. Slagle, and C. Xu, *Wave function and strange correlator of short-range entangled states*, *Phys. Rev. Lett.* **112** (Jun, 2014) 247202.

[72] A. M. Polyakov, *Gauge Fields and Strings*, *Contemp. Concepts Phys.* **3** (1987) 1–301.

[73] D. A. Ivanov, *Non-abelian statistics of half-quantum vortices in p-wave superconductors*, *Phys. Rev. Lett.* **86** (Jan, 2001) 268–271.

[74] C. Wang and M. Levin, *Braiding statistics of loop excitations in three dimensions*, *Phys. Rev. Lett.* **113** (Aug, 2014) 080403.

[75] H. Moradi and X.-G. Wen, *Universal topological data for gapped quantum liquids in three dimensions and fusion algebra for non-abelian string excitations*, *Phys. Rev. B* **91** (Feb, 2015) 075114.

[76] J. C. Wang and X.-G. Wen, *Non-abelian string and particle braiding in topological order: Modular $\mathrm{SL}(3,\mathbb{Z})$ representation and $(3+1)$-dimensional twisted gauge theory*, *Phys. Rev. B* **91** (Jan, 2015) 035134.

[77] S. Jiang, A. Mesaros, and Y. Ran, *Generalized modular transformations in $(3+1)$D topologically ordered phases and triple linking invariant of loop braiding*, *Phys. Rev. X* **4** (Sep, 2014) 031048.

[78] C.-M. Jian and X.-L. Qi, *Layer construction of 3d topological states and string braiding statistics*, *Phys. Rev. X* **4** (Dec, 2014) 041043.

[79] Z. Bi, A. Rasmussen, and C. Xu, *Line defects in three-dimensional symmetry-protected topological phases*, *Phys. Rev. B* **89** (May, 2014) 184424.

[80] H. Li and F. D. M. Haldane, *Entanglement spectrum as a generalization of entanglement entropy: Identification of topological order in non-abelian fractional quantum hall effect states*, *Phys. Rev. Lett.* **101** (Jul, 2008) 010504.

[81] X.-L. Qi, H. Katsura, and A. W. W. Ludwig, *General relationship between the entanglement spectrum and the edge state spectrum of topological quantum states*, *Phys. Rev. Lett.* **108** (May, 2012) 196402.

[82] R. Shankar and A. Vishwanath, *Equality of bulk wave functions and edge correlations in some topological superconductors: A spacetime derivation*, *Phys. Rev. Lett.* **107** (Sep, 2011) 106803.

[83] E. Witten, *Instatons, the quark model, and the 1/n expansion*, *Nuclear Physics B* **149** (1979), no. 2 285 – 320.

[84] I. Affleck, T. Kennedy, E. H. Lieb, and H. Tasaki, *Valence bond ground states in isotropic quantum antiferromagnets*, *Comm. Math. Phys.* **115** (1988), no. 3 477–528.

[85] M. den Nijs and K. Rommelse, *Preroughening transitions in crystal surfaces and valence-bond phases in quantum spin chains*, *Phys. Rev. B* **40** (Sep, 1989) 4709–4734.

[86] T. Kennedy, E. H. Lieb, and H. Tasaki, *A two-dimensional isotropic quantum antiferromagnet with unique disordered ground state*, *Journal of Statistical Physics* **53** (1988), no. 1 383–415.

[87] Z.-X. Liu, M. Liu, and X.-G. Wen, *Gapped quantum phases for the $s = 1$ spin chain with D_{2h} symmetry*, *Phys. Rev. B* **84** (Aug, 2011) 075135.

[88] T.-C. Wei, I. Affleck, and R. Raussendorf, *Two-dimensional affleck-kennedy-lieb-tasaki state on the honeycomb lattice is a universal resource for quantum computation*, *Phys. Rev. A* **86** (Sep, 2012) 032328.

[89] A. Miyake, *Quantum computational capability of a 2D valence bond solid phase*, *Annals of Physics* **326** (July, 2011) 1656–1671, [arXiv:1009.3491].

[90] S. R. White, *Density matrix formulation for quantum renormalization groups*, *Phys. Rev. Lett.* **69** (Nov, 1992) 2863–2866.

[91] U. Schollwöck, *The density-matrix renormalization group in the age of matrix product states*, *Annals of Physics* **326** (Jan., 2011) 96–192, [arXiv:1008.3477].

[92] B. Nienhuis, *Exact critical point and critical exponents of* O(n) *models in two dimensions*, *Phys. Rev. Lett.* **49** (Oct, 1982) 1062–1065.

[93] J. L. Jacobsen, N. Read, and H. Saleur, *Dense loops, supersymmetry, and goldstone phases in two dimensions*, *Phys. Rev. Lett.* **90** (Mar, 2003) 090601.

[94] J. Cardy, *Linking numbers for self-avoiding loops and percolation: Application to the spin quantum hall transition*, *Phys. Rev. Lett.* **84** (Apr, 2000) 3507–3510.

[95] M. Levin and C. P. Nave, *Tensor renormalization group approach to two-dimensional classical lattice models*, *Phys. Rev. Lett.* **99** (Sep, 2007) 120601.

[96] Z.-C. Gu, M. Levin, B. Swingle, and X.-G. Wen, *Tensor-product representations for string-net condensed states*, *Phys. Rev. B* **79** (Feb, 2009) 085118.

[97] Z.-C. Gu and X.-G. Wen, *Tensor-entanglement-filtering renormalization approach and symmetry-protected topological order*, *Phys. Rev. B* **80** (Oct, 2009) 155131.

[98] T. Scaffidi and Z. Ringel, *Wave functions of symmetry-protected topological phases from conformal field theories*, *Phys. Rev. B* **93** (Mar, 2016) 115105.

[99] M. Levin and X.-G. Wen, *Detecting topological order in a ground state wave function*, *Phys. Rev. Lett.* **96** (Mar, 2006) 110405.

[100] A. Kitaev and J. Preskill, *Topological entanglement entropy*, *Phys. Rev. Lett.* **96** (Mar, 2006) 110404.

[101] Z. Wang, X.-L. Qi, and S.-C. Zhang, *Topological order parameters for interacting topological insulators*, *Phys. Rev. Lett.* **105** (Dec, 2010) 256803.

[102] Z. Wang, X.-L. Qi, and S.-C. Zhang, *Topological invariants for interacting topological insulators with inversion symmetry*, *Phys. Rev. B* **85** (Apr, 2012) 165126.

[103] Z. Wang and S.-C. Zhang, *Simplified topological invariants for interacting insulators*, *Phys. Rev. X* **2** (Aug, 2012) 031008.

[104] Z. Wang and S.-C. Zhang, *Strongly correlated topological superconductors and topological phase transitions via green's function*, *Phys. Rev. B* **86** (Oct, 2012) 165116.

[105] M. P. Zaletel, *Detecting two-dimensional symmetry-protected topological order in a ground-state wave function*, *Phys. Rev. B* **90** (Dec, 2014) 235113.

[106] Z. Bi, Y.-Z. You, and C. Xu, *Exotic quantum critical point on the surface of three-dimensional topological insulator*, *Phys. Rev. B* **94** (Jul, 2016) 024433.

[107] Z. Bi, A. Rasmussen, Y. BenTov, and C. Xu, *Stable Interacting (2 + 1)d Conformal Field Theories at the Boundary of a class of (3 + 1)d Symmetry Protected Topological Phases*, *ArXiv e-prints* **1605.05336** (May, 2016) [arXiv:1605.0533].

[108] C.-M. Jian, Z. Bi, and C. Xu, *Lieb-Schultz-Mattis Theorem and its generalizations from the Perspective of the Symmetry Protected Topological phase*, *ArXiv e-prints* (Apr., 2017) [arXiv:1705.0001].

[109] R. Roy, *Topological superfluids with time reversal symmetry*, *ArXiv e-prints* (Mar., 2008) [arXiv:0803.2868].

[110] L. Fidkowski, X. Chen, and A. Vishwanath, *Non-abelian topological order on the surface of a 3d topological superconductor from an exactly solved model*, *Phys. Rev. X* **3** (Nov, 2013) 041016.

[111] X. Chen, L. Fidkowski, and A. Vishwanath, *Symmetry enforced non-abelian topological order at the surface of a topological insulator*, *Phys. Rev. B* **89** (Apr, 2014) 165132.

[112] P. Bonderson, C. Nayak, and X.-L. Qi, *A time-reversal invariant topological phase at the surface of a 3d topological insulator*, *Journal of Statistical Mechanics: Theory and Experiment* **2013** (2013), no. 09 P09016.

[113] C. Wang, A. C. Potter, and T. Senthil, *Gapped symmetry preserving surface state for the electron topological insulator*, *Phys. Rev. B* **88** (Sep, 2013) 115137.

[114] L. Fu and C. L. Kane, *Superconducting proximity effect and majorana fermions at the surface of a topological insulator*, *Phys. Rev. Lett.* **100** (Mar, 2008) 096407.

[115] D. T. Son, *Is the composite fermion a dirac particle?*, *Phys. Rev. X* **5** (Sep, 2015) 031027.

[116] M. A. Metlitski and A. Vishwanath, *Particle-vortex duality of two-dimensional dirac fermion from electric-magnetic duality of three-dimensional topological insulators*, *Phys. Rev. B* **93** (Jun, 2016) 245151.

[117] C. Wang and T. Senthil, *Dual dirac liquid on the surface of the electron topological insulator*, *Phys. Rev. X* **5** (Nov, 2015) 041031.

[118] C. Wang and T. Senthil, *Half-filled landau level, topological insulator surfaces, and three-dimensional quantum spin liquids*, *Phys. Rev. B* **93** (Feb, 2016) 085110.

[119] C. Dasgupta and B. I. Halperin, *Phase transition in a lattice model of superconductivity*, *Phys. Rev. Lett.* **47** (Nov, 1981) 1556–1560.

[120] M. P. A. Fisher and D. H. Lee, *Correspondence between two-dimensional bosons and a bulk superconductor in a magnetic field*, *Phys. Rev. B* **39** (Feb, 1989) 2756–2759.

[121] C. Xu and Y.-Z. You, *Self-dual quantum electrodynamics as boundary state of the three-dimensional bosonic topological insulator*, *Phys. Rev. B* **92** (Dec, 2015) 220416.

[122] O. I. Motrunich and A. Vishwanath, *Emergent photons and transitions in the* O(3) *sigma model with hedgehog suppression*, *Phys. Rev. B* **70** (Aug, 2004) 075104.

[123] T. Senthil, A. Vishwanath, L. Balents, S. Sachdev, and M. P. A. Fisher, *"deconfined" quantum critical points*, *Science* **303** (2004) 1490.

[124] T. Senthil, L. Balents, S. Sachdev, A. Vishwanath, and M. P. A. Fisher, *Quantum criticality beyond the landau-ginzburg-wilson paradigm*, *Phys. Rev. B* **70** (Oct, 2004) 144407.

[125] D. F. Mross, J. Alicea, and O. I. Motrunich, *Explicit derivation of duality between a free dirac cone and quantum electrodynamics in* $(2+1)$ *dimensions*, *Phys. Rev. Lett.* **117** (Jun, 2016) 016802.

[126] M. P. A. Fisher, *Quantum phase transitions in disordered two-dimensional superconductors*, *Phys. Rev. Lett.* **65** (Aug, 1990) 923–926.

[127] M. P. A. Fisher, G. Grinstein, and S. M. Girvin, *Presence of quantum diffusion in two dimensions: Universal resistance at the superconductor-insulator transition*, *Phys. Rev. Lett.* **64** (Jan, 1990) 587–590.

[128] P. Calabrese, A. Pelissetto, and E. Vicari, *The Critical behavior of magnetic systems described by Landau-Ginzburg-Wilson field theories*, cond-mat/0306273.

[129] M.-C. Cha, M. P. A. Fisher, S. M. Girvin, M. Wallin, and A. P. Young, *Universal conductivity of two-dimensional films at the superconductor-insulator transition*, *Phys. Rev. B* **44** (Oct, 1991) 6883–6902.

[130] G. G. Batrouni, B. Larson, R. T. Scalettar, J. Tobochnik, and J. Wang, *Universal conductivity in the two-dimensional boson hubbard model*, *Phys. Rev. B* **48** (Oct, 1993) 9628–9635.

[131] W. Witczak-Krempa, E. S. Sorensen, and S. Sachdev, *The dynamics of quantum criticality revealed by quantum monte carlo and holography*, *Nature Physics* **10** (2014) 361.

[132] K. Chen, L. Liu, Y. Deng, L. Pollet, and N. Prokof'ev, *Universal conductivity in a two-dimensional superfluid-to-insulator quantum critical system*, *Phys. Rev. Lett.* **112** (Jan, 2014) 030402.

[133] F. Kos, D. Poland, D. Simmons-Duffin, and A. Vichi, *Bootstrapping the o(n) archipelago*, *Journal of High Energy Physics* **2015** (2015), no. 11 106.

[134] M. Hermele, T. Senthil, and M. P. A. Fisher, *Algebraic spin liquid as the mother of many competing orders*, *Phys. Rev. B* **72** (Sep, 2005) 104404.

[135] J. Alicea, O. I. Motrunich, M. Hermele, and M. P. A. Fisher, *Criticality in quantum triangular antiferromagnets via fermionized vortices*, *Phys. Rev. B* **72** (Aug, 2005) 064407.

[136] C. Xu and S. Sachdev, *Global phase diagrams of frustrated quantum antiferromagnets in two dimensions: Doubled chern-simons theory*, *Phys. Rev. B* **79** (Feb, 2009) 064405.

[137] E. Katz, S. Sachdev, E. S. Sørensen, and W. Witczak-Krempa, *Conformal field theories at nonzero temperature: Operator product expansions, monte carlo, and holography*, *Phys. Rev. B* **90** (Dec, 2014) 245109.

[138] S. Kachru, M. Mulligan, G. Torroba, and H. Wang, *Mirror symmetry and the half-filled landau level*, *Phys. Rev. B* **92** (Dec, 2015) 235105.

[139] K. Intriligator and N. Seiberg, *Mirror symmetry in three dimensional gauge theories*, *Physics Letters B* **387** (1996), no. 3 513 – 519.

[140] J. de Boer, K. Hori, H. Ooguri, and Y. Oz, *Mirror symmetry in three-dimensional gauge theories, quivers and d-branes*, *Nuclear Physics B* **493** (1997), no. 1 101 – 147.

[141] A. Kapustin and M. J. Strassler, *On mirror symmetry in three dimensional abelian gauge theories*, *Journal of High Energy Physics* **1999** (1999), no. 04 021.

[142] D. T. Son, *Is the composite fermion a dirac particle?*, *Phys. Rev. X* **5** (Sep, 2015) 031027.

[143] S. Sachdev and X. Yin, *Quantum phase transitions beyond the landauginzburg paradigm and supersymmetry*, *Annals of Physics* **325** (2010), no. 1 2 – 15. January 2010 Special Issue.

[144] E.-G. Moon, *Skyrmions with quadratic band touching fermions: A way to achieve charge* 4*e superconductivity*, *Phys. Rev. B* **85** (Jun, 2012) 245123.

[145] K. Slagle, Y.-Z. You, and C. Xu, *Exotic quantum phase transitions of strongly interacting topological insulators*, *Phys. Rev. B* **91** (Mar, 2015) 115121.

[146] Y.-Y. He, H.-Q. Wu, Y.-Z. You, C. Xu, Z. Y. Meng, and Z.-Y. Lu, *Bona fide interaction-driven topological phase transition in correlated SPT states*, *ArXiv e-prints* (Aug., 2015) [arXiv:1508.0638].

[147] T. Senthil and M. P. A. Fisher, *Competing orders, nonlinear sigma models, and topological terms in quantum magnets*, *Phys. Rev. B* **74** (Aug, 2006) 064405.

[148] A. G. Abanov, *Hopf term induced by fermions*, *Physics Letters B* **492** (2000), no. 3–4 321 – 323.

[149] C. Wang and T. Senthil, *Interacting fermionic topological insulators/superconductors in three dimensions*, *Phys. Rev. B* **89** (May, 2014) 195124.

[150] S. Hikami, *Renormalization group functions of orthogonal and symplectic non-linear σ models*, *Progress of Theoretical Physics* **64** (1980), no. 4 1466.

[151] E. Brezin, S. Hikami, and J. Zinn-Justin, *Generalized Nonlinear σ Models With Gauge Invariance*, *Nucl. Phys.* **B165** (1980) 528–544.

[152] B. I. Halperin, T. C. Lubensky, and S.-k. Ma, *First-order phase transitions in superconductors and smectic-a liquid crystals*, *Phys. Rev. Lett.* **32** (Feb, 1974) 292–295.

[153] R. K. Kaul and S. Sachdev, *Quantum criticality of u(1) gauge theories with fermionic and bosonic matter in two spatial dimensions*, *Phys. Rev. B* **77** (Apr, 2008) 155105.

[154] M. E. Fisher, S.-k. Ma, and B. G. Nickel, *Critical exponents for long-range interactions*, *Phys. Rev. Lett.* **29** (Oct, 1972) 917–920.

[155] K. Gawędski and A. Kupiainen, *Renormalization of a non-renormalizable quantum field theory*, *Nuclear Physics B* **262** (1985), no. 1 33 – 48.

[156] D. F. Mross, J. McGreevy, H. Liu, and T. Senthil, *Controlled expansion for certain non-fermi-liquid metals*, *Phys. Rev. B* **82** (Jul, 2010) 045121.

[157] C. Nayak and F. Wilczek, *Non-fermi liquid fixed point in 2 + 1 dimensions*, *Nuclear Physics B* **417** (1994), no. 3 359 – 373.

[158] C. Nayak and F. Wilczek, *Renormalization group approach to low temperature properties of a non-fermi liquid metal*, *Nuclear Physics B* **430** (1994), no. 3 534 – 562.

[159] S.-S. Lee, *Low-energy effective theory of fermi surface coupled with u(1) gauge field in $2+1$ dimensions*, *Phys. Rev. B* **80** (Oct, 2009) 165102.

[160] E. Frey and L. Balents, *Critical behavior of the supersolid transition in bose-hubbard models*, *Phys. Rev. B* **55** (Jan, 1997) 1050–1067.

[161] C. Xu, M. Müller, and S. Sachdev, *Ising and spin orders in the iron-based superconductors*, *Phys. Rev. B* **78** (Jul, 2008) 020501.

[162] X.-G. Wen, *Artificial light and quantum order in systems of screened dipoles*, *Phys. Rev. B* **68** (Sep, 2003) 115413.

[163] R. Moessner and S. L. Sondhi, *Three-dimensional resonating-valence-bond liquids and their excitations*, *Phys. Rev. B* **68** (Nov, 2003) 184512.

[164] M. Hermele, M. P. A. Fisher, and L. Balents, *Pyrochlore photons: The $u(1)$ spin liquid in a $s = \frac{1}{2}$ three-dimensional frustrated magnet*, *Phys. Rev. B* **69** (Feb, 2004) 064404.

[165] T. Gregoire and J. G. Wacker, *Mooses, topology and higgs*, *Journal of High Energy Physics* **2002** (2002), no. 08 019.

[166] N. Arkani-Hamed, A. G. Cohen, E. Katz, and A. E. Nelson, *The littlest higgs*, *Journal of High Energy Physics* **2002** (2002), no. 07 034.

[167] D. E. Kaplan and M. Schmaltz, *The little higgs from a simple group*, *Journal of High Energy Physics* **2003** (2003), no. 10 039.

[168] M. Oshikawa, *Commensurability, excitation gap, and topology in quantum many-particle systems on a periodic lattice*, *Phys. Rev. Lett.* **84** (Feb, 2000) 1535–1538.

[169] M. B. Hastings, *Lieb-schultz-mattis in higher dimensions*, *Phys. Rev. B* **69** (Mar, 2004) 104431.

[170] I. Kimchi, S. A. Parameswaran, A. M. Turner, F. Wang, and A. Vishwanath, *Featureless and nonfractionalized mott insulators on the honeycomb lattice at 1/2 site filling*, *Proceedings of the National Academy of Sciences* **110** (2013), no. 41 16378–16383, [http://www.pnas.org/content/110/41/16378.full.pdf].

[171] C.-M. Jian and M. Zaletel, *Existence of featureless paramagnets on the square and the honeycomb lattices in 2+1 dimensions*, *Phys. Rev. B* **93** (Jan, 2016) 035114.

[172] P. Kim, H. Lee, S. Jiang, B. Ware, C.-M. Jian, M. Zaletel, J. H. Han, and Y. Ran, *Featureless quantum insulator on the honeycomb lattice*, *Phys. Rev. B* **94** (Aug, 2016) 064432.

[173] D. S. Freed, *Anomalies and Invertible Field Theories*, *Proc. Symp. Pure Math.* **88** (2014) 25–46, [arXiv:1404.7224].

[174] D. S. Freed, *Short-range entanglement and invertible field theories*, arXiv:1406.7278.

[175] Z. Bi and C. Xu, *Construction and field theory of bosonic-symmetry-protected topological states beyond group cohomology*, *Phys. Rev. B* **91** (May, 2015) 184404.

[176] M. Cheng, M. Zaletel, M. Barkeshli, A. Vishwanath, and P. Bonderson, *Translational symmetry and microscopic constraints on symmetry-enriched topological phases: A view from the surface*, *Phys. Rev. X* **6** (Dec, 2016) 041068.

[177] H. C. Po, H. Watanabe, C.-M. Jian, and M. P. Zaletel, *Lattice Homotopy Constraints on Phases of Quantum Magnets*, *ArXiv e-prints* (Mar., 2017) [arXiv:1703.0688].

[178] I. Affleck, *Exact critical exponents for quantum spin chains, non-linear σ models at $\theta = \pi$ and the quantum hall effect*, *Nuclear Physics B* **265** (1986), no. 3 409 – 447.

[179] I. Affleck, *The quantum hall effects, σ-models at $\theta = \pi$ and quantum spin chains*, *Nuclear Physics B* **257** (1985) 397 – 406.

[180] N. Read and S. Sachdev, *Some features of the phase diagram of the square lattice su(n) antiferromagnet*, *Nuclear Physics B* **316** (1989), no. 3 609 – 640.

[181] A. M. M. Pruisken, M. A. Baranov, and M. Voropaev, *The large N theory exactly reveals the quantum Hall effect and theta-renormalization*, *eprint arXiv:cond-mat/0101003* (Dec., 2001) [cond-mat/0101003].

[182] K. Duivenvoorden and T. Quella, *Topological phases of spin chains*, *Phys. Rev. B* **87** (Mar, 2013) 125145.

[183] H.-H. Tu, G.-M. Zhang, and T. Xiang, *Class of exactly solvable so(n) symmetric spin chains with matrix product ground states*, *Phys. Rev. B* **78** (Sep, 2008) 094404.

[184] H.-H. Tu and R. Orús, *Effective field theory for the* SO(n) *bilinear-biquadratic spin chain*, *Phys. Rev. Lett.* **107** (Aug, 2011) 077204.

[185] C. Wang, A. Nahum, M. A. Metlitski, C. Xu, and T. Senthil, *Deconfined quantum critical points: symmetries and dualities*, arXiv:1703.0242.

[186] C. Xu, F. Wang, Y. Qi, L. Balents, and M. P. A. Fisher, *Spin liquid phases for spin-1 systems on the triangular lattice*, *Phys. Rev. Lett.* **108** (Feb, 2012) 087204.

[187] N. Read and S. Sachdev, *Valence-bond and spin-peierls ground states of low-dimensional quantum antiferromagnets*, *Phys. Rev. Lett.* **62** (Apr, 1989) 1694–1697.

[188] N. Read and S. Sachdev, *Spin-peierls, valence-bond solid, and néel ground states of low-dimensional quantum antiferromagnets*, *Phys. Rev. B* **42** (Sep, 1990) 4568–4589.

[189] M. Hermele, *Su(2) gauge theory of the hubbard model and application to the honeycomb lattice*, *Phys. Rev. B* **76** (Jul, 2007) 035125.

[190] O. I. Motrunich and T. Senthil, *Origin of artificial electrodynamics in three-dimensional bosonic models*, *Phys. Rev. B* **71** (Mar, 2005) 125102.

[191] G. Chen, J. Gukelberger, S. Trebst, F. Alet, and L. Balents, *Coulomb gas transitions in three-dimensional classical dimer models*, *Phys. Rev. B* **80** (Jul, 2009) 045112.

[192] P. Hosur, S. Ryu, and A. Vishwanath, *Chiral topological insulators, superconductors, and other competing orders in three dimensions*, *Phys. Rev. B* **81** (Jan, 2010) 045120.

[193] C.-M. Jian, To appear.

[194] T. Hahn, ed., *International Tables for Crystallography*, vol. A: Space-group symmetry. Springer, 5th ed., 2006.

[195] Y.-Z. You, Z. Bi, A. Rasmussen, M. Cheng, and C. Xu, *Bridging fermionic and bosonic short range entangled states*, *New Journal of Physics* **17** (2015), no. 7 075010.

[196] Z. Bi, R. Zhang, Y.-Z. You, A. Young, L. Balents, C.-X. Liu, and C. Xu, *Bilayer graphene as a platform for bosonic symmetry-protected topological states*, *Phys. Rev. Lett.* **118** (Mar, 2017) 126801.

[197] Y.-Z. You, Z. Bi, D. Mao, and C. Xu, *Quantum phase transitions between bosonic symmetry-protected topological states without sign problem: Nonlinear sigma model with a topological term*, *Phys. Rev. B* **93** (Mar, 2016) 125101.

[198] X.-L. Qi, T. L. Hughes, S. Raghu, and S.-C. Zhang, *Time-reversal-invariant topological superconductors and superfluids in two and three dimensions*, *Phys. Rev. Lett.* **102** (May, 2009) 187001.

[199] S. Ryu, A. P. Schnyder, A. Furusaki, and A. W. W. Ludwig, *Topological insulators and superconductors: tenfold way and dimensional hierarchy*, *New Journal of Physics* **12** (2010), no. 6 065010.

[200] L. Fidkowski and A. Kitaev, *Effects of interactions on the topological classification of free fermion systems*, *Phys. Rev. B* **81** (Apr, 2010) 134509.

[201] L. Fidkowski and A. Kitaev, *Topological phases of fermions in one dimension*, *Phys. Rev. B* **83** (Feb, 2011) 075103.

[202] X.-L. Qi, *A new class of (2+1)-dimensional topological superconductors with $\mathbb{Z}_8$ topological classification*, *New Journal of Physics* **15** (2013), no. 6 065002.

[203] S. Ryu and S.-C. Zhang, *Interacting topological phases and modular invariance*, *Phys. Rev. B* **85** (Jun, 2012) 245132.

[204] Z.-C. Gu and M. Levin, *Effect of interactions on two-dimensional fermionic symmetry-protected topological phases with Z_2 symmetry*, *Phys. Rev. B* **89** (May, 2014) 201113.

[205] H. Yao and S. Ryu, *Interaction effect on topological classification of superconductors in two dimensions*, *Phys. Rev. B* **88** (Aug, 2013) 064507.

[206] Y.-M. Lu and D.-H. Lee, *Quantum phase transitions between bosonic symmetry-protected topological phases in two dimensions: Emergent* qed_3 *and anyon superfluid*, *Phys. Rev. B* **89** (May, 2014) 195143.

[207] T. Grover and A. Vishwanath, *Quantum phase transition between integer quantum hall states of bosons*, *Phys. Rev. B* **87** (Jan, 2013) 045129.

[208] Z. Wang, X.-L. Qi, and S.-C. Zhang, *Topological field theory and thermal responses of interacting topological superconductors*, *Phys. Rev. B* **84** (Jul, 2011) 014527.

[209] S. Ryu, J. E. Moore, and A. W. W. Ludwig, *Electromagnetic and gravitational responses and anomalies in topological insulators and superconductors*, *Phys. Rev. B* **85** (Jan, 2012) 045104.

[210] A. Abanov and P. Wiegmann, *Theta-terms in nonlinear sigma-models*, *Nuclear Physics B* **570** (2000), no. 3 685 – 698.

[211] X. Chen, L. Fidkowski, M. Metlitski, and A. Vishwanath *unpublished* (2014).

[212] E. Plamadeala, M. Mulligan, and C. Nayak, *Short-range entangled bosonic states with chiral edge modes and ¡span class="aps-inline-formula"¿¡math¿¡mi¿t¡/mi¿¡/math¿¡/span¿ duality of heterotic strings*, *Phys. Rev. B* **88** (Jul, 2013) 045131.

[213] M. Cheng and Z.-C. Gu, *Topological response theory of abelian symmetry-protected topological phases in two dimensions*, *Phys. Rev. Lett.* **112** (Apr, 2014) 141602.

[214] J. Cano, M. Cheng, M. Mulligan, C. Nayak, E. Plamadeala, and J. Yard, *Bulk-edge correspondence in (2 + 1)-dimensional abelian topological phases*, *Phys. Rev. B* **89** (Mar, 2014) 115116.

[215] Y. Ran, A. Vishwanath, and D.-H. Lee, *Spin-charge separated solitons in a topological band insulator*, *Phys. Rev. Lett.* **101** (Aug, 2008) 086801.

[216] S. V. Isakov, M. B. Hastings, and R. G. Melko, *Topological entanglement entropy of a bose?hubbard spin liquid*, *Nature Physics* **7** (2011) 772.

[217] S. V. Isakov, M. B. Hastings, and R. G. Melko, *Universal signatures of fractionalized quantum critical points*, *Science* **335** (2012) 193.

[218] T. Senthil and M. Levin, *Integer quantum hall effect for bosons*, *Phys. Rev. Lett.* **110** (Jan, 2013) 046801.

[219] J. C. Wang, Z.-C. Gu, and X.-G. Wen, *Field-theory representation of gauge-gravity symmetry-protected topological invariants, group cohomology, and beyond*, *Phys. Rev. Lett.* **114** (Jan, 2015) 031601.

[220] D. A. Abanin, P. A. Lee, and L. S. Levitov, *Spin-filtered edge states and quantum hall effect in graphene*, *Phys. Rev. Lett.* **96** (May, 2006) 176803.

[221] M. Kharitonov, *Canted antiferromagnetic phase of the ν=0 quantum hall state in bilayer graphene*, *Phys. Rev. Lett.* **109** (Jul, 2012) 046803.

[222] P. Maher, C. R. Dean, A. F. Young, T. Taniguchi, K. Watanabe, K. L. Shepard, J. Hone, and P. Kim, *Evidence for a spin phase transition at charge neutrality in bilayer graphene*, *Nature Physics* **9** (2013) 154–158.

[223] M. Kharitonov, *Edge excitations of the canted antiferromagnetic phase of the $\nu = 0$ quantum hall state in graphene: A simplified analysis*, *Phys. Rev. B* **86** (Aug, 2012) 075450.

[224] J. González, F. Guinea, and M. A. H. Vozmediano, *Marginal-fermi-liquid behavior from two-dimensional coulomb interaction*, *Phys. Rev. B* **59** (Jan, 1999) R2474–R2477.

[225] B. M. Hunt, J. I. A. Li, A. A. Zibrov, L. Wang, T. Taniguchi, K. Watanabe, J. Hone, C. R. Dean, M. Zaletel, R. C. Ashoori, and A. F. Young, *Competing valley, spin, and orbital symmetry breaking in bilayer graphene*, *ArXiv e-prints* (July, 2016) [arXiv:1607.0646].

[226] T. Martin, *Course 5 noise in mesoscopic physics*, *Les Houches* **81** (2005) 283 – 359.

[227] J. Maciejko, C. Liu, Y. Oreg, X.-L. Qi, C. Wu, and S.-C. Zhang, *Kondo effect in the helical edge liquid of the quantum spin hall state*, *Phys. Rev. Lett.* **102** (Jun, 2009) 256803.

[228] C. L. Kane and M. P. A. Fisher, *Transmission through barriers and resonant tunneling in an interacting one-dimensional electron gas*, *Phys. Rev. B* **46** (Dec, 1992) 15233–15262.

[229] M. Kharitonov, *Edge excitations of the canted antiferromagnetic phase of the $\nu = 0$ quantum hall state in graphene: A simplified analysis*, *Phys. Rev. B* **86** (Aug, 2012) 075450.

[230] N. Read and G. Moore, *Fractional quantum hall effect and nonabelian statistics*, *Progress of Theoretical Physics Supplement* **107** (01, 1992) 157–166.

[231] L. Ju, Z. Shi, N. Nair, Y. Lv, C. Jin, J. Velasco Jr, C. Ojeda-Aristizabal, H. A. Bechtel, M. C. Martin, A. Zettl, J. Analytis, and F. Wang, *Topological valley transport at bilayer graphene domain walls*, *Nature* **520** (04, 2015) 650–655.

[232] J. Li, K. Wang, K. J. McFaul, Z. Zern, Y. Ren, K. Watanabe, T. Taniguchi, Z. Qiao, and J. Zhu, *Gate-controlled topological conducting channels in bilayer graphene*, *Nat Nano* **11** (12, 2016) 1060–1065.

[233] V. Mazo, C.-W. Huang, E. Shimshoni, S. T. Carr, and H. A. Fertig, *Superfluid-insulator transition of quantum hall domain walls in bilayer graphene*, *Phys. Rev. B* **89** (Mar, 2014) 121411.

[234] V. Mazo, E. Shimshoni, C.-W. Huang, S. T. Carr, and H. A. Fertig, *Helical quantum hall edge modes in bilayer graphene: a realization of quantum spin-ladders*, *Physica Scripta* **2015** (2015), no. T165 014019.

[235] L. P. Kadanoff, *Lattice coulomb gas representations of two-dimensional problems*, *Journal of Physics A: Mathematical and General* **11** (1978), no. 7 1399.

[236] P. di Francesco, H. Saleur, and J. B. Zuber, *Relations between the coulomb gas picture and conformal invariance of two-dimensional critical models*, *Journal of Statistical Physics* **49** (1987), no. 1 57–79.

[237] J. T. Chalker and P. D. Coddington, *Percolation, quantum tunnelling and the integer hall effect*, *Journal of Physics C: Solid State Physics* **21** (1988), no. 14 2665.

[238] Y.-Z. You, Z. Bi, A. Rasmussen, M. Cheng, and C. Xu, *Bridging fermionic and bosonic short range entangled states*, *New Journal of Physics* **17** (July, 2015) 075010, [arXiv:1404.6256].

[239] C. L. Kane and M. P. A. Fisher, *Nonequilibrium noise and fractional charge in the quantum hall effect*, *Phys. Rev. Lett.* **72** (Jan, 1994) 724–727.

[240] C. d. C. Chamon, D. E. Freed, and X. G. Wen, *Tunneling and quantum noise in one-dimensional luttinger liquids*, *Phys. Rev. B* **51** (Jan, 1995) 2363–2379.

[241] P. Fendley, A. W. W. Ludwig, and H. Saleur, *Exact nonequilibrium dc shot noise in luttinger liquids and fractional quantum hall devices*, *Phys. Rev. Lett.* **75** (Sep, 1995) 2196–2199.

[242] R. de Picciotto, M. Reznikov, M. Heiblum, V. Umansky, G. Bunin, and D. Mahalu, *Direct observation of a fractional charge*, *Nature* **389** (1997) 162.

[243] R.-X. Zhang and C.-X. Liu, *Fingerprints of bosonic symmetry protected topological state in a quantum point contact*, *ArXiv e-prints* (Oct., 2016) [arXiv:1610.0123].

[244] X. Chen, Z.-X. Liu, and X.-G. Wen, *Two-dimensional symmetry-protected topological orders and their protected gapless edge excitations*, *Phys. Rev. B* **84** (Dec, 2011) 235141.

[245] S. D. Geraedts and O. I. Motrunich, *Exact realization of integer and fractional quantum hall phases in models in*, *Annals of Physics* **334** (2013) 288 – 315.

[246] S. D. Geraedts and O. I. Motrunich, *Monte carlo study of a $u(1) \times u(1)$ system with π-statistical interaction*, *Phys. Rev. B* **85** (Jan, 2012) 045114.

[247] Z.-X. Liu, Z.-C. Gu, and X.-G. Wen, *Microscopic realization of two-dimensional bosonic topological insulators*, *Phys. Rev. Lett.* **113** (Dec, 2014) 267206.

[248] Y.-C. He, S. Bhattacharjee, R. Moessner, and F. Pollmann, *Bosonic integer quantum hall effect in an interacting lattice model*, *Phys. Rev. Lett.* **115** (Sep, 2015) 116803.

[249] Z.-X. Liu, J.-W. Mei, P. Ye, and X.-G. Wen, *$u(1) \times u(1)$ symmetry-protected topological order in gutzwiller wave functions*, *Phys. Rev. B* **90** (Dec, 2014) 235146.

[250] C. Wu and S.-C. Zhang, *Sufficient condition for absence of the sign problem in the fermionic quantum monte carlo algorithm*, *Phys. Rev. B* **71** (Apr, 2005) 155115.

[251] Z.-X. Li, Y.-F. Jiang, and H. Yao, *Solving the fermion sign problem in quantum Monte Carlo simulations by Majorana representation*, *Phys. Rev. B* **91** (June, 2015) 241117, [arXiv:1408.2269].

[252] Z.-X. Li, Y.-F. Jiang, and H. Yao, *Fermion-sign-free Majarana-quantum-Monte-Carlo studies of quantum critical phenomena of Dirac fermions in two dimensions*, *New Journal of Physics* **17** (Aug., 2015) 085003, [arXiv:1411.7383].

[253] H. Isobe and L. Fu, *Theory of interacting topological crystalline insulators*, *Phys. Rev. B* **92** (Aug, 2015) 081304.

[254] M. Barkeshli and X.-G. Wen, *Effective field theory and projective construction for Z_k parafermion fractional quantum hall states*, *Phys. Rev. B* **81** (Apr, 2010) 155302.

[255] F. J. Burnell, X. Chen, L. Fidkowski, and A. Vishwanath, *Exactly soluble model of a three-dimensional symmetry-protected topological phase of bosons with surface topological order*, *Phys. Rev. B* **90** (Dec, 2014) 245122.